PCSK9 AS A DRIVER OF LIPID METABOLISM AND KIDNEY DISEASE

PCSK9 AS A DRIVER OF LIPID METABOLISM AND KIDNEY DISEASE

By

Jae Hyun Byun, Hons. B. Sc.

A Thesis Submitted to the School of Graduate Studies in Partial Fulfilment of the Requirements for the Degree Master of Science

McMaster University MASTER OF SCIENCE (2020) Hamilton, ON
Department of Medical Sciences

TITLE: PCSK9 AS A DRIVER OF LIPID METABOLISM AND KIDNEY DISEASE
AUTHOR: Jae Hyun Byun (H. B.Sc. McMaster University)
SUPERVISOR: Dr. Richard C. Austin, Ph.D.
PAGES: xiii, 133

Abstract

The global prevalence of chronic kidney disease (CKD) has risen at an accelerating rate, increasing the global healthcare burden for long-term and chronic care costs. Multiple risk factors including hypertension, diabetes, and dyslipidemia synergistically induce the progression of CKD. Chief among these factors are dyslipidemia and obesity; increased free fatty acid uptake due to excess consumption of lipid-rich diets has been shown to promote intra-renal lipid accumulation in several in vivo models and in patients in various stages of CKD. Furthermore, patients with renal disease are also at a substantially higher risk for atherosclerotic cardiovascular disease (CVD). In the general population, as well as in patients with renal disease, circulating low-density lipoprotein cholesterol (LDLc) is a well-established driver of atherosclerotic lesion development and CVD progression. In 2003, the proprotein convertase subtilisin/kexin type-9 (PCSK9) was identified as the third locus of familial hypercholesterolemia and was further characterized for its ability to enhance the degradation of the low-density lipoprotein receptor (LDLR). Since this seminal discovery, the development of monoclonal antibodies targeted against PCSK9 demonstrated a significant reduction in LDLc and subsequent CVD risk, establishing the remarkable *'bench to bedside'* transition. However, the inherent role of PCSK9 in regulating lipid homeostasis remained unknown in different pathological conditions. In the first chapter of my thesis, I demonstrate that PCSK9 regulates the LDLR as a feedback mechanism to protect against non-alcoholic steatohepatitis (NASH) progression induced by a high-fat diet (HFD) challenge.

Since its seminal discovery, PCSK9 was also characterized to modulate a wide variety of receptors known to play a crucial role in lipid metabolism including the cluster of differentiation 36 (CD36), the very low-density lipoprotein receptor (VLDLR), and the apolipoprotein E

receptor 2 (ApoER2). Previously, we have demonstrated that the absence of PCSK9 promotes diet-induced non-alcoholic steatohepatitis and liver injury through increased surface expression of CD36. Given that these same receptors are well-expressed on renal epithelia, the second chapter of my thesis demonstrates that PCSK9 is also able to modulate renal lipid metabolism by attenuating tubular lipid accumulation and subsequent renal injury.

Furthermore, when PCSK9 was first characterized by Seidah and colleagues in 2003, in situ hybridization of murine PCSK9 demonstrated that it was primarily expressed in the liver, but also well-expressed in the kidney cortex, cerebellum, and small intestines. Despite its expression in a wide range of tissues, the secretion of PCSK9 was exclusive to the liver, thus, questioning what the intracellular role of PCSK9 may be. Hence, my last chapter of my masters studies lies in establishing the role of intracellular PCSK9 expression in a cellular process known as endoplasmic reticulum (ER) stress in the kidney. ER stress is a phenomena which primarily occurs due to increased accumulation of misfolded polypeptides, and has been implicated in numerous metabolic diseases including hepatic steatosis, CKD, and neurodegenerative pathologies. Previously, we have demonstrated that overexpressing wild-type and variants of PCSK9 in a *Pcsk9*$^{-/-}$ mouse does not induce the activation of the unfolded protein response (UPR) and attenuates hepatic ER stress. Using a well-established CKD model, I show that *Pcsk9*$^{-/-}$ mice exhibit increased renal ER stress and injury relative to wild-type controls. Overall, my findings demonstrate for the first time that both extracellular and intracellular PCSK9 has the ability to modulate renal injury using two distinct mechanism to protect against CKD progression.

Acknowledgements

I would like to first express my sincere gratitude to my supervisor, Dr. Richard C. Austin, for providing the foundation of my scientific discipline and ongoing support throughout my masters education. My transition to investigating the molecular biology of PCSK9 in a wet lab setting from the clinical setting of PCSK9 inhibition is the prime example of the '*bench to bedside'* concept. As such, I am grateful for experiencing both of these sides throughout my education. As well, I thank Dr. Gregory P. Curnew for becoming the role model that I aspire to be in clinical practice. I am inspired how you go above and beyond to ensure your patients get the optimal amount of care that they need; from after-clinic workshops, patient pancake breakfasts, online YouTube videos, to CN tower climbs, I can only aspire to be a quarter of what you have accomplished in your career. Next, I wanted to express my utmost gratitude to Paul F. Lebeau, who first introduced me to the exciting aspects of research and experimental design. You have instilled in me a discipline that will surely go beyond my scientific career; from rigorous days of running around executing countless experiments to sitting down every Monday to go over the weekly agendas, I learned to set realistic, and reasonable goals for myself and work hard at achieving them. As well, thank you for the comedic relief that would make countless failed experiments more enjoyable: *Yep, out of 10 experiments, expect only 3 of them to work at most. Also, always remember to* ***look pretty*** *before this happens. If all fails, at least you'll* ***look pretty****.* Lastly, I would like to thank my committee members Dr. Jeffrey G. Dickhout and Dr. Joan C. Krepinsky for their input and guidance throughout the course of my education. Altogether, my academic progression would not have been made possible without the phenomenal support from both the lab and the clinic.

I would next like to thank my family and friends for their constant support in believing the dreams and goals that I aspire to accomplish. My inherent drive and discipline stems from my parents; they are the rock that I had grew from and a place where I can always call *home.* As well, I thank my girlfriend, Lorraine Leung, for her constant emotional support throughout my masters education. You made me realize that there are so many things worth celebrating; from journal publications to my academic successes... but above all, it is about your unconditional will to stay by my side when things turn 180 on any given day. I look forward to our future together as we continue to journey through several mountains that have yet to be explored. As well, to all my friends, I thank you for all the moral support and for the countless amount of genuine conversations that we would have over religion, life, family, and the future.

The drive behind the curation of this thesis would not have been possible without any of the acknowledged individuals on this page. I thank you all for always believing in me when all else seems to fail. I am forever grateful for all of your unconditional support throughout the years.

Table of Contents

Abbreviations

ATF6	activating transcription factor 6
apoB	apolipoprotein B
apoE	apolipoprotein E
apoER2	apoE receptor-2
BSA	bovine serum albumin
CD36	cluster of differentiation 36
CKD	chronic kidney disease
CVD	cardiovascular disease
EGF-a	epidermal growth factor a
ENaC	epithelial sodium channel
ESRD	end-stage renal disease
ER	endoplasmic reticulum
ERAI	endoplasmic reticulum activated indicator
FAS	fatty acid synthase
FFA	free fatty acid;
FH	familial hypercholesterolemia
GFR	glomerular filtration rate
GOF	gain-of-function
GRP78	glucose-regulated protein of 78 kDa
GRP94	glucose-regulated protein 94 kDa
HDAC	histone deacetylase
HDL	high-density lipoprotein

HFD	high-fat diet;
HMGCR	HMG-CoA reductase
HRP	horse radish peroxidase
IHC	immunohistochemical
INSIG-1	insulin-induced gene-1
IRE1	inositol-requiring enzyme I
LDLc	low-density lipoprotein cholesterol
LDLR	low-density lipoprotein receptor
LOF	loss-of-function
mAb	monoclonal antibody
NAFLD	non-alcoholic fatty liver disease
n-ATF6	nuclear ATF6
NCD	normal control diet
OA	oleic acid
OD	optical density
ORO	oil-red-o
ox-LDL	oxidized-LDL
PA	palmitate
PBS	phosphate-buffered saline
PPAR	peroxisome proliferator-activated receptor
PCSK9	proprotein convertase subtilisin/kexin type-9
peIF2α	phosphorylated eukaryotic initiation factor 2α
p-PERK	phosphorylated-PERK

PERK	protein kinase RNA-like ER kinase
PSR	picro sirius red
qRT-PCR	quantitative real-time PCR
ROS	reactive oxygen species
SCAP	SREBP cleavage-activating protein
SERCA	sarco/endoplasmic reticulum Ca^{2+}-ATPase
siCD36	small interfering CD36
siRNA	small interfering RNA
siScrambled	small interfering scrambled
SREBP	sterol-regulatory binding proteins
sXBP1	spliced XBP1
S1	site-1
S2	site-2
SREBP-1	sterol regulatory element binding protein-1
TG	thapsigargin
TM	tunicamycin
TBS	tris-buffered saline
Unx	uninephrectomy
UPR	unfolded protein response
VLDLR	very low-density lipoprotein receptor
XBP1	x-box binding protein-1
4-PBA	4-phenylbutyrate

Declaration of Academic Achievement

This is a *sandwich-formatted* thesis which is composed of 8 chapters. Chapter 1 consists of an introduction and provides the context of my research focus. Chapter 2 and 3 outlines my research objectives and hypotheses, which also includes the experimental methods necessary for the curation of all figures. Chapter 4 to 6 are articles which have either been published or submitted for review at the time this thesis was prepared. I am the primary author in all articles presented in this thesis. Chapters 7 and 8 serves as a conclusion, discussing the overall contributions of my work to the scientific community, as well as future directions and limitations of this research. I have personally accomplished most of the research, laboratory experiments and procedures necessary for the curation of all figures. As a team, Dr. Richard C. Austin and Dr. Paul F. Lebeau provided insight into experimental design and analysis. Our PhD student and research technician, Khrystyna Platko and Melissa E. Macdonald respectively, provided assistance with animal handling and the use of *in vivo* models.

This thesis is primarily composed of three manuscripts, all of which have either been published or currently submitted for review:

Lebeau P*, **Byun JH*,** Platko K, MacDonald M, Poon S, Faiyaz M, Seidah N, Austin RC. Diet-induced hepatic steatosis abrogates cell-surface LDLR by inducing de novo PCSK9 expression in mice. *Journal of Biological Chemistry*, 294:9037-9047 * co-first authors

Byun JH*, Lebeau P*, Platko K, Carlisle R, Faiyaz M, Dickhout JG, Krepinsky JC, Austin RC. PCSK9 blocks surface CD36 expression to prevent tubular lipid accumulation and renal injury. *Submitted to the Journal of the American Society of Nephrology*

Byun JH, Lebeau P, Platko K, Carlisle R, Faiyaz M, Esselman R, Dickhout JG, Krepinsky JC, Seidah NG, Austin RC. Renal PCSK9 protects against AngII/DOCA induced progression of CKD in mice. *Prepared for the Journal of Scientific Reports*

In addition to the works in my thesis, I contributed to the following published manuscripts:

Lebeau P*, **Byun JH*,** Yousof T, Austin RC. Pharmacologic Inhibition of S1P attenuates ATF6 expression, causes ER stress and contributes to apoptotic cell death. *Toxicology and Applied Pharmacology*, 2018; 349:1-7. * co-first authors

Lebeau, P.F.*, **Byun, J.H.*,** Platko, K.*, Al-Hashimi, A. A., Lhoták, Š., Macdonald, M. E., … Austin, R. C. (2019). Pcsk9 knockout exacerbates diet-induced non-alcoholic steatohepatitis, fibrosis and liver injury in mice. *JHEP Reports*, 1(6), 418–429. doi: 10.1016/j.jhepr.2019.10.009 * co-first authors

Platko K*, Lebeau P*, **Byun JH**, Poon S, Day E, MacDonald M, Holzapfel N, Mejia-Benitez A, Maclean K, Krepinsky J, Austin RC. GDF10 blocks hepatic PPARγ activation to protect against diet-induced liver injury. *Molecular Metabolism*, 27, 62–74. doi: 10.1016/j.molmet.2019.06.021

Lebeau P, Platko K, Al-Hashimi AA, **Byun JH**, Lhotak S, Holzapfel N, Gyulay G, Igdoura SA, Cool D, Trigatti B, Austin RC. Loss-of-function PCSK9 mutants evade the unfolded protein response sensor GRP78 and fail to induce endoplasmic reticulum stress when retained. *Journal of Biological Chemistry* 2018; 293:7329-7343.

Lynn E, Lhotak S, Lebeau P, **Byun JH**, Chen J, Platko K, Shi C, O'Brien E, Austin RC. 4-Phenylbutyrate protects against atherosclerotic lesion growth by increasing the expression of HSP25 in macrophages and in the circulation of ApoE-/- mice. *The FASEB Journal*, 33(7), 8406–8422. doi: 10.1096/fj.201802293rr

Crane ED, Al-Hashimi AA, Chen J, Lynn EG, Won KD, Lhotak S, Naeium M, Platko K, Lebeau P, **Byun JH**, Shayegan B, Krepinsky JC, Rayner KJ, Marchio S, Pasqualini R, Arap W, Austin RC. Anti-GRP78 autoantibodies induce endothelial cell activation and accelerate the development of atherosclerotic lesions. 2018; 3:24.

Lebeau P, Chen J, **Byun JH**, Platko K, Austin RC. The trypan blue cellular debris assay: a novel low-cost method for the rapid quantification of cell death. *MethodsX*. 2019; 6:1174-1180

Platko K, Lebeau P, Gyulay G, Lhotak S, MacDonald M, Pacher G, **Byun JH**, Boivin F, Igdoura S, Bridgewater D, Ingram A, Krepinsky J, Austin RC et al. TDAG51 is a key modulator of vascular calcification and osteogenic differentiation of arterial smooth muscle cells. *Accepted into Atherosclerosis, Thrombosis, and Vascular Biology*

1. Introduction

1.1 Elucidating the crosstalk between CKD and CVD

Chronic kidney disease (CKD) is considered one of the leading worldwide health concerns that is increasing at an alarming rate, thereby negatively impacting the global healthcare burden for long-term and chronic care costs (1). In 2017, the prevalence of CKD at various stages reached approximately 47 million people in North America, comprising 15-20% of the population (2). Hence, focusing on therapeutic approaches in alleviating the prevalence and economic burden caused by CKD is of critical importance.

The diagnosis of CKD is defined as a persistent abnormality in renal structural integrity and function (i.e. glomerular filtration rate (GFR) <60mL/min/m^2 or albuminuria >30 mg per day) and is commonly attributed to risk factors including family history, hypertension, diabetes, and obesity (3). The progression of CKD consists of multiple stages, ranging from stage 1 normal function (>60% renal function; GFR >90mL/min/m^2) to stage 5 renal failure (<15% renal function; GFR <15mL/min/m^2) (Figure 1). As the disease progresses, CKD patients develop severe renal interstitial fibrosis, proteinuria, glomerulonephritis, tubular atrophy, nephron loss, and compromised creatinine clearance (4). Despite the wide range in etiology, cardiovascular disease (CVD) risk is arguably considered a significant risk factor for CKD progression (5, 6, 7).

1.1.1 The CVD influence

CVD remains as the primary driver of morbidity and mortality in North America, accounting for more than 40% of annual deaths. In addition to total mortality, the inadequate management of CVD often leads to long-term disabilities from complications of heart attacks,

strokes, heart failure, and end-stage renal disease (ESRD) (9, 10, 11). A prominent risk factor of CVD is obesity, which is considered a major generator of metabolic syndrome (12). In the context of CKD, early stages of obesity-induced metabolic syndrome promote glomerular hyperfiltration, glomerular basement membrane thickening, mesangial cell proliferation, and expansion of Bowman's capsule (13, 14). Although not fully understood, several mechanisms have been proposed to contribute to the pathogenesis of renal injury, one of which include abnormal lipid metabolism (15). The first line of evidence originates from Kimmelstiel and Wilson et al. in 1936 (17), demonstrating the presence of lipid deposits in the kidneys of diabetic patients, suggesting a role in the progression of renal disease. Since then, several other studies have shown a significant correlation between serum lipid, renal lipid deposition, and proteinuria with a progressive decline in renal function (15, 16). In the early 1990s, large-scale studies focusing on the link between dyslipidemia and CKD reported that the hazard ratio of proteinuria was significantly elevated in CKD patients with high circulating cholesterol (18); regardless of gender, these patients presented with low high-density lipoprotein (HDL) and significantly elevated levels of triglyceride. In support of these findings, a recent meta-analysis (19) reported that 90% of patients diagnosed with CKD exhibited significantly higher levels of circulating cholesterol (> 240 mg/dL), and that more than 80% of those who were not treated with hemodialysis had elevated LDLc levels above 130 mg/dL. Thus, in the literature, there is a substantial amount of epidemiological evidence to reason a causative influence that CVD has over CKD progression and severity.

				Albuminuria categories		
				A1	**A2**	**A3**
				Normal to mildly increased	Moderately increased	Severely increased
				<30 mg/g <3 mg/mmol	30-299 mg/g 3-29 mg/mmol	≥300 mg/g ≥30 mg/mmol
GFR Stages	**G1**	Normal or high	≥90			
	G2	Mildly decreased	60-90			
	G3a	Mildly to moderately decreased	45-59			
	G3b	Moderately to severely decreased	30-44			
	G4	Severely decreased	15-29			
	G5	Kidney failure	<15			

Figure 1. Relative risk for progression, morbidity, and mortality of chronic kidney disease at various stages predicted by GFR and albuminuria (86).

1.2 ER Stress: Implications in CKD

1.2.1 ER structure and function

The endoplasmic reticulum (ER) is an essential organelle ubiquitously exhibited in mammalian cells and plays an important role in Ca^{2+} homeostasis, lipid synthesis, detoxification of chemicals and *de novo* protein synthesis and subsequent maturation (20). An important component of ER function is the quality control of protein folding, as misfolded proteins are recognized before their transition to the Golgi apparatus where it undergoes lysosomal and proteasomal degradation. Molecular chaperones, which reside in the ER lumen, are charged with these diverse tasks and rely on a tightly regulated oxidizing environment provided to them by the ER (21). Disturbances in this optimal environment for proper protein folding reduce the chaperone activity and eventually mitigate the net efficiency of proper polypeptide folding. With an increased aggregation in misfolded polypeptides, this in turn promotes ER stress, an established driver of a variety of human diseases including kidney, cardiovascular, neurodegenerative, and several metabolic diseases (21, 22).

1.2.2 ER stress and UPR activation

Given that the ER is chiefly responsible for the synthesis and proper folding of all secretory, transmembrane, and ER luminal proteins, the accumulation of misfolded proteins are detected via a highly conserved signaling cascade (23) known as the unfolded protein response (UPR). The activation of the UPR is dependent on the dissociation of ER-resident chaperones such as the glucose-regulated protein of 78kDa (GRP78) from three transmembrane sensors in the ER lumen, which all work in concert at an attempt in mitigating ER stress.

The first of the three transmembrane 'arm of the UPR' is the highly conserved inositol-requiring enzyme-1 (IRE1). The activation of the UPR promotes the auto-phosphorylation and dimerization of IRE1 (26), which then enables IRE1 to act as an endoribonuclease and splices the X-box-binding protein-1 (XBP1) (27). The activated spliced form of XBP1 (sXBP1) then translocate to the nucleus and enhances the expression of genes involved in endoplasmic reticulum associated degradation (ERAD) and represses global translation of proteins (28). The phosphorylation of the protein kinase RNA-like ER kinase (PERK) represents the second arm of the UPR. Upon UPR activation, this promotes the phosphorylation of the eukaryotic initiation factor 2α (peIF2α) (29). pEIF2α then acts to reduce the influx of *de novo* polypeptides entering the ER at an attempt to attenuate global protein synthesis (29, 30). As expected, the final arm of the UPR is the activating transcription factor 6 (ATF6). UPR activation causes the transition of ATF6 from the ER membrane to the Golgi apparatus for processing and activation by site-1 (S1) and site-2 (S2) proteases (24), both of which are also well known to process the activation of the sterol regulatory element binding proteins (SREBP), key players in several lipogenic pathways (25). The active fragment of ATF6 then translocate to the nucleus and promotes the transcription of chaperones, as well as the ERAD process. Overall, the chronic activation of these transmembrane proteins and their downstream signaling pathways result in cellular apoptosis, inflammation, and fibrosis in the context of CKD progression (31, 32).

1.2.3 Chronic ER stress in renal injury

Much of the debate on CKD progression through pro-fibrotic and inflammatory activation focuses on whether this phenotype is a maladaptive progressive mechanism or an adaptive response to injury. Likewise, UPR activation in the context of ER stress represents a

compensatory response to increase the proper folding efficiency of the ER, which then is represented as a pathological state in chronic conditions (31). Aside, it is known that the structural integrity of the kidney is compromised as a result of a dynamic combination in the activation of cellular apoptosis, inflammation, and fibrosis (33). As such, several recent studies have suggested a therapeutic approach at combatting this dynamic combination through the inhibition of prolonged ER stress and UPR activation.

Chemical agents, such as 4-phenylbutyrate (4-PBA) have been suggested as an inhibitor of ER stress and UPR activation. 4-PBA was primarily approved by the Food and Drug Administration for the clinical use in urea cycle disorders. It acts as an ammonia scavenger (34), a weak histone deacetylase (HDAC) inhibitor (35), and an ER stress inhibitor (36, 37). As an ER stress inhibitor, it acts as a low molecular weight chemical chaperone by preventing protein mislocalization and aggregation. Similar to chaperones like GRP78, 4-PBA uses its hydrophobic regions to interact with the exposed hydrophobic regions of misfolded polypeptides (38). In the context of CKD, 4-PBA has been reported to attenuate blood pressure, albuminuria, and tubular casts in mouse models through the inhibition of ER stress (39). Others have also demonstrated that 4-PBA was able to attenuate ER stress-induced renal tubular cell apoptosis and renal fibrosis in vivo (88). Thus, the inhibition of ER stress through chemical chaperones like 4-PBA may represent a promising therapeutic approach in targeting CKD progression.

1.3 CD36: A driver of renal injury and CKD progression

The fatty acid translocase, CD36, is a transmembrane scavenger receptor that plays an important role in the progression of several metabolic diseases including atherosclerosis, non-alcoholic fatty liver disease (NAFLD) (40), diabetes mellitus (41), and metastatic cancer (42). In

the kidney, CD36 has been reported to play a pivotal role in promoting intra-renal lipid accumulation, cellular apoptosis, and both inflammatory and pro-fibrotic signalling pathways (43, 44, 45) (Figure 2). Mechanistically, CD36 acts as a multifunctional receptor that mediates the cellular uptake of long-chain fatty acids and oxidized lipoproteins and is abundantly expressed in the proximal and distal tubular epithelium, as well as on podocytes, mesangial cells, and interstitial macrophages (46, 47, 48). Previous studies demonstrated that disruption of CD36-dependent pathways can modulate the development of kidney fibrosis. In mice, transgenic overexpression of tubular CD36 led to an increase in intra-renal lipid accumulation and resulted in the up-regulation of pro-fibrotic genes and markers of UPR activation (44). In podocytes, CD36-dependent uptake of palmitic acid led to a dose-dependent increase in ER stress, mitochondrial reactive oxygen species (ROS) production, ATP depletion, and apoptosis (47). Furthermore, CD36-deficient mice on HFD developed significantly less renal fibrosis compared with wild-type mice at days 3, 7, and 14 after unilateral ureteral obstruction surgery (89). As such, accumulating evidence strongly suggest that CD36 stands as a key driver of renal damage and its potential use as a therapeutic target for the management of renal disease has yet to be fully elucidated.

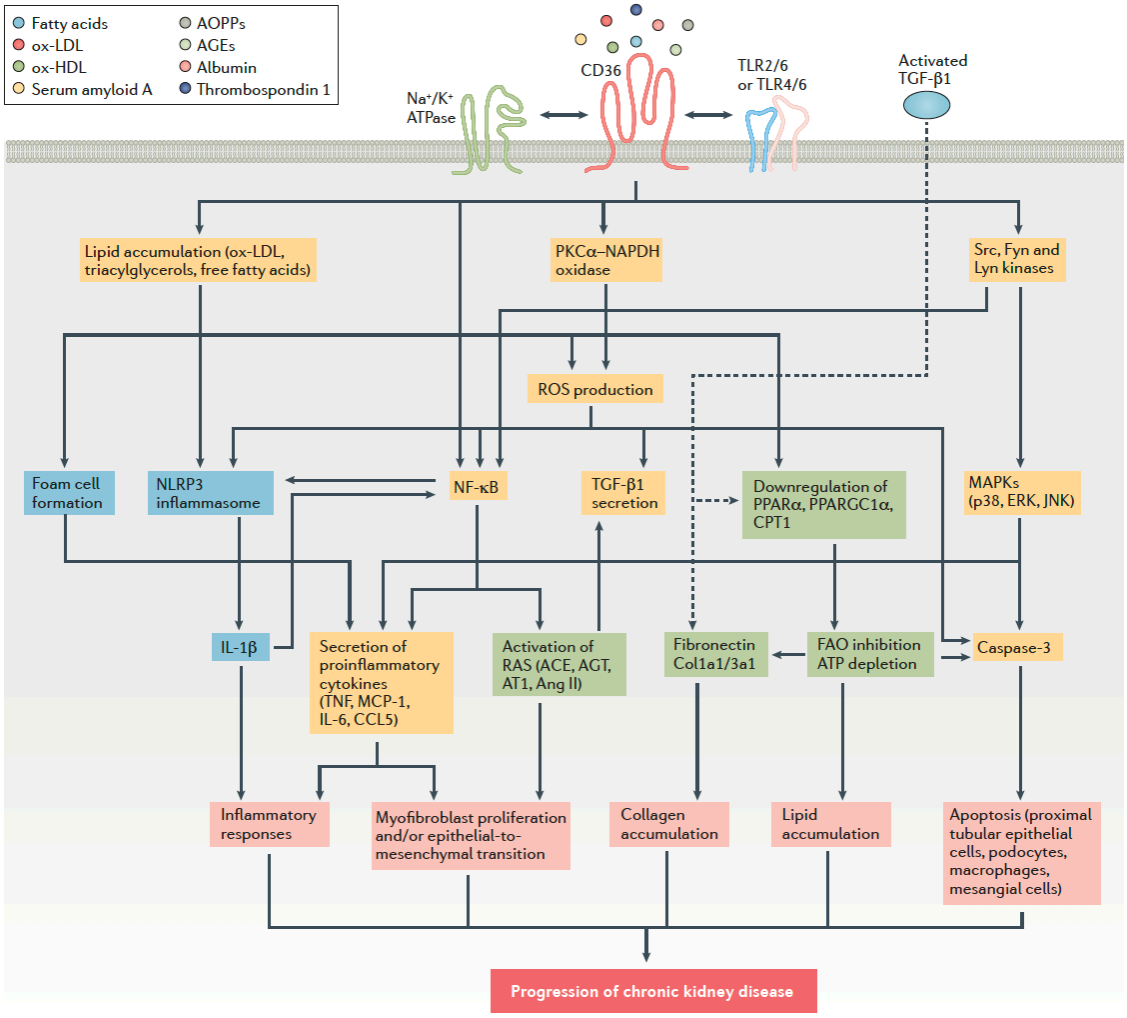

Figure 2. CD36 as an established driver of renal injury and disease through the activation of pro-inflammatory, fibrotic, and apoptotic pathways (85).

1.4 PCSK9: From bench to bedside

1.4.1 Structure, function, and expression

The proprotein convertase subtilisin/kexin type 9 (PCSK9) is a 692 amino acid zymogen that is primarily expressed in the liver, kidney cortex, small intestine, and the cerebellum. Upon translation, nascent PCSK9 undergoes autocatalytic cleavage at position VFAQ152↓, a necessary step for its maturation and secretion from the ER (49). Following zymogen cleavage, PCSK9 traffics through the Golgi apparatus and is secreted into the blood. Since its seminal discovery by Seidah et al. in 2003, secreted PCSK9 has been shown to bind to surface LDLR (50) through the epidermal growth factor (EGF)-a domain at Kd ranging between 90-840 nmol/L. Upon binding, the PCSK9-LDLR complex undergoes endocytosis where it gets degraded in the lysosome. From a biological standpoint, the binding half-life of PCSK9 to the LDLR for degradation is 5-10 minutes, which is subsequently followed with an internalization half-life of 2-3 hours. Interestingly, although PCSK9 has been shown to be expressed in multiple tissues (Figure 3), the vast majority of circulating PCSK9 which interacts with surface LDLR is secreted by hepatocytes (51).

The SREBP family, which are well-known to regulate *de novo* lipogenesis and triglyceride production, plays a major role in the synthesis of PCSK9 (52). SREBP-2 specifically, which upon activation promotes cholesterol synthesis and uptake, also transcriptionally regulates the LDLR. With this paradoxical relationship, the dual transcriptional regulation of PCSK9 and the LDLR suggests that secreted PCSK9 may act as a negative feedback regulator of surface LDLR in excess amounts. Overall, this entire process is initiated upon detection of low intracellular lipid levels by the sterol-sensing domain of the insulin-induced gene-1 (INSIG-1), which primarily anchors the inactive SREBP-2 in the ER lumen.

Upon release, SREBP-2 localizes to the Golgi apparatus with the SREBP cleavage-activating protein (SCAP), a necessary binding partner of SREBP-2 for its proteolytic cleavage and activation by S1-protease and S2-protease. Upon activation, SREBP-2 translocate to the nucleus and enhances the expression of cholesterol regulatory genes to increase intracellular cholesterol levels as a homeostatic response (53). Given the recent discovery of SREBP-2 to regulate PCSK9 expression, it suggests that there may exist a hinderance in the efficacy of LDLc-lowering therapies. Statins for example, which act to suppress *de novo* lipogenesis through inhibiting HMG-CoA reductase (HMGCR) activity, in turn been shown to activate the SREBP family and thus, increase the expression and secretion of PCSK9 (52).

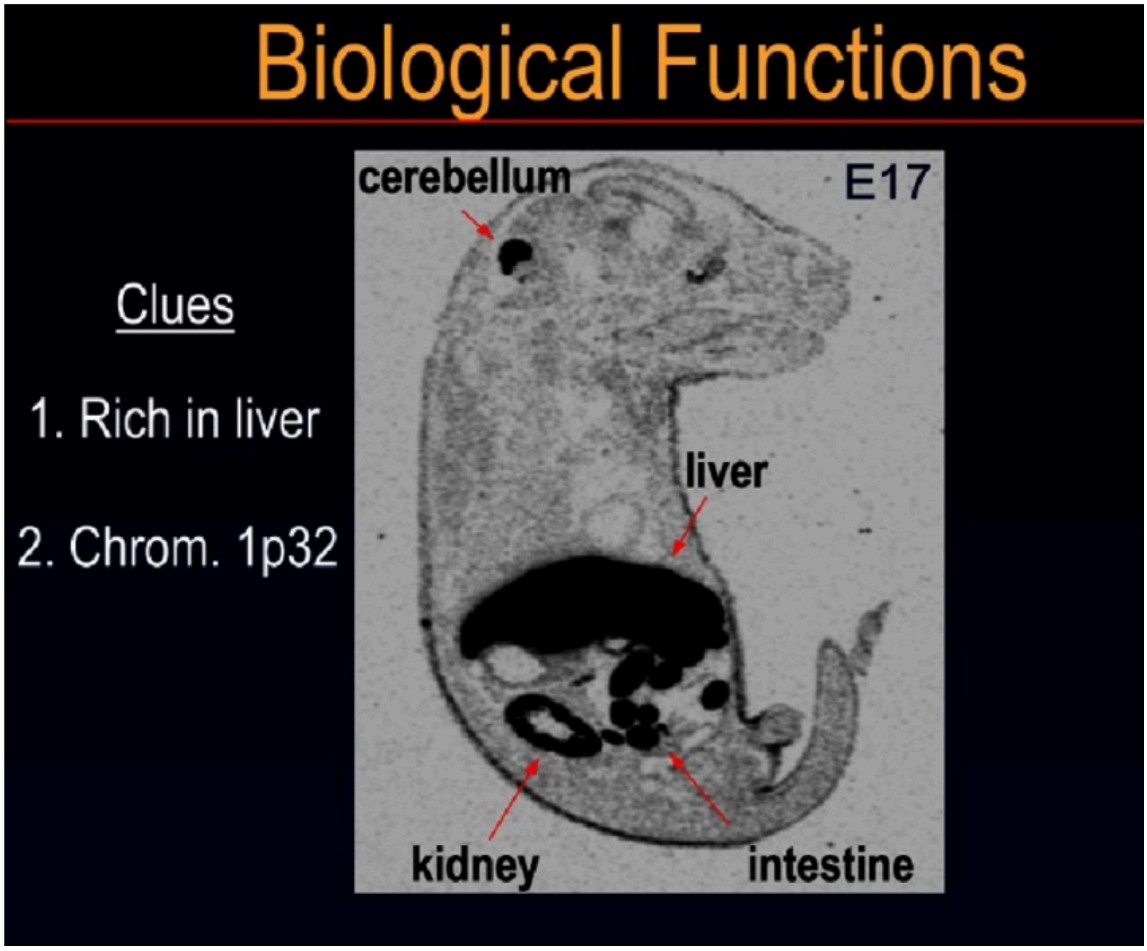

Figure 3. Murine in-situ hybridization of PCSK9 suggests abundant expression in liver, kidney cortex, small intestine, and cerebellum (87). (Approved and credited to creative commons at *creativecommons.org.* No changes were made in this figure.)

The cloning and localization of the *PCSK9* gene on the short arm of chromosome 1p32 (49) represents the third familial hypercholesterolemia (FH) locus, with the first two represented by the *LDLR* and its ligand apolipoprotein B (*apoB*). Following its cloning, gain-of-function (GOF) mutations of the *PCSK9* gene at positions F216L and S127R were first identified as the cause of the hypercholesterolemic phenotype observed in two French families, exhibiting approximately 2-fold and 4-fold increase in circulating LDLc respectively (54). In contrast, loss-of-function (LOF) mutations in PCSK9 lowers circulating LDLc levels, as demonstrated by the R46L mutation for example, which resulted in a 47% reduction in the risk of CVD. Overall, the identification of circulating PCSK9 and its ability to modulate surface LDLR levels represents a major phenotype in regulating circulating LDLc levels.

1.4.2 Current and future clinical therapies

As PCSK9 positively correlates with LDLc levels through its interaction with the LDLR, fully human monoclonal antibodies (mAbs) that target against PCSK9, Alirocumab and Evolocumab were recently FDA-approved in 2016 (56). These anti-PCSK9 mAbs consist of fully human IgG subtypes that inherently bind with an approximate 1:1 stoichiometry to circulating PCSK9 and block its binding to the LDLR through the EGF-a domain. The efficacy of this biologic was examined within the 'Further Cardiovascular Outcomes Research with PCSK9 Inhibition in Subjects with Elevated Risk' (FOURIER) trial which demonstrated a 60% reduction (from a median of 92 mg/dL to 30 mg/dL) in LDLc levels using Evolocumab in patients at risk of CVD (55). On an average 2 year follow-up, a reduction in primary cardiovascular outcomes (i.e. cardiovascular death, myocardial infarction (MI), stroke, hospitalization for angina) with Evolocumab administration suggested a 15% relative risk

reduction with the use of PCSK9 mAbs. Thus, the inhibition of PCSK9 through mAb therapy represents a novel approach to reduce circulating LDLc levels and combat against CVD.

However, given the high cost and lack of affordability of PCSK9 mAbs, this perpetuated the need of finding alternative therapeutic approaches at targeting PCSK9 inhibition. Very recently, the development of inclisiran, a small interfering RNA (siRNA) targeted against PCSK9 has recently been approved for PHASE III clinical trials (57). In the randomized, double-blind, phase II ORION-1 trial, a two-dose regimen of inclisiran exhibited approximately a 70% reduction in circulating PCSK9 and a corresponding 53% reduction in LDLc levels. Thus, the use of inclisiran also represents a promising approach, given that ironically, the inhibition of PCSK9 using PCSK9 mAbs have recently been reported to increase circulating PCSK9 levels 7-10 fold in patients with CVD (58). The extent to determine the mechanism for this observation, as well as the activity and retained functionality of *de novo* circulating PCSK9, have yet to be elucidated.

Other preliminary approaches that have yet to reach the clinical setting include blocking the interaction of PCSK9 to the LDLR using EGF-a mimetics, and to inhibit proPCSK9 autocatalytic cleavage in the ER lumen (59). Specifically, the latter represents the ER retention approach for PCSK9, which we have previously reported to not cause UPR activation and in turn, protect against ER stress-induced liver injury (Lebeau et al., submitted). However, two permanent PCSK9 inhibition strategies have been proposed, which include PCSK9 vaccination and CRISPR-Cas9 gene silencing of PCSK9 (60, 61). Although novel, these approaches on the permanent silencing of PCSK9 expression raises concern on its long-term effects.

1.4.3 PCSK9: Beyond the PCSK9-LDLR interaction

Since the seminal discovery of PCSK9 by Seidah and colleagues, others have demonstrated that PCSK9 can promote the degradation of other surface receptors. These include the structural homologues of the LDLR; both the very low-density lipoprotein receptor (VLDLR) (62) and apolipoprotein (apoE) receptor-2 (ApoER2) (63), the CD81 receptor for hepatitis C virus (64), the epithelial sodium channel (ENaC) for blood pressure regulation (65), and beta secretase for Alzheimer's disease progression (66). Most notably however, is the ability of PCSK9 to degrade CD36. Using a variety of methods, including subcellular tracking, co-immunoprecipitation, and surface plasmon resonance, Demers et al. demonstrate that PCSK9 binds to the extracellular loop of CD36 to mediate its internalization and subsequent degradation (63). The authors then demonstrate that both GOF and LOF models of PCSK9 were able to alter surface expression of CD36 and was the first to implicate the potential role of PCSK9 in triglyceride metabolism. In our laboratory, we confirmed this phenotype as PCSK9 was able to protect against CD36-mediated liver injury *in vivo* using a mouse model of HFD (67).

On the other hand, our laboratory also demonstrate the effect of PCSK9 intracellular retention by overexpressing the $PCSK9^{Q152H}$ variant (69), which fails to undergo autocatalytic cleavage and secretion from the ER (68). Although we first observed that overexpressing such a protein did not induce UPR activation, we observed that overexpression of PCSK9 protected against ER stress-inducing agents such as thapsigargin (TG) and tunicamycin (TM) (Lebeau et al. unpublished). To elucidate a mechanism for this effect, we demonstrated that PCSK9 increases the stability and abundance of ER-resident chaperones, most notably, GRP78 and GRP94, to protect against ER stress. In support of these findings, the robust ER stress observed in mice overexpressed with the LDLR retention variant, $LDLR^{G544V}$, was attenuated with co-

overexpression of the PCSK9^{Q152H}. Thus, while inherently reducing circulating PCSK9 through its retention in the ER, the intracellular role of PCSK9 may also act as a potential therapeutic target to combat against CVD.

2. Research Objectives and Hypotheses

The first aim of my MSc research project was to characterize the role of PCSK9 in hepatic lipid metabolism within the context of NAFLD. Recent studies demonstrated that liver steatosis grade in patients were positively correlated with circulating PCSK9 levels (78). However, no mechanism underlying this observation has been proposed and thus, remained unclear. Given that PCSK9 is almost exclusively secreted by the liver, and that we have previously demonstrated that ER stress induces *de novo* PCSK9 expression, I hypothesized that diet-induced hepatic ER stress promoted *de novo* PCSK9 expression. Furthermore, I also hypothesized that these changes could be a mechanism to the dyslipidemia that is exhibited in patients with NAFLD.

Since its seminal discovery in 2003, PCSK9 has been shown to promote the degradation of several other well-known receptors that promote extracellular lipid uptake into tissue, such as the VLDLR, apoER2, and CD36. Previously, we have demonstrated that circulating PCSK9 can protect against CD36-driven NAFLD to protect against CVD risk. Given the abundant expression of CD36 in the proximal and distal tubules of the kidney cortex (43, 44, 45), I hypothesized that the absence of circulating PCSK9 would promote excess renal lipid accumulation to induce the onset/progression of diet-induced kidney injury.

Lastly, given that PCSK9 is well-expressed in the kidney cortex, we sought to investigate the role of renal PCSK9 in the context of renal disease. Recent papers have demonstrated that circulating PCSK9 may play a role in the dyslipidemia that is exhibited in patients with nephrotic syndrome. However, no papers to date have investigated the endogenous role of PCSK9 in kidney function and thus, remains to be elucidated. Previously, we have demonstrated that intracellular retention of PCSK9 is able to protect against ER stress-induced liver disease. As

such, I hypothesized that renal PCSK9 could also protect against ER stress-induced kidney disease in a mouse model of CKD by upregulating ER chaperones independent of UPR activation.

2.1.1 Part 1: Diet-induced hepatic steatosis abrogates cell-surface LDLR by inducing de novo PCSK9 expression in mice.

Published: Lebeau & Byun et al. 2019. Diet-induced hepatic steatosis abrogates cell-surface LDLR by inducing de novo PCSK9 expression in mice. *J. Biol. Chem.* 294, 9037-9047

Research summary: The worldwide prevalence of NAFLD is increasing rapidly. Although this condition is generally benign, accumulating evidence now suggests that patients with NAFLD are also at increased risk of CVD; the leading cause of death in developed nations. Despite the well-established role of the liver as a central regulator of circulating LDLc levels, a known driver of CVD, the mechanism(s) by which hepatic steatosis contributes to CVD remains elusive. Interestingly, a recent study has shown that circulating PCSK9 levels correlate positively with liver steatosis grade. Given that PCSK9 degrades the LDLR and prevents the removal of LDL from the blood into the liver, in the present study we examined the effect of hepatic steatosis on LDLR expression and circulating LDL cholesterol levels. We now report that in a manner consistent with findings in human patients, diet-induced steatosis increases circulating PCSK9 levels as a result of *de novo* expression in mice. We also report the novel finding that steatosis abrogates hepatic LDLR expression and increases circulating LDL levels in a PCSK9-dependent manner. These findings provide important mechanistic insights as to how hepatic steatosis

modulates lipid regulatory genes like PCSK9 and the LDLR, and also highlights a novel mechanism by which liver disease may contribute to CVD.

2.1.2 Part 2: PCSK9 blocks renal surface CD36 expression to prevent tubular lipid accumulation and renal injury

Submitted: Byun et al. 2019. PCSK9 blocks renal surface CD36 expression to prevent tubular lipid accumulation and renal injury. *J. Am. Soc. Nephrol.*, December 11, 2019

Research summary: The discovery of the PCSK9 has led to the development of a new line of therapeutics capable of significantly lowering circulating cholesterol levels. Since this discovery, PCSK9 has been reported to modulate the uptake of circulating lipids through a range of receptors including the LDLR and CD36, all of which are ubiquitously expressed on hepatocytes and renal epithelia. In the kidney, CD36 is reported to promote renal injury through pro-inflammatory and fibrotic pathways. In this study, we sought to investigate the role of PCSK9 in modulating renal lipid accumulation and injury through CD36 in a diet-induced mouse model. The effect of PCSK9 on lipid uptake and accumulation was first examined in cultured renal cells. Lipid accumulation was then assessed in *Pcsk9*$^{-/-}$ mice for diet-induced renal injury. As a result of PCSK9 deficiency, we observed that heightened CD36 levels increased the uptake of free fatty acids (FFA) in renal cells. Our results indicate that the uptake of long-chain saturated FFAs promote ER stress, which was further exacerbated in the absence of exogenous PCSK9 *in vitro*. Consistent with these observations, *Pcsk9*$^{-/-}$ mice fed a HFD displayed elevated ER stress, inflammation, fibrosis, and renal injury relative to controls. Overall, we report that circulating PCSK9 modulates renal lipid

uptake in a manner dependent on renal CD36. In the context of increased dietary fat consumption, the absence of circulating PCSK9 may promote renal lipid accumulation and subsequent renal injury.

2.1.3 Part 3: Renal PCSK9 protects against AngII/DOCA induced progression of renal injury in mice

In preparation: Byun et al. 2020. Renal PCSK9 protects against AngII/DOCA induced progression of renal injury in mice. *J. Sci. Reports*

Research summary: CKD is a global health concern due to its increasing worldwide prevalence and its cause remains to be elucidated. However, several lines of evidence implicate the association between ER stress and CKD progression demonstrated in clinical patients and multiple animal models. Recently, we have identified the role of intracellular PCSK9 as a co-chaperone in the ER lumen by upregulating ER-resident chaperones independent of UPR activation in order to alleviate ER stress. Given that PCSK9 is highly expressed in hepatocytes and also in the renal cortex, we sought to investigate whether renal PCSK9 can protect against ER-stress induced renal injury using an established model of CKD. To investigate the role of renal PCSK9, cultured renal cells and *Pcsk9*$^{-/-}$ mice were overexpressed with human PCSK9 and assessed for UPR activation either in the presence or absence of ER-stress inducing agents, thapsigargin or tunicamycin. *Pcsk9*$^{-/-}$ mice were then assessed for ER-stress induced renal injury using an AngII/DOCA CKD model. We observed that overexpression of PCSK9 in cultured renal cells can protect against basal UPR activation or with an agent that is well-known to induce

ER stress. Consistent with these observations, we also observed that *Pcsk9*$^{-/-}$ mice exhibit increased renal fibrosis, inflammation, and apoptosis with the AngII/DOCA therapy relative to WT controls. Overall, we demonstrate here that the depletion of intracellular PCSK9 in the kidney exacerbates renal ER stress and subsequent injury. In multiple mouse models, the expression of renal PCSK9 is able to modulate ER stress through the attenuation of UPR activation.

3. Materials and Methods

Cell Culture, Transfections and FFA treatments:

Human immortalized proximal tubule epithelial (HK-2), hepatocytes (Huh-7 and HepG2), embryonic kidney (HEK293), and primary rat mesangial cell lines were used. All cells were cultured in Dulbecco's Modified Eagle Medium (Gibco, ThermoFisher Scientific) supplemented with 10% fetal bovine serum (FBS) (Sigma-Aldrich), and 50 IU/ml of penicillin and 100µg/ml streptomycin (Sigma-Aldrich). All cells were maintained in 5% CO_2 at 37°C. Cells were plated at a confluence of 60% for transfection experiments. Transfection cocktail consisted of the following ratio: 1µg DNA:3 µl X-tremeGENE HP DNA reagent:100 µl Opti-MEM. The cDNA of human WT PCSK9 and the $PCSK9^{Q152H}$ retention variant was cloned into pIRES-EGFP with a V5-tag inserted between the N-terminal signal peptide. Moreover, as a relative measure of ER stress and UPR activation in cells, HK-2 cells were transfected with an ER stress-activated indicator (ERAI) plasmid (79). Briefly, under conditions of ER stress, the ER stress-specific intron is spliced and removed from the ERAI mRNA transcript leading to a frameshift and subsequent production of functional FLAG-spliced XBP1 protein. Cells were treated with LDL (Lee Biosolutions), oxidized low-density lipoprotein (ox-LDL) (Alfa Aesar), oleate (Alfa Aesar), and palmitate (Sigma-Aldrich) that were conjugated to FA-free bovine serum albumin (BSA). All treatments were carried out overnight for 24 h unless specified otherwise.

HFD Model Animal Studies

6-week old male *Pcsk9*$^{-/-}$ mice on a C57BL/6J background and age-matched controls were placed on either a normal control diet (NCD) (n=10) or HFD (60% fat/Kcal; ENVIGO #TD06414;

n=10) for 12 weeks with *ad libitum* access to food and water. All animal procedures were approved by the McMaster University Animal Research Ethics Board.

Tunicamycin Model Animal Studies

Both 12-week and 50-week old mice on a C57BL/6J background and age-matched controls were given intraperitoneal injection of either phosphate-buffered saline (PBS) or TM (0.5mg/kg) and sacrificed 3 days later. All animal procedures were approved in accordance with McMaster University animal care guidelines.

PCSK9 Transgenic Model Animal Studies

Briefly, a composite human albumin promoter containing a 235 bp SV40 enhancer element and a 213 bp albumin promoter element (pDRIVE-SV40-hAlb, InvivoGen, San Diego, CA) was used to control the expression of full-length human PCSK9 cDNA containing a C-terminal V5 tag. To enhance this expression, a chimeric intron (pRL-SV40, Promega, Madison, Wisconsin) was inserted between the PCSK9 cDNA and the promoter. The V5-tagged hPCSK9 construct was injected into the pronucleus of fertilized eggs from the C57BL6J/N strain mice. Confirmation of transgenic founders and their offspring was identified by a PCR product amplified from insulator sequences. These transgenic animals were a generous gift by Dr. Nabil Seidah, IRCM, Montreal.

CKD Model Animal Studies

10-week old mice on a C57BL/6J background and age-matched controls underwent uninephrectomy (Unx) 2 weeks before the initiation of the experiment. Mice were then given 1% sodium chloride in the drinking water and implanted subcutaneously with a DOCA pellet

(Innovative Research of America, M-121) and an angiotensin II (AngII)-infused (Sigma) model 1004 ALZET osmotic pump. The DOCA was a 50 mg 21-day releasing pellet while 1.5ng of AngII was delivered per minute per gram of bodyweight by the osmotic pump. All mice were sacrificed on day 14 after the initial implantation. All animal procedures were approved by the McMaster University Animal Research Ethics Board and were in collaboration with Drs. Jeffrey Dickhout and Rachel Carlisle at the Hamilton Centre for Kidney Research.

Blood Pressure Measurements

Blood pressures of mice were obtained through tail cuff plethysmography using a CODA (Kent Scientific) blood pressure analyzer. Mice were positioned on a heating pad and were placed in restraint to be provided with the tail cuff apparatus. The cuff measured absolute systolic blood pressure, diastolic blood pressure, heart rate, and flow rate.

Immunoblotting

Cells and tissues were lysed in SDS-containing buffer containing protease and phosphatase inhibitor (Roche), as described previously (69). Protein concentrations were measured using a modified Lowry protein assay (Bio-Rad). Samples were then electrophoretically resolved on 7-10% polyacrylamide gels and subsequently transferred to nitrocellulose membranes. Membranes were blocked using 5% w/v skimmed milk in tris-buffered saline (TBS) containing Tween-20 for 1 h and subsequently incubated in primary antibody overnight for 18 h at 4˚C. To detect bound primary antibodies, horse radish peroxidase (HRP) conjugated antibodies were used (goat anti-rabbit, Bio-Rad; donkey anti-goat, Santa Cruz, goat anti-mouse, Bio-Rad) and developed using a

chemiluminescent reagent (FroggaBio). Quantification of immunoblots was assessed after normalization to β-actin (Sigma-Aldrich).

Real-time Polymerase Chain Reaction (PCR)

Total RNA from tissues and cell culture was isolated using an RNA purification kit according to manufacturer's instructions (ThermoFisher Scientific). A total of 2 μg of RNA was reverse-transcribed to cDNA using SuperScript Vilo IV cDNA synthesis kit (ThermoFisher Scientific). Quantitative real-time PCR (qRT-PCR) assessment of different mRNA species was used in conjunction with FAST SYBR Green (ThermoFisher Scientific). All primer sequences are listed in Table 2.

Oil-Red-O (ORO) staining

Cells were fixed using 4% paraformaldehyde and stained with ORO (Sigma-Aldrich) for 5 min. After washing, cells were counterstained with Gills hematoxylin (no.5, Sigma Aldrich) and mounted on a glass slide. For quantification purposes, ORO stain was extracted from cells using isopropanol for 20 minutes on an orbital shaker at 37ºC. Optical density of ORO-exposed isopropanol extracts was quantified using a spectrophotometer (molecular devices) at a wavelength of 520nm. For ORO staining of *in vivo* models, 10 μm thick sections of mouse OCT-embedded kidneys were washed with propylene glycol and stained with ORO for 10 min. Following staining, tissues were repeatedly washed with propylene glycol and counterstained using alum hematoxylin.

Triglyceride and Creatinine Quantification

Renal cortical tissue was assessed for triglyceride content using a triglyceride assay kit (Abcam) according to manufacturer's instructions. All data was normalized to tissue weight. Plasma creatinine (Sigma-Aldrich) was measured using a colorimetric assay as per manufacturer's instructions.

PCSK9 ELISA

Quantification of PCSK9 in media was determined as per the manufacturer's instructions using the R&D systems human Quantikinine PCSK9 ELISA.

Immunohistochemical (IHC) Staining

4 μm thick sections were deparaffinized, blocked in 5% v/v serum and subsequently incubated with primary antibodies for 18 h at 4˚C. Sections were incubated with biotin-labeled secondary antibodies (Vector Laboratories). Streptavidin-labeled HRP solution (Vector Laboratories) and NovaRed developing solution (Vector Laboratories) were used to visualize the staining. Slides were examined using a Nikon light microscope (Nikon DS-Ri2). Relative staining intensity was quantified using ImageJ software (n=10). For Picro Sirius Red (PSR) staining, kidney sections were exposed to saturated picric acid solution and stained with Sirius red F3B (Color Index 35782).

Statistical Analysis

Statistical analysis for two-group comparisons was conducted using unpaired Student's *t*-test and for multiple group comparison, one-way ANOVA was used. Statistically significant differences were considered at $p<0.05$. All error bars are represented as standard deviation of the mean.

4. Publication in the Journal of Biological Chemistry, 2019

Lebeau, P. F.*, Byun, J. H.*, Platko, K., MacDonald, M. E., Poon, S. V., Faiyaz, M., Seidah, N. G., and Austin, R. C. (2019) Diet-induced hepatic steatosis abrogates cell-surface LDLR by inducing de novo PCSK9 expression in mice. The Journal of biological chemistry **294**, 9037-9047

Author Contributions: P. F. L., J. H. B., K. P., N. G. S., and R. C. A. conceptualization; P. F. L., J. H. B., K. P., S. V. P., M. F., and R. C. A. data curation; P. F. L. software; P. F. L. formal analysis; P. F. L. supervision; P. F. L. validation; P. F. L., J. H. B., K. P., M. E. M., S. V. P., and R. C. A. investigation; P. F. L. visualization; P. F. L., J. H. B., K. P., M. E. M., S. V. P., and N. G. S. methodology; P. F. L. writing original draft; P. F. L., J. H. B., and R. C. A. project administration; P. F. L., J. H. B., K. P., M. F., N. G. S., and R. C. A. writing-review and editing; R. C. A. resources; R. C. A. funding acquisition.

Personal thesis contribution: As the co-primary author of this paper, I have provided most of the *in vitro* and *in vivo* data curation and experimental analysis which contributed towards all the figures of this manuscript. In addition, I provided revision of the primary draft and assisted in the publication process of this paper into the Journal of Biological Chemistry.

JBC ARTICLE

Diet-induced hepatic steatosis abrogates cell-surface LDLR by inducing *de novo* PCSK9 expression in mice

Received for publication, February 19, 2019, and in revised form, April 9, 2019 Published, Papers in Press, April 19, 2019, DOI 10.1074/jbc.RA119.008094

Paul F. Lebeau[‡1], Jae Hyun Byun[‡1], Khrystyna Platko[‡], Melissa E. MacDonald[‡], Samantha V. Poon[‡], Mahi Faiyaz[‡], Nabil G. Seidah[§], and Richard C. Austin[‡2]

From the [‡]Department of Medicine, McMaster University, The Research Institute of St. Joe's Hamilton, Hamilton, Ontario L8N 4A6 and the [§]Laboratory of Biochemical Neuroendocrinology, Montreal Clinical Research Institute, University of Montreal, Montreal, Quebec H2W 1R7, Canada

Edited by George N. DeMartino

The worldwide prevalence of non-alcoholic fatty liver disease (NAFLD) is increasing rapidly. Although this condition is generally benign, accumulating evidence now suggests that patients with NAFLD are also at increased risk of cardiovascular disease (CVD); the leading cause of death in developed nations. Despite the well-established role of the liver as a central regulator of circulating low-density lipoprotein (LDL) cholesterol levels, a known driver of CVD, the mechanism(s) by which hepatic steatosis contributes to CVD remains elusive. Interestingly, a recent study has shown that circulating proprotein convertase subtilisin/kexin type 9 (PCSK9) levels correlate positively with liver steatosis grade. Given that PCSK9 degrades the LDL receptor (LDLR) and prevents the removal of LDL from the blood into the liver, in the present study we examined the effect of hepatic steatosis on LDLR expression and circulating LDL cholesterol levels. We now report that in a manner consistent with findings in patients, diet-induced steatosis increases circulating PCSK9 levels as a result of *de novo* expression in mice. We also report the finding that steatosis abrogates hepatic LDLR expression and increases circulating LDL levels in a PCSK9-dependent manner. These findings provide important mechanistic insights as to how hepatic steatosis modulates lipid regulatory genes, including *PCSK9* and the *LDLR*, and also highlights a novel mechanism by which liver disease may contribute to CVD.

Liver fat accumulation due to reasons other than excessive alcohol consumption, or more often referred to as NAFLD,[3] currently has an estimated occurrence of 30–46% in developed nations (1). Given the current trends in global consumption of unhealthy dietary fats and sugars, it is no surprise that NAFLD is increasing in prevalence as these factors play a central role in its development (2). Although NAFLD is described as liver fat accumulation with no sign of liver injury, this initial stage often progresses to non-alcoholic steatohepatitis (NASH); a state characterized histologically by necroinflammation and hepatocyte damage (3). NAFLD and its complications are estimated to be the primary cause of liver-related mortality and liver transplantation within the next 20 years (4).

Evidence that patients with NAFLD are at higher risk of developing CVD, which is among the leading causes of death worldwide (5), is now accumulating (6–9). Given that both NAFLD and CVD share many comorbidities and frequently develop in patients at the same time, it has been a major challenge to discern the exact mechanism(s) by which one contributes to the other (10). Despite this challenge, several reports have demonstrated that NAFLD increases the expression or prevalence of factors known to contribute to CVD. These factors include circulating proinflammatory mediators, prothrombotic factors, hyperlipidemia, and risk of type-2 diabetes. Recent studies have shown a link between the presence of NAFLD and increased intima-media thickness, impaired arterial vasodilation, plaque development, as well as coronary artery calcium scores (10).

Interestingly, two independent clinical studies have also demonstrated that patients with NAFLD have increased levels of circulating PCSK9 (11, 12). PCSK9 is an established driver of atherosclerotic lesion development and CVD due to its ability to enhance the degradation of cell-surface LDLR, thereby reducing the ability of the liver to clear pro-atherogenic LDL cholesterol from the circulation (13–15). Seminal studies in this field have also shown that gain-of-function mutations in *PCSK9* correlate with increased risk of CVD in humans (16), and in a reciprocal manner, loss-of-function mutations have the opposite outcome (17). Pre-clinical data also demonstrate that

This work was supported by the Heart and Stroke Foundation of Canada Research Grants G-13-0003064 and G-15-0009389 and Canadian Institutes of Health Research Grant 74477 (to R. C. A.), Leducq Foundation Grant 13 CVD 03, CIHR Foundation Grant 148363, and Canada Research Chair Grant 216684 (to N. G. S.), and the Research Institute of St. Joe's Hamilton. The authors declare that they have no conflicts of interest with the contents of this article.

[1] Both authors contributed equally to this work.

[2] A Career Investigator of the Heart and Stroke Foundation of Ontario and holds the Amgen Canada Research Chair in the Division of Nephrology at The Research Institute of St. Joe's Hamilton and McMaster University. To whom correspondence should be addressed: 50 Charlton Ave. East, Rm. T-3313, Hamilton, Ontario L8N 4A6, Canada. Tel.: 905-522-1155 (ext. 35175); Fax: 905-540-6589; E-mail: austinr@taari.ca.

[3] The abbreviations used are: NAFLD, non-alcoholic fatty liver disease; 4PBA, 4-phenylbutyrate; ApoB, apolipoprotein-B; ATF4, activating transcription factor 4; CASP, caspase; CHOP, C/EBP homologous protein; CVD, cardiovascular disease; ER, endoplasmic reticulum; FN1, fibronectin 1; GFP, green fluorescent protein; GRP, glucose-regulated protein; H&E, hematoxylin and eosin; HFD, high-fat diet; HMG-CoA, 3-hydroxy-3-methylglutaryl-CoA; IRE1α, inositol-requiring enzyme 1α; LDL, low-density lipoprotein; LDLR, LDL receptor; Met, metformin; NASH, non-alcoholic steatohepatitis; NCD, normal control diet; ORO, Oil Red O; PA, palmitate; PCSK9, proprotein convertase subtilisin/kexin type 9; PERK, PKR-like endoplasmic reticulum kinase; SREBP, sterol regulatory element-binding protein; TBS, Tris-buffered saline; UPR, unfolded protein response; XBP1, X-box–binding protein.

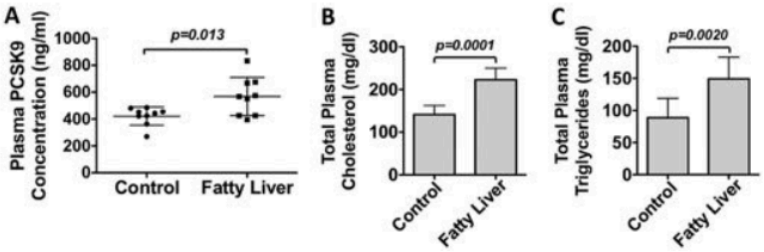

Figure 1. Circulating PCSK9 levels are increased in patients with hepatic steatosis. *A–C*, circulating PCSK9 levels, as well as total cholesterol and triglyceride levels, were assessed in patients with fatty liver ($n = 9$) and compared with healthy volunteers ($n = 9$). All samples were acquired from males over the age of 50.

adenoviral-mediated overexpression of PCSK9 in mice, or hepatocyte-specific transgenic overexpression of PCSK9 leads to a similar phenotype as that of the well-established $Ldlr^{-/-}$ mouse model used for the study of atherosclerosis (18, 19). In line with these data, human monoclonal antibodies targeted against PCSK9 were recently shown to reduce circulating LDL cholesterol levels by up to 60% in patients at high risk of CVD (20).

In the present study, we examined the effect of diet-induced hepatic steatosis on the expression and abundance of established drivers of CVD. Here, we show that the uptake and accumulation of the saturated fatty acid palmitate (PA), as well as high-fat diet (HFD), cause endoplasmic reticulum (ER) stress in cultured hepatocytes, and in the livers of mice, respectively. ER stress is a pathological cellular response that contributes to the development of liver disease and is also known to promote the activation of the sterol regulatory element-binding protein-2 (SREBP2); the major transcription factor responsible for the *de novo* synthesis of cholesterol regulatory proteins including PCSK9 and the LDLR. Accordingly, we also observed increased expression of PCSK9 in PA-treated hepatocytes, as well as in the livers and circulation of HFD-fed mice. Given the consistency of these data with studies done in patients with NAFLD, we next investigated the effect of this outcome on circulating LDL cholesterol and on the expression of its receptor in the liver. We also report the novel finding that HFD-induced hepatic steatosis caused a significant reduction of cell-surface LDLR expression and increased circulating LDL cholesterol levels in mice. Furthermore, because LDLR expression and serum LDL levels were unaffected by the HFD in $Pcsk9^{-/-}$ mice, we also identify that diet-induced hepatic steatosis affected these parameters in a PCSK9-dependent manner. Collectively, our data highlight a novel mechanism by which NAFLD may contribute to CVD by increasing PCSK9 expression to attenuate liver-mediated LDL cholesterol clearance.

Results

HFD increases circulating PCSK9 levels and attenuates hepatic cell-surface LDLR expression in mice

Consistent with previous studies (12), we first confirmed that patients with liver fat accumulation exhibit increased plasma PCSK9 levels (Fig. 1*A*; $p = 0.013$; $n = 9$), as well as circulating cholesterol (Fig. 1*B*; $p = 0.0001$; $n = 9$) and triglyceride levels (Fig. 1*C*; $p = 0.0020$; $n = 9$). Given that (*a*) PCSK9 contributes to CVD by degrading the LDLR and increasing plasma LDL levels (21), and (*b*) accumulating evidence suggests that hepatic steatosis contributes to CVD (10), we next examined the effect of steatosis on hepatic LDLR expression. Accordingly, male C57BL/6J mice were fed HFD or normal control diet (NCD) for a total of 12 weeks. Hepatic steatosis in these mice was confirmed via visualization of lipid droplets using H&E, as well as Oil Red O (ORO) (Fig. 2*A*). Strikingly, immunohistochemical staining revealed that HFD-fed mice had markedly reduced cell-surface LDLR expression compared with NCD-fed controls (Fig. 2*B*). As expected, LDLR antibody staining specificity was confirmed by the absence of staining in the livers of $Ldlr^{-/-}$ mice. In contrast, immunoblotting revealed a modest reduction in LDLR expression in the livers of HFD-fed mice (Fig. 2*C*). These data are representative of whole-cell LDLR abundance, however, and not strictly of the cell-surface LDLR population. Therefore, these data suggest a strong presence of an intracellular LDLR population in liver hepatocytes, which is not affected by the HFD. ORO and LDLR immunohistochemical staining intensities were also quantified using ImageJ software (Fig. 2*D*). Consistent with previous studies, we observed that hepatic LDLR expression was inversely correlated with circulating PCSK9 levels in mice (Fig. 2*D*) (14). The surrogate marker of circulating LDL cholesterol, apolipoprotein-B (ApoB) (22), as well as total cholesterol and triglyceride levels were also examined and found to be increased in HFD-fed mice compared with NCD-fed controls (Fig. 2, *E–G*). These findings demonstrate a diet-induced hepatic steatosis effect on the PCSK9-LDLR axis, which could explain the observed increase in circulating lipid levels.

Diet-induced hepatic steatosis causes hepatic ER stress and promotes de novo PCSK9 expression

Our research group has previously demonstrated that ER stress causes the activation of SREBP2 (23, 24) and expression of PCSK9 in cultured hepatocytes (25). As such, we next examined the livers of HFD-fed mice for markers of ER stress. Consistent with other reports (26, 27), increased expression of ER stress and pro-apoptotic markers, including the glucose-regulated proteins (GRP78 and GRP94), C/EBP homologous protein (CHOP), activating transcription factor 4 (ATF4), PKR-like endoplasmic reticulum kinase (PERK), as well as pro-fibrotic and apoptotic markers fibronectin 1 (FN1), Bcl-2–binding component 3 (BBC3), caspases (CASP1 and CASP3), inositol-

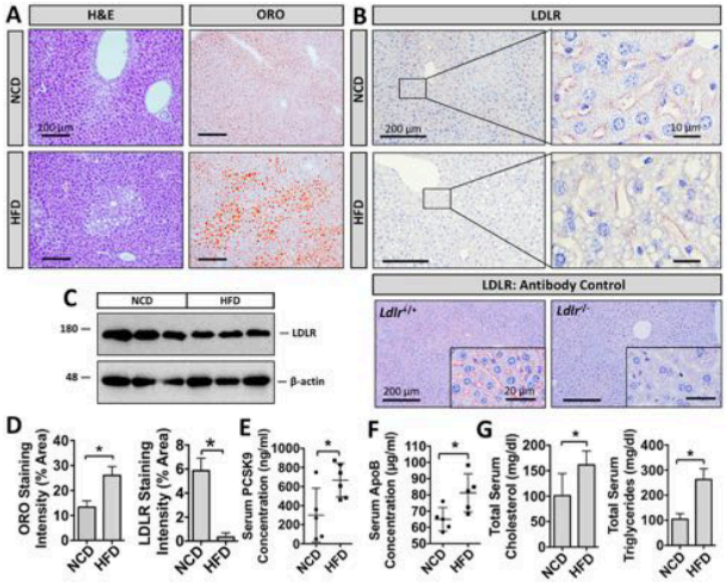

Figure 2. Diet-induced hepatic steatosis increases circulating PCSK9 levels and blocks cell-surface LDLR expression in mice. C57BL/6J mice were fed either a NCD ($n = 10$) or a HFD ($n = 10$) *ad libitum* starting at 6 weeks of age, for an additional 12 weeks. *A*, hepatic lipid droplet accumulation was confirmed using H&E as well as ORO staining. *B*, cell-surface LDLR protein expression was examined via immunohistochemical staining. LDLR antibody staining specificity was confirmed in the livers of $Ldlr^{-/-}$ mice. *C*, total hepatic LDLR expression was also examined via immunoblot analysis. *D*, ORO and LDLR staining intensities were quantified using ImageJ software. *E* and *F*, circulating PCSK9 and ApoB protein levels were examined using ELISAs ($n = 5$). *G*, total cholesterol and triglyceride levels were also examined in the serum of NCD- and HFD-fed mice. *, $p < 0.05$. *Error bars* represent values presented as the mean ± S.D.

requiring enzyme 1α (IRE1α), and spliced X-box–binding protein 1 (sXBP1) was observed in the livers of HFD-fed mice compared with controls via immunohistochemical staining, real-time PCR, and immunoblotting (Fig. 3, *A–C*). Furthermore, similar to our previous studies done in cultured cells (25), we observed that hepatic ER stress was associated with increased mRNA expression of SREBP2, as well as PCSK9 and the LDLR (Fig. 3*C*). Increased intracellular PCSK9 protein abundance was also observed in the livers of HFD-fed mice compared with NCD-fed controls (Fig. 3*D*). Additional modulators of cholesterol and triglyceride homeostasis, including the SREBP2-regulated HMG-CoA reductase, SREBP1, fatty acid synthase, and ApoB were examined via real-time PCR and found to be induced in the livers of HFD-fed mice (Fig. 3*F*). Overall, because circulating PCSK9 originates almost exclusively from liver hepatocytes (20, 28), these findings suggest that diet-induced hepatic ER stress represents a significant contributor in the observed increase in circulating PCSK9 levels in the context of liver fat accumulation.

Pharmacologic inhibition of ER stress, or lipid accumulation, blocks lipid-driven PCSK9 expression and restores LDLR function and expression in hepatocytes

To further examine the effect of lipid-induced ER stress on PCSK9 expression, cultured hepatocytes were treated with the fatty acid, PA. PA represents one of many saturated fatty acids that are highly abundant in animal-derived dietary fats (29) and is also a well-established inducer of ER stress in a variety of cultured cell models (30–32). Similar to the livers of mice exposed to high levels of dietary fats from the HFD, cultured human HepG2 hepatocytes treated with bovine serum albumin (BSA)-conjugated PA yielded increased mRNA expression of SREBP2, PCSK9, and LDLR compared with those treated with the BSA vehicle control (Fig. 4*A*). Because previous studies have shown that metformin (Met) and 4-phenylbutyrate (4PBA) attenuate hepatic lipid accumulation and protect against ER stress (33–35), two additional groups of cells were also pretreated with these agents for 24 h prior to PA treatment. Consistent with other studies, we observed that both agents reduced lipid accumulation (Fig. 4*B*) (36, 37) and attenuated PA-induced expression of the ER stress markers, GRP78, GRP94, and IRE1α. Furthermore, Met and 4PBA also blocked the PA-induced expression of SREBP2, PCSK9, and LDLR. SREBP2 transcriptional activity was then assessed in HuH7 cultured human hepatocytes transfected with a sterol-regulatory element (SRE)-driven GFP reporter construct (Fig. 4*C*). Similar to mRNA transcript levels of SREBP2, PA increased GFP fluorescence intensity, which was in turn blocked by Met and 4PBA. Met and 4PBA also significantly reduced PA-induced secreted PCSK9 levels in the medium harvested from HepG2 and HuH7 cells (Fig. 4*D*). To assess whether these treatments were affecting all secreted proteins, or if PCSK9 was affected with an acceptable level of specificity, medium harvested from these cells was electrophoretically resolved and stained using Coomassie Brilliant Blue protein stain. Given that the relative abundance of secreted proteins was not markedly affected by these treatments, these data suggest that PA, Met, and 4PBA-induced

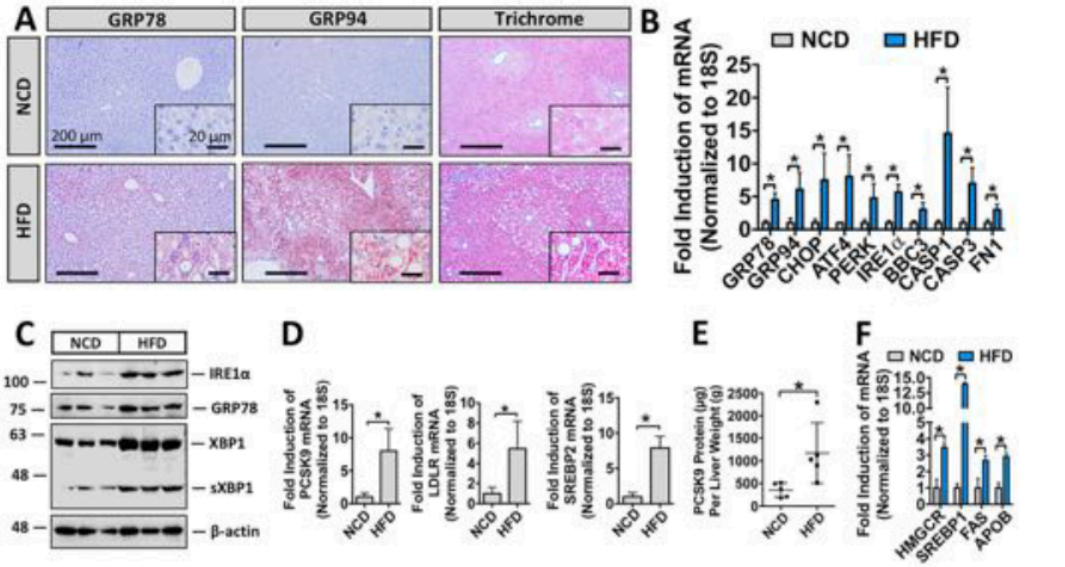

Figure 3. HFD-fed mice exhibit hepatic ER stress and increased expression of SREBP2 and PCSK9. C57BL/6J mice were fed either a *NCD* ($n = 10$) or a HFD ($n = 10$) *ad libitum* starting at 6 weeks of age, for an additional 12 weeks. *A,* immunohistochemical staining of the ER stress markers, GRP78 and GRP94, as well as Masson's trichrome staining for fibrotic collagen deposition (*blue*) in the livers of HFD-fed mice. *B,* real-time PCR analysis of hepatic ER stress marker expression (GRP78, GRP94, CHOP, ATF4, PERK, and IRE1α), apoptosis, and fibrosis markers (CASP1, CASP3, and FN1). *C,* immunoblots used to examine LDLR expression in the livers of HFD-fed mice from Fig. 2*C* were re-probed for ER stress markers GRP78, IRE1α, and XBP1. *D,* real-time PCR analysis of hepatic PCSK9, LDLR, and SREBP2 mRNA transcript levels. *E,* assessment of liver PCSK9 protein levels using an ELISA. *F,* analysis of mRNA transcript abundance of established cholesterol and triglyceride modulators HMG-CoA reductase (*HMGR*), SREBP1, fatty acid synthase (*FAS*), and ApoB via real-time PCR. *, $p < 0.05$. *Error bars* represent values presented as the mean ± S.D.

changes in secreted PCSK9 levels are not the result of changes in global protein secretion.

Next, a quantitative assessment of fluorescently-labeled DiI-LDL uptake was carried out in HepG2 cells treated with vehicle, Met, or 4PBA in the presence or absence of PA (Fig. 4*E*). Consistent with previous studies, elevated secreted PCSK9 levels were associated with a reduction of LDL uptake (38, 39). Met and 4PBA also attenuated the PA-mediated inhibition of DiI-LDL uptake observed in these cells. PCSK9 mRNA expression and secretion in response to PA treatment was also examined in primary human hepatocytes, yielding findings that were consistent with those observed in HepG2 and HuH7 cells (Fig. 4*F*).

Given our observation that 4PBA can attenuate PA-induced ER stress and PCSK9 expression in cultured cells, an additional cohort of mice was fed HFD in the presence or absence of 4PBA in the drinking water. Similar to PA-treated HepG2 cells, we observed that 4PBA attenuated the ability of the HFD to block LDLR expression (Fig. 4*G*). A reduction in the expression of the ER stress markers, GRP78 and GRP94, as well as the fibrosis marker, fibronectin, was also observed in the livers of HFD-fed mice exposed to 4PBA (Fig. 4*H*).

Diet-induced hepatic steatosis attenuates hepatic LDLR expression in a PCSK9-dependent manner

Because LDLR expression is known to be affected by other proteins and conditions (40), our final aim was to identify the extent to which PCSK9 contributed to the observed reduction of cell-surface LDLR expression in HFD-fed mice. Accordingly, *Pcsk9*$^{-/-}$ mice on a C57BL/6J background were also fed a HFD for 12 weeks starting at 6 weeks of age. Similar to wild-type C57BL/6J mice, a significant increase in hepatic lipid content was observed in HFD-fed *Pcsk9*$^{-/-}$ mice compared with those fed the NCD (Fig. 5, *A* and *B*). Strikingly, immunohistochemical staining revealed that the HFD did not significantly reduce LDLR expression in these mice. ORO and LDLR staining intensities were also quantified using ImageJ software (Fig. 5*C*). Consistent with immunohistochemical staining of cell-surface LDLR, immunoblot data also demonstrate that HFD did not markedly reduce LDLR expression in the livers of *Pcsk9*$^{-/-}$ mice (Fig. 5*D*). Furthermore, HFD also failed to increase circulating ApoB-containing LDL cholesterol in *Pcsk9*$^{-/-}$ mice (Fig. 5*E*). PCSK9 knockout in these mice was confirmed using an ELISA for circulating PCSK9 (Fig. 5*F*).

Collectively, these data suggest that intracellular lipid accumulation causes ER stress, which induces *de novo* PCSK9 expression and secretion from hepatocytes (Fig. 6). In turn, heightened circulating PCSK9 levels enhance the degradation of hepatic cell-surface LDLR and increase the levels of circulating LDL cholesterol in the context of diet-induced hepatic steatosis.

Discussion

Hepatocytes, like all secretory cells, are rich in ER and are thus susceptible to injury and damage as a result of conditions that lead to ER stress (41). It is well-established that lipid accumulation in hepatocytes can promote the activation of the

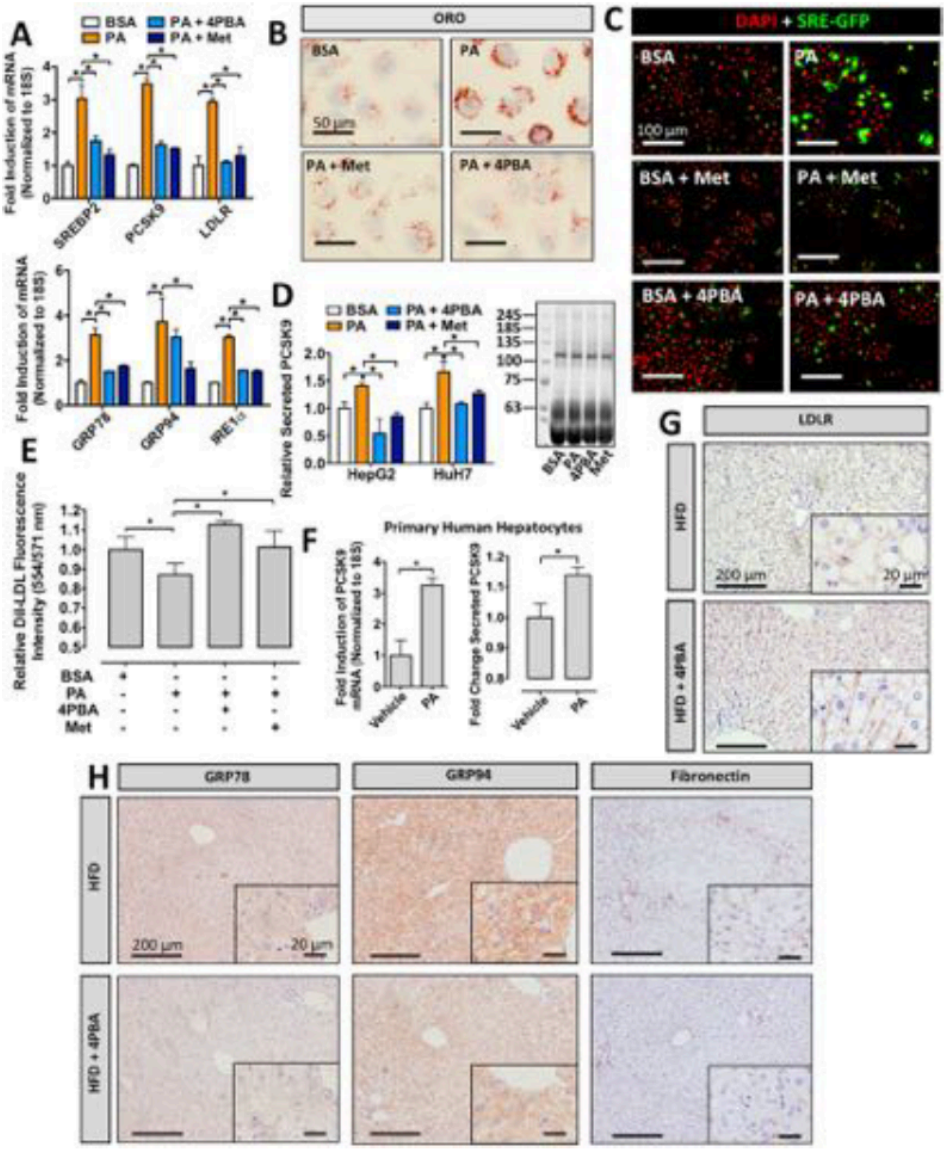

Figure 4. Blocking ER stress and lipid accumulation attenuates PCSK9 expression and restores LDLR expression and function. *A,* HepG2 cells were pre-treated with Met (1 mM) or 4PBA (1 mM) for 24 h and subsequently treated with BSA-conjugated PA (300 μM). SREBP2, PCSK9, and LDLR, as well as the ER stress markers GRP78, GRP94, and IRE1α expression was assessed using real-time PCR. *B,* lipid droplet accumulation in these cells was also assessed via ORO staining. *C,* HepG2 cells were transfected with a SRE reporter plasmid encoding GFP and subsequently pre-treated with Met (1 mM) or 4PBA (1 mM) in the presence or absence of BSA-conjugated PA (300 μM). SREBP2-mediated GFP expression was assessed using a fluorescent microscope. *D,* secreted PCSK9 levels from HepG2 and HuH7 cells grown in FBS-free medium were examined via ELISA. Coomassie staining of electrophoretically resolved medium harvested from these cells demonstrates that treatments did not affect global protein secretion. *E,* fluorescently-labeled DiI-LDL uptake was examined in treated HepG2 cells. *F,* experiments were repeated in cultured primary human hepatocytes (PA, 300 μM, 24 h). *G* and *H,* male C57BL/6J mice were fed a HFD in the presence or absence of 4PBA in the drinking water. Hepatic LDLR expression, as well as GRP78, GRP94, and fibronectin expression was examined via immunohistochemical staining. *, $p < 0.05$. *Error bars* represent values presented as the mean ± S.D.

unfolded protein response (UPR), a highly conserved signaling cascade that attempts to resolve ER stress (42). In a reciprocal manner, studies have also shown that ER stress can lead to intracellular lipid accumulation by inducing *de novo* lipid synthesis in a manner dependent on specific transcription factors, such as SREBP1 (42, 43). Given that both processes appear to

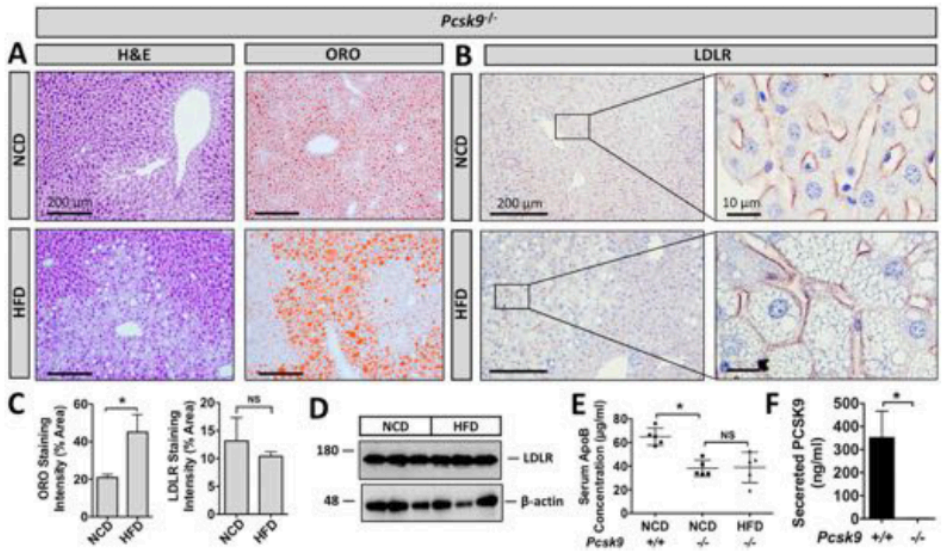

Figure 5. HFD fails to affect hepatic cell-surface LDLR and plasma LDL in *Pcsk9*$^{-/-}$ mice. *A*, *Pcsk9*$^{-/-}$ mice on a C57BL/6J background were fed either NCD ($n = 5$) or HFD ($n = 5$) *ad libitum* for 12 weeks starting at 6 weeks of age. *A* and *B*, hepatic lipid droplet accumulation was assessed via H&E and *ORO* and cell-surface LDLR expression via immunohistochemical staining. *C*, staining intensity was quantified using ImageJ Software (*, $p < 0.05$; $n = 5$). *D*, hepatic LDLR expression was also examined via immunoblot analysis. *E*, circulating ApoB levels were assessed using an ELISA. *F*, PCSK9 knockout was also confirmed via ELISA of circulating PCSK9 (*, $p < 0.05$). *Error bars* represent values presented as the mean ± S.D.

occur at the same time, however, it has been challenging to discern which of the two factors in this paradoxical relationship contributes most to the development of liver disease (10). Nonetheless, in a manner consistent with previous studies, we observed a significant increase in the expression of mediators of the UPR during conditions of hepatic steatosis in response to HFD (Fig. 3, *A* and *B*) (27). Although previous studies have demonstrated that HFD increases SREBP1 expression (44, 45), we also report the finding that diet-induced hepatic steatosis increases the expression of SREBP2 (Fig. 3*C*). Furthermore, we demonstrate that hepatic ER stress caused a significant increase in PCSK9 expression and secretion (Figs. 3*C* and 2*D*, respectively); a process that we previously demonstrated to be dependent on SREBP2 (25). We also observed that PA, a saturated fatty acid known to cause ER stress in secretory cell types (46), increased SREBP2 activity and PCSK9 expression and secretion in cultured human hepatocytes (Fig. 4). In response to elevated secreted PCSK9 levels, we observed that the livers of mice and cultured hepatocytes exhibited a significant reduction in LDLR expression and activity (Figs. 2*B* and 4*E*, respectively). Given that this phenotype was not observed in HFD-fed *Pcsk9*$^{-/-}$ mice, we conclude that the effect of diet-induced hepatic steatosis on LDLR expression occurs in a manner dependent on *de novo* SREBP2-driven PCSK9 expression and secretion (Fig. 6).

In a previous study, we observed that ER stress resulting from ER Ca^{2+} depletion, but not from the inhibition of *N*-glycosylation, caused a significant increase in SREBP2 activation and PCSK9 expression in hepatocytes (25). These findings suggest that PCSK9 expression is affected only by certain ER stress-inducing stimuli. Despite increased PCSK9 protein abundance as a result of thapsigargin treatment, we observed that thapsigargin and tunicamycin blocked the exit of PCSK9 from hepatocytes. Interestingly, in the present study we demonstrate that lipid accumulation in hepatocytes increases SREBP2 activity and promotes PCSK9 expression, suggesting that this process could occur as a result of ER Ca^{2+} depletion. Consistent with this notion, previous studies have also demonstrated that fatty acid uptake and accumulation causes ER Ca^{2+} depletion, ER stress, and apoptosis in a variety of cell lines (30, 47). In contrast to our previous study, however, diet-induced hepatic steatosis and ER stress not only increased the expression of PCSK9, but also increased its secretion from hepatocytes. Given the intricacies of the UPR and ER cargo receptors that are known to play a role in the secretion of PCSK9 and regulation of cholesterol (48, 49), it is not surprising that different conditions of ER stress affect PCSK9 in different ways. Although ER stress can increase its expression, *PCSK9* is also a lipid-responsive gene and therefore further studies are required to delineate the exact mechanism by which lipid accumulation influences PCSK9 secretion from hepatocytes.

Consistent with previous studies, we also observed that circulating PCSK9 levels were positively correlated with circulating LDL cholesterol levels, but inversely correlated with hepatic LDLR expression (Fig. 2, *B*, *D*, and *E*) (38, 50). Importantly, *de novo* synthesis of PCSK9 and the LDLR is regulated by the same transcription factor, and thus differences in the relative abundance of these proteins in the context of SREBP2 activation/inhibition can be attributed to differences in the stimuli being studied. Here, we observed that diet-induced hepatic steatosis increased *de novo* expression of the LDLR at the mRNA level (Fig. 3*C*), but blocked its expression at the protein level

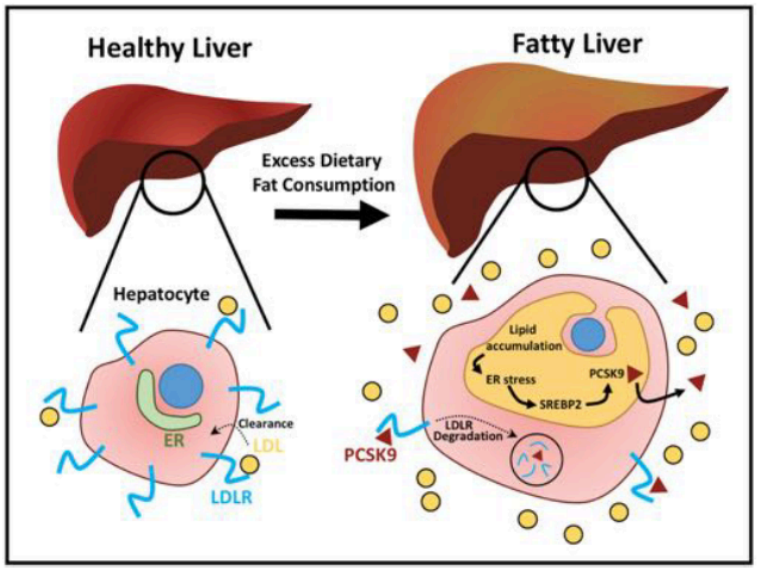

Figure 6. Fatty liver increases *de novo* PCSK9 to block cell-surface LDLR expression. The healthy liver regulates circulating LDL cholesterol levels by means of expressing high levels of cell-surface LDLR compared with most tissue types. Diet-induced hepatic steatosis, however, causes ER stress, which leads to an increase in SREBP2 activation and expression of the natural inhibitor of the LDLR, PCSK9. In this pathologic milieu, PCSK9 prevails over the LDLR and contributes to dyslipidemia and risk of CVD.

(Fig. 4*A*). Consistent with our observations, LDLR expression is inversely correlated with SREBP2 activation in naringin-treated mice and in monkeys treated with siRNA targeted against the SREBP cleavage-activating protein (51, 52); a protein known to interact with and stabilize the SREBPs (53). In contrast, it is also well-established that HMG-CoA reductase inhibitors activate SREBP2 and increase hepatic LDLR expression, as well as circulating PCSK9 levels (54, 55). Interestingly, a recent study has demonstrated that HMG-CoA reductase inhibitors can increase circulating PCSK9 levels while blocking the occurrence of a gain-of-function phosphorylation at position 688 (56). Given that HMG-CoA reductase inhibitors are well-known to reduce CVD risk (57), the aforementioned findings rectify the long-lasting PCSK9-statin anomaly. Furthermore, with a half-life of only 5 min (58), PCSK9 protein expression is more likely dependent on *do novo* synthesis than the LDLR, which has a half-life of 12 h (59).

Although we are the first to demonstrate that diet-induced liver fat accumulation increases circulating PCSK9 levels in mice, similar reports in patients have been controversial. The Dallas Heart study was the first to report a modest but significant positive correlation between hepatic steatosis and circulating PCSK9 levels (11). Ruscica and colleagues (12) also reported a statistically significant positive correlation between steatosis grade and circulating PCSK9 levels. Although our findings also demonstrate that patients with hepatic steatosis exhibit increased plasma PCSK9 levels, the statistical power of the result in this study is limited by low patient number. In contrast to the aforementioned data, a recent study by Wargny and colleagues (60) demonstrated that no significant correlation was observed between circulating PCSK9 levels and liver fat accumulation, plasma transaminase activity, NASH activity score, or lobular/portal inflammation in three patient cohorts. Inconsistencies in these data sets, however, are likely attributable to differences in liver disease severity between patient cohorts (60).

The liver is a central regulator of lipid homeostasis and yet despite the established role of lipid in the development of atherosclerosis and other cardiovascular complications, the contribution of liver disease to CVD remains elusive. Although previous studies have also demonstrated that a HFD can increase circulating LDL cholesterol levels (61), we are the first to highlight a role of the liver in this process. Because recent studies have also demonstrated that PCSK9 itself has proinflammatory properties (62), it is also possible that steatosis-driven PCSK9 expression may contribute to CVD in a manner independent of LDL cholesterol. Collectively, the present study delineates a novel mechanism by which diet-induced liver fat accumulation can influence CVD by affecting the expression of central regulators in its development, PCSK9 and the LDLR.

Experimental procedures

Patient cohort and ELISAs

Plasma samples from healthy controls and patients with fatty liver disease were acquired from Discovery Life Sciences (Huntsville, AL). All samples were acquired from males over the age of 50. PCSK9 levels in human and mouse plasma samples, as well as mouse liver lysates, were examined using commercially available ELISAs (R&D Systems). Mouse ApoB levels were also assessed using ELISAs (Abcam).

Table 1
Antibodies used for immunoblotting and immunohistochemical (IHC) staining

Antibody	Catalog No.	Application	Dilution
GRP78	SC-1050, Santa Cruz Biotechnology	IHC[a]	1:40, no retrieval
GRP94	ADI-SPA-850, Enzo Life Sciences	IHC	1:100, HIER[c]
LDLR	AF-2255, R and D Systems	IHC	1:100, HIER
Fibronectin	PA5–29578, ThermoFisher Scientific	IHC	1:200, HIER
GRP78	610979, BD Bioscience	IB[b]	1:1000
IRE1α	14C10, Cell Signaling Technologies	IB	1:500
XBP1	Sc-8015, Santa Cruz Biotechnology	IB	1:2000
β-Actin	MA5–15739, ThermoFisher Scientific	IB	1:5000
LDLR	AF2255, R and D Systems	IB	1:1000

[a] IHC, immunohistochemistry.
[b] IB, immunoblot.
[c] HIER, heat-induced epitope retrieval.

Table 2
Primers used for real-time PCR

Gene	Species	Forward	Reverse
ApoB	Mouse	AAGCACCTCCGAAAGTACGTG	CTCCAGCTCTACCTTACAGTTGA
ATF4	Mouse	ATGGCCGGCTATGGATGAT	CGAAGTCAAACTCTTTCAGATCCATT
BBC3	Mouse	TGTGGAGGAGGAGGAGTGG	TGCTGCTCTTCTTGTCTCCG
CASP1	Mouse	TCCGCGGTTGAATCCTTTTCAGA	ACCACAATTGCTGTGTGTGCGCA
CASP3	Mouse	CCTCAGAGAGACATTCATGG	GCAGTAGTCGCCTCTGAAGA
CHOP	Mouse	CTGCCTTTCACCTTGGAGAC	CGTTTCCTGGGGATGAGATA
FAS	Mouse	GCGATGAAGAGCATGGTTTAG	GGCTCAAGGGTTCCATGTT
FN1	Mouse	CGAGGTGACAGAGACCACAA	CTGGAGTCAAGCCAGACACA
GRP78	Mouse	GTCCTGCATCATCAGCGAAAG	GGTAGCCACATACTGAACACCA
GRP94	Mouse	GATGGTCTGGCAACATGGAG	CGCCTTGGTGTCTGGTAGAA
HMGCR	Mouse	CTTTCAGAAACGAACTGTAGC TCAC	CTAGTGGAAGATGAATGGACATGAT
LDLR	Mouse	GAGGAGCAGCCACATGGTAT	GCTCGTCCTCTGTGGTCTTC
PCSK9	Mouse	TTGCAGCAGCTGGGAACTT	CCGACTGTGATGACCTCTGGA
PERK	Mouse	GATGACTGCAATTACGCTATCAAGA	CCTTCTCCCGTGCCAACTC
SREBP1	Mouse	GGAGCCATGGATTGCACATT	GGCCCGGGAAGTCACTGT
SREBP2	Mouse	GCGTTCTGGAGACCATGGA	ACAAAGTTGCTCTGAAAACAAATCA

Cholesterol and triglyceride assays

Circulating plasma total cholesterol and triglyceride levels were examined using commercially available colorimetric assays and were carried out as per the manufacturer's instructions (Wako Diagnostics).

Immunohistochemical staining

Formalin-fixed paraffin-embedded liver sections were deparaffinized and stained with primary antibodies for 18 h following heat-induced epitope retrieval. Excess primary antibodies were removed via washing prior to exposure of sections to secondary antibodies conjugated to horseradish peroxidase. Staining was visualized using Nova Red (Vector Labs) and quantified using ImageJ. For quantification purposes, 20 representative images were taken from each treatment group at a magnification power of ×20. See Table 1 for antibodies used.

Cell culture studies

HepG2 cells were treated with BSA-conjugated PA (300 μM; Sigma-Aldrich) for 24 h in the presence or absence of Met (1 mM; Sigma-Aldrich) or 4PBA (1 mM; Sigma-Aldrich). Cells were fixed in 4% paraformaldehyde for the assessment of lipid droplet accumulation via ORO (Sigma-Aldrich) staining. SREBP2 transcriptional activity was assessed in HepG2 cells transfected with a reporter plasmid encoding a SRE-driven GFP (9) using X-tremeGENE HP transfection reagent (Sigma-Aldrich). PCSK9 mRNA expression and ELISAs were repeated in Hepatosure® 100-donor primary human hepatocytes purchased from Xenotech (Kansas City, KS). For the quantitative assessment of LDL uptake, HepG2 cells were seeded in black clear-bottom 96-well plates and treated with the indicated interventions for 24 h. Five hours prior to quantification using a fluorescent spectrophotometer (Molecular Devices, Gemini EM; excitation 554/emission 571), cells were treated with DiI fluorescently-labeled LDL (100 ng/ml; Alpha Aesar). Excess DiI-LDL in the medium was removed and the cell monolayer was vigorously washed with Hank's buffered saline solution containing HEPES (20 mM).

Animal studies

Pcsk9$^{-/-}$ (n = 5) and age-matched *Pcsk9*$^{+/+}$ controls on a C57BL/6J background (n = 10) were started on HFD (60% fat; Harland Tecklad) *ad libitum* at 6 weeks of age and sacrificed at 18 weeks of age. A second cohort of C57BL/6J mice were started on the HFD at 10–11 weeks of age and provided with either normal drinking water (n = 8) or water containing 4PBA (n = 9; 1 g/kg/day) for 12 weeks. Mice were fasted for 12 h prior to sacrifice. All animal studies were performed in accordance with the McMaster University animal care guidelines.

Immunoblot analysis

Cells were lysed in 4× SDS-PAGE sample buffer and separated on 10% polyacrylamide gels in reducing conditions, as described previously (63), and transferred to nitrocellulose membranes using a Trans-Blot Semi-Dry transfer apparatus (Bio-Rad). Following transfer, membranes were blocked in 1× Tris-buffered saline (TBS) and 5% BSA for 45 min. Membranes were then incubated with primary antibodies (diluted in TBS containing 1% BSA) for 18 h at 4 °C. Following primary antibody incubation, membranes were exposed to secondary antibodies conjugated to horseradish

peroxidase. EZ-ECL chemiluminescent reagent (FroggaBio) was used to visualize membranes on Amersham Biosciences Hyperfilm (GE Healthcare), which were developed using a Kodak X-Omat 1000A processor.

RNA isolation and quantitative real-time PCR

Total RNA was isolated using RNeasy Mini Kit (Qiagen) and reverse-transcribed to cDNA using High-capacity cDNA Reverse Transcription kit (Applied Biosystems). Real-time PCR was performed using Fast SYBR Green Master Mix (Applied Biosystems). Primer sequences used for real-time PCR are listed in Table 2.

Statistical analysis

Error bars represent values expressed as the mean ± S.D. Comparisons between two groups were carried out using the unpaired Student's *t* test and those involving multiple groups using a one-way analysis of variance. Differences between groups were considered significant at $p < 0.05$.

Author contributions—P. F. L., J. H. B., K. P., N. G. S., and R. C. A. conceptualization; P. F. L., J. H. B., K. P., S. V. P., M. F., and R. C. A. data curation; P. F. L. software; P. F. L. formal analysis; P. F. L. supervision; P. F. L. validation; P. F. L., J. H. B., K. P., M. E. M., S. V. P., and R. C. A. investigation; P. F. L. visualization; P. F. L., J. H. B., K. P., M. E. M., S. V. P., and N. G. S. methodology; P. F. L. writing-original draft; P. F. L., J. H. B., and R. C. A. project administration; P. F. L., J. H. B., K. P., M. F., N. G. S., and R. C. A. writing-review and editing; R. C. A. resources; R. C. A. funding acquisition.

References

1. Vernon, G., Baranova, A., and Younossi, Z. M. (2011) Systematic review: the epidemiology and natural history of non-alcoholic fatty liver disease and non-alcoholic steatohepatitis in adults. *Aliment. Pharmacol. Ther.* **34,** 274–285 CrossRef Medline
2. Sayiner, M., Koenig, A., Henry, L., and Younossi, Z. M. (2016) Epidemiology of nonalcoholic fatty liver disease and nonalcoholic steatohepatitis in the United States and the rest of the world. *Clin. Liver Dis.* **20,** 205–214 CrossRef Medline
3. Benedict, M., and Zhang, X. (2017) Non-alcoholic fatty liver disease: an expanded review. *World J. Hepatol.* **9,** 715–732 CrossRef Medline
4. Calzadilla Bertot, L., and Adams, L. A. (2016) The natural course of non-alcoholic fatty liver disease. *Int. J. Mol. Sci.* **17,** e774 Medline
5. World Health Organization (2016) *Hearts: technical package for cardiovascular disease management in primary health care.* World Health Organization, Switzerland
6. Söderberg, C., Stål, P., Askling, J., Glaumann, H., Lindberg, G., Marmur, J., and Hultcrantz, R. (2010) Decreased survival of subjects with elevated liver function tests during a 28-year follow-up. *Hepatology* **51,** 595–602 CrossRef Medline
7. Pickhardt, P. J., Hahn, L., Muñoz del Rio, A., Park, S. H., Reeder, S. B., and Said, A. (2014) Natural history of hepatic steatosis: observed outcomes for subsequent liver and cardiovascular complications. *Am. J. Roentgenol.* **202,** 752–758 CrossRef Medline
8. Ekstedt, M., Hagström, H., Nasr, P., Fredrikson, M., Stål, P., Kechagias, S., and Hultcrantz, R. (2015) Fibrosis stage is the strongest predictor for disease-specific mortality in NAFLD after up to 33 years of follow-up. *Hepatology* **61,** 1547–1554 CrossRef Medline
9. Patil, R., and Sood, G. K. (2017) Non-alcoholic fatty liver disease and cardiovascular risk. *World J. Gastrointest. Pathophysiol.* **8,** 51–58 CrossRef Medline
10. Francque, S. M., van der Graaff, D., and Kwanten, W. J. (2016) Non-alcoholic fatty liver disease and cardiovascular risk: pathophysiological mechanisms and implications. *J. Hepatol.* **65,** 425–443 CrossRef Medline
11. Lakoski, S. G., Lagace, T. A., Cohen, J. C., Horton, J. D., and Hobbs, H. H. (2009) Genetic and metabolic determinants of plasma PCSK9 levels. *J. Clin. Endocrinol. Metab.* **94,** 2537–2543 CrossRef Medline
12. Ruscica, M., Ferri, N., Macchi, C., Meroni, M., Lanti, C., Ricci, C., Maggioni, M., Fracanzani, A. L., Badiali, S., Fargion, S., Magni, P., Valenti, L., and Dongiovanni, P. (2016) Liver fat accumulation is associated with circulating PCSK9. *Ann. Med.* **48,** 384–391 CrossRef Medline
13. Benjannet, S., Rhainds, D., Essalmani, R., Mayne, J., Wickham, L., Jin, W., Asselin, M. C., Hamelin, J., Varret, M., Allard, D., Trillard, M., Abifadel, M., Tebon, A., Attie, A. D., Rader, D. J., *et al.* (2004) NARC-1/PCSK9 and its natural mutants: zymogen cleavage and effects on the low density lipoprotein (LDL) receptor and LDL cholesterol. *J. Biol. Chem.* **279,** 48865–48875 CrossRef Medline
14. Maxwell, K. N., and Breslow, J. L. (2004) Adenoviral-mediated expression of Pcsk9 in mice results in a low-density lipoprotein receptor knockout phenotype. *Proc. Natl. Acad. Sci. U.S.A.* **101,** 7100–7105 CrossRef Medline
15. Seidah, N. G., Abifadel, M., Prost, S., Boileau, C., and Prat, A. (2017) The proprotein convertases in hypercholesterolemia and cardiovascular diseases: emphasis on proprotein convertase subtilisin/kexin 9. *Pharmacol. Rev.* **69,** 33–52 Medline
16. Abifadel, M., Varret, M., Rabès, J. P., Allard, D., Ouguerram, K., Devillers, M., Cruaud, C., Benjannet, S., Wickham, L., Erlich, D., Derré, A., Villéger, L., Farnier, M., Beucler, I., Bruckert, E., *et al.* (2003) Mutations in PCSK9 cause autosomal dominant hypercholesterolemia. *Nat. Genet.* **34,** 154–156 CrossRef Medline
17. Mayne, J., Dewpura, T., Raymond, A., Bernier, L., Cousins, M., Ooi, T. C., Davignon, J., Seidah, N. G., Mbikay, M., and Chrètien, M. (2011) Novel loss-of-function PCSK9 variant is associated with low plasma LDL cholesterol in a French-Canadian family and with impaired processing and secretion in cell culture. *Clin. Chem.* **57,** 1415–1423 CrossRef Medline
18. Kumar, S., Kang, D. W., Rezvan, A., and Jo, H. (2017) Accelerated atherosclerosis development in C57Bl6 mice by overexpressing AAV-mediated PCSK9 and partial carotid ligation. *Lab. Invest.* **97,** 935–945 CrossRef Medline
19. Denis, M., Marcinkiewicz, J., Zaid, A., Gauthier, D., Poirier, S., Lazure, C., Seidah, N. G., and Prat, A. (2012) Gene inactivation of PCSK9 reduces atherosclerosis in mice. *Circulation* **125,** 894–901 CrossRef Medline
20. Sabatine, M. S., Giugliano, R. P., Keech, A. C., Honarpour, N., Wiviott, S. D., Murphy, S. A., Kuder, J. F., Wang, H., Liu, T., Wasserman, S. M., Sever, P. S., Pedersen, T. R., and FOURIER Steering Committee and Investigators. (2017) Evolocumab and clinical outcomes in patients with cardiovascular disease. *N. Engl. J. Med.* **376,** 1713–1722 CrossRef Medline
21. Seidah, N. G. (2017) The PCSK9 revolution and the potential of PCSK9-based therapies to reduce LDL-cholesterol. *Global Cardiol. Sci. Pract.* **2017,** e201702 Medline
22. Wadhera, R. K., Steen, D. L., Khan, I., Giugliano, R. P., and Foody, J. M. (2016) A review of low-density lipoprotein cholesterol, treatment strategies, and its impact on cardiovascular disease morbidity and mortality. *J. Clin. Lipidol.* **10,** 472–489 CrossRef Medline
23. Colgan, S. M., Tang, D., Werstuck, G. H., and Austin, R. C. (2007) Endoplasmic reticulum stress causes the activation of sterol regulatory element binding protein-2. *Int. J. Biochem. Cell Biol.* **39,** 1843–1851 CrossRef Medline
24. Colgan, S. M., Hashimi, A. A., and Austin, R. C. (2011) Endoplasmic reticulum stress and lipid dysregulation. *Expert. Rev. Mol. Med.* **13,** e4 CrossRef Medline
25. Lebeau, P., Al-Hashimi, A., Sood, S., Lhoták, Š., Yu, P., Gyulay, G., Paréé, G., Chen, S. R., Trigatti, B., Prat, A., Seidah, N. G., and Austin, R. C. (2017) Endoplasmic reticulum stress and Ca^{2+} depletion differentially modulate the sterol regulatory protein PCSK9 to control lipid metabolism. *J. Biol. Chem.* **292,** 1510–1523 CrossRef Medline
26. Li, J., Huang, J., Li, J. S., Chen, H., Huang, K., and Zheng, L. (2012) Accumulation of endoplasmic reticulum stress and lipogenesis in the liver through generational effects of high fat diets. *J. Hepatol.* **56,** 900–907 CrossRef Medline

27. Lee, H. Y., Lee, G. H., Bhattarai, K. R., Park, B. H., Koo, S. H., Kim, H. R., and Chae, H. J. (2016) Bax inhibitor-1 regulates hepatic lipid accumulation via ApoB secretion. *Sci. Rep.* **6,** 27799 CrossRef Medline
28. Zaid, A., Roubtsova, A., Essalmani, R., Marcinkiewicz, J., Chamberland, A., Hamelin, J., Tremblay, M., Jacques, H., Jin, W., Davignon, J., Seidah, N. G., and Prat, A. (2008) Proprotein convertase subtilisin/kexin type 9 (PCSK9): hepatocyte-specific low-density lipoprotein receptor degradation and critical role in mouse liver regeneration. *Hepatology* **48,** 646–654 CrossRef Medline
29. Carta, G., Murru, E., Banni, S., and Manca, C. (2017) Palmitic acid: physiological role, metabolism and nutritional implications. *Front. Physiol.* **8,** 902 CrossRef Medline
30. Zhang, Y., Xue, R., Zhang, Z., Yang, X., and Shi, H. (2012) Palmitic and linoleic acids induce ER stress and apoptosis in hepatoma cells. *Lipids Health Dis.* **11,** 1 CrossRef Medline
31. Cui, W., Ma, J., Wang, X., Yang, W., Zhang, J., and Ji, Q. (2013) Free fatty acid induces endoplasmic reticulum stress and apoptosis of beta-cells by Ca^{2+}/calpain-2 pathways. *PLoS ONE* **8,** e59921 CrossRef Medline
32. Zhang, Y., Miao, L., Zhang, H., Wu, G., Zhang, Z., and Lv, J. (2018) Chlorogenic acid against palmitic acid in endoplasmic reticulum stress-mediated apoptosis resulting in protective effect of primary rat hepatocytes. *Lipids Health Dis.* **17,** 270 CrossRef Medline
33. Ben Mosbah, I., Alfany-Fernandez, I., Martel, C., Zaouali, M. A., Bintanel-Morcillo, M., Rimola, A., Rodes, J., Brenner, C., Rosello-Catafau, J., and Peralta, C. (2010) Endoplasmic reticulum stress inhibition protects steatotic and non-steatotic livers in partial hepatectomy under ischemia-reperfusion. *Cell Death Dis.* **1,** e52 CrossRef Medline
34. Ford, R. J., Fullerton, M. D., Pinkosky, S. L., Day, E. A., Scott, J. W., Oakhill, J. S., Bujak, A. L., Smith, B. K., Crane, J. D., Blümer, R. M., Marcinko, K., Kemp, B. E., Gerstein, H. C., and Steinberg, G. R. (2015) Metformin and salicylate synergistically activate liver AMPK, inhibit lipogenesis and improve insulin sensitivity. *Biochem. J.* **468,** 125–132 CrossRef Medline
35. Zabielski, P., Hady, H. R., Chacinska, M., Roszczyc, K., Gorski, J., and Blachnio-Zabielska, A. U. (2018) The effect of high fat diet and metformin treatment on liver lipids accumulation and their impact on insulin action. *Sci. Rep.* **8,** 7249 CrossRef Medline
36. Woo, S. L., Xu, H., Li, H., Zhao, Y., Hu, X., Zhao, J., Guo, X., Guo, T., Botchlett, R., Qi, T., Pei, Y., Zheng, J., Xu, Y., An, X., Chen, L., *et al.* (2014) Metformin ameliorates hepatic steatosis and inflammation without altering adipose phenotype in diet-induced obesity. *PLoS ONE* **9,** e91111 CrossRef Medline
37. Nissar, A. U., Sharma, L., Mudasir, M. A., Nazir, L. A., Umar, S. A., Sharma, P. R., Vishwakarma, R. A., and Tasduq, S. A. (2017) Chemical chaperone 4-phenyl butyric acid (4-PBA) reduces hepatocellular lipid accumulation and lipotoxicity through induction of autophagy. *J. Lipid Res.* **58,** 1855–1868 CrossRef Medline
38. Khera, A. V., Qamar, A., Reilly, M. P., Dunbar, R. L., and Rader, D. J. (2015) Effects of niacin, statin, and fenofibrate on circulating proprotein convertase subtilisin/kexin type 9 levels in patients with dyslipidemia. *Am. J. Cardiol.* **115,** 178–182 CrossRef Medline
39. Gu, L., Wang, Y., Xu, Y., Tian, Q., Lei, G., Zhao, C., Gao, Z., Pan, Q., Zhao, W., Nong, L., and Tan, S. (2017) Lunasin functionally enhances LDL uptake via inhibiting PCSK9 and enhancing LDLR expression *in vitro* and *in vivo*. *Oncotarget* **8,** 80826–80840 Medline
40. Zelcer, N., Hong, C., Boyadjian, R., and Tontonoz, P. (2009) LXR regulates cholesterol uptake through Idol-dependent ubiquitination of the LDL receptor. *Science* **325,** 100–104 CrossRef Medline
41. Dara, L., Ji, C., and Kaplowitz, N. (2011) The contribution of endoplasmic reticulum stress to liver diseases. *Hepatology* **53,** 1752–1763 CrossRef Medline
42. Basseri, S., Lhoták, S., Sharma, A. M., and Austin, R. C. (2009) The chemical chaperone 4-phenylbutyrate inhibits adipogenesis by modulating the unfolded protein response. *J. Lipid Res.* **50,** 2486–2501 CrossRef Medline
43. Ruiz, R., Jideonwo, V., Ahn, M., Surendran, S., Tagliabracci, V. S., Hou, Y., Gamble, A., Kerner, J., Irimia-Dominguez, J. M., Puchowicz, M. A., DePaoli-Roach, A., Hoppel, C., Roach, P., and Morral, N. (2014) Sterol regulatory element-binding protein-1 (SREBP-1) is required to regulate glycogen synthesis and gluconeogenic gene expression in mouse liver. *J. Biol. Chem.* **289,** 5510–5517 CrossRef Medline
44. Shimomura, I., Bashmakov, Y., and Horton, J. D. (1999) Increased levels of nuclear SREBP-1c associated with fatty livers in two mouse models of diabetes mellitus. *J. Biol. Chem.* **274,** 30028–30032 CrossRef Medline
45. Jo, H. K., Kim, G. W., Jeong, K. J., Kim, D. Y., and Chung, S. H. (2014) Eugenol ameliorates hepatic steatosis and fibrosis by down-regulating SREBP1 gene expression via AMPK-mTOR-p70S6K signaling pathway. *Biol. Pharm. Bull.* **37,** 1341–1351 Medline
46. Cao, J., Dai, D. L., Yao, L., Yu, H. H., Ning, B., Zhang, Q., Chen, J., Cheng, W. H., Shen, W., and Yang, Z. X. (2012) Saturated fatty acid induction of endoplasmic reticulum stress and apoptosis in human liver cells via the PERK/ATF4/CHOP signaling pathway. *Mol. Cell. Biochem.* **364,** 115–129 CrossRef Medline
47. Xu, S., Nam, S. M., Kim, J. H., Das, R., Choi, S. K., Nguyen, T. T., Quan, X., Choi, S. J., Chung, C. H., Lee, E. Y., Lee, I. K., Wiederkehr, A., Wollheim, C. B., Cha, S. K., and Park, K. S. (2015) Palmitate induces ER calcium depletion and apoptosis in mouse podocytes subsequent to mitochondrial oxidative stress. *Cell Death Dis.* **6,** e1976 CrossRef Medline
48. Chen, X. W., Wang, H., Bajaj, K., Zhang, P., Meng, Z. X., Ma, D., Bai, Y., Liu, H. H., Adams, E., Baines, A., Yu, G., Sartor, M. A., Zhang, B., Yi, Z., Lin, J., *et al.* (2013) SEC24A deficiency lowers plasma cholesterol through reduced PCSK9 secretion. *eLife* **2,** e00444 CrossRef Medline
49. Emmer, B. T., Hesketh, G. G., Kotnik, E., Tang, V. T., Lascuna, P. J., Xiang, J., Gingras, A. C., Chen, X. W., and Ginsburg, D. (2018) The cargo receptor SURF4 promotes the efficient cellular secretion of PCSK9. *eLife* **7,** e38839 CrossRef Medline
50. Li, H., Dong, B., Park, S. W., Lee, H. S., Chen, W., and Liu, J. (2009) Hepatocyte nuclear factor 1α plays a critical role in *PCSK9* gene transcription and regulation by the natural hypocholesterolemic compound berberine. *J. Biol. Chem.* **284,** 28885–28895 CrossRef Medline
51. Jensen, K. K., Tadin-Strapps, M., Wang, S. P., Hubert, J., Kan, Y., Ma, Y., McLaren, D. G., Previs, S. F., Herath, K. B., Mahsut, A., Liaw, A., Wang, S., Stout, S. J., Keohan, C., Forrest, G., *et al.* (2016) Dose-dependent effects of siRNA-mediated inhibition of SCAP on PCSK9, LDLR, and plasma lipids in mouse and rhesus monkey. *J. Lipid Res.* **57,** 2150–2162 CrossRef Medline
52. Sui, G. G., Xiao, H. B., Lu, X. Y., and Sun, Z. L. (2018) Naringin activates AMPK resulting in altered expression of SREBPs, PCSK9, and LDLR to reduce body weight in obese C57BL/6J mice. *J. Agric. Food Chem.* **66,** 8983–8990 CrossRef Medline
53. Shao, W., and Espenshade, P. J. (2014) Sterol regulatory element-binding protein (SREBP) cleavage regulates Golgi-to-endoplasmic reticulum recycling of SREBP cleavage-activating protein (SCAP). *J. Biol. Chem.* **289,** 7547–7557 CrossRef Medline
54. Mayne, J., Dewpura, T., Raymond, A., Cousins, M., Chaplin, A., Lahey, K. A., Lahaye, S. A., Mbikay, M., Ooi, T. C., and Chrétien, M. (2008) Plasma PCSK9 levels are significantly modified by statins and fibrates in humans. *Lipids Health Dis.* **7,** 22 CrossRef Medline
55. Welder, G., Zineh, I., Pacanowski, M. A., Troutt, J. S., Cao, G., and Konrad, R. J. (2010) High-dose atorvastatin causes a rapid sustained increase in human serum PCSK9 and disrupts its correlation with LDL cholesterol. *J. Lipid Res.* **51,** 2714–2721 CrossRef Medline
56. Gauthier, M. S., Awan, Z., Bouchard, A., Champagne, J., Tessier, S., Faubert, D., Chabot, K., Garneau, P. Y., Rabasa-Lhoret, R., Seidah, N. G., Ridker, P. M., Genest, J., and Coulombe, B. (2018) Posttranslational modification of proprotein convertase subtilisin/kexin type 9 is differentially regulated in response to distinct cardiometabolic treatments as revealed by targeted proteomics. *J. Clin. Lipidol.* **12,** 1027–1038 CrossRef Medline
57. LaRosa, J. C., Grundy, S. M., Waters, D. D., Shear, C., Barter, P., Fruchart, J. C., Gotto, A. M., Greten, H., Kastelein, J. J., Shepherd, J., Wenger, N. K., and Treating to New Targets (TNT) Investigators (2005) Intensive lipid lowering with atorvastatin in patients with stable coronary disease. *N. Engl. J. Med.* **352,** 1425–1435 CrossRef Medline
58. Giunzioni, I., and Tavori, H. (2015) New developments in atherosclerosis: clinical potential of PCSK9 inhibition. *Vasc. Health Risk Manag.* **11,** 493–501 Medline

59. Wang, Y., Huang, Y., Hobbs, H. H., and Cohen, J. C. (2012) Molecular characterization of proprotein convertase subtilisin/kexin type 9-mediated degradation of the LDLR. *J. Lipid Res.* **53,** 1932–1943 CrossRef Medline
60. Wargny, M., Ducluzeau, P. H., Petit, J. M., Le May, C., Smati, S., Arnaud, L., Pichelin, M., Bouillet, B., Lannes, A., Blanchet, O., Lefebvre, P., Francque, S., Van Gaal, L., Staels, B., Vergès, B., Boursier, J., and Cariou, B. (2018) Circulating PCSK9 levels are not associated with the severity of hepatic steatosis and NASH in a high-risk population. *Atherosclerosis* **278,** 82–90 CrossRef Medline
61. Retterstøl, K., Svendsen, M., Narverud, I., and Holven, K. B. (2018) Effect of low carbohydrate high fat diet on LDL cholesterol and gene expression in normal-weight, young adults: a randomized controlled study. *Atherosclerosis* **279,** 52–61 CrossRef Medline
62. Ricci, C., Ruscica, M., Camera, M., Rossetti, L., Macchi, C., Colciago, A., Zanotti, I., Lupo, M. G., Adorni, M. P., Cicero, A. F. G., Fogacci, F., Corsini, A., and Ferri, N. (2018) PCSK9 induces a pro-inflammatory response in macrophages. *Sci. Rep.* **8,** 2267 CrossRef Medline
63. Lebeau, P., Platko, K., Al-Hashimi, A. A., Byun, J. H., Lhoták, Š., Holzapfel, N., Gyulay, G., Igdoura, S. A., Cool, D. R., Trigatti, B., Seidah, N. G., and Austin, R. C. (2018) Loss-of-function PCSK9 mutants evade the unfolded protein response sensor GRP78 and fail to induce endoplasmic reticulum stress when retained. *J. Biol. Chem.* **293,** 7329–7343 CrossRef Medline

5. Manuscript submitted to the Journal of the American Society of Nephrology 2019

Byun J. H.*, P. F. Lebeau*, K. Platko, R. E. Carlisle, M. Faiyaz, J. Chen, M. E. MacDonald, J. G. Dickhout, J. C. Krepinsky, and R. C. Austin (2019) PCSK9 reduces surface CD36 expression to prevent tubular lipid accumulation and renal injury. *Submitted to the Journal of the American Society of Nephrology Dec 2019*

Author Contributions: J.H.B., P.F.L., and R.C.A. conceptualization; J.H.B., P.F.L., K.P., R.C., and M.F data curation; J.H.B software; J.H.B formal analysis; J.H.B and P.F.L supervision; J.H.B. validation; J.H.B., P.F.L, K.P., R.C., M.F., J.C., M.E.M., J.G.D., J.C.K., and R.C.A. investigation; J.H.B. visualization; J.H.B., P.F.L., and K.P. methodology; J.H.B. writing original draft; J.H.B., P.F.L., and R.C.A. project administration; J.H.B., P.F.L, K.P., R.C., M.F., J.C., M.E.M., J.G.D., J.C.K., and R.C.A. writing-review and editing; R.C.A. resources; R.C.A. funding acquisition.

Personal thesis contribution: As the primary author of this paper, I have provided most of the *in vitro* and *in vivo* data curation and experimental analysis which contributed towards all the figures of this manuscript. In addition, I wrote the original draft of this manuscript and oversaw the publication process of this paper into the Journal of the American Society of Nephrology.

Journal of the American Society of NEPHROLOGY

JASN

PCSK9 reduces surface CD36 expression to prevent tubular lipid accumulation and renal injury

Journal:	*Journal of the American Society of Nephrology*
Manuscript ID	JASN-2019-12-1281
Manuscript Type:	Original Article - Basic Research
Date Submitted by the Author:	11-Dec-2019
Complete List of Authors:	Byun, Jae Hyun; McMaster University, Medicine Lebeau, Paul; McMaster University, Medicine Platko, Khrystyna; McMaster University, Medicine Carlisle, Rachel; McMaster University, Medicine Faiyaz, Mahi; McMaster University, Medicine Chen, Jack; McMaster University, Medicine MacDonald, Melissa; McMaster University, Medicine Dickhout, Jeffrey; McMaster University, Medicine Krepinsky, Joan; McMaster University, Medicine Austin, Richard; McMaster University, Medicine
Keywords:	endoplasmic reticulum stress, chronic kidney disease, PCSK9, CD36, renal injury, lipid accumulation

Significance Statement:

The proprotein convertase subtilisin/kexin type 9 (PCSK9) plays an essential role in lipid metabolism through its ability to interact with a variety of receptors known to promote lipid uptake from circulation. Given that these receptors are abundantly expressed on renal epithelia, we examined relative renal lipid accumulation in the context of PCSK9 deficiency. In this study, it was observed that PCSK9 can protect against saturated fatty acid-induced cytotoxicity in cultured renal cells and diet-induced renal injury in PCSK9 knockout mice.

PCSK9 reduces surface CD36 expression to prevent tubular lipid accumulation and renal injury

Jae Hyun Byun, Paul F. Lebeau*, Khrystyna Platko, Rachel E. Carlisle, Mahi Faiyaz, Jack Chen, Melissa E. MacDonald, Jeffrey G. Dickhout, Joan C. Krepinsky, and Richard C. Austin†*

Affiliations: *From the Department of Medicine, Division of Nephrology, McMaster University, St. Joseph's Healthcare Hamilton and Hamilton Centre for Kidney Research, Hamilton, Ontario L8N 4A6, Canada.*

* Co-first authors

† To whom correspondence should be addressed: Richard C. Austin, PhD, 50 Charlton Ave East, Room T-3313, Hamilton, Ontario, L8N 4A6

Running Title: PCSK9 protects against CD36-mediated renal injury.

Conflict of interest: The authors do not have competing interests to declare.

Financial Support: This work was supported in part by research grants to Richard C. Austin from the Heart and Stroke Foundation of Canada (G-13-0003064 and G-15-0009389), the Canadian Institutes of Health Research (74477), CIHR foundation grant (148363) and Canada Research Chair (216684). Financial support from the Research Institute of St. Joseph's Healthcare Hamilton is acknowledged. Richard C. Austin is a Career Investigator of the Heart and Stroke Foundation of Ontario and holds the Amgen Canada Research Chair in the Division of Nephrology at St. Joseph's Healthcare and McMaster University.

Author Contributions: JHB, PL, and RCA conceived the studies. JHB, PL, KP, RC, and MF performed all of the in vitro and in vivo studies. The manuscript was written by JHB, PL, and RCA and revised by KP, RC, JD, and JK.

Keywords: ER stress, renal injury, PCSK9, CD36, lipid accumulation, CKD

Abbreviations: ATF6, activating transcription factor 6; BSA, bovine serum albumin; CD36, cluster of differentiation 36; CKD, chronic kidney disease; CVD, cardiovascular disease; ER, endoplasmic reticulum; FAS, fatty acid synthase; FFA, free fatty acid; GFR, glomerular filtration rate; GOF, gain-of-function; GRP78, glucose-regulated protein of 78 kDa; GRP94, glucose-regulated protein 94 kDa; HFD, high-fat diet; HRP, horse radish peroxidase; IHC, immunohistochemical; IRE1, inositol-requiring enzyme I; LDLc, low-density lipoprotein cholesterol; LDLR, low-density lipoprotein receptor; LOF, loss-of-function; mAb, monoclonal antibody; n-ATF6, nuclear ATF6; NCD, normal control diet; OA, oleic acid; ORO, oil-red-o; PERK, ox-LDL, oxidized-LDL; PA, palmitate; PPAR, peroxisome proliferator-activated receptor; PCSK9, proprotein convertase subtilisin/ kexin type 9; p-PERK, phosphorylated-PERK; PERK,

protein kinase RNA-like ER kinase; qRT-PCR, quantitative real-time PCR, ROS, reactive oxygen species; SERCA, sarco/endoplasmic reticulum Ca^{2+}-ATPase; siCD36, small interfering CD36; siScrambled, small interfering scrambled; SREBP-1, sterol regulatory element binding protein-1; TBS, tris-buffered saline; UPR, unfolded protein response

Significance Statement:

The proprotein convertase subtilisin/kexin type 9 (PCSK9) plays an essential role in lipid metabolism through its ability to interact with a variety of receptors known to promote lipid uptake from circulation. Given that these receptors are abundantly expressed on renal epithelia, we examined relative renal lipid accumulation in the context of PCSK9 deficiency. In this study, it was observed that PCSK9 can protect against saturated fatty acid-induced cytotoxicity in cultured renal cells and diet-induced renal injury in PCSK9 knockout mice.

Abstract

Background: The discovery of the proprotein convertase subtilisin/kexin type 9 (PCSK9) has led to the development of a new line of therapeutics capable of significantly lowering circulating cholesterol levels. Since this discovery, PCSK9 has been reported to modulate the uptake of circulating lipids through a range of receptors including the low-density lipoprotein receptor (LDLR) and CD36, all of which are ubiquitously expressed on hepatocytes and renal epithelia. In the kidney, CD36 is reported to promote renal injury through pro-inflammatory and fibrotic pathways. In this study, we sought to investigate the role of PCSK9 in modulating renal lipid accumulation and injury through CD36 in a diet-induced mouse model.
Methods: The effect of PCSK9 on lipid uptake and accumulation was examined in cultured renal cells. Lipid accumulation was then assessed in Pcsk9-/- mice and assessed for diet-induced renal injury.
Results: As a result of PCSK9 deficiency, we observed that heightened CD36 levels increased the uptake of free fatty acids (FFA) in renal cells. Our results indicate that the uptake of long-chain saturated FFAs promote ER stress, which was further exacerbated in the absence of exogenous PCSK9 in vitro. Consistent with these observations, *Pcsk9*$^{-/-}$ mice on a high fat diet (HFD) displayed elevated ER stress, inflammation, fibrosis, and renal injury relative to controls.
Conclusions: Overall, we report that circulating PCSK9 modulates renal lipid uptake in a manner dependent on renal CD36. In the context of increased dietary fat consumption, the absence of circulating PCSK9 may promote renal lipid accumulation and subsequent renal injury.

Electronic word count: 150 (including abstract), 5212 (including introduction, methods, results, discussion, references and figure captions)

Figure Count: 8 figures

Introduction

The global prevalence of chronic kidney disease (CKD) has risen at an alarming rate, increasing the global healthcare burden for long-term and chronic care costs (1). The progression of CKD in affected individuals commonly develops as a result of interstitial fibrosis, proteinuria, and tubular atrophy (2), which compromises the overall filtration capacity of the kidney. Dyslipidemia and obesity are also considered prominent risk factors in CKD (3, 4, 5, 6). Increased free fatty acid (FFA) uptake due to excess consumption of diets rich in fats has been shown to promote intra-renal lipid accumulation in several animal models and patients at various stages of CKD (7, 8, 9, 10). As a result, excess renal uptake of FFAs has been shown to damage podocytes, mesangial cells, and proximal tubular epithelial cells through various mechanisms by increasing reactive oxygen species (ROS) production and lipid peroxidation. This in turn promotes mitochondrial dysfunction and tissue inflammation, resulting in the formation of glomerular and tubular lesions (11, 12).

Among the underlying mechanisms of FFA-induced CKD progression is the induction of endoplasmic reticulum (ER) stress (13). Changes in the lipid composition of the ER membrane has been shown to antagonize the sarco/endoplasmic reticulum Ca^{2+}-ATPase (SERCA) pump, leading to the depletion of ER Ca^{2+} levels (14). Because the chaperones expressed in the ER lumen that function to properly folding *de novo* proteins are dependent on Ca^{2+}, this state of Ca^{2+} depletion commonly leads to the accumulation and subsequent aggregation of misfolded proteins in this organelle. The ER is responsible for the synthesis and proper folding of secretory, transmembrane, and ER luminal proteins and addresses the accumulation of misfolded protein via a highly conserved signaling cascade known as the unfolded protein response (UPR) (13). The activation of the UPR is dependent on the dissociation of ER chaperones such as the glucose-regulated protein of 78 kDa (GRP78) from three transmembrane sensors in the ER lumen; namely the activating transcription factor 6 (ATF6), the protein kinase RNA (PKR)-like ER kinase (PERK), and the inositol-requiring enzyme I (IRE1). Chronic activation of these transmembrane proteins and their downstream signaling pathways result in cellular apoptosis, inflammation, and fibrosis in the context of CKD progression (13, 15).

Recently, the scavenger receptor known as the cluster of differentiation 36 (CD36) has been reported to play a pivotal role in promoting intra-renal lipid accumulation, inflammatory signaling, cellular apoptosis and pro-fibrotic signaling pathways (16, 17, 18). CD36 is a multifunctional receptor that mediates the cellular uptake of long-chain fatty acids and oxidized lipoproteins and is abundantly expressed in the proximal and distal tubular epithelium, on podocytes, mesangial cells, and interstitial macrophages (11, 19, 20, 21). Previous studies demonstrated that disruption of CD36-dependent pathways can modulate the development of kidney fibrosis. In mice, transgenic overexpression of tubular CD36 led to an increase in intra-renal lipid accumulation and resulted in an up-regulation in the expression of pro-fibrotic genes and markers of UPR activation (17). In podocytes, CD36-dependent uptake of palmitic acid led to a dose-dependent increase in ER stress, mitochondrial reactive oxygen species (ROS) production, ATP depletion, and apoptosis (20). As such, accumulating evidence strongly suggest that CD36 stands as a key driver of renal damage and its potential use as a therapeutic target for the management of renal disease has yet to be fully elucidated.

Patients with renal disease also are at a substantially higher risk for atherosclerotic cardiovascular diseases (CVD) (22). In the general population, as well as in CKD patients, circulating low-density lipoprotein cholesterol (LDLc) is a well-known driver of atherosclerotic lesion development and CVD progression. In 2003, the third locus of familial hypercholesterolemia was identified as the proprotein convertase subtilisin kexin/type 9 (PCSK9), and was further characterized for its ability to degrade the low-density lipoprotein receptor (LDLR). Chief among these discoveries was the identification of patients with loss-of-function (LOF) PCSK9 mutations, which conferred significantly lower LDLc levels, while gain-of-function (GOF) mutations increased plasma LDLc levels (23, 24, 25). The development of monoclonal antibodies targeted against PCSK9, capable of reducing plasma LDLc levels by 60% in patients at high risk of CVD, now stand as testament of PCSK9 being an important mediator of CVD risk. In recent years, PCSK9 has been shown to promote the degradation of several other receptors well-known to promote extracellular lipid uptake into tissue, such as the LDLR-related protein-1, the very low-density lipoprotein receptor (26), and CD36 (27). Given the abundant expression of CD36 in the tubular structures of the kidney, the deficiency of circulating PCSK9 may affect the expression of these receptors, thereby promoting renal lipid accumulation and injury via the enhancement of FFA and lipoprotein uptake. In this study, we examine this hypothesis and report that *Pcsk9*$^{-/-}$ mice exhibit elevated levels of renal tubular CD36 expression and elevated renal lipid levels. As a result, we also observed that *Pcsk9*$^{-/-}$ mice exhibit elevated levels of high-fat diet (HFD)-induced renal ER stress, inflammation, and fibrosis relative to wild-type (WT) controls. Given these observations, we report here that PCSK9 has the ability to modulate renal lipid uptake to protect against lipid-induced renal injury.

Materials and Methods

Cell Culture, Transfections and free fatty acid (FA) treatments:

Human immortalized proximal tubule epithelial (HK-2), hepatocytes (Huh-7), embryonic kidney (HEK293), and primary rat mesangial cell lines were used. All cells were cultured in Dulbecco's Modified Eagle Medium (Gibco, ThermoFisher Scientific) supplemented with 10% fetal bovine serum (FBS) (Sigma-Aldrich), and 50 IU/ml of penicillin and 100µg/ml streptomycin (Sigma-Aldrich). All cells were maintained in 5% CO_2 at 37°C. Cells were plated at a confluence of 60% for transfection experiments. Transfection cocktail consisted of the following ratio: 1µg DNA:3 µl X-tremeGENE HP DNA reagent:100 µl Opti-MEM. The cDNA of human WT PCSK9 and the PCSK9^{Q152H} retention variant was cloned into pIRES-EGFP with a V5-tag inserted between the N-terminal signal peptide. Cells were treated with LDL (Lee Biosolutions), oxLDL (Alfa Aesar), oleate (Alfa Aesar), and palmitate (Sigma-Aldrich) that were conjugated to FA-free bovine serum albumin (BSA). All treatments were carried out overnight for 24 h unless specified otherwise.

Animal Studies

6-week old male *Pcsk9*$^{-/-}$ mice on a C57BL/6J background and age-matched C57BL/6J controls were placed on either a normal control diet (NCD) (n=10) or HFD (60% fat/Kcal; ENVIGO #TD06414; n=10) for 12 weeks *ad libitum* access to food and water. All animal procedures were approved by the McMaster University Animal Research Ethics Board.

Alirocumab Administration

10-week old male WT mice on a C57BL/6J background were administered with PCSK9 monoclonal antibody (mAb) (n=10) or saline (n=10) at 10 mg/kg via orbital injection and

sacrificed 10 days later. All animal procedures were approved by the McMaster University Animal Research Ethics Board.

Immunoblotting

Protein samples were electrophoretically resolved on 7-10% polyacrylamide gels and transferred onto nitrocellulose membranes. Membranes were then blocked using 5% w/v skimmed milk in tris-buffered saline (TBS) containing Tween-20 for 1 h and incubated in primary antibody overnight for 18 h at 4˚C. To detect bound primary antibodies, horse radish peroxidase (HRP) conjugated antibodies were used (goat anti-rabbit, Bio-Rad; donkey anti-goat, Santa Cruz, goat anti-mouse, Bio-Rad) and developed using a chemiluminescent reagent (FroggaBio). Quantification of immunoblots was assessed after normalization to β-actin (Sigma-Aldrich). Please refer to Table 1 for a list of the antibodies used for this study.

Real-time PCR

Total RNA from tissues and cell culture was isolated using RNA purification kit according to manufacturer's instructions (ThermoFisher Scientific). A total of 2 µg of RNA was reverse-transcribed to cDNA using SuperScript Vilo IV cDNA synthesis kit (ThermoFisher Scientific). Quantitative real-time PCR (qRT-PCR) assessment of different mRNA species was used in conjunction with FAST SYBR Green (ThermoFisher Scientific). All primer sequences are listed in Table 2.

Immunofluorescent staining

Cells were fixed using 4% paraformaldehyde and either non-permeabilized or permeabilized with 0.025% Triton-X in PBS, and blocked with 1% BSA for 30 min. Cells were then stained with anti-LDLR (catalog no. AF2148, R&D Systems), anti-CD36 (catalog no. NB400-144, Novus Biologicals) or anti-ATF6 (catalog no. NBP1-40256, Novus Biologicals) for 1h. Following primary antibody incubation, cells were fluorescently labelled with either Alexa 647 (catalog no. 21245, Thermo Fisher Scientific), Alexa 594 (catalog no. A11058, Thermo Fisher Scientific), or Alexa 488 (catalog no. A10468) as well as DAPI. Slides were mounted using permafluor and visualized using the EVOS FL color imaging system.

Oil-Red-O (ORO) staining

Cells were fixed using 4% paraformaldehyde and stained with ORO (Sigma-Aldrich) for 5 min. After washing, cells were counterstained with Gills hematoxylin (no.5, Sigma Aldrich) and mounted on a glass slide. For quantification purposes, ORO stain was extracted from cells using isopropanol for 20 minutes on an orbital shaker at 37ºC. Optical density of ORO-exposed isopropanol extracts was quantified using a spectrophotometer (molecular devices) at a wavelength of 520nm. 10µm thick sections of mouse OCT-embedded kidneys were washed with propylene glycol and stained with ORO for 10 min. Following staining, tissues were repeatedly washed with propylene glycol and counterstained using alum hematoxylin.

Thioflavin-T/S staining

Thioflavin staining is a tool commonly used for the visualization of misfolded protein aggregate accumulation occurring as a result of ER stress (28). Cells were fixed using 4% paraformaldehyde and stained with Thioflavin-T (Sigma-Aldrich) for 15 min at 37ºC. For tissue, 10µm thick sections

of mouse OCT-embedded kidneys were stained with Thioflavin-S staining for 15 min. All images and quantifications were collected using a fluorescent microscope (EVOS FL).

Trigylceride Quantification

Renal cortical tissue was assessed for triglyceride content using a triglyceride assay kit (Abcam) according to manufacturer's instructions. All data were normalized to tissue weight.

PCSK9 ELISA

Quantification of PCSK9 in media was determined using the R and D systems human Quantikinine PCSK9 ELISA.

Immunohistochemical (IHC) Staining

4 µm thick sections were deparaffinized, blocked in 5% v/v serum and subsequently incubated with primary antibodies for 18 h at 4˚C. Sections were incubated with biotin-labeled secondary antibodies (Vector Laboratories). Streptavidin-labeled HRP solution (Vector Laboratories) and NovaRed developing solution (Vector Laboratories) were used to visualize the staining. Slides were examined using a Nikon light microscope (Model no. DS-Ri2). Relative staining intensity was quantified using ImageJ software (n=10). For picro Sirius red (PSR) staining, kidney sections were exposed to saturated picric acid solution and stained with Sirius red F3B (Colour Index 35782). Please refer to table 1 for a list of the antibodies used for this study.

Statistical Analysis

Statistical analysis for two-group comparisons was conducted using unpaired Student's *t*-test and for multiple group comparison, one-way ANOVA was used. Statistically significant differences were considered at $p<0.05$. All error bars are represented as standard deviation of the mean.

Results

Secreted PCSK9 regulates surface CD36 and LDLR in cultured renal cells

Given that renal proximal tubular cells express a number of receptors known to be regulated by PCSK9, and that PCSK9 is secreted into the blood almost exclusively by the liver (16, 18), we developed an *in vitro* model to mimic the effect of liver-secreted PCSK9 on HK-2 cells. In these experiments, cultured HuH7 human hepatoma cells were transfected with either WT PCSK9 or the $PCSK9^{Q152H}$ LOF mutant that fails to be secreted from cells (39). PCSK9-containing medium from $PCSK9^{WT}$-transfected cells, or control medium from $PCSK9^{Q152H}$-transfected cells that does not contain PCSK9 was harvested and used to culture HK-2 cells. Western blot and immunofluorescence analysis demonstrated that HK-2 cells exposed to PCSK9-containing medium express reduced levels of LDLR and CD36 (Fig. 1A-C). To confirm these observations, Immunofluorescent staining intensity was quantified using ImageJ software (Fig. 1D; *, $p<0.05$). Secreted PCSK9 was also measured in medium from HuH7 cells, along with non-transfected HuH7 cells compared to HK-2 cells, confirming that the majority of secreted PCSK9 originated from hepatocytes (Fig. 1E-F; *, $p<0.05$). qRT-PCR analysis revealed that relative mRNA transcripts of PCSK9 and SREBP2 in HK-2 cells were not significantly affected with the media swap experimental design (Fig. 1G; NS, non-significant). Collectively, these data demonstrate that PCSK9 secreted from hepatocytes downregulates CD36 expression on the surface of renal-derived cells.

PCSK9 blocks OA- and LDL-induced lipid droplet accumulation in renal cells

We then examined whether exogenous PCSK9 could regulate lipid uptake in a variety of renal-derived cell lines. HK-2 cells were exposed to medium harvested from PCSK9-transfected HuH7 cells, treated with oleic acid (OA), and stained with the ORO lipid stain. HK-2 cells exposed to medium from WT-PCSK9 transfected HuH7 cells exhibited attenuated lipid accumulation relative to cells exposed to control medium (Fig. 2A). Consistent with visual observations, quantification of ORO staining via densitometry of isopropanol extract at 520 nm suggests that PCSK9 blocks OA-induced lipid accumulation in HK-2 cells (Fig. 2B, *, $p<0.05$). To further confirm this observation, both HK-2 and primary mesangial cells exposed to PCSK9-containing medium were treated with fluorescently-labelled DiI-LDL in order to visualize LDL uptake. Attenuation in fluorescence intensity suggests that cells exposed to PCSK9-containing medium yielded less uptake of DiI-labelled LDL in HK-2 cells (Fig. 2C), which was also quantified using a black clear-bottom 96-well plate (Fig. 2D-E, *, $p<0.05$). Furthermore, to confirm that the observed differences in lipid accumulation was due to the exogenous V5-labelled PCSK9, anti-V5 antibodies were added to media and stained for lipid accumulation via ORO. Compared to IgG controls, the addition of anti-V5 antibody reversed the attenuating effects of lipid accumulation by exogenous V5-PCSK9 in the media (Fig. 2F). Altogether, these observations demonstrate that secreted PCSK9 modulates lipid uptake in renal-derived cell lines.

PCSK9 attenuates lipid accumulation in renal-derived cells in a manner dependent of CD36

Given that PCSK9 regulates CD36 expression (27), and that CD36 is a well-established scavenger receptor for FFA in renal cells (16), we examined whether PCSK9 regulates FFA uptake and subsequent accumulation in a manner dependent on CD36. First, ORO staining and quantification was carried out in HK-2 cells treated with SSO, a well-established blocker of CD36 (Fig. 3A-B, *, $p<0.05$) (42). Then, HK-2 cells were treated with OA in the presence of either scrambled small interfering (si)RNA (siScrambled) or siRNA targeted against CD36 (siCD36). Treatment with siCD36 was able to attenuate OA-induced lipid accumulation (Fig. 3C-D, *, $p<0.05$) Next, HK-2 cells were treated with DiI-oxLDL for 5 h. Visualization and fluorescent staining quantification revealed that exogenous PCSK9 was able to attenuate DiI-oxLDL uptake (Fig. 3E-F, *, $p<0.05$). The effectiveness of siRNA-mediated knockdown of CD36 was assessed via immunobloting (Fig. 3G). Lastly, intracellular triglyceride content was measured in HK-2 cells following CD36 knockdown and OA treatment. Results revealed that knockdown of CD36 expression using siCD36 was able to attenuate relative triglyceride content in HK-2 cells compared to relative controls (Fig. 3H, *, $p<0.05$). In addition to regulating CD36 expression, these data demonstrate that PCSK9 also regulates the uptake and accumulation of FFA in cultured renal cells.

PCSK9 attenuates palmitate- and oxidized LDL-induced ER stress in vitro

CD36 is a well-established contributor of ER stress in proximal tubular cells in a manner dependent on excess uptake of ER stress-inducing lipoproteins and FFAs, such as oxidized-LDL (ox-LDL) and palmitate (PA), respectively (20). Therefore, we next examined whether PCSK9 could protect against ER stress in the presence of ox-LDL and PA resulting from the attenuation of CD36 expression. Immunofluorescent staining of UPR markers nuclear ATF6 (n-ATF6) demonstrated that PCSK9-containing medium reduces ox-LDL-induced ER stress (Fig. 4A), which was also quantified (Fig. 4B, *, $p<0.05$). Next, qRT-PCR assessment revealed that PCSK9-containing medium was able to attenuate relative UPR activation induced by PA (Fig. 4C-F, *, $p<0.05$). To

further correlate the lipotoxic effects of PA on the observed UPR activation, relative triglyceride content was measured in HK-2 cells treated with PA in the presence or absence of exogenously added PCSK9. Results demonstrated that the presence of PCSK9 was able to significantly reduce triglyceride uptake in HK-2 cells with the treatment of PA (Fig. 4G, $p<0.05$). Lastly, protein aggregate accumulation, a hallmark characteristic of ER stress, was assessed via quantification of live staining in HK-2 cells with Thioflavin-T. We observed reduced fluorescence in Thioflavin-T staining in HK-2 cells exposed to exogenous PCSK9 treated with PA, indicative of a reduction in misfolded protein aggregates (Fig. 4H, *, $p<0.05$; NS, non-significant). Together, these observations suggest that PCSK9 is able to protect against PA and oxLDL-induced ER stress by reducing extracellular FFA uptake.

Pcsk9$^{-/-}$ mice exhibit increased renal lipid accumulation

To gain insight into the ability of PCSK9 to modulate renal lipid uptake/accumulation *in vivo*, male *Pcsk9*$^{-/-}$ mice and age-matched C57BL/6J *Pcsk9*$^{+/+}$ controls that were fed NCD, were sacrificed at 12 weeks of age. Immunohistochemical analysis of renal cortex revealed that *Pcsk9*$^{-/-}$ mice exhibited increased in tubular lipid accumulation assessed via ORO staining relative to the controls (Fig. 5A). This observation was consistent with increased CD36 and lipid droplet marker perilipin, staining in the *Pcsk9*$^{-/-}$ mice. Immunoblot analysis also demonstrated that *Pcsk9*$^{-/-}$ mice had increased protein expression of CD36 and LDLR, receptors known to promote lipid uptake in a variety of tissues including the kidney (Fig. 5B, *, $p<0.05$) (16, 17, 18). Interestingly, as a compensatory response, *Pcsk9*$^{-/-}$ mice also exhibited increased β oxidation through increased peroxisome proliferator-activated receptor (PPAR)α expression and simultaneously, reduced sterol regulatory element binding protein (SREBP)-1 and fatty acid synthase (FAS) expression, which are well-established markers of lipogenesis (Fig. 5B) (41). In line with these observations, qRT-PCR analysis also showed a decrease in markers of lipogenesis accompanied by marked increase in FA oxidation and lipolysis (Fig. 5C-F, *, $p<0.05$; NS, non-significant). Renal triglyceride content in the cortex was also significantly higher in the *Pcsk9*$^{-/-}$ mice relative to controls (Fig 5G, *, $p<0.05$). Similar to our *in vitro* findings, these data suggest that PCSK9 modulates renal CD36 expression and renal lipid levels *in vivo*.

Pcsk9$^{-/-}$ mice exhibit increased renal ER stress on a HFD

To further investigate the role of PCSK9 of renal lipid accumulation *in vivo*, 6-week old male *Pcsk9*$^{-/-}$ mice and age-matched C57BL/6J controls were fed either NCD, or HFD for 12 weeks prior to sacrifice. IHC analysis revealed an increase in the expression of ER stress marker phosphorylated-PERK (p-PERK) in the kidneys of HFD-fed *Pcsk9*$^{-/-}$ compared to HFD-fed *Pcsk9*$^{-/-}$ controls (Fig. 6A-B, *, $p<0.05$). CD36 and perilipin expression was induced by HFD and elevated in the *Pcsk9*$^{-/-}$ mice fed both NCD and HFD (Fig. 6A, C-D, *, $p<0.05$). Along with these observations, qRT-PCR also revealed an increase in mRNA abundance of ER stress markers in *Pcsk9*$^{-/-}$ compared to controls (Fig 6E, *, $p<0.05$). To correlate with these observations, renal triglyceride content was also observed to be significantly higher in *Pcsk9*$^{-/-}$ mice on both NCD and HFD (Fig 6F, *, $p<0.05$). Lastly, Thioflavin-S (28) also revealed increased fluorescence of protein aggregation in the HFD-fed *Pcsk9*$^{-/-}$ mice relative to its HFD-fed controls (Fig. 6G). These data suggest that PCSK9 is able to attenuate HFD-induced ER stress by modulating lipid uptake within the cortex of the kidney.

HFD-fed Pcsk9$^{-/-}$ mice exhibit increased renal fibrosis and inflammation

Next, we investigated the effect of NCD or HFD on renal injury in *Pcsk9*$^{-/-}$ mice. Initially, IHC staining revealed an increase in the expression of pro-inflammatory and pro-fibrotic markers, including NFκB p65, α-smooth muscle actin (SMA) and fibronectin in the *Pcsk9*$^{-/-}$ mice on HFD relative to its controls (Fig. 7A-D, *, $p<0.05$). To support these initial observations, qRT-PCR analysis also revealed that *Pcsk9*$^{-/-}$ mice on HFD exhibit increased pro-fibrotic, pro-apoptotic, and pro-inflammatory markers relative to controls (Fig. 7E, *, $p<0.05$). Together, these data demonstrate that *Pcsk9*$^{-/-}$ mice exhibit increased renal lipid accumulation as well as preliminary signs of renal injury and response.

Anti-PCSK9 mAb modulates surface expression of CD36 on renal epithelia

Commercially-available antibodies targeted against PCSK9 are well known to prevent the interaction between PCSK9 and the LDLR. Importantly, however, the location in which PCSK9 interacts with CD36 is not yet known and therefore, the effect of such antibodies on CD36 levels is not fully understood. To explore the outcome of this intruiging question, male C57BL/6J mice (n=10) were treated with Alirocumab (10 mg/kg) for seven days. Consistent with previous reports, ELISA data demonstrate that Alirocumab significantly increased circulating PCSK9 levels (Fig. 8A, *, $p<0.05$). IHC analysis then demonstrated that the administration of alirocumab significantly reduce surface and total staining of CD36 on renal epithelia (Fig. 8B-C, *, $p<0.05$). Immunoblots also support a reduction in CD36 protein expression (Fig. 8D, *, $p<0.05$). At the mRNA level, qRT-PCR demonstrate that markers of lipid metabolism, known to be upregulated during sterol deprivation were significantly reduced with the administration of PCSK9 mAbs, with the exception of the LDLR (Fig. 8E, *, $p<0.05$; NS, non-significant). Altogether, these findings suggest that the administration of PCSK9 mAbs is able to modulate relative expression of CD36 on the renal epithelia.

Discussion:

The lipid nephrotoxicity hypothesis, first postulated by Moorhead et al. in 1982 (29), suggests that dyslipidemia promotes CKD progression by inducing oxidative, inflammatory, and ER stress (7). Since this time, several studies have bridged the gap between renal lipid accumulation and kidney disease using a variety of in vitro and in vivo models, as well as clinical observations (5,6,7,8). Herein, we report that *Pcsk9*$^{-/-}$ mice exhibit increased expression of tubular CD36 and LDLR, which was associated with increased renal lipid accumulation. Consistent with our observations, others have demonstrated that PCSK9 is able to interact with surface receptors expressed on renal epithelia, although not to the same extent as the liver (30). Previous studies have also demonstrated the pathological role of CD36 in promoting intra-renal oxidative and ER stress by driving the uptake of modified lipoproteins and FFAs. Given that HFD is reported to induce renal ER stress, inflammation, and fibrosis (31, 32), we sought to investigate the effect of a HFD challenge in the context of elevated renal CD36 expression occurring as a result of PCSK9 deficiency.

PCSK9 is primarily expressed in the liver, the small intestine and the kidney (33). Despite our knowledge of its presence in the kidney, little is currently known about its potential role in kidney function and renal disease. Preliminary studies demonstrated that circulating PCSK9 is significantly elevated in multiple in vivo models of renal pathology (34,45). Recent studies have also shown a connection between circulating PCSK9 and its role in nephrotic syndrome (36). The

primary pathology associated with nephrotic syndrome is damage to the glomeruli and podocytes. Patients with this disease are also at an increased risk of atherosclerosis and thromboembolism due to a well-established dyslipidemia observed in most patients with CKD (43). Haas et al. demonstrated that podocyte damage-induced nephrotic syndrome increases plasma PCSK9 levels and leads to dyslipidemia; a dyslipidemia that was markedly attenuated in PCSK9 knockout mice (36). The up-regulation of circulating PCSK9 in multiple pathophysiological conditions is also consistent with our previous findings where we demonstrated that diet-induced hepatic steatosis also increases plasma PCSK9 concentrations (35). Overall, accumulating evidence suggest that the absence of PCSK9 has a protective effect against dyslipidemia in patients with renal disease. As circulating PCSK9 concentrations positively correlate with plasma cholesterol levels, these important findings highlight the role of PCSK9 as a driver of dyslipidemia in patients with CKD. In our studies, we demonstrate for the first time that PCSK9 deficiency promotes renal lipid deposition, likely occurring as a result of increased expression of receptors known to uptake lipids from circulation, such as CD36 and LDLR.

Clinically, current FDA-approved monoclonal antibodies against PCSK9, such as alirocumab and evolocumab, bind to the EGFa-binding domain of PCSK9 in order to prevent the interaction of PCSK9 with the LDLR (44). Recent studies have demonstrated that such antibodies increase circulating PCSK9 levels 7-fold as a result of the reduced rate of LDLR-mediated removal of PCSK9 from the circulation (37). Given that the domain in which PCSK9 interacts with CD36 remains unclear and may potentially differ from the LDLR, it is worth noting that the compensatory increase in circulating PCSK9 may enhance the degradation of renal CD36 and protect against lipid-induced renal injury. Herein for the first time, we report that PCSK9 mAbs such as alirocumab are able to reduce the surface expression of CD36 on the renal epithelia. These data strongly suggest that PCSK9 interacts with CD36 via a different domain that it does with the LDLR. Interestingly, qRT-PCR data also revealed that alirocumab reduced CD36 mRNA levels, thereby highlighting a second mechanism as to the observed reduction in surface CD36 expression. Given that alirocumab increases cellular cholesterol uptake through the LDLR (44), reduced expression of SREBP2, PCSK9 and CD36 may represent a negative feedback loop in order to reduce further lipid uptake and accumulation. Although we have shown that mAbs targeted against PCSK9 modulate renal CD36 levels, additional studies are required to determine whether anti-PCSK9 antibodies can attenuate diet-induced renal lipid accumulation in modulating renal injury.

Overall, we report here for the first time that PCSK9 has an extensive effect beyond hepatic lipid homeostasis by modulating the LDLR and CD36 on the renal epithelia. Given this effect, we observed that in turn, PCSK9 is able to attenuate CD36-driven ER stress, inflammation, and fibrosis in the context of diet-induced renal disease. Data demonstrating the extent to which the observed renal injury in *Pcsk9*$^{-/-}$ occurs as a result of excess diet-induced lipid uptake represents a limitation of this study. Recently, we have identified a mechanism in which the form of PCSK9 acts as a co-chaperone of the UPR in the liver (Lebeau et al., unpublished data), as well as in kidney (Byun et al., unpublished data) by promoting the stability of ER chaperones, GRP78 and GRP94. This raises the question of whether the observed increased ER stress in HFD-fed *Pcsk9*$^{-/-}$ may have occurred as a result of (1) increased lipid uptake, and also (2) as a result of increased sensitivity of ER stress due to a lack of renal stress-response chaperones. In addition to clarifying this point, future studies will also aim to determine whether intracellular or extracellular expression

of PCSK9 plays a bigger factor in the ER stress observed within this study using different models of CKD, and whether clinically-approved mAbs against PCSK9 affect renal lipid accumulation.

Figure Legends

Fig. 1 Secreted PCSK9 regulates the LDLR and CD36 in cultured renal cells
(A) Immunoblot of HuH7 cells transfected with either WT-PCSK9 or Q152H-PCSK9 and confirming relative secretion in media. (B) Relative protein expression of CD36 in HK-2 cells exposed to media harvested from HuH7 cells. (C,D) Immunofluorescence microscopy staining for surface CD36 and LDLR in HK-2 cells post-media swap experiment (*, $p<0.05$). (E) Relative secreted PCSK9 measured in HuH7 cells transfected with either WT-PCSK9 or Q152H-PCSK9 after 24 hours (*, $p<0.05$). (F) Secreted PCSK9 was also measured in HuH7 and HK-2 cells to confirm that renal cells do not secrete PCSK9 relative to hepatocytes in vitro (*, $p<0.05$; NS, non-significant). (G) mRNA transcript levels of PCSK9 and SREBP2 in HK-2 cells confirming that modulation of surface receptors were through exogenously added PCSK9 from hepatocytes (NS, non-significant). Data are represented as the mean and errors as the standard deviation. Differences between groups were determined using *t*-tests or ANOVAs. Scale bars, 200 μm.

Fig. 2 PCSK9 blocks OA and LDL-induced lipid droplet accumulation in renal cells
(A,B) ORO staining of HK-2 cells treated with OA (200 μM) for 18 hours in the presence or absence of PCSK9 from media (*, $p<0.05$). (C,D,E) HK-2 and rat mesangial cells were treated with fluorescently-labelled DiI-LDL cholesterol and quantified (*, $p<0.05$). (F) ORO staining of HK-2 cells showing the effects of V5 antibody (2μg/mL) in the absence of PCSK9 with the treatment of OA (*, $p<0.05$). Data are represented as the mean and errors as the standard deviation. Differences between groups were determined using *t*-tests or ANOVAs. Scale bars, (A) 10 μm. (C) 200 μm.

Fig. 3 PCSK9 regulates lipid accumulation in renal-derived cells in a manner dependent on CD36
(A,B) ORO staining of HK-2 cells treated with OA and or SSO (10μM), a well-established blocker of CD36 activity for 18 hours (*, $p<0.05$). (C,D) The effect of an siRNA targeted against CD36 was also assessed via ORO staining with the treatment of OA in HK-2 cells (*, $p<0.05$). (E,F) Uptake of fluorescently-labeled oxLDL was also measured in HK-2 cells and quantified using a spectrophotometer (*, $p<0.05$). (G) Immunoblot of CD36 confirming knockdown of its expression using siRNA targeted against CD36 (*, $p<0.05$). (H) Relative intracellular triglyceride levels measured in HK-2 cells treated with OA with the modulation of CD36 expression (*, $p<0.05$). Data are represented as the mean and errors as the standard deviation. Differences between groups were determined using *t*-tests or ANOVAs. Scale bars, 200 μm.

Fig. 4 PCSK9 protects from palmitate and oxidized LDL-induced ER stress in vitro
(A,B) Immunofluorescence microscopy of HK-2 cells stained for n-ATF6 treated with ox-LDL either in the presence or absence of PCSK9 (*, $p<0.05$). (C,D,E,F) qRT-PCR analysis of UPR activation markers in HK-2 cells (*, $p<0.05$). (G) Relative intracellular triglyceride levels measured in HK-2 cells treated with PA in the presence or absence of PCSK9 (*, $p<0.05$). (H) Quantification of Thioflavin-T fluorescent staining in HK-2 cells treated with PA in media

harvested from transfected HuH7 cells (*, $p<0.05$; NS, non-significant). Data are represented as the mean and errors as the standard deviation. Differences between groups were determined using *t*-tests or ANOVAs. Scale bars, 200 μm.

Fig. 5 *Pcsk9*$^{-/-}$ mice exhibit increased renal lipid accumulation on NCD
(A) Immunohistochemistry analysis staining for ORO, CD36, and perilipin levels to measure relative lipid accumulation in the renal cortex in vivo. (B) Immunoblot of the renal cortex in *Pcsk9*$^{-/-}$ mice and its relative controls for different markers of lipid metabolism (*, $p<0.05$). (C,D,E,F) qRT-PCR analysis of different genes involved in lipid droplet formation, lipogenesis, fatty acid oxidation, and lipolysis (*, $p<0.05$; NS, non-significant). (G) Relative intra-renal triglyceride content assessed in *Pcsk9*$^{-/-}$ relative to controls (*, $p<0.05$). Data are represented as the mean and errors as the standard deviation. Differences between groups were determined using *t*-tests or ANOVAs. Scale bars, 100 μm.

Fig. 6 *Pcsk9*$^{-/-}$ mice exhibit increased renal ER stress on a high-fat diet
(A,B,C,D) IHC analysis and quantification of the renal cortex of *Pcsk9*$^{-/-}$ mice and relevant controls on HFD for p-PERK, CD36, and perilipin (*, $p<0.05$). (E) qRT-PCR analysis of UPR activation in the renal cortex of the mice (*, $p<0.05$). (F) Relative intra-renal triglyceride content assessed in *Pcsk9*$^{-/-}$ mice placed under NCD or HFD relative to controls (*, $p<0.05$). (G) Thioflavin-S staining of the renal cortex to confirm intracellular protein aggregation. Data are represented as the mean and errors as the standard deviation. Differences between groups were determined using *t*-tests or ANOVAs. Scale bars, 100 μm.

Fig. 7 *Pcsk9*$^{-/-}$ mice exhibit increased renal fibrosis and inflammation on a high-fat diet
(A,B,C,D) IHC staining of markers of inflammation and fibrosis assessed in *Pcsk9*$^{-/-}$ mice placed either on NCD or HFD relative to controls (*, $p<0.05$). (E) qRT-PCR analysis of pro-fibrotic, inflammatory, and apoptotic markers confirming initial observations made in the renal cortex of these mice (*, $p<0.05$). Data are represented as the mean and errors as the standard deviation. Differences between groups were determined using *t*-tests or ANOVAs. Scale bars, 100 μm.

Fig. 8 PCSK9 mAb modulates surface expression of CD36 on renal epithelia
(A) Relative secreted PCSK9 measured in WT mice treated with either vehicle or alirocumab (*, $p<0.05$). (B,C) IHC of CD36 assessed in WT mice with relative quantifications (*, $p<0.05$). (D) Immunoblot of CD36 protein expression in renal cortex (*, $p<0.05$). (E) qRT-PCR analysis of lipid metabolism in renal cortex (*, $p<0.05$; NS, non-significant). Data are represented as the mean and errors as the standard deviation. Differences between groups were determined using *t*-tests or ANOVAs. Scale bars, 100 μm.

References

1. Hill NR, Fatoba ST, Oke JL, Hirst JA, O'Callaghan CA, Lasserson DS, Hobbs FDR: Global prevalence of chronic kidney disease – a systematic review and meta-Analysis. *PLoS One* 11: e0158765, 2016
2. Metcalfe W: How does early chronic kidney disease progress?: A background paper prepared for the UK consensus conference on early chronic kidney disease. *Nephrol. Dial. Transplant.* 22: ix26–ix30, 2007
3. Bigot A, Gusto G, Copin N, Sautenet B, Lantieri O, Halimi J-M: Body mass index, fatty liver index and other metabolic disturbances differentially affect albuminuria and glomerular filtration rate in the general population. *J. Diabetes Metab.* 05: 1000387, 2014
4. Singh GM, Danaei G, Farzadfar F, Stevens GA, Woodward M, Wormser D, Kaptoge S, Whitlock G, Qiao Q, Lewington S, Di Angelantonio E, vander Hoorn S, Lawes CMM, Ali MK, Mozaffarian D, Ezzati M: The age-specific quantitative effects of metabolic risk factors on cardiovascular diseases and diabetes: A pooled analysis. *PLoS One* 8: e65174, 2013
5. GBD 2015 Obesity Collaborators: Health effects of overweight and obesity in 195 Countries over 25 years. *N. Engl. J. Med.* 377: 13–27, 2017
6. Lee SM, Park M, Yoon H-J: Association of body mass index with estimated glomerular filtration rate and incident proteinuria In: *Proceedings of the 11th International Joint Conference on Biomedical Engineering Systems and Technologies*, pp 587–590, 2018
7. Kuwahara S, Hosojima M, Kaneko R, Aoki H, Nakano D, Sasagawa T, Kabasawa H, Kaseda R, Yasukawa R, Ishikawa T, Suzuki A, Sato H, Kageyama S, Tanaka T, Kitamura N, Narita I, Komatsu M, Nishiyama A, Saito A: Megalin-mediated tubuloglomerular alterations in high-fat diet–induced kidney disease. *J. Am. Soc. Nephrol.* 27: 1996–2008, 2016
8. Aukema HM: Lipids in chronic kidney disease: Alterations and interventions. *Lipid Technol.* 25: 207–209, 2013
9. Martino-Costa AL, Malhão F, Lopes C, Dias-Pereira P: Renal interstitial lipid accumulation in cats with chronic kidney disease. *J. Comp. Pathol.* 157: 75–79, 2017
10. Kume S, Uzu T, Araki S, Sugimoto T, Isshiki K, Chin-Kanasaki M, Sakaguchi M, Kubota N, Terauchi Y, Kadowaki T, Haneda M, Kashiwagi A, Koya D: Role of altered renal lipid metabolism in the development of renal injury induced by a high-fat diet. *J. Am. Soc. Nephrol.* 18: 2715–2723, 2007
11. Yang P, Xiao Y, Luo X, Zhao Y, Zhao L, Wang Y, Wu T, Wei L, Chen Y: Inflammatory stress promotes the development of obesity-related chronic kidney disease via CD36 in mice. *J. Lipid Res.* 58: 1417–1427, 2017
12. de Vries APJ, Ruggenenti P, Ruan XZ, Praga M, Cruzado JM, Bajema IM, D'Agati VD, Lamb HJ, Barlovic DP, Hojs R, Abbate M, Rodriquez R, Mogensen CE, Porrini E: Fatty kidney: emerging role of ectopic lipid in obesity-related renal disease. *Lancet Diabetes Endocrinol.* 2: 417–426, 2014
13. Inagi R, Ishimoto Y, Nangaku M: Proteostasis in endoplasmic reticulum—new mechanisms in kidney disease. *Nat. Rev. Nephrol.* 10: 369–378, 2014
14. Fu S, Yang L, Li P, Hofmann O, Dicker L, Hide W, Lin X, Watkins SM, Ivanov AR, Hotamisligil GS: Aberrant lipid metabolism disrupts calcium homeostasis causing liver endoplasmic reticulum stress in obesity. *Nature* 473: 528–531, 2011

15. Dickhout JG, Carlisle RE, Austin RC: Interrelationship between cardiac hypertrophy, heart failure, and chronic kidney disease. *Circ. Res.* 108: 629–642, 2011
16. Kennedy DJ, Chen Y, Huang W, Viterna J, Liu J, Westfall K, Tian J, Bartlett DJ, Tang WHW, Xie Z, Shapiro JI, Silverstein RL: CD36 and Na/K-ATPase-α1 form a proinflammatory signaling loop in kidney. *Hypertension* 61: 216–224, 2013
17. Susztak K, Ciccone E, McCue P, Sharma K, Böttinger EP: Multiple metabolic hits converge on CD36 as novel mediator of tubular epithelial apoptosis in diabetic nephropathy. *PLoS Med.* 2: e45, 2005
18. Okamura DM, López-Guisa JM, Koelsch K, Collins S, Eddy AA: Atherogenic scavenger receptor modulation in the tubulointerstitium in response to chronic renal injury. *Am. J. Physiol. Physiol.* 293: F575–F585, 2007
19. Hua W, Huang H, Tan L, Wan J, Gui H, Zhao L, Ruan X, Chen X, Du X: CD36 Mediated fatty acid-induced podocyte apoptosis via oxidative stress. *PLoS One* 10: e0127507, 2015
20. Ruan XZ, Varghese Z, Powis SH, Moorhead JF: Human mesangial cells express inducible macrophage scavenger receptor. *Kidney Int.* 56: 440–451, 1999
21. Zoccali C: Traditional and emerging cardiovascular and renal risk factors: An epidemiologic perspective. *Kidney Int.* 70: 26–33, 2006
22. Goldsmith DJ: Cardiovascular disease and chronic kidney disease: overview. In: *Oxford Textbook of Clinical Nephrology*, 4th ed., edited by Turner NN, Lameire N, Goldsmith DJ, Winearls CG, Himmelfard J, Rumuzzi G, Bennet WG, de Broe ME, Chapman JR, Covic A, Vivekanad J, Sheerin N, Unwin R, Woolf A, Oxford, Oxford University Press, 2015
23. Fasano T, Cefalù AB, Di Leo E, Noto D, Pollaccia D, Bocchi L, Valenti V, Bonardi R, Guardamagna O, Averna M, Tarugi P: A novel loss of function mutation of PCSK9 gene in white Ssubjects with low-plasma low-density lipoprotein cholesterol. *Arterioscler. Thromb. Vasc. Biol.* 27: 677–681, 2007
24. Cohen J, Pertsemlidis A, Kotowski IK, Graham R, Garcia CK, Hobbs HH: Low LDL cholesterol in individuals of African descent resulting from frequent nonsense mutations in PCSK9. *Nat. Genet.* 37: 161–165, 2005
25. Cohen JC, Boerwinkle E, Mosley TH, Hobbs HH: Sequence variations in PCSK9, low LDL, and protection against coronary heart disease. *N. Engl. J. Med.* 354: 1264–1272, 2006
26. Demers A, Samami S, Lauzier B, Des Rosiers C, Sock ETN, Ong H, Mayer G: PCSK9 induces CD36 degradation and affects long-chain fatty acid uptake and triglyceride metabolism in adipocytes and in mouse liver significance. *Arterioscler. Thromb. Vasc. Biol.* 35: 2517–2525, 2015
27. Poirier S, Mayer G, Benjannet S, Bergeron E, Marcinkiewicz J, Nassoury N, Mayer H, Nimpf J, Prat A, Seidah NG: The proprotein convertase PCSK9 induces the degradation of low density lipoprotein receptor (LDLR) and its closest family members VLDLR and ApoER2. *J. Biol. Chem.* 283: 2363–2372, 2008
28. Bussière T, Bard F, Barbour R, Grajeda H, Guido T, Khan K, Schenk D, Games D, Seubert P, Buttini M: Morphological characterization of thioflavin-S-positive amyloid plaques in transgenic Alzheimer mice and effect of passive Aβ immunotherapy on their clearance. *Am. J. Pathol.* 165: 987–995, 2004
29. Mayne J, Dewpura T, Raymond A, Bernier L, Cousins M, Ooi TC, Davignon J, Seidah NG, Mbikay M, Chretien M: Novel loss-of-function PCSK9 variant is associated with low

Plasma LDL cholesterol in a french-canadian family and with impaired processing and secretion in cell culture. *Clin. Chem.* 57: 1415–1423, 2011

30. Lebeau PF, Byun JH, Platko K, Al-Hashimi AA, Lhoták Š, MacDonald ME, Mejia-Benitez A, Prat A, Igdoura SA, Trigatti B, Maclean KN, Seidah NG, Austin RC: PCSK9 knockout exacerbates diet-induced non-alcoholic steatohepatitis, fibrosis and liver injury in mice. *J. Heptatology Reports* 2019
31. Sekiya M, Yahagi N, Matsuzaka T, Takeuchi Y, Nakagawa Y, Takahashi H, Okazaki H, Iizuka Y, Ohashi K, Gotoda T, Ishibashi S, Nagai R, Yamazaki T, Kadowaki T, Yamada N, Osuga J, Shimano H: SREBP-1-independent regulation of lipogenic gene expression in adipocytes. *J. Lipid Res.* 48: 1581–1591, 2007
32. Moorhead JF, El-Nahas M, Chan MK, Varghese Z: Lipid nephrotoxicity in chronic progressive glomerular and tubulo-interstitial disease. *Lancet* 320: 1309–1311, 1982
33. Schmidt RJ, Beyer TP, Bensch WR, Qian Y-W, Lin A, Kowala M, Alborn WE, Konrad RJ, Cao G: Secreted proprotein convertase subtilisin/kexin type 9 reduces both hepatic and extrahepatic low-density lipoprotein receptors in vivo. *Biochem. Biophys. Res. Commun.* 370: 634–640, 2008
34. Sleeman P, Patel NN, Lin H, Walkden GJ, Ray P, Welsh GI, Satchell SC, Murphy GJ: High fat feeding promotes obesity and renal inflammation and protects against post cardiopulmonary bypass acute kidney injury in swine. *Crit. Care* 17: R262, 2013
35. Noeman SA, Hamooda HE, Baalash AA: Biochemical study of oxidative stress markers in the liver, kidney and heart of high fat diet induced obesity in rats. *Diabetol. Metab. Syndr.* 3: 17, 2011
36. Seidah NG, Benjannet S, Wickham L, Marcinkiewicz J, Jasmin SB, Stifani S, Basak A, Prat A, Chretien M: The secretory proprotein convertase neural apoptosis-regulated convertase 1 (NARC-1): Liver regeneration and neuronal differentiation. *Proc. Natl. Acad. Sci.* 100: 928–933, 2003
37. Konarzewski M, Szolkiewicz M, Sucajtys-Szulc E, Blaszak J, Lizakowski S, Swierczynski J, Rutkowski B: Elevated circulating PCSK-9 concentration in renal failure patients is corrected by renal replacement therapy. *Am. J. Nephrol.* 40: 157–163, 2014
38. Sucajtys-Szulc E, Szolkiewicz M, Swierczynski J, Rutkowski B: Up-regulation of liver Pcsk9 gene expression as a possible cause of hypercholesterolemia in experimental chronic renal failure. *Mol. Cell. Biochem.* 411: 281–287, 2016
39. Haas ME, Levenson AE, Sun X, Liao W-H, Rutkowski JM, de Ferranti SD, Schumacher VA, Scherer PE, Salant DJ, Biddinger SB: The role of proprotein convertase subtilisin/kexin type 9 in nephrotic syndrome-associated hypercholesterolemia. *Circulation* 134: 61–72, 2016
40. Agrawal S, Zaritsky JJ, Fornoni A, Smoyer WE: Dyslipidaemia in nephrotic syndrome: mechanisms and treatment. *Nat. Rev. Nephrol.* 14: 57–70, 2018
41. Lebeau PF, Byun JH, Platko K, MacDonald ME, Poon S V., Faiyaz M, Seidah NG, Austin RC: Diet-induced hepatic steatosis abrogates cell-surface LDLR by inducing de novo PCSK9 expression in mice. *J. Biol. Chem.* 294: 9037–9047, 2019
42. Seidah NG: The PCSK9 revolution and the potential of PCSK9-based therapies to reduce LDL-cholesterol. *Glob. Cardiol. Sci. Pract.* 2017: 2017
43. Shapiro MD, Miles J, Tavori H, Fazio S: Diagnosing resistance to a proprotein convertase subtilisin/kexin type 9 Inhibitor. *Ann. Intern. Med.* 168: 376, 2018

Figure 1.

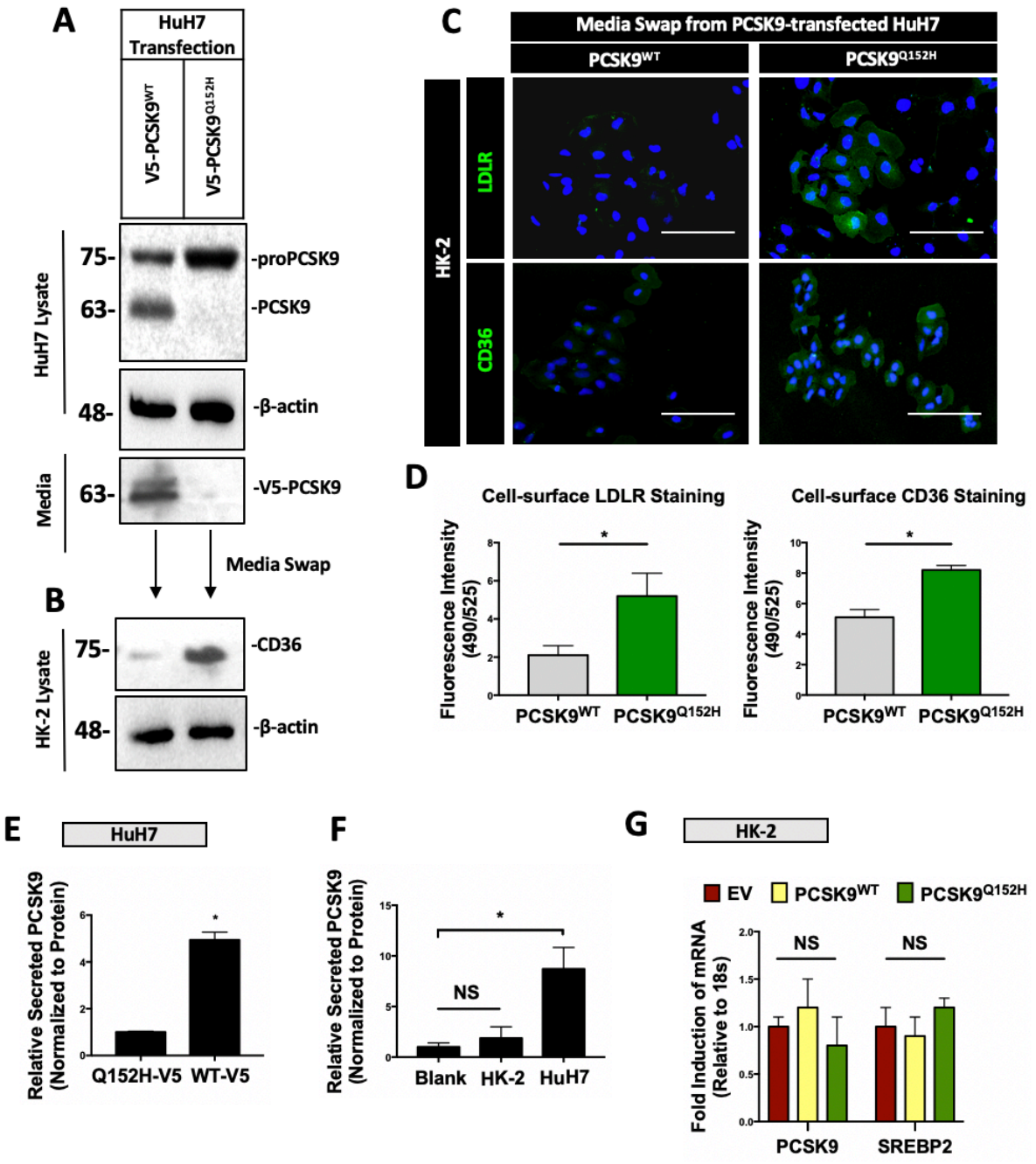
A
HuH7 Transfection
V5-PCSK9WT
V5-PCSK9Q152H
HuH7 Lysate
75-
63-
-proPCSK9
-PCSK9
48-
-β-actin
Media
63-
-V5-PCSK9
Media Swap
B
HK-2 Lysate
75-
-CD36
48-
-β-actin
C
Media Swap from PCSK9-transfected HuH7
PCSK9WT
PCSK9Q152H
HK-2
LDLR
CD36
D
Cell-surface LDLR Staining
Cell-surface CD36 Staining
Fluorescence Intensity (490/525)
PCSK9WT
PCSK9Q152H
E
HuH7
Relative Secreted PCSK9 (Normalized to Protein)
Q152H-V5
WT-V5
F
Relative Secreted PCSK9 (Normalized to Protein)
NS
Blank
HK-2
HuH7
G
HK-2
EV
PCSK9WT
PCSK9Q152H
Fold Induction of mRNA (Relative to 18s)
NS
NS
PCSK9
SREBP2

Figure 2.

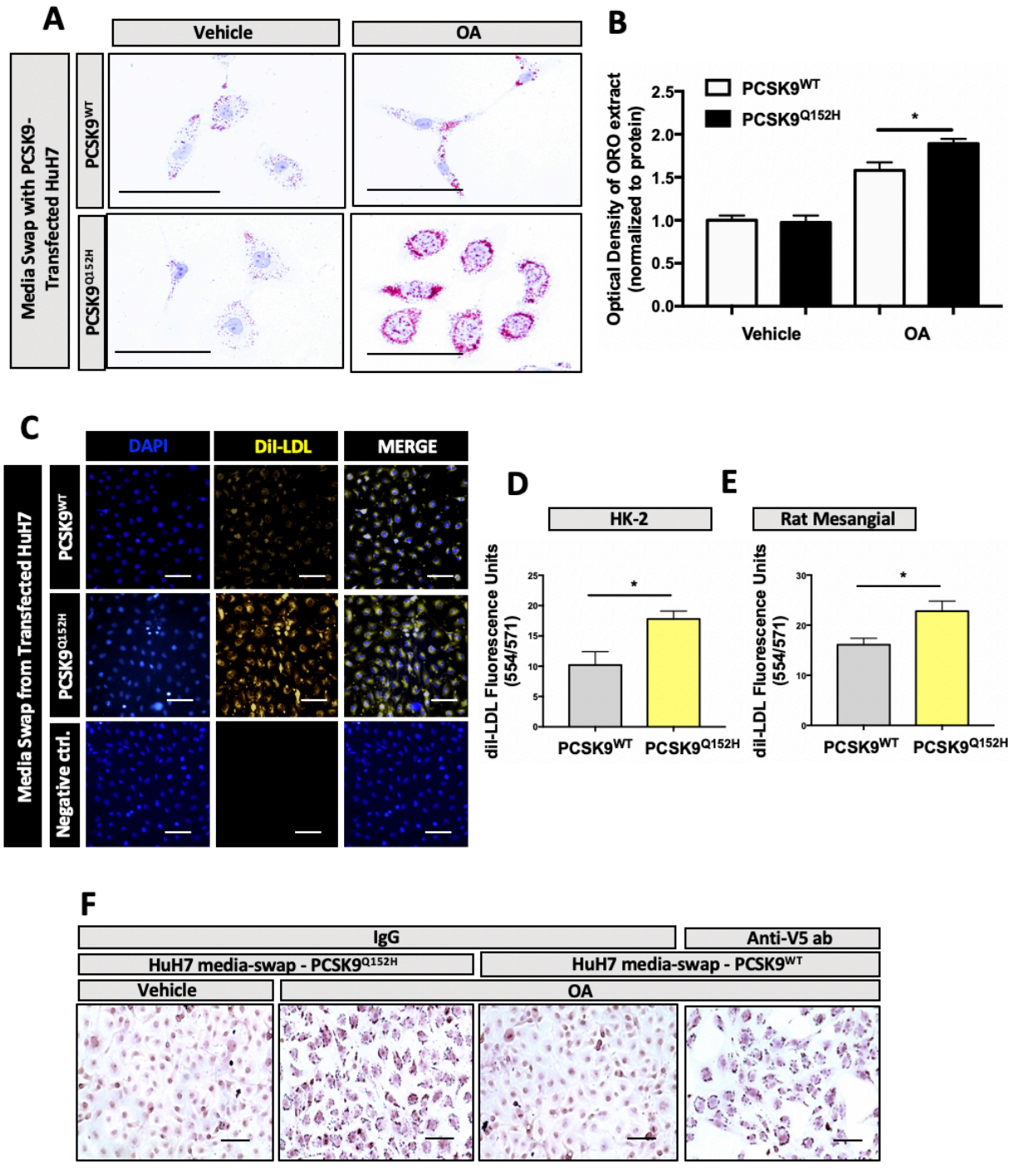
A
Vehicle
OA
Media Swap with PCSK9-Transfected HuH7
PCSK9WT
PCSK9Q152H
B
Optical Density of ORO extract (normalized to protein)
PCSK9WT
PCSK9Q152H
*
2.5
2.0
1.5
1.0
0.5
0.0
Vehicle
OA
C
DAPI
DiI-LDL
MERGE
Media Swap from Transfected HuH7
PCSK9WT
PCSK9Q152H
Negative ctrl.
D
HK-2
dil-LDL Fluorescence Units (554/571)
*
PCSK9WT
PCSK9Q152H
E
Rat Mesangial
dil-LDL Fluorescence Units (554/571)
*
PCSK9WT
PCSK9Q152H
F
IgG
Anti-V5 ab
HuH7 media-swap - PCSK9Q152H
HuH7 media-swap - PCSK9WT
Vehicle
OA

Figure 3.

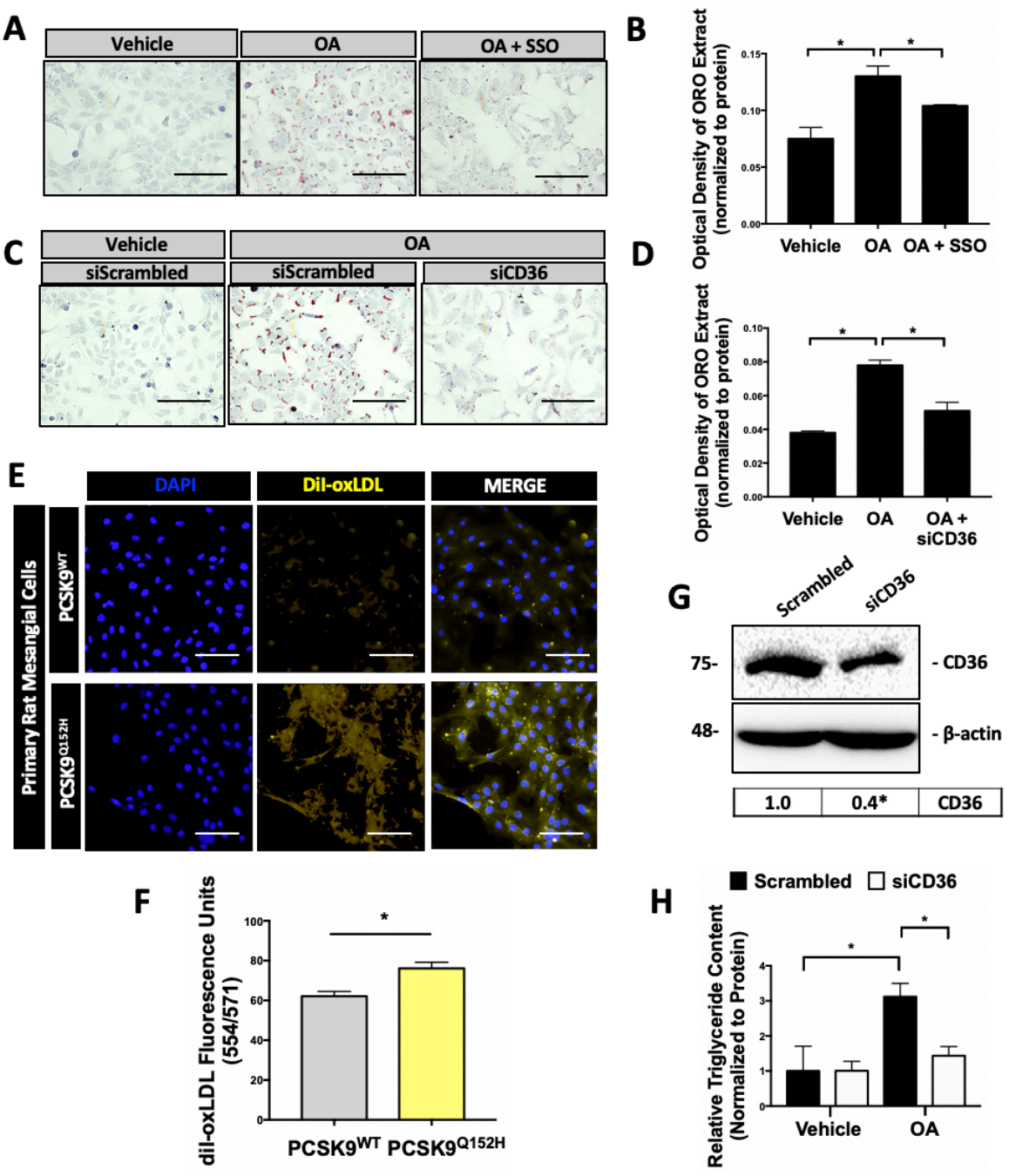
A
Vehicle
OA
OA + SSO
B
Optical Density of ORO Extract (normalized to protein)
Vehicle
OA
OA + SSO
C
Vehicle
OA
siScrambled
siScrambled
siCD36
D
Optical Density of ORO Extract (normalized to protein)
Vehicle
OA
OA + siCD36
E
DAPI
DiI-oxLDL
MERGE
Primary Rat Mesangial Cells
PCSK9WT
PCSK9Q152H
F
dil-oxLDL Fluorescence Units (554/571)
PCSK9WT
PCSK9Q152H
G
Scrambled
siCD36
75-
- CD36
48-
- β-actin
1.0
0.4*
CD36
H
Scrambled
siCD36
Relative Triglyceride Content (Normalized to Protein)
Vehicle
OA

Figure 4.

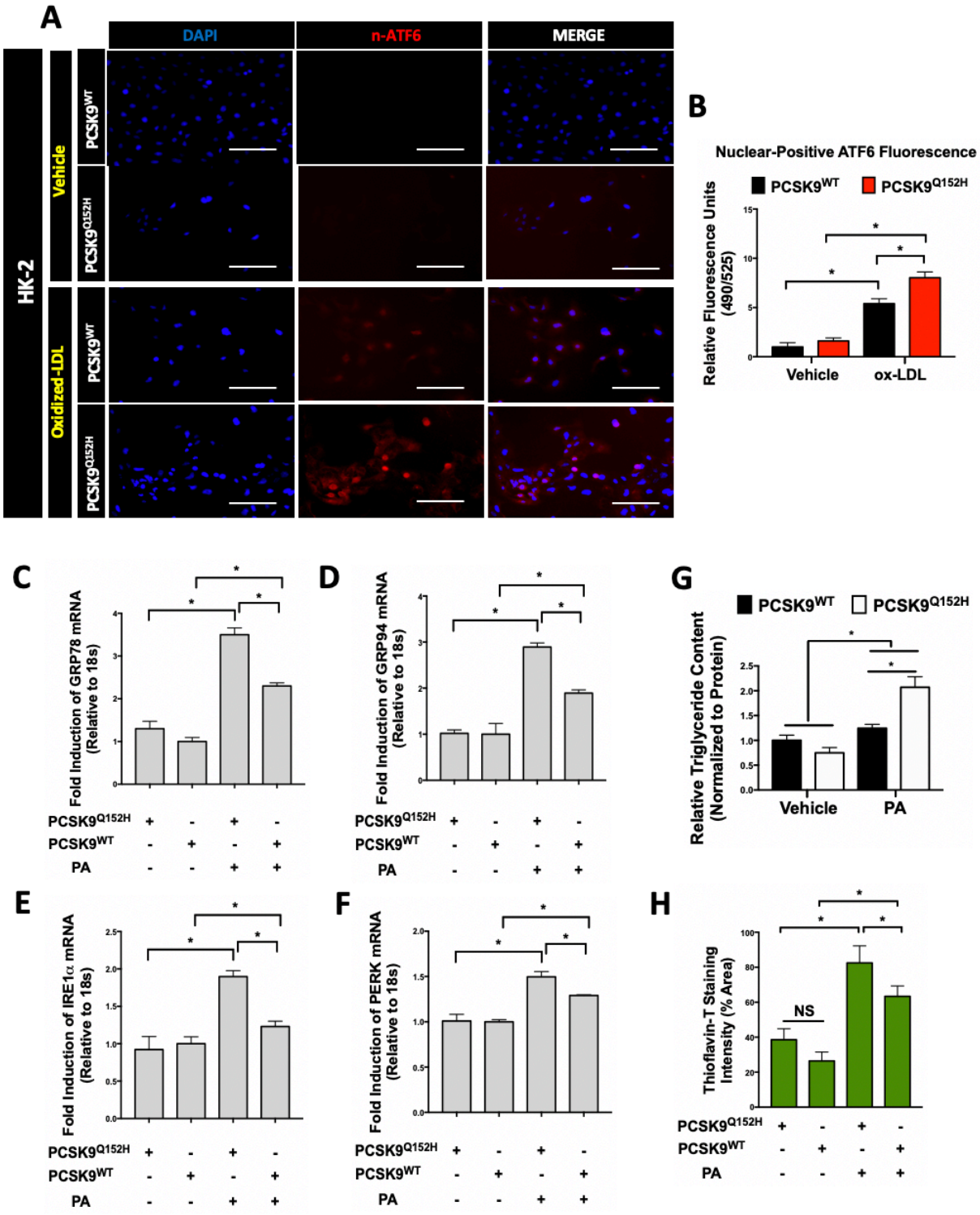
A
DAPI
n-ATF6
MERGE
HK-2
Vehicle
Oxidized-LDL
PCSK9WT
PCSK9Q152H
B
Nuclear-Positive ATF6 Fluorescence
PCSK9WT
PCSK9Q152H
Relative Fluorescence Units (490/525)
Vehicle
ox-LDL
C
Fold Induction of GRP78 mRNA (Relative to 18s)
D
Fold Induction of GRP94 mRNA (Relative to 18s)
G
Relative Triglyceride Content (Normalized to Protein)
Vehicle
PA
E
Fold Induction of IRE1α mRNA (Relative to 18s)
F
Fold Induction of PERK mRNA (Relative to 18s)
H
Thioflavin-T Staining Intensity (% Area)
NS

Figure 5.

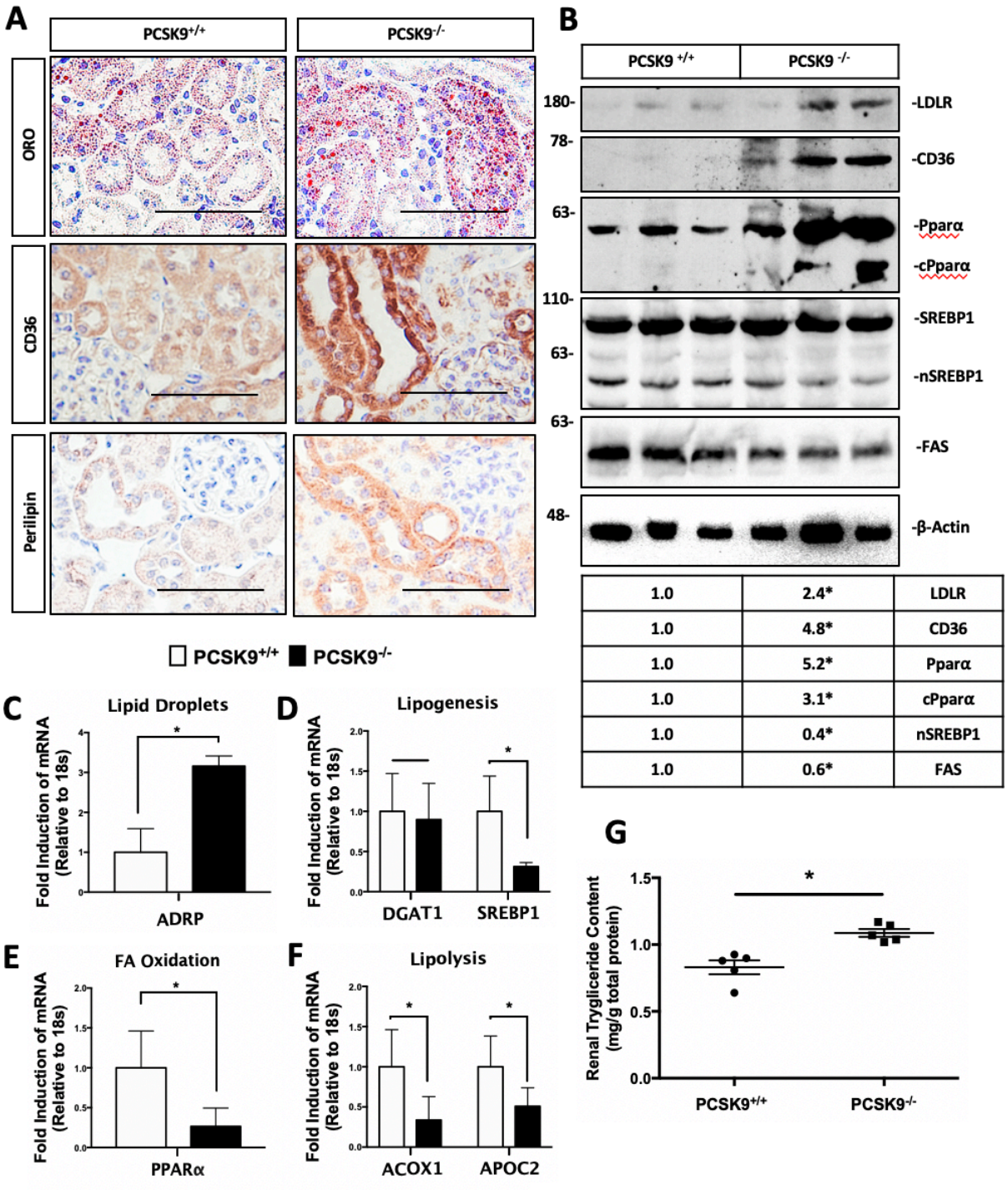

1.0	2.4*	LDLR
1.0	4.8*	CD36
1.0	5.2*	Pparα
1.0	3.1*	cPparα
1.0	0.4*	nSREBP1
1.0	0.6*	FAS

Figure 6.

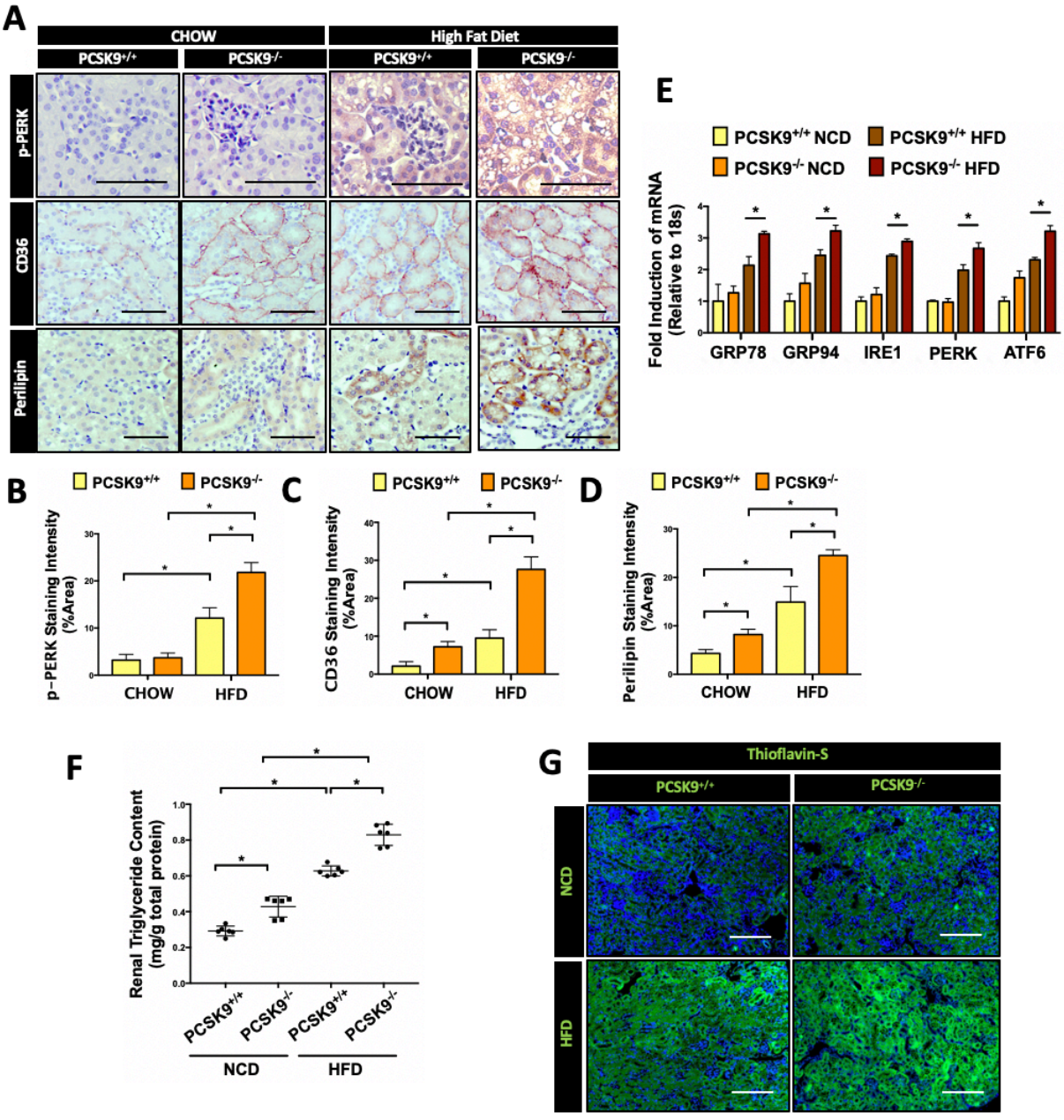
A
CHOW
High Fat Diet
PCSK9+/+
PCSK9-/-
PCSK9+/+
PCSK9-/-
p-PERK
CD36
Perilipin
E
PCSK9+/+ NCD
PCSK9+/+ HFD
PCSK9-/- NCD
PCSK9-/- HFD
Fold Induction of mRNA (Relative to 18s)
GRP78
GRP94
IRE1
PERK
ATF6
B
PCSK9+/+
PCSK9-/-
p-PERK Staining Intensity (%Area)
CHOW
HFD
C
PCSK9+/+
PCSK9-/-
CD36 Staining Intensity (%Area)
CHOW
HFD
D
PCSK9+/+
PCSK9-/-
Perilipin Staining Intensity (%Area)
CHOW
HFD
F
Renal Triglyceride Content (mg/g total protein)
PCSK9+/+
PCSK9-/-
PCSK9+/+
PCSK9-/-
NCD
HFD
G
Thioflavin-S
PCSK9+/+
PCSK9-/-
NCD
HFD

Figure 7.

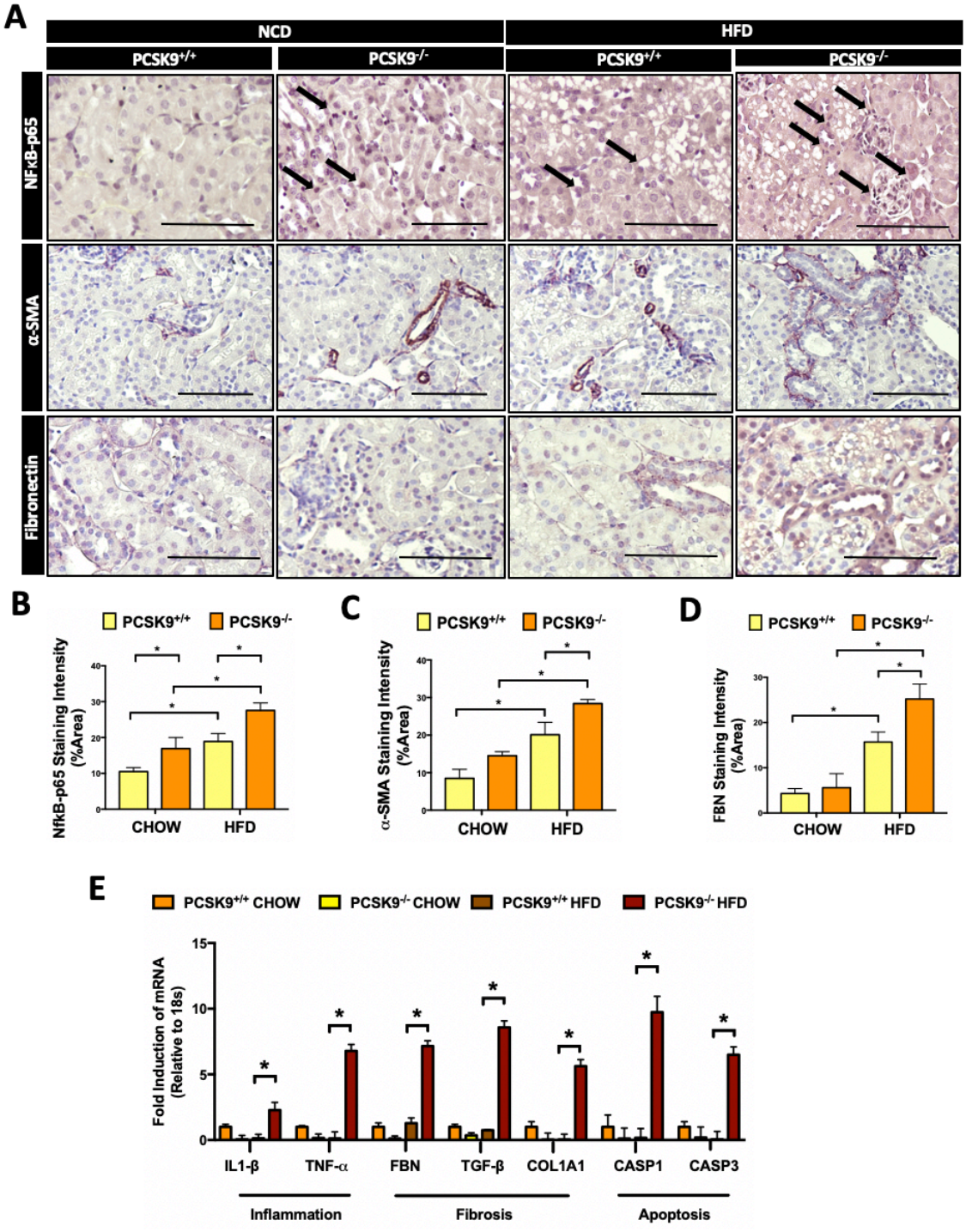
A
NCD
HFD
PCSK9+/+
PCSK9-/-
PCSK9+/+
PCSK9-/-
NFκB-p65
α-SMA
Fibronectin
B
PCSK9+/+
PCSK9-/-
NfkB-p65 Staining Intensity (%Area)
CHOW
HFD
C
PCSK9+/+
PCSK9-/-
α-SMA Staining Intensity (%Area)
CHOW
HFD
D
PCSK9+/+
PCSK9-/-
FBN Staining Intensity (%Area)
CHOW
HFD
E
PCSK9+/+ CHOW
PCSK9-/- CHOW
PCSK9+/+ HFD
PCSK9-/- HFD
Fold Induction of mRNA (Relative to 18s)
IL1-β
TNF-α
FBN
TGF-β
COL1A1
CASP1
CASP3
Inflammation
Fibrosis
Apoptosis

Figure 8.

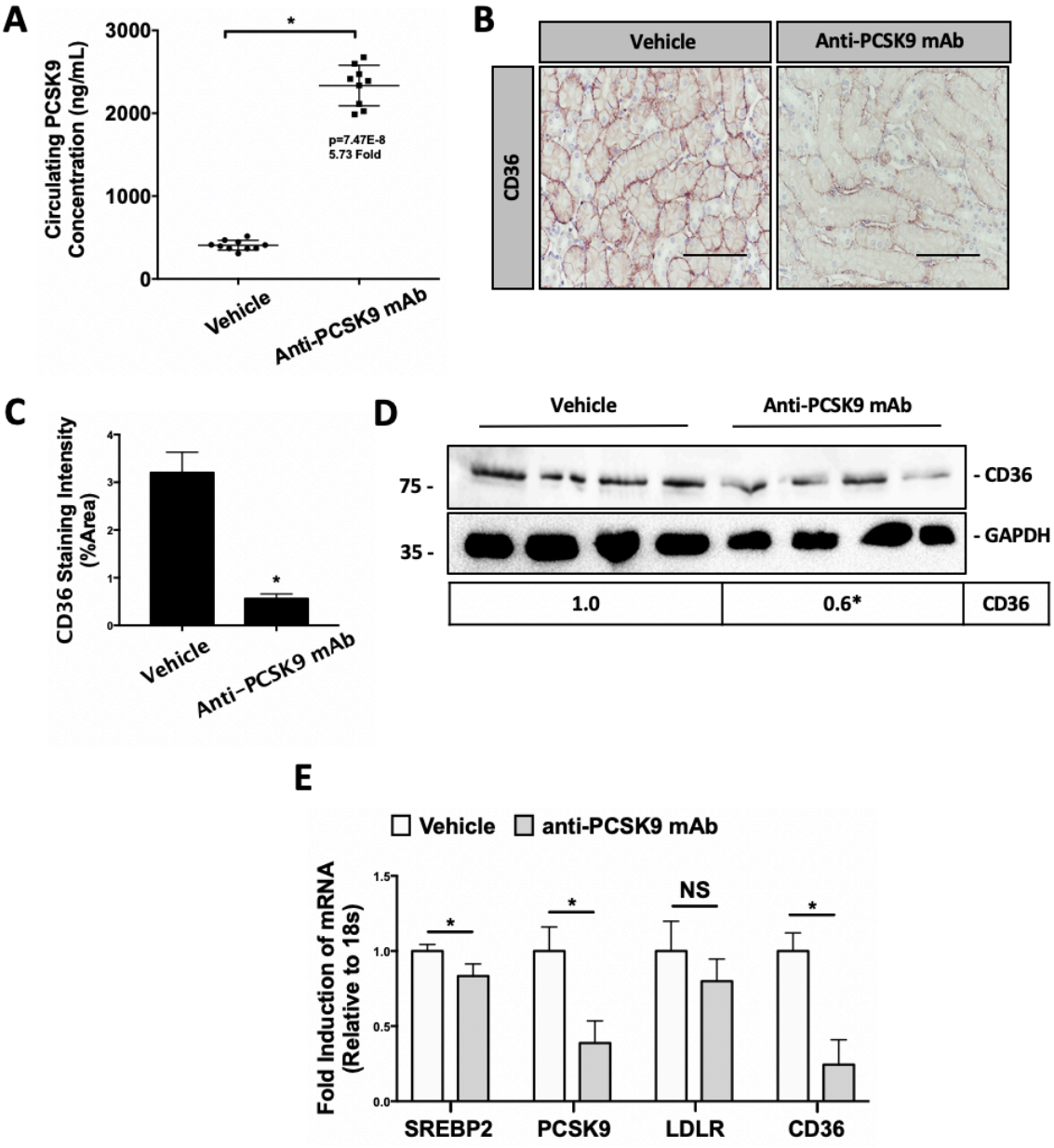
A
Circulating PCSK9 Concentration (ng/mL)
3000
2000
1000
0
*
p=7.47E-8
5.73 Fold
Vehicle
Anti-PCSK9 mAb
B
Vehicle
Anti-PCSK9 mAb
CD36
C
CD36 Staining Intensity (%Area)
4
3
2
1
0
*
Vehicle
Anti-PCSK9 mAb
D
Vehicle
Anti-PCSK9 mAb
75 -
35 -
- CD36
- GAPDH
1.0
0.6*
CD36
E
Vehicle
anti-PCSK9 mAb
Fold Induction of mRNA (Relative to 18s)
1.5
1.0
0.5
0.0
*
*
NS
*
SREBP2
PCSK9
LDLR
CD36

Table 1. Antibodies used for immunoblotting and immunohistochemical analysis

Gene	Catalog no.	Application	Dilution
PCSK9	NB300-959, Novus Biologicals	IB	1:500
B-Actin	A2228, Sigma-Aldrich	IB	1:3000
CD36	NB400-144, Novus Biologicals	IB/IHC	1:1000/1:500
Perilipin	ab3526, Abcam	IHC	1:100
LDLR	AF2255, R and D Systems	IB	1:1000
PPARα	SC-398394	IB	1:1000
SREBP1	ab28481	IB	1:1000
FAS	ab110021, Abcam	IB	1:1000
GRP78	610979	IB	1:1000
GRP94	ADI-SPA-850, Enzo Life Sciences	IB	1:1000
IRE1α	14C10, Cell Signaling	IB	1:1000
p-PERK	ab192591, Abcam	IHC	1:100
NfkB-p65			
α-SMA	MA5-11547, ThermoFisher Scientific	IHC	1:100
FBN-1	ab2413, Abcam	IHC	1:200

Table 2. Primers used for quantitative real time PCR.

Gene	Species	Forward	Reverse
GRP78	**Human**	CATCACGCCG TCCTATGTCG	CGTCAAAGAC CGTGTTCTCG
GRP94	**Human**	GCTTCGGTCA GGGTATCTTT	AGGCTCTTCT TCCACCTTTG
PERK	**Human**	GTCCGGAACC AGACGATGAG	GGCTGGATGA CACCAAGGAA
IRE1α	**Human**	GAAAAGGAAT CCCTGGATGG	TCAGAGGGCG TCTGGAGTC
ADRP	**Mouse**	TCTCAGGGGT GGTGGATAAG	TCTACCAGCA GCTCCGACTT
DGAT1	**Mouse**	CTGATCCTGA GTAATGCAAG GTT	TGGATGCAAT AATCACGCAT GG
SREBP1	**Mouse**	GCCGGCGCCA TGGACGAGCT GGCC	CAGGAAGGCT TCCAGAGAGG AGGC
PPARα	**Mouse**	GAAGGGCACA CGCGTGCGAG TTTCAG	CTGTGATGAC AACGTCTTGT TCCCGAACT
ACOX1	**Mouse**	TCTCAGGGGT GGTGGATAAG	TCTACCAGCA GTCCGACTT
APOC2	**Mouse**	CTCTGCTGGG CACGGTGCA	GCCGCCGAGC TTTTGCTGTAC
GRP78	**Mouse**	GTCCTGCATC ATCAGCAAAG	GGTAGCCACA TACTGAACAC C
GRP94	**Mouse**	GATGGTCTGG CAACATGGAG	CGCCTTGGTG TCTGGTAGAA
IRE1α	**Mouse**	TGAAACACCC CTTCTTCTG	CCTCCTTTTCT ATTCGGTCAC TT
PERK	**Mouse**	AAAAAGCAGT GGGATTTGGA	CTGGAATATA CCGAAGTTCA AAG
ATF6	**Mouse**	GGACGAGGTG GTGTCAGAG	GACAGCTCTT CGCTTTGGAC

6. Manuscript prepared for the Journal of Scientific Reports, Nature

Byun J. H., P. F. Lebeau, K. Platko, R. E. Carlisle, M. Faiyaz, M.E. Macdonald, R. Esselman, J. G. Dickhout, J. C. Krepinsky, N.G. Seidah, and R. C. Austin (2020) Renal PCSK9 protects against AngII/DOCA induced progression of CKD in mice. *Prepared for the Journal of Scientific Reports, Jan 2020*

Author Contributions: J.H.B., N.G.S., and R.C.A. conceptualization; J.H.B., P.F.L., K.P., R.C., R.E., and M.F data curation; J.H.B software; J.H.B formal analysis; J.H.B and P.F.L supervision; J.H.B. validation; J.H.B., P.F.L, K.P., R.C., M.F., J.C., M.E.M., J.G.D., J.C.K., and R.C.A. investigation; J.H.B. visualization; J.H.B., R.C., K.P., and J.G.D. methodology; J.H.B. writing original draft; J.H.B., P.F.L., and R.C.A. project administration; J.H.B., P.F.L, K.P., R.C., M.E.M., J.G.D., J.C.K., N.G.S., and R.C.A. writing-review and editing; R.E., N.G.S., and R.C.A. resources; R.C.A. funding acquisition.

Personal thesis contribution: As the primary author of this paper, I have provided most of the *in vitro* and *in vivo* data curation and experimental analysis which contributed towards all the figures of this manuscript. In addition, I wrote the original draft of the manuscript and am currently overseeing the publication process of this paper into the Journal of Scientific Reports.

Renal PCSK9 protects against AngII/DOCA induced progression of CKD in mice

Jae Hyun Byun[*], *Paul F. Lebeau*[1], *Khrystyna Platko*[1], *Rachel E. Carlisle*[1], *Mahi Faiyaz*[1], *Melissa E. Macdonald*[1] , *Rachid Esselman*[2], *Jeffrey G. Dickhout*[1], *Joan C. Krepinsky*[1], *Nabil G. Seidah*[2], *and Richard C. Austin*[1†]

Affiliations: [1]*From the Department of Medicine, Division of Nephrology, McMaster University, St. Joseph's Healthcare Hamilton and Hamilton Centre for Kidney Research, Hamilton, Ontario L8N 4A6, Canada, the* [2]*Laboratory of Biochemical Neuroendocrinology, Clinical Research Institute of Montreal, affiliated to the University of Montreal, Montreal, Quebec H2W 1R7, Canada*

† To whom correspondence should be addressed: Richard C. Austin, PhD, 50 Charlton Ave East, Room T-3313, Hamilton, Ontario, L8N 4A6

Running Title: PCSK9 protects against ER-stress induced CKD progression

Conflict of interest: The authors do not have competing interests to declare.

Financial Support: This work was supported in part by research grants to Richard C. Austin from the Heart and Stroke Foundation of Canada (G-13-0003064 and G-15-0009389), the Canadian Institutes of Health Research (74477), CIHR foundation grant (148363) and Canada Research Chair (216684). Financial support from the Research Institute of St. Joseph's Healthcare Hamilton is acknowledged. Richard C. Austin is a Career Investigator of the Heart and Stroke Foundation of Ontario and holds the Amgen Canada Research Chair in the Division of Nephrology at St. Joseph's Healthcare and McMaster University.

Author Contributions: JHB, NGS, and RCA conceived the studies. JHB, PL, KP, RC, and MF performed all of the in vitro and in vivo studies. The manuscript was written by JHB, PL, NGS, and RCA and revised by KP, RC, JD, and JK.

Keywords: CKD, renal injury, PCSK9, ER stress, inflammation, fibrosis, apoptosis

Abbreviations: CKD, chronic kidney disease; CVD, cardiovascular disease; ESRD, end-stage renal disease; PCSK9, proprotein convertase subtilisin/kexin type-9; LDLc, low-density lipoprotein cholesterol; AngII, angiotensin II; ER, endoplasmic reticulum; UPR, unfolded protein response; GRP78, glucose-regulated protein of 78kDa; ATF6, activating transcription factor 6; IRE1, inositol-requiring enzyme I; PERK, PKR-like ER kinase; LDLR, low-density lipoprotein receptor; LOF, loss-of-function; GOF, gain-of-function; WT, wild-type; FBS, fetal bovine serum; ERAI, ER stress-activated indicator; TG, thapsigargin; TM, tunicamycin; PBS, phosphate-buffered saline; UNX, uninephrectomy; IHC, immunohistochemical; n-, nuclear; GRP94, glucose-regulated protein of 94kDa; XBP1, x-box binding protein-1; p-PERK, phospho-PERK; 4-PBA, 4-phenylbutyric acid; SREBP, sterol-regulatory element binding protein

GRP94, glucose-regulated protein of 94kDa; XBP1, x-box binding protein-1; p-PERK, phospho-PERK; 4-PBA, 4-phenylbutyric acid; SREBP, sterol-regulatory element binding protein

Abstract

Background: Chronic kidney disease (CKD) is a global health concern due to its increasing worldwide prevalence and its cause remains to be elucidated. However, several lines of evidence implicate the association between endoplasmic reticulum (ER) stress and CKD progression demonstrated in clinical patients and multiple animal models. Recently, we have identified the role of intracellular proprotein convertase subtilisin/kexin type-9 (PCSK9) as a co-chaperone in the ER lumen by upregulating ER-resident chaperones independent of UPR activation in order to alleviate ER stress. Given that PCSK9 is well-expressed in hepatocytes and also in the renal cortex, we sought to investigate whether renal PCSK9 can protect against ER-stress induced renal injury using an established model of CKD.
Methods: To investigate the role of renal PCSK9, cultured renal cells and Pcsk9$^{-/-}$ mice were overexpressed with human PCSK9 and assessed for UPR activation either in the presence or absence of ER-stress inducing agents, thapsigargin or tunicamycin. Pcsk9$^{-/-}$ mice were then assessed for ER-stress induced renal injury using an AngII/DOCA CKD model.
Results: We observed that overexpression of PCSK9 in cultured renal cells can protect against basal UPR activation or with an agent that is well-known to induce ER stress. Consistent with these observations, we also observed that Pcsk9$^{-/-}$ mice exhibit increased renal fibrosis, inflammation, and apoptosis with the AngII/DOCA therapy relative to wild-type (WT) controls.
Conclusions: Overall, we demonstrate here that the depletion of intracellular PCSK9 in the kidney exacerbates renal ER stress and subsequent injury. In multiple mouse models, the expression of renal PCSK9 is able to modulate ER stress through the attenuation of UPR activation.

Introduction

Chronic kidney disease (CKD) is a rising global health concern due to its increasingly worldwide prevalence (1). Several profound risk factors including proteinuria, hypertension, and poor glucose control all work in concert to increase the progression of CKD, in which patients eventually result in end stage renal disease (ESRD) (2). Patients reaching ESRD require renal replacement therapy consisting of dialysis and renal transplants that are extremely costly, contributing to the economic burden of healthcare by approximately $35 billion per year in the United States (2,3). Moreover, these individuals are also associated with various complications including cardiovascular disease (CVD), cognitive decline, anemia, and imbalance in bone and mineral deposition (1). Currently, there is no absolute cure for CKD, as present available treatments are only responsible for reducing the rate of CKD progression. Thus, studies investigating therapeutics aimed at halting CKD is an important public health initiative and of high importance.

A crucial regulator of kidney pathogenesis and injury may be attributed to endoplasmic reticulum (ER) stress (4,5). The ER is responsible for the global synthesis of secretory,

transmembrane, and ER-resident proteins. In pathological conditions, this leads to the imbalance between the protein folding demand and the protein folding capacity, resulting in the accumulation and aggregation of misfolded proteins. As a compensatory response, the ER triggers the activation of the unfolded protein response (UPR). Upon activation, the UPR induces the dissociation of ER-resident chaperones such as the glucose-regulated protein of 78kDa (GRP78) from three transmembrane proteins, namely: the activating transcription factor 6 (ATF6), inositol-requiring enzyme I (IRE1), and protein kinase RNA (PKR)-like ER kinase (PERK). The activation of these three transducers often results in cell death, inflammation, and fibrosis in the context of CKD progression (6,7). Clinically, ER stress has shown to be highly associated in the pathogenesis of various renal diseases including glomerulonephritis (8), diabetic nephropathy (9), and acute kidney injury (AKI) (10).

CKD patients are also highly associated with an increased risk in CVD (13). In the general population, circulating LDL cholesterol (LDLc) is a crucial driver of atherosclerotic lesion formation and CVD progression. In 2003, the proprotein convertase subtilisin kexin/type-9 (PCSK9) was primarily discovered by Seidah and colleagues as a crucial regulator of lipid homeostasis due to its ability to modulate the cell-surface expression of the low-density lipoprotein (LDL) receptor (LDLR) (11). Clinically, loss-of-function (LOF) PCSK9 mutations conferred significantly attenuated LDLc levels, while gain-of-function (GOF) mutations increased plasma LDLc levels (12). Thus, the development of monoclonal antibodies targeted against PCSK9, capable of reducing circulating LDLc by approximately 60%, strongly suggests that PCSK9 acts as a crucial regulator of lipid metabolism and subsequent CVD risk.

Independent of lipid metabolism, the current landscape of studies investigating the relationship between PCSK9 and other pathologies is not well-known. However, given that chronic ER stress contributes to the progression of CKD (4,5,7,8), emerging studies are targeting at the alleviation of renal ER stress as a therapeutic approach to kidney disease. In our lab, we are first to report that ER retention of PCSK9 does not induce UPR activation in hepatocytes. Furthermore, hepatic overexpression of PCSK9 and its retention variant, the $PCSK9^{Q152H}$, further protected against ER stress by increasing the protein abundance of GRP78 and the glucose-regulated protein of 94kDa (GRP94) independent of UPR activation. Altogether, these initial emerging studies suggest that PCSK9 may have a distinct intracellular, ER-resident role as a co-chaperone to attenuate ER stress and protect against liver disease. Given that PCSK9 is well-expressed in hepatocytes and also in the kidney, we investigated in this study whether PCSK9 is capable of modulating UPR activation in the context of an established CKD model in vivo. We observed that *Pcsk9*$^{-/-}$ mice exhibit significantly increased renal ER stress, inflammation, and fibrosis relative to wild-type (WT) controls on the Angiotensin II (AngII)/DOCA salt model. Given these observations, we report for the first time that intracellular renal PCSK9 is capable of attenuating ER-stress induced renal injury.

Materials and Methods

Cell Culture, Transfections and ER stress-inducing treatments:

Human immortalized proximal tubule epithelial (HK-2) and immortalized hepatocytes (Huh-7) were cultured in Dulbecco's Modified Eagle Medium (Gibco, ThermoFisher Scientific) and

supplemented with 10% fetal bovine serum (FBS) (Sigma-Aldrich), 50 IU/ml of penicillin and 100µg/ml streptomycin (Sigma-Aldrich). All cells were maintained in 5% CO_2 at 37°C. For culture experiments, cells were plated at a confluence of 60% and transfected with a cocktail consisting of the following ratio: 1µg DNA:3 µl X-tremeGENE HP DNA reagent:100 µl Opti-MEM. The cDNA of human WT PCSK9 was cloned into pIRES-EGFP with a V5-tag inserted between the N-terminal signal peptide. Moreover, as a relative measure of ER stress and UPR activation in cells, HK-2 cells were transfected with an ER stress-activated indicator (ERAI) plasmid. Briefly, under conditions of ER stress, the ER stress-specific intron is spliced and removed from the ERAI mRNA transcript leading to a frameshift and subsequent production of functional FLAG-spliced x-box binding protein-1 (XBP1). Cells were treated with either thapsigargin (TG) (100nM) or tunicamycin (TM) (1µg/mL) for 18h, unless otherwise stated.

TM Model Animal Studies

Both 12-week and 50-week old mice on a C57BL/6J background and age-matched controls were given intraperitoneal injection of either phosphate-buffered saline (PBS) or TM (0.5mg/kg) and sacrificed 3 days later. All animal procedures were approved in accordance with McMaster University animal care guidelines.

PCSK9 Transgenic Model Animal Studies

Briefly, a composite human albumin promoter containing a 235 bp SV40 enhancer element and a 213 bp albumin promoter element (pDRIVE-SV40-hAlb, InvivoGen, San Diego, CA) was used to control the expression of full-length human PCSK9 cDNA containing a C-terminal V5 tag. To enhance this expression, a chimeric intron (pRL-SV40, Promega, Madison, Wisconsin) was inserted between the PCSK9 cDNA and the promoter to enhance the expression. The V5-tagged hPCSK9 construct was injected into the pronucleus of fertilized eggs from the C57BL6J/N strain mice. Confirmation of transgenic founders and their offspring was identified by a PCR product amplified from insulator sequences. These transgenic animals were sacrificed at 12 weeks of age and were a generous gift by Dr. Nabil Seidah.

CKD Model Animal Studies

10-week old mice on a C57BL/6J background and age-matched controls underwent uninephrectomy (Unx) 2 weeks before the initiation of the experiment. The mice were then given 1% sodium chloride in the drinking water and implanted subcutaneously with a DOCA pellet (Innovative Research of America, M-121) and an angiotensin II (AngII)-infused (Sigma) model 1004 ALZET osmotic pump. The DOCA was a 50 mg 21-day releasing pellet while 1.5ng of AngII was delivered per minute per gram of bodyweight by the osmotic pump. All mice were sacrificed on day 14 after the initial implantation. All animal procedures were approved and were in collaboration with Dr. Jeffrey Dickhout's group by the McMaster University Animal Research Ethics Board.

Blood Pressure Measurements

Blood pressure of mice was obtained through tail cuff plethysmography using a CODA (Kent Scientific) blood pressure analyzer. Mice were positioned on a heating pad and were placed in restraint to be provided with the tail cuff. The cuff measured absolute systolic blood pressure, diastolic blood pressure, heart rate, and flow rate.

Immunoblotting
Cells and tissues were lysed in SDS-containing buffer containing protease and phosphatase inhibitor (Roche). Protein concentrations were measured using a modified Lowry protein assay (Bio-Rad), electrophoretically resolved on 7-10% polyacrylamide gels, and subsequently transferred to nitrocellulose membranes. Membranes were blocked using 5% w/v skimmed milk in tris-buffered saline (TBS) containing Tween-20 for 1 h and incubated in primary antibody overnight for 18 h at 4˚C. To detect bound primary antibodies, horse radish peroxidase (HRP) conjugated antibodies were used (goat anti-rabbit, Bio-Rad; donkey anti-goat, Santa Cruz, goat anti-mouse, Bio-Rad) and developed using a chemiluminescent reagent (FroggaBio). Quantification of immunoblots was assessed after normalization to β-actin (Sigma-Aldrich). Please refer to Table 1 for a list of the antibodies used for this study.

Real-time Polymerase Chain Reaction (PCR)
Total RNA was isolated using RNA purification kit according to manufacturer's instructions (ThermoFisher Scientific). A total of 2 µg of RNA was reverse-transcribed to cDNA using SuperScript Vilo IV cDNA synthesis kit (ThermoFisher Scientific). Quantitative real-time PCR (qRT-PCR) assessment of different mRNA species was used in conjunction with FAST SYBR Green (ThermoFisher Scientific). All primer sequences are listed in Table 2.

Immunofluorescent staining
Cells were fixed using 4% paraformaldehyde and either non-permeabilized or permeabilized with 0.025% Triton-X in PBS, and blocked with 1% BSA for 30 min. Cells were then stained with anti-FLAG (catalog no. SC-121-G, Santa Cruz Biotechnology) or anti-GRP78 (catalog no. catalog no. 610979, BD Biosciences) for 1h. Following primary antibody incubation, cells were fluorescently labelled with Alexa 594 (catalog no. A11058, Thermo Fisher Scientific) as well as DAPI. Slides were mounted using permafluor and visualized using the EVOS FL color imaging system.

Creatinine Quantification
Plasma creatinine (Sigma-Aldrich) was measured using a colorimetric assay as per manufacturer's instructions.

PCSK9 ELISA
Quantification of PCSK9 in media was determined as per manufacturer's instructions using the R and D systems human Quantikinine PCSK9 ELISA.

Immunohistochemical (IHC) Staining
4 µm thick sections were deparaffinized, blocked in 5% v/v serum and subsequently incubated with primary antibodies for 18 h at 4˚C. Sections were incubated with biotin-labeled secondary antibodies (Vector Laboratories). Streptavidin-labeled HRP solution (Vector Laboratories) and NovaRed developing solution (Vector Laboratories) were used to visualize the staining. Slides were examined using a Nikon light microscope (Nikon DS-Ri2). Relative staining intensity was quantified using ImageJ software (n=10). For Picro Sirius Red (PSR) staining, kidney sections were exposed to saturated picric acid solution and stained with Sirius red F3B (Color Index 35782).

Statistical Analysis
Statistical analysis for two-group comparisons was conducted using unpaired Student's *t*-test and for multiple group comparison, one-way ANOVA was used. Statistically significant differences were considered at $p<0.05$. All error bars are represented as standard deviation of the mean.

Results

Overexpression of hPCSK9 increases chaperone abundance independent of UPR activation in HK-2 cells
Given that PCSK9 is also expressed in the kidney (40), we wanted to assess the effects of intracellular overexpression of PCSK9 in HK-2 cells. In this experiment, HK-2 cells were transfected with a CMV-driven plasmid overexpressing PCSK9 with a C-terminal V5 tag. We initially observed an increase in chaperone protein expression, GRP78 and GRP94, with an attenuation in UPR activation as shown with IRE1α, and n-ATF6 (Fig. 1A). The increase in GRP78 chaperone expression was also confirmed using immunofluorescent microscopy with the overexpression of PCSK9, which was subsequently quantified (Fig. 1B-C; *, $p<0.05$). Quantitative real-time PCR also confirmed that overexpression of PCSK9 was able to attenuate UPR activation on the transcriptional level (Fig. 1D; *, $p<0.05$). Lastly, circulating PCSK9 confirmed that the majority of its expression was intracellular compared to the HuH7 hepatocyte cell line (Fig 1E; *, $p<0.05$). This was normalized to relative GFP fluorescence, which was also normalized to relative protein concentration. Altogether, this data suggests that overexpression of PCSK9 is able to attenuate basal UPR activation by upregulating ER chaperones, GRP78 and GRP94.

Overexpression of hPCSK9 attenuates ER stress and cytotoxicity in renal cells
Next, we wanted to assess if intracellular PCSK9 in HK-2 cells was able to attenuate ER-stress induced UPR activation. Firstly, HK-2 cells were transfected with an ER stress-activated indicator (ERAI) plasmid which inherently expresses the Flag-sXBP1 protein. Subsequently, WT PCSK9 was overexpressed in HK-2 cells and treated with an ER Ca^{2+} depleting agent, thapsigargin, to induce ER stress. Western blot of p-IRE1 and flag-sXBP1 demonstrated that overexpression of PCSK9 is able to reduce thapsigargin-induced ER stress in HK-2 cells (Fig. 2A; *, $p<0.05$). Immunofluorescence microscopy of Flag-sXBP1 confirmed that PCSK9 is able to attenuate thapsigargin-induced immunofluorescence in HK-2 cells (Fig 2B-C; *, $p<0.05$). Moreover, overexpression of PCSK9 was able to reduce relative percent cellular cytotoxicity induced by thapsigargin and tunicamycin (Fig 2D; *, $p<0.05$). Lastly, quantitative real-time PCR also confirmed that overexpression of PCSK9 was able to attenuate mRNA levels of UPR activation induced by thapsigargin (Fig 2E; *, $p<0.05$). Collectively, the data suggests that overexpression of PCSK9 is able to attenuate thapsigargin and tunicamycin-induced ER stress and cellular cytotoxicity in cultured renal cells.

Overexpression of hPCSK9 increases chaperone abundance independent of UPR activation and attenuates ER stress in Pcsk9$^{-/-}$ mice
To further characterize the co-chaperone role of renal PCSK9 in vivo, we investigated the effects of transgenic overexpression of human PCSK9 (hPCSK9) into a *Pcsk9*$^{-/-}$ mouse model in the kidney. The presence of hPCSK9 was first assessed using IHC staining to confirm the experimental design. Subsequently, we observed that the transgenic overexpression of hPCSK9

increased GRP78 and GRP94 IHC staining, with a corresponding reduction in UPR activation through the assessment of phospho-PERK staining intensity (Fig 3A-B; *, $p<0.05$). To confirm our initial findings, qRT-PCR analysis of the kidney cortex also demonstrated a significant reduction in mRNA levels of UPR activation (Fig 3C; *, $p<0.05$). Similar to our initial observations from IHC, western blots confirmed that overexpression of hPCSK9 is able to increase the expression of ER-resident chaperones while reducing UPR activation (Fig 3D; *, $p<0.05$). Taken together, this suggests that transgenic overexpression of hPCSK9 is able to attenuate basal UPR activation by stabilizing GRP78 and GRP94 expression.

Pcsk9*$^{-/-}$ *mice exhibit increased ER stress and UPR activation induced by tunicamycin

Subsequently, we wanted to assess the effects of UPR activation in the absence of PCSK9. IHC analysis of 12-week old *Pcsk9*$^{-/-}$ mice exhibited reduced GRP78 expression with both PBS and TM treatment. As a potential compensatory response, nuclear CHOP staining was increased in the *Pcsk9*$^{-/-}$ mice with tunicamycin treatment (Fig 4A-C; *, $p<0.05$). Furthermore, in 50-week old mice, the treatment of an ER-stress inducing agent, tunicamycin, *Pcsk9*$^{-/-}$ mice exhibited increased mRNA of UPR activation relative to wild-type controls (Fig. 4D-G; *, $p<0.05$) This observation was also confirmed using western blot analysis (Fig. 4H; *, $p<0.05$).

Pcsk9*$^{-/-}$ *mice exhibit increased CKD-induced ER stress in DOCA/AngII mouse model

Next, we wanted to investigate whether the absence of PCSK9 is able to further induce ER stress in a DOCA/AngII CKD mouse model. Initially, we observed that *Pcsk9*$^{-/-}$ mice exhibited modestly heavier renal tissue weight than wild-type controls with the DOCA/AngII therapy (Fig. 5A, *, $p<0.05$). Given that this is a hypertensive model, the systolic blood pressure of *Pcsk9*$^{-/-}$ mice were significantly increased, but with no significant differences in overall diastolic blood pressure (Fig 5B-C, *, $p<0.05$). Next, relative UPR activation was assessed by staining for phospho-PERK using IHC. Quantified using ImageJ, *Pcsk9*$^{-/-}$ mice exhibited increased staining of phospho-PERK on the AngII/DOCA therapy relative to the wild-type controls (Fig 5D-E; *, $p<0.05$). To confirm this observation, we also observed that *Pcsk9*$^{-/-}$ mice increased UPR activation with a simultaneous reduction in chaperone expression of GRP78 (Fig 5F; *, $p<0.05$). Lastly, relative mRNA transcript levels of UPR activation demonstrated that *Pcsk9*$^{-/-}$ mice exhibited increased UPR activation with and without the AngII/DOCA therapy (Fig 5G-J; *, $p<0.05$). Overall, the data suggests that the absence of PCSK9 in the kidney significantly increases ER stress and systolic blood pressure relative to wild-type controls in a murine model of CKD.

Pcsk9*$^{-/-}$ *mice exhibit increased renal fibrosis and inflammation in DOCA/AngII mouse model

As our final objective, we aimed to characterize renal injury in the sham or AngII/DOCA *Pcsk9*$^{-/-}$ mice relative to controls. CD36 and picro sirius red staining, markers of inflammation and fibrosis respectively, were significantly greater in the *Pcsk9*$^{-/-}$ mice on the AngII/DOCA therapy relative to the wild type controls. Interestingly however, periodic acid-Schiff (PAS) staining demonstrated that *Pcsk9*$^{-/-}$ mice exhibited significantly less protein cast formation than their respective controls (Fig 6A-D; *, $p<0.05$). As a measure of renal function and clearance, serum creatinine levels were significantly higher in the *Pcsk9*$^{-/-}$ mice on the AngII/DOCA therapy (Fig. 6E; *, $p<0.05$). Lastly, to confirm our initial observations, mRNA levels of pro-fibrotic, inflammatory, and apoptotic markers were also significantly higher in the *Pcsk9*$^{-/-}$ mice than the wild-type controls (Fig. 6F; *, $p<0.05$).

Discussion

Since its seminal discovery by Seidah and colleagues (14), PCSK9 has been established as a crucial regulator of lipid metabolism through its ability to degrade the hepatic LDLR and thus, increase circulating LDLc levels (12). In recent years however, circulating PCSK9 has been shown to modulate a variety of other receptors known to play an important role in HIV (17), sodium homeostasis (16), and triglyceride uptake (18). However, despite our extensive knowledge in the role of circulating PCSK9, its intracellular role in tissue still remains to be elucidated.

PCSK9 has been shown to be primarily expressed in the liver, but also well-expressed in the kidney cortex, cerebellum, and the intestines (14). Thus, it asks the question why PCSK9 is exclusively secreted by hepatocytes (19) and what the role of non-secreted, intracellular PCSK9 may be in other tissues. Herein, we report that in the absence of intracellular renal PCSK9, *Pcsk9*$^{-/-}$ mice exhibit increased renal injury as a response to the AngII/DOCA therapy. Recently, we have identified a mechanism in which the intracellular retention of PCSK9 encourages its capability to act as a co-chaperone of the UPR in the liver (Lebeau et al., unpublished). Given this observation, we also demonstrate here that the kidney cortex of *Pcsk9*$^{-/-}$ mice exhibit reduced chaperone expression and subsequent UPR activation. As a result, *Pcsk9*$^{-/-}$ mice also displayed significantly increased serum creatinine levels and markers of renal fibrosis and inflammation compared to WT controls.

Consistent with these observations, others have demonstrated that ER stress is able to promote renal injury using the same AngII/DOCA salt murine model of CKD (20). As a way to inhibit UPR activation, Mohammed et al. reported that the administration of a chemical chaperone, 4-phenylbutyric acid (4-PBA) was able to decrease blood pressure, interstitial fibrosis, and renal inflammation induced by this CKD model. Interestingly, as the DOCA/AngII model was able to upregulate markers of UPR activation, the PCSK9 gene was also significantly upregulated, with a greater increase with the administration of 4-PBA. Given that chaperones such as GRP78 and GRP94 are heavily upregulated in conditions of ER stress (21), the observation that the DOCA/AngII therapy is able to increase PCSK9 expression suggests that this may possibly be a compensatory response and implies a chaperone-like role that it may have in the ER lumen.

Similarly, our group has previously reported the role of ER stress in the modulation of hepatic PCSK9 and LDLR. Using agents that cause ER Ca^{2+} depletion, Lebeau et al. demonstrated that changes in Ca^{2+} levels in the ER lumen has a distinct effect on the transcriptional regulation of endogenous PCSK9 via Ca^{2+}-dependent sterol regulatory element binding protein (SREBP)-2 activation (22). Furthermore, others have shown that TG-mediated activation of the SREBP family and ER stress could be reversed with the treatment of the Ca^{2+}-chelating agents such as BAPTA (23). In the present study, given that the overexpression of PCSK9 is also able to reduce thapsigargin-induced ER stress in cultured renal cells, it is worth investigating if the endogenous retention of PCSK9 is able to increase ER luminal Ca^{2+} levels in order to attenuate UPR activation.

Interestingly however, despite the increased transcriptional activity of PCSK9, Lebeau and colleagues also concluded that ER stress was able to block the secretion of PCSK9 and increase cell-surface LDLR in primary hepatocytes (22). Although its mechanism remains to be elucidated, recent reports identified GRP94 as an ER-resident binding partner of PCSK9, and thus, its upregulation through ER stress may explain how it is able to hinder the exit of PCSK9 from the ER lumen (24). However, the inherent biological reason as to why ER stress promotes the retention of PCSK9 despite increasing its expression remains unknown, but suggests again, that PCSK9 may have a distinct role inside the ER lumen. Given that intracellular PCSK9 is able to stabilize the expression of chaperones such as GRP78 and GRP94, future studies should elucidate if the absence of these chaperones can promote the secretion of PCSK9 in other tissues aside from the liver.

In the clinical context of PCSK9 inhibition, recent studies have demonstrated that monoclonal antibodies targeted against PCSK9 is able to reduce circulating cholesterol levels of up to 70% in combination with statin therapy. However, given its high cost and lack of affordability, this perpetuates the need at finding alternative therapeutic approaches at reducing PCSK9. Since this time, the development of inclisiran, an siRNA targeted against PCSK9 has recently been approved to transition into Phase III clinical trials (25). In the randomized, double-blind, phase II ORION-1 trial, a two-dose regimen of inclisiran exhibited approximately a 70% reduction in circulating PCSK9 and a corresponding 53% reduction in LDLc levels (25). Other approaches using nucleic acid antisense inhibitor were not as successful; mild to moderate injection site reactions and significant renal toxicity were reported with the administration of this drug. Despite a significant 49% reduction in circulating PCSK9, there was a transient significant increase in serum creatinine, appearance of urinary granular casts, and elevations of urinary kidney damage markers in healthy individuals (26). Taken together, studies investigating the effects of silencing the expression of endogenous PCSK9 will be crucial in order to compliment the siRNA and oligonucleotide therapeutic approach at modulating circulating LDLc levels to reduce the risk of CVD and CKD progression.

Overall, we report here a novel role for intra-renal PCSK9 in the modulation of UPR activation through its ability to stabilize the expression of ER-resident chaperones. Given this observed effect, we demonstrate that re-introducing or overexpressing PCSK9 was able to attenuate basal ER-stress and in conditions induced by tunicamycin or the AngII/DOCA therapy in vivo. A limitation of our study is confirming if the observed renal UPR activation induced by the AngII/DOCA therapy is solely due to the depletion of PCSK9 in the kidney. Given that the models we used were a total-body knockout of PCSK9 expression, we cannot confirm that the renal injury induced by the AngII/DOCA model is solely due to the absence of intracellular expression of renal PCSK9. In future studies, given that the majority of renal PCSK9 expression is localized in the proximal and distal tubules, relative renal injury will be assessed using kidney-specific tubular knockouts of PCSK9 in other relevant mouse models of CKD.

Figure Legends

Fig. 1 Overexpression of hPCSK9 increases chaperone abundance independent of UPR activation in renal cells

(A) HK-2 cells were overexpressed with WT-PCSK9 for 72 hours and assessed for relative chaperone expression and UPR activation (*, $p<0.05$). (B,C) Immunofluorescence microscopy of GRP78 was assessed and quantified in HK-2 cells overexpressed with WT-PCSK9 (*, $p<0.05$). (D) qRT-PCR analysis confirmed no UPR activation with the overexpression of WT-PCSK9 in HK-2 cells (*, $p<0.05$). (E) PCSK9 ELISA confirms majority of intracellular PCSK9 is retained in HK-2 cells relative to HuH7 cells (*, p<0.05).

Fig. 2 Overexpression of hPCSK9 attenuates ER stress and cytotoxicity in renal cells
(A) Immunoblot analysis of UPR activation in HK-2 cells treated with thapsigargin after transfected with an empty vector or the CMV-driven plasmid overexpressing WT-PCSK9. (B,C) Quantification and immunofluorescent microscopy of flag-sXBP1 confirming the effects of PCSK9 overexpression in modulating UPR activation (*, $p<0.05$). (D) Percent cytotoxicity was assessed in HK-2 cells overexpressed with WT-PCSK9 either in the presence or absence of thapsigargin or tunicamycin (*, $p<0.05$). (E) qRT-PCR analysis confirming the attenuation of UPR activation in HK-2 cells overexpressed with WT-PCSK9 (*, $p<0.05$).

Fig. 3 Overexpression of hPCSK9 increases chaperone abundance independent of UPR activation and attenuates ER stress in *Pcsk9*$^{-/-}$ mice
(A,B) Immunohistochemical staining of hPCSK9 initially confirmed the validation of the experiment, and then further assessed for relative staining of chaperones and UPR activation (*, $p<0.05$). (C) qRT-PCR analysis confirmed the attenuation of UPR activation in the renal cortex of PCSK9 transgenic mice (*, $p<0.05$). (D) This was also confirmed in the renal cortex of these mice through immunoblot analysis (*, $p<0.05$).

Fig. 4 *Pcsk9*$^{-/-}$ mice exhibit increased renal ER stress and subsequent UPR activation
(A,B,C) Immunohistochemical staining of markers of UPR activation assessed in *Pcsk9*$^{-/-}$ mice treated with either PBS or tunicamycin relative to controls (*, $p<0.05$). (D-G) qRT-PCR analysis of UPR activation was also assessed in mice treated with tunicamycin or saline in *Pcsk9*$^{-/-}$ mice relative to WT controls (*, $p<0.05$). (H) Immunoblot analysis of markers of UPR activation also confirmed the initial observations made from the renal cortex of these mice (*, $p<0.05$).

Fig. 5 *Pcsk9*$^{-/-}$ mice exhibit increased CKD-induced ER stress in DOCA/AngII mouse model
(A) Kidney tissue weight was assessed in *Pcsk9*$^{-/-}$ mice receiving either sham or the AngII/DOCA therapy (*, $p<0.05$). (B,C) Systolic and diastolic blood pressure was also assessed in the *Pcsk9*$^{-/-}$ mice under these conditions relative to controls (*, $p<0.05$). (D,E) Immunohistochemical staining of phospho-PERK was assessed as a marker of UPR activation and quantified (*, $p<0.05$). (F) Immunoblot analysis of UPR activation and chaperone expression was assessed in the renal cortex of these mice (*, $p<0.05$). (G,H,I,J) qRT-PCR analysis was also assessed for UPR activation in *Pcsk9*$^{-/-}$ mice placed either in sham surgery or AngII/DOCA therapy (*, $p<0.05$).

Fig. 6 *Pcsk9*$^{-/-}$ mic exhibit increased fibrosis and inflammation in DOCA/AngII mouse model
(A,B,C) Immunohistochemical staining of CD36 and picrosirius red staining was assessed in the renal cortex of *Pcsk9*$^{-/-}$ mice either on sham or AngII/DOCA therapy relative to controls (*, $p<0.05$). (D) Serum creatinine levels were measured in these mice to assess for renal clearance

activity (NS, non-significant; *, p<0.05). (E) qRT-PCR analysis of pro-fibrotic, inflammatory, and apoptotic markers were assessed in the *Pcsk9*$^{-/-}$ mice relative to controls placed on sham or AngII/DOCA therapy (*, $p<0.05$).

References

1. Hill, N. R., Fatoba, S. T., Oke, J. L., Hirst, J. A., O'Callaghan, C. A., Lasserson, D. S., & Hobbs, F. D. R. (2016). Global Prevalence of Chronic Kidney Disease – A Systematic Review and Meta-Analysis. *Plos One*, *11*(7). doi: 10.1371/journal.pone.0158765

2. Ojo A. Addressing the global burden of chronic kidney disease through clinical and translational research. Trans Am Clin Climatol Assoc 125, 229–243 (2014).

3. Jha V. et al.. Chronic kidney disease: global dimension and perspectives. Lancet 382, 260–272 (2013).

4. Dickhout J. G. & Krepinsky J. C. Endoplasmic reticulum stress and renal disease. Antioxid Redox Signal 11, 2341–2352 (2009).

5. Inagi R., Ishimoto Y. & Nangaku M. Proteostasis in endoplasmic reticulum--new mechanisms in kidney disease. Nat Rev Nephrol 10, 369–378 (2014).

6. Dickhout J. G., Carlisle R. E. & Austin R. C. Interrelationship between cardiac hypertrophy, heart failure, and chronic kidney disease: endoplasmic reticulum stress as a mediator of pathogenesis. Circ Res 108, 629–642 (2011).

7. Mohammed-Ali Z., Cruz G. L. & Dickhout J. G. Crosstalk between the unfolded protein response and NF-kappaB-mediated inflammation in the progression of chronic kidney disease. J Immunol Res2015, 428508 (2015).

8. Kirchhoff F. et al.. Rapid development of severe end-organ damage in C57BL/6 mice by combining DOCA salt and angiotensin II. Kidney Int 73, 643–650 (2008).

9. Lindenmeyer M. T. et al.. Proteinuria and hyperglycemia induce endoplasmic reticulum stress. J Am Soc Nephrol 19, 2225–2236 (2008).

10. Markan S. et al.. Up regulation of the GRP-78 and GADD-153 and down regulation of Bcl-2 proteins in primary glomerular diseases: a possible involvement of the ER stress pathway in glomerulonephritis. Mol Cell Biochem 324, 131–138 (2009).

11. Poirier S, Mayer G, Benjannet S, Bergeron E, Marcinkiewicz J, Nassoury N, Mayer H, Nimpf J, Prat A, Seidah NG. The proprotein convertase pcsk9 induces the degradation of low density lipoprotein receptor (ldlr) and its closest family members vldlr and apoer2. The Journal of biological chemistry. 2008;283:2363–2372.

12. Fasano T, Cefalù AB, Di Leo E, Noto D, Pollaccia D, Bocchi L, Valenti V, Bonardi R, Guardamagna O, Averna M, Tarugi P. A novel loss of function mutation of PCSK9 gene in white subjects with low-plasma low-density lipoprotein cholesterol.Arterioscler Thromb Vasc Biol. 2007; *27*:677–681. doi: 10.1161/01.ATV.0000255311.26383.2f

13. Zoccali, C. Traditional and emerging cardiovascular and renal risk factors: an epidemiologic perspective. *Kidney Int.* **70**, 26–33

14. 56. Seidah, N. G., Benjannet, S., Wickham, L., Marcinkiewicz, J., Jasmin, S. B., Stifani, S., …Chretien, M. (2003). The secretory proprotein convertase neural apoptosis-regulated convertase 1 (NARC-1): Liver regeneration and neuronal differentiation. Proceedings of the National Academy of Sciences, 100(3), 928–933. doi: 10.1073/pnas.0335507100

15. Fasano T, Cefal. AB, Di Leo E, Noto D, Pollaccia D, Bocchi L, Valenti V, Bonardi R, Guardamagna O, Averna M, Tarugi P. A novel loss of function mutation of PCSK9 gene in white subjects with low-plasma low-density lipoprotein cholesterol.Arterioscler Thromb Vasc Biol. 2007; 27:677–681. doi: 10.1161/01.ATV.0000255311.26383.2f

16. Sharotri V, Collier DM, Olson DR, Zhou R, Snyder PM. Regulation of epithelial sodium channel trafficking by proprotein convertase subtilisin/kexin type 9 (pcsk9) The Journal of biological chemistry. 2012;287:19266–19274.

17. Labonte P, Begley S, Guevin C, Asselin MC, Nassoury N, Mayer G, Prat A, Seidah NG. Pcsk9 impedes hepatitis c virus infection in vitro and modulates liver cd81 expression. Hepatology. 2009;50:17–24.

18. Demers A, Samami S, Lauzier B, Des Rosiers C, Sock ET, Ong H, Mayer G. Pcsk9 induces cd36 degradation and affects long-chain fatty acid uptake and triglyceride metabolism in adipocytes and in mouse liver. Arteriosclerosis, thrombosis, and vascular biology. 2015

19. Seidah N. G. (2017). The PCSK9 revolution and the potential of PCSK9-based therapies to reduce LDL-cholesterol. Global cardiology science & practice, 2017(1), e201702. doi:10.21542/gcsp.2017.2

20. Mohammed-Ali, Z., Lu, C., Marway, M. K., Carlisle, R. E., Ask, K., Lukic, D., Krepinsky, J. C., … Dickhout, J. G. (2017). Endoplasmic reticulum stress inhibition attenuates hypertensive chronic kidney disease through reduction in proteinuria. Scientific reports, 7, 41572. doi:10.1038/srep41572

21. Inagi R., Ishimoto Y. & Nangaku M. Proteostasis in endoplasmic reticulum--new mechanisms in kidney disease. Nat Rev Nephrol 10, 369–378 (2014).

22. Lebeau, P., Al-Hashimi, A., Sood, S., Lhot.k, Š., Yu, P., Gyulay, G., … Austin, R. C. (2016). Endoplasmic Reticulum Stress and Ca2 Depletion Differentially Modulate the Sterol Regulatory Protein PCSK9 to Control Lipid Metabolism. Journal of Biological

Chemistry, 292(4), 1510–1523. doi: 10.1074/jbc.m116.744235

23. Lauressergues, E., Bert, E., Duriez, P., Hum, D., Majd, Z., Staels, B., and Cussac, D. (2012) Does endoplasmic reticulum stress participate in APD-induced hepatic metabolic dysregulation? Neuropharmacology 62, 784 –796

24. Poirier, S., Mamarbachi, M., Chen, W. T., Lee, A. S., and Mayer, G. (2015) GRP94 regulates circulating cholesterol levels through blockade of PCSK9-induced LDLR degradation. Cell Rep. 13, 2064–2071

25. Ray, K. K., Landmesser, U., Leiter, L. A., Kallend, D., Dufour, R., Karakas, M., … Kastelein, J. J. (2017). Inclisiran in Patients at High Cardiovascular Risk with Elevated LDL Cholesterol. New England Journal of Medicine, 376(15), 1430–1440. doi: 10.1056/nejmoa1615758

26. Poelgeest, E. P. V., Hodges, M. R., Moerland, M., Tessier, Y., Levin, A. A., Persson, R., … Burggraaf, J. (2015). Antisense-mediated reduction of proprotein convertase subtilisin/kexin type 9 (PCSK9): a first-in-human randomized, placebo-controlled trial. British Journal of Clinical Pharmacology, 80(6), 1350–1361. doi: 10.1111/bcp.12738

Figure 1 *Byun et al., 2019*

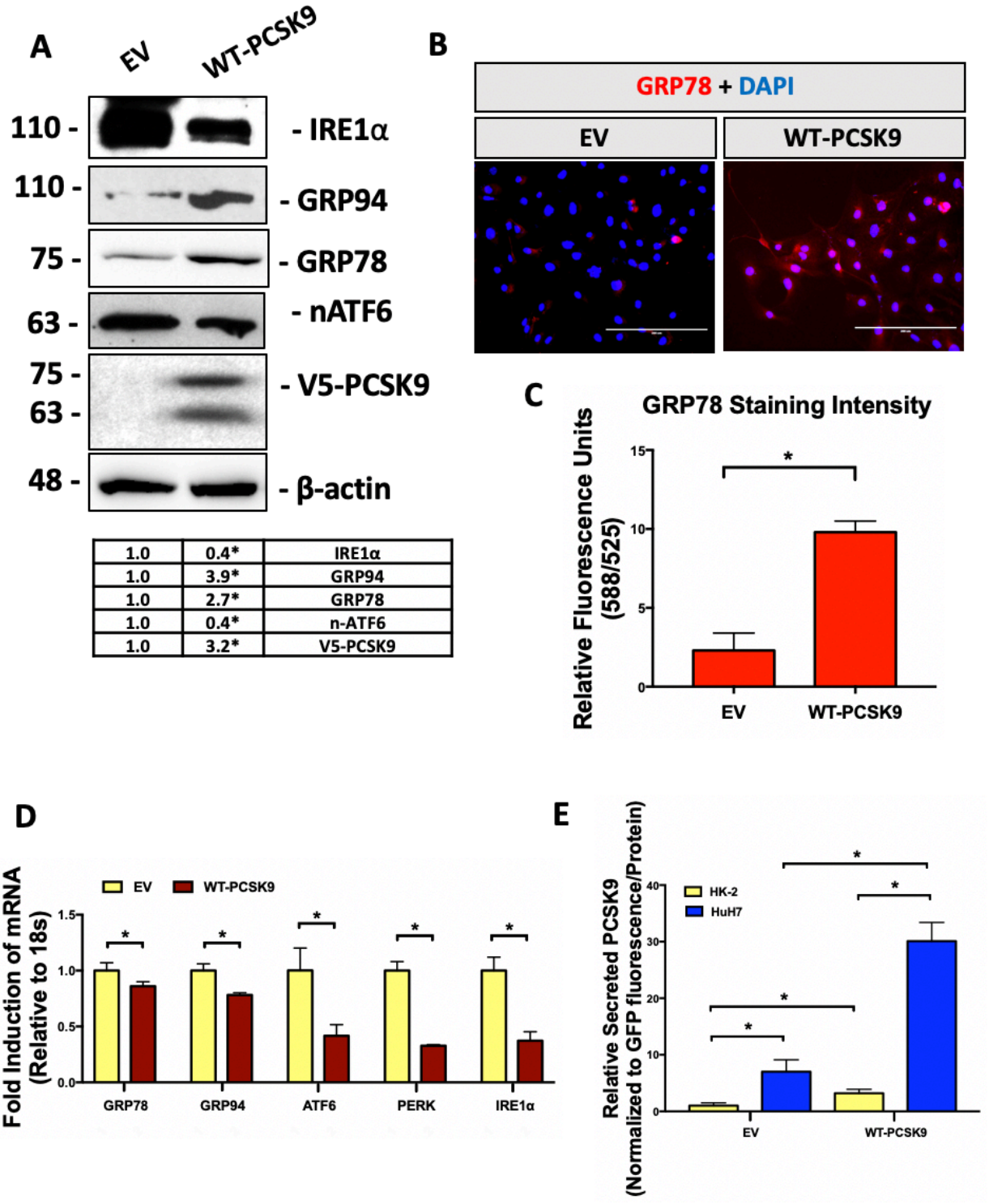

1.0	0.4*	IRE1α
1.0	3.9*	GRP94
1.0	2.7*	GRP78
1.0	0.4*	n-ATF6
1.0	3.2*	V5-PCSK9

Figure 2

Byun et al., 2019

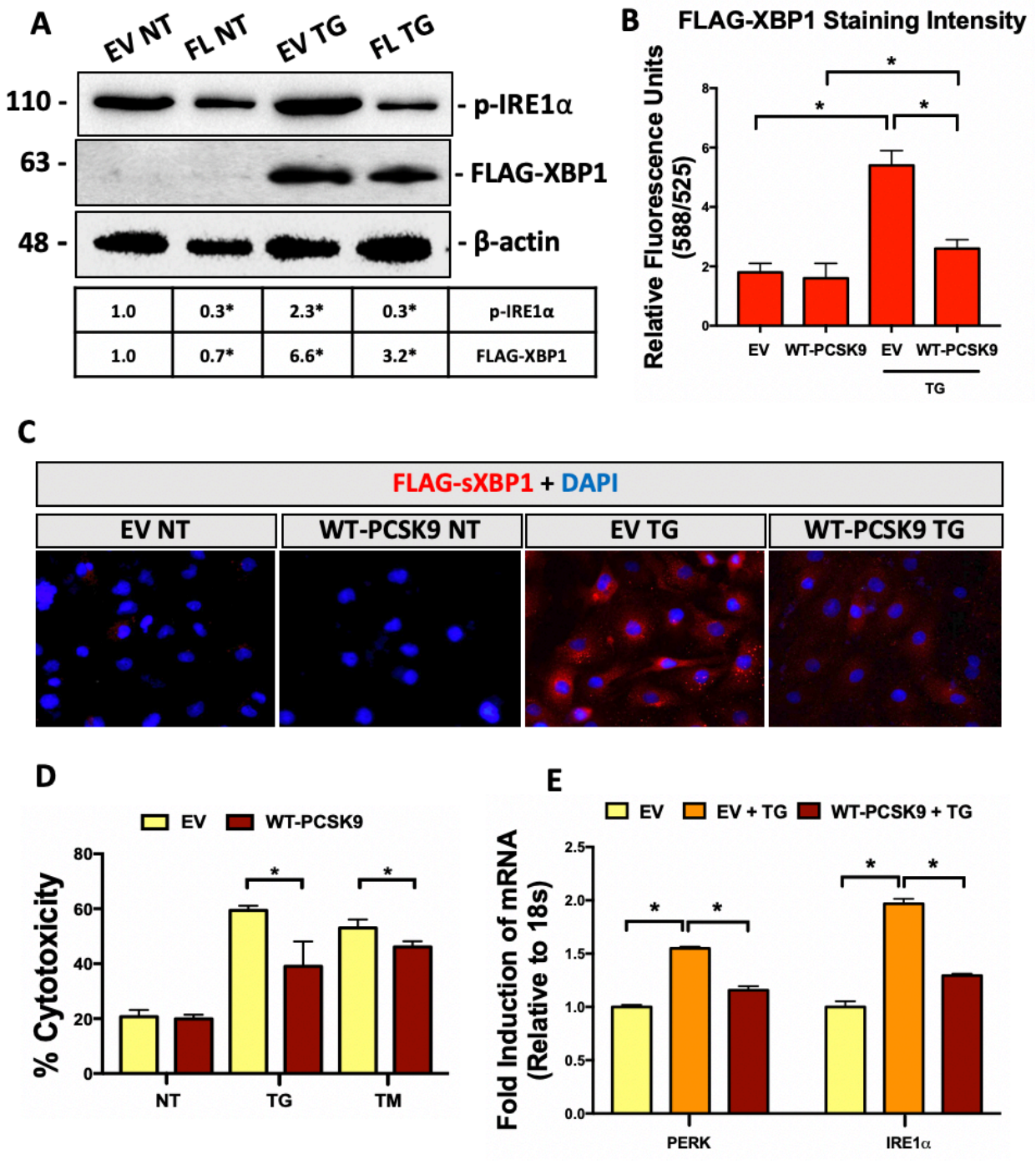

Figure 3 ***Byun et al., 2019***

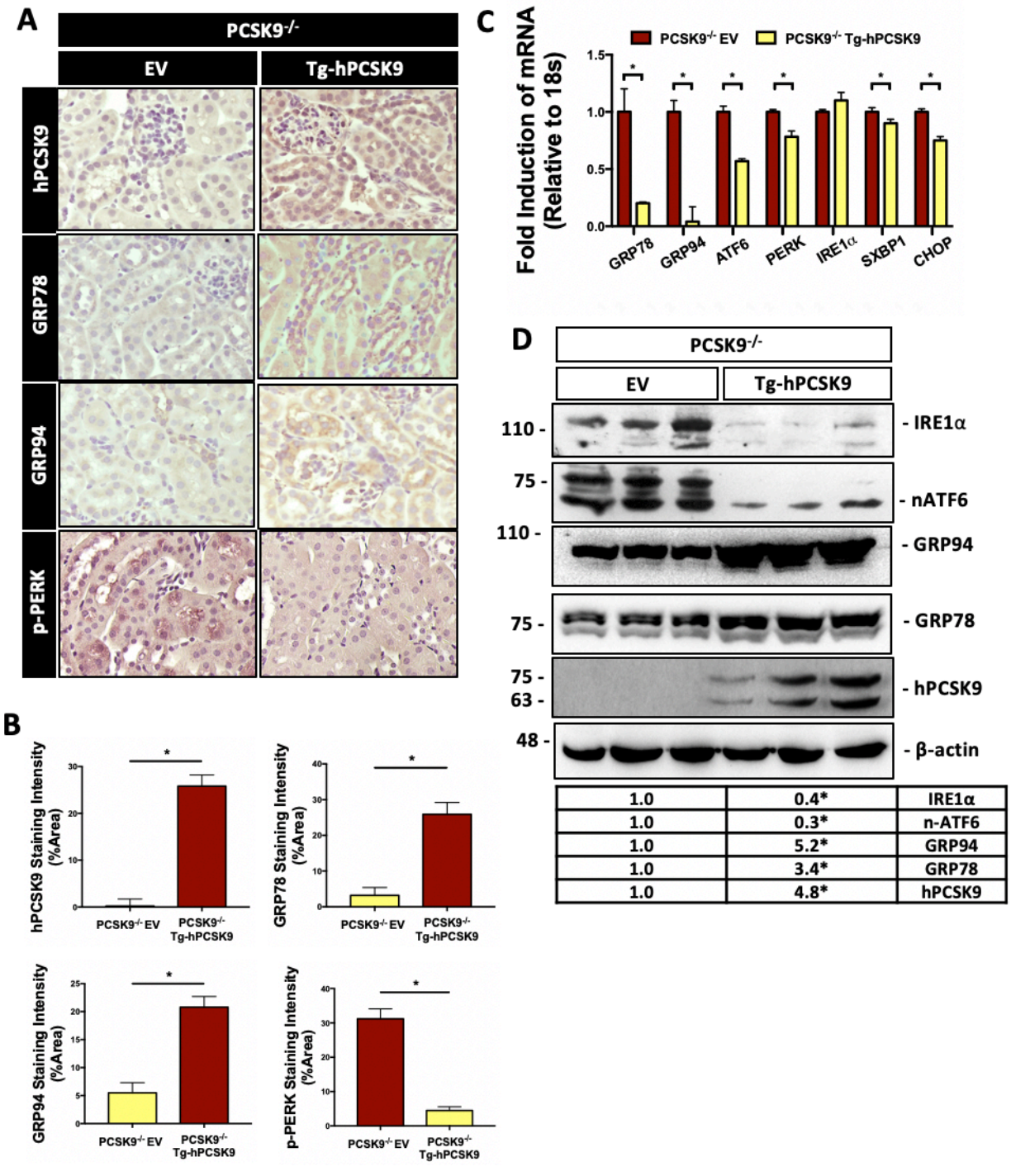

Figure 4 *Byun et al., 2019*

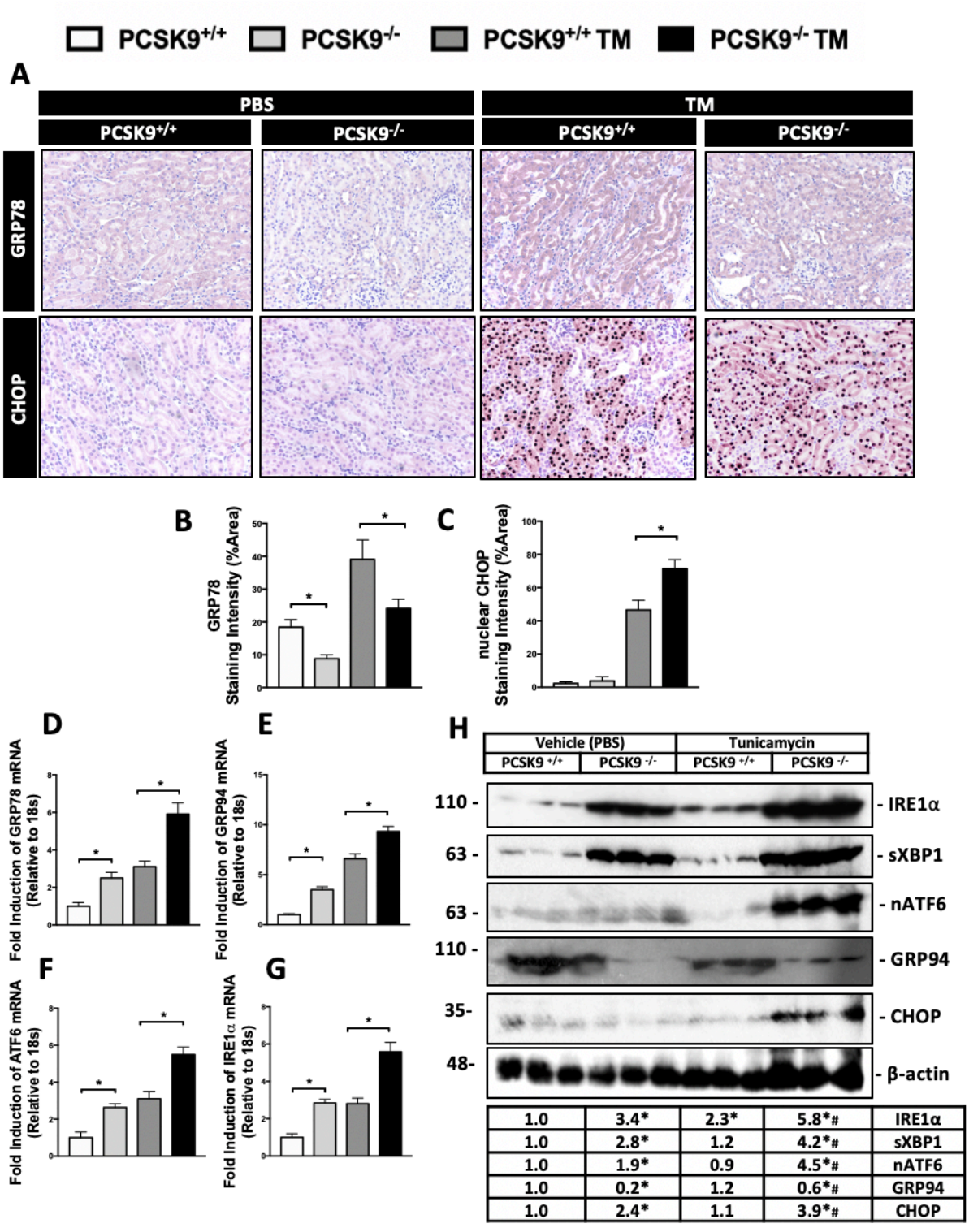

1.0	3.4*	2.3*	5.8*#	IRE1α
1.0	2.8*	1.2	4.2*#	sXBP1
1.0	1.9*	0.9	4.5*#	nATF6
1.0	0.2*	1.2	0.6*#	GRP94
1.0	2.4*	1.1	3.9*#	CHOP

Figure 5

Byun et al., 2019

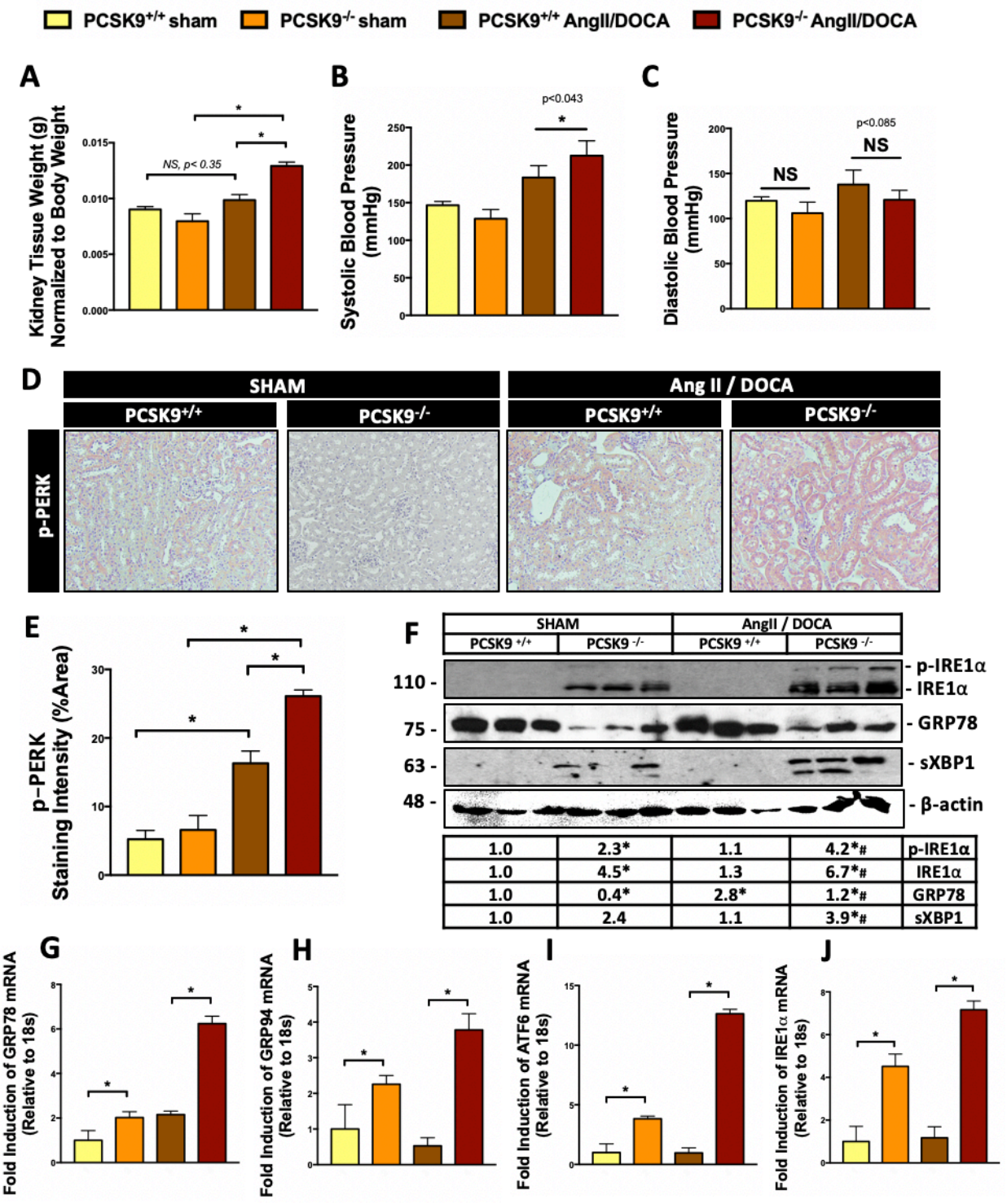

Figure 6 *Byun et al., 2019*

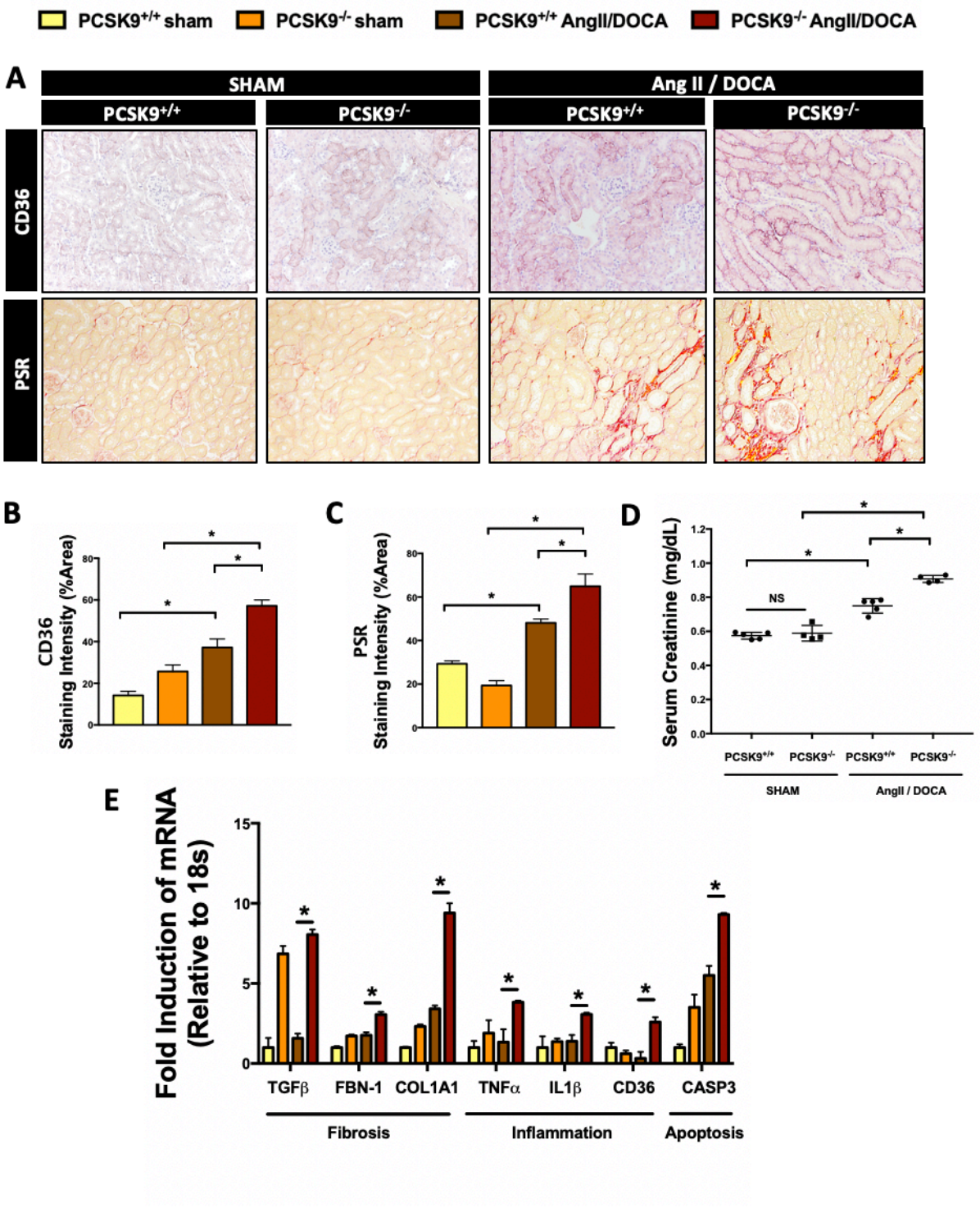

7. Discussion

Since the seminal discovery of PCSK9 and its ability to modulate LDLc levels through the LDLR, transition into the development of clinically-available mAbs within the decade now stands as testament of PCSK9 being an important mediator of CVD risk (55). This also emphasizes the importance of biomedical research as a foundation for translational clinical application, where targeting PCSK9 as a therapeutic target is a prime example of the *'bench to bedside'* concept. Nevertheless, it is still unknown the long-term effects of targeting PCSK9 inhibition in patients, thus, ongoing investigations within the field of cardiovascular research and renal disease are of utmost importance.

The overall objective of my thesis was to investigate the potential influence that PCSK9 may have in association with renal disease. Although extensively studied in association with liver function and CVD, very little is known within the current literature pertaining to the role that PCSK9 may have in modulating renal function and disease. Given that the kidney also expresses both endogenous PCSK9 and the receptors that it has been demonstrated to interact with on the renal epithelia (85) , we sought to investigate the effect of PCSK9 in the context of renal function and/or injury. Herein, **my first objective** was to initially elucidate the role PCSK9 in homeostatic lipid metabolism using a diet-induced mouse model (75). Consistent with clinical findings, our studies revealed that diet-induced model of HFD in mice exhibited significantly elevated levels of circulating PCSK9 (74). We reported that by exposing hepatocytes to FFA consisting of both long-chain saturated and unsaturated fatty acids resulted in a reduction in surface LDLR, suggesting that the increase in circulating PCSK9 acts as a negative feedback regulator to prevent excess lipid deposition and accumulation in the liver.

In the context of renal disease, others have also demonstrated that circulating PCSK9 is significantly elevated in several *in vivo* models of kidney pathology (70, 71). Recent studies have shown a connection between circulating PCSK9 and its role in nephrotic syndrome. The primary pathology associated with nephrotic syndrome is damage to the glomeruli and podocytes, with the secondary pathology being dyslipidemia. Haas et al. demonstrated that podocyte damage-induced nephrotic syndrome increases plasma PCSK9 levels and leads to dyslipidemia: a dyslipidemia that was markedly attenuated in PCSK9 knockout mice (72). These findings demonstrate that dyslipidemia has an influence in renal disease, and thus, targeting PCSK9 may have an effect in attenuating renal injury.

However, an interesting inconsistency was observed during the course of these studies. Previously, Lebeau et al. demonstrated that ER stress blocked PCSK9 secretion despite its increased expression in hepatocytes (69). Given that excessive lipid uptake is widely reported to cause ER stress via ER Ca^{2+} depletion (80), we in turn, observed that intracellular uptake of FFAs *in vitro* and in HFD conditions *in vivo* increased PCSK9 secretion from hepatocytes. The discrepancy in the secretion of PCSK9 in both of these conditions may be explained through multiple reasons. Firstly, despite others reporting that PCSK9 acts as an ER stress-induced gene (39, 69), it is well-established that PCSK9 transcription is also strongly induced by fluxes in lipid regulation (81). Given that long-chain saturated FFAs like palmitate simultaneously act to induce ER stress and disrupt lipid homeostasis (80), differentiating which stimulus has a greater effect in PCSK9 secretion remains to be elucidated. A possible mechanism could be through the upregulation of ER-resident chaperones through UPR activation in conditions of both pharmacologic treatment of ER stress-inducing agents and/or excess intracellular uptake of FFAs. As ER-resident chaperones such as GRP94 have been reported to be a strong binding partner of

PCSK9 (77), perhaps the magnitude of UPR activation in influencing the upregulation of ER-resident chaperones can explain the discrepancy in both of these conditions. Given that pharmacologic agents such as thapsigargin or tunicamycin treatment are strong inducers of ER stress, these agents may increase ER chaperone abundance to a significantly greater extent than in conditions of HFD or uptake of saturated FFAs. Overall, however, these findings suggest that increased PCSK9 secretion in conditions of diet-induced liver disease represent a protective stance by acting as a negative feedback loop to prevent excess hepatic lipid uptake.

The **second objective of my thesis** was to assess renal injury in the context of PCSK9 deficiency. We sought to investigate the effect of ablating PCSK9 as a negative feedback regulator from promoting excess lipid accumulation in a variety of tissues, including the kidney. Herein, we demonstrated that PCSK9 deficiency in mice promotes renal lipid deposition, likely occurring as a result of increased expression of surface receptors known to uptake lipids from circulation, such as CD36 and the LDLR. The lipid nephrotoxicity hypothesis, first postulated by Moorhead et al. in 1982 (73), suggests that dyslipidemia promotes CKD progression by inducing oxidative, inflammatory, and ER stress. Our studies also are in accordance with this hypothesis that increased renal lipid deposition promoted HFD-induced ER stress, inflammation, and renal fibrosis as a result of a deficiency in circulating PCSK9.

In the current landscape of studies investigating the role of CD36 in renal disease, CD36 has been shown to induce renal injury through several distinct mechanisms (45, 46). Herein, we provide a mechanistic insight of CD36 in promoting renal injury through its ability to enhance excess lipid uptake into renal tissue. Other studies have reported that independent of lipid uptake and deposition, CD36 enhances renal injury through pathways pertaining to inflammation, fibrosis, and apoptosis (47, 48). In the adriamycin-induced nephropathy mouse model of focal segmental

glomerulosclerosis, podocyte injury was caused by CD36-dependent apoptosis via activation of the p38MAPK pathway (82). In streptozotocin-treated mouse model of diabetic nephropathy, insulin treatment was able to attenuate CD36-driven hyperglycemia (83). Therefore, it is possible that perhaps the deficiency of PCSK9 can have an effect on CD36-driven renal injury independent of HFD conditions and excess FFA uptake.

Interestingly, these findings are also in line with our previous data suggesting that PCSK9 deficiency also enhances diet-induced hepatic steatosis (67). Given that both the LDLR and CD36 are also heavily expressed on the surface of hepatocytes, we also observed that excess FFA uptake induced ER stress and liver injury to a greater extent in *Pcsk9*$^{-/-}$ mice compared to controls. These findings support the notion from my first objective that PCSK9 may have a protective stance against diet-induced pathologies such as non-alcoholic fatty liver disease (NAFLD) and lipid driven renal injury (75). Thus, this yields the question whether PCSK9 deficiency can modulate the pathogenic progression of various other tissues that also express the LDLR and CD36 such as the pancreas, skeletal muscle, macrophages, and the heart.

Clinically, this provides an insight into the current FDA-approved mAbs against PCSK9, which binds to the EGF-a-binding domain of PCSK9 to prevent its interaction with the LDLR (55). Recent studies have demonstrated that such antibodies increase circulating PCSK9 levels 7-fold as a result of the reduced rate of LDLR-mediated removal of PCSK9 from circulation (70). Given that the domain in which PCSK9 interacts with CD36 remains unclear and may potentially differ from the LDLR, we realized that a whole-body knockout of PCSK9 did not accurately represent the long-term effects of these PCSK9 mAbs. Thus, we also sought to investigate if mAb-bound PCSK9 still has the ability to enhance the degradation of renal CD36 to protect against lipid-induced renal injury. Herein, we also reported that the administration of alirocumab is able to

reduce the surface expression of CD36 on the renal epithelia (Byun et al., unpublished). These data strongly suggest that PCSK9 interacts with CD36 via a different domain than it does with the LDLR. Interestingly, mRNA transcript levels of CD36 were also significantly reduced with alirocumab administration, thereby highlighting a second mechanism as to the observed reduction in surface CD36 expression. Given that alirocumab increases cellular cholesterol uptake through the LDLR, reduced expression of SREBP-2, PCSK9, and CD36 may represent a negative feedback loop in order to reduce further lipid uptake and accumulation.

The **last objective of my thesis** was to elucidate the role of endogenously expressed renal PCSK9 (Byun et al., unpublished). The data thus far, demonstrating the extent to which the observed renal injury in *Pcsk9*$^{-/-}$ mice occurs as a result of excess diet-induced lipid uptake, represents a limitation of my previous objective. Previously, we have identified a mechanism in which the retention of PCSK9 acts as a co-chaperone to attenuate ER stress in hepatocytes by promoting the stability of ER chaperones, GRP78 and GRP94. Thus, this raises the question of whether the observed increase in ER stress due to HFD conditions in *Pcsk9*$^{-/-}$ mice may have occurred as a result of (1) increased lipid uptake, and also (2) increased sensitivity of ER stress due to a lack of renal stress-response chaperones. Furthermore, others have demonstrated that ER stress has a direct effect in upregulating genes responsible for the upregulation of *de novo* lipogenesis. Lhotak et al. demonstrated that ER stress contributed to renal proximal tubule injury by increasing SREBP-2 mediated lipid accumulation and cellular apoptosis (76). To reverse these effects, overexpression of ER-resident chaperones was able to attenuate ER stress-induced renal lipid accumulation. As such, we investigated if renal PCSK9 also acts as a co-chaperone to modulate ER stress in a murine model of CKD.

Consistent with its intracellular role in hepatocytes, we demonstrated that in the absence of intracellular renal PCSK9, *Pcsk9*$^{-/-}$ mice exhibit increased renal injury as a response to the AngII/DOCA therapy. Given this observation, we also observed that the kidney cortex of *Pcsk9*$^{-/-}$ mice exhibit reduced expression of ER-resident chaperones and subsequent UPR activation. In line with this data, others have demonstrated that ER stress is able to promote renal injury using the same AngII/DOCA murine model of CKD (39). Mohammed et al. reported that administration of 4-PBA was able to significantly decrease blood pressure and interstitial fibrosis induced by this CKD model. Interestingly, as this model was able to significantly upregulate markers of UPR activation, the *PCSK9* gene was also significantly upregulated, with a greater increase with the 4-PBA treatment. Given that ER-resident chaperones such as GRP78 and GRP94 are heavily upregulated in conditions of ER stress, the observation that the AngII/DOCA model is able to increase PCSK9 expression suggests that this may possibly be a compensatory response and implies a chaperone-like role for PCSK9 with in the ER lumen.

Furthermore, Lebeau et al. previously reported the role of ER stress in the modulation of hepatic PCSK9 and LDLR (75). Using ER stress-inducing agents that cause ER Ca^{2+} depletion, it was observed that changes in Ca^{2+} levels in the ER lumen has a distinct effect on upregulating the transcriptional regulation of endogenous PCSK9 via SREBP-2 activation. Interestingly, however, despite the increased PCSK9 mRNA, Lebeau et al. also concluded that ER stress was able to block the secretion of PCSK9 and increase surface LDLR in primary hepatocytes. Although its mechanism remains to be elucidated, recent reports identified GRP94 as an ER-resident binding partner of PCSK9 (77), and thus, its upregulation through ER stress may explain how it is able to hinder the exit of PCSK9 from the ER lumen. However, the inherent biological reason as to why

ER stress promotes the retention of PCSK9 despite increasing its expression remains unknown, but suggests again that PCSK9 may have a distinct role inside the ER lumen.

Overall, my research objectives were an attempt to characterize the role of PCSK9 in modulating renal injury using a variety of different *in vivo* models of renal disease. Herein, we first determined that the upregulation of circulating PCSK9 in the context of HFD represents a protective, negative feedback response to reduce excess uptake of FFAs into the liver. As a result, we then observed that under HFD conditions in the context of PCSK9 deficiency, *Pcsk9*$^{-/-}$ mice also enhanced lipid uptake and deposition into the renal cortex in a CD36-dependent manner. Lastly, we suggest a novel intracellular role of PCSK9 in the renal cortex. Despite the wide range of studies demonstrating that ER protein retention induces pathological ER stress, Lebeau et al. shows that intracellular retention of PCSK9 stabilizes ER-resident chaperones to protect against UPR activation (Lebeau et al., submitted). Likewise, we observed that kidney-expressed PCSK9 also plays a co-chaperone-like role in the ER lumen to protect against chronic UPR activation induced by multiple *in vivo* models of renal disease. Given these three research objectives however, it is currently challenging to discern if either depletion of circulating or intracellular renal PCSK9 expression plays a bigger role in the ER stress observed *in vitro* and *in vivo* (Figure 4). Thus, further elucidating the distinction between the intracellular and extracellular protective role that PCSK9 may partake in attenuating renal disease is of utmost importance for these future ongoing studies in the Austin Laboratory.

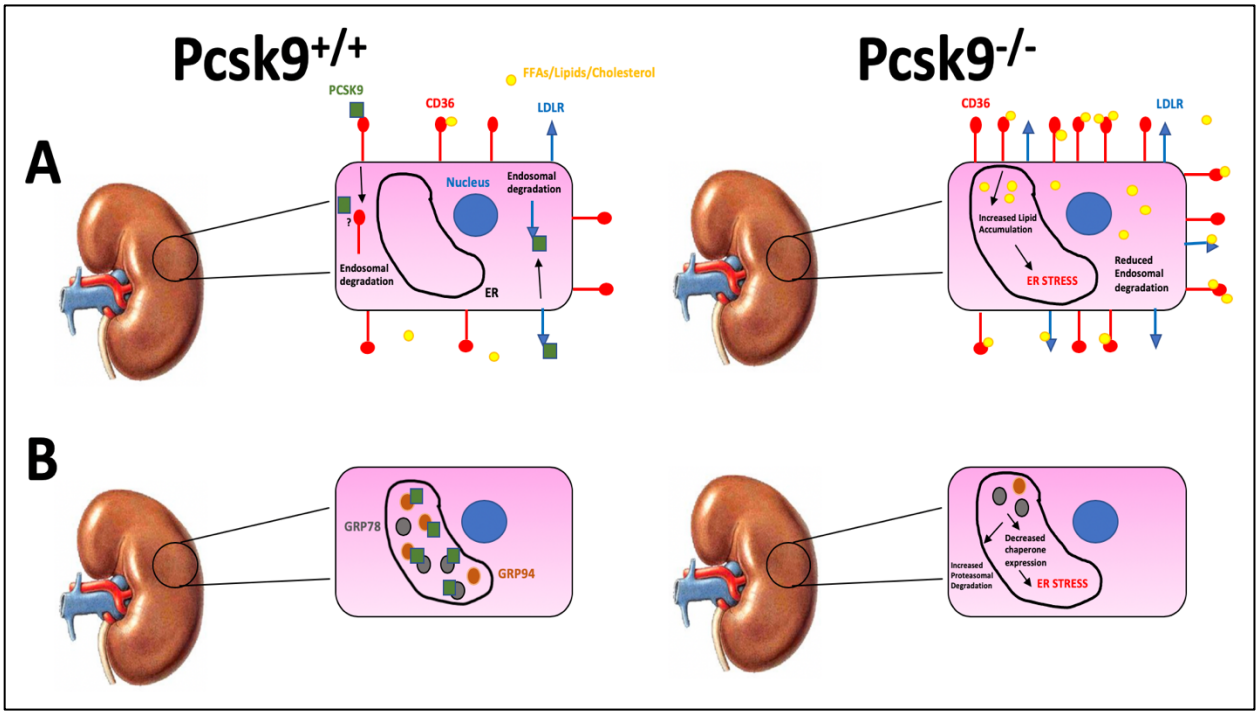

Figure 4. Schematic diagram on the proposed roles of PCSK9 in attenuating renal ER stress to attenuate renal disease progression and injury. Mechanism A emphasizes on CD36-driven lipid uptake to induce ER stress in the absence of PCSK9. Mechanism B emphasizes on ER stress as a result of attenuated chaperone expression in the absence of PCSK9.

8. Overall Findings and Future Directions

Overall, my thesis demonstrates that PCSK9 has an extensive role beyond hepatic lipid homeostasis and may have a novel effect in modulating renal injury using our established *in vitro* and *in vivo* models of CKD. We have initially demonstrated the effects of extracellular circulating PCSK9 in the context of diet-induced renal injury. Likewise, we also provide evidence of the effects of intracellular PCSK9 deficiency in the context of ER stress-induced renal inflammation, fibrosis, and compromised clearance of serum creatinine.

Given that targeting PCSK9 remains as a novel therapeutic approach in combatting against CVD, ongoing investigations to elucidate novel mechanisms at reducing the secretion of PCSK9 remains of high importance. Upon the initial discovery of PCSK9 and of its relative bodily expression using in situ hybridization (51), it was concluded that the secretion of PCSK9 was solely responsible by hepatocytes, as *in vivo* models of liver-specific *Pcsk9*$^{-/-}$ mice exhibited undetectable levels of it in circulation (84). Thus, this suggests that other tissues such as the kidney that also express PCSK9 may have an inherent mechanism as to how it is retained intracellularly. Taken together, the identification of the inherent mechanism as to how the kidney retains PCSK9 despite its relatively abundant expression may represent a novel therapeutic avenue at reducing CVD risk and subsequent CKD progression. Given that the ER-resident chaperone GRP94 is a binding partner of PCSK9, it is worth investigating if the relative abundance or binding of chaperones to PCSK9 may have an effect in the ER retention of PCSK9. Key future experiments for this proposal include:

Does reduced expression of ER chaperones modulate PCSK9 secretion? Previously, we have shown that ER-resident chaperones such as GRP94 binds to PCSK9 to evade UPR detection and

subsequent activation (69). Based on these findings, future studies will investigate whether the expression of GRP78 and GRP94 can modulate the secretion of PCSK9. In order to carry out this experiment, cells that express, but do not secrete PCSK9 (i.e. renal cells) will be treated with siRNA targeted against GRP78 and/or GRP94 and then assayed for secreted PCSK9 using ELISA. Likewise, secreted PCSK9 should also be measured in cells co-overexpressed with WT-PCSK9 with either GRP78 or GRP94. The latter experiment will determine if overexpressing ER-resident chaperones can hinder the secretion of PCSK9 from these cells. To compare differences, optical density (OD) of ELISA will be normalized relative to protein abundance. Overall, these findings will determine a novel therapeutic strategy through the modulation of ER-resident chaperone expression to reduce circulating PCSK9 and ultimately, CVD progression.

Furthermore, I have demonstrated that PCSK9 mAbs may have the ability to enhance the degradation of surface CD36, a well-known driver of several renal diseases that contribute towards the overall progression of CKD (43, 44, 45, 46) by inducing pro-inflammatory, fibrotic, and apoptotic pathways. Given that CD36 plays a crucial role in enhancing renal injury, it is worth investigating if currently approved PCSK9 mAbs can protect against CD36-dependent activation of renal pathogenesis.

What is the effect of PCSK9 mAbs in the context of diet-induced and/or -independent renal injury? Based on these preliminary findings, future studies will investigate if PCSK9 mAbs can have a protective effect by attenuating CD36-driven renal injury in a diet-induced *in vivo* model. Briefly, mice will be placed in HFD conditions for 12 weeks with bi-weekly injections of alirocumab and/or evolocumab (30mg/kg) and assessed for diet-induced renal ER stress and injury. Other well-established *in vivo* models of CKD including unilateral ureter obstruction,

streptozotocin, and AngII/DOCA treatments can be used to evaluate if PCSK9 mAbs can protect against these conditions of renal disease. The results of these findings can suggest other attractive therapeutic mechanisms that the current FDA-approved PCSK9 mAbs may have at combatting against CVD and CKD.

Lastly, a limitation of this study is the use of a whole body knockout of PCSK9 in our *in vivo* models to assess for renal lipid accumulation. As we have previously observed, both the extracellular and intracellular depletion of PCSK9 can promote ER stress-induced renal injury. Inherently, we cannot be certain that increased lipid uptake under HFD conditions was the sole culprit to the ER stress observed in these studies. This is certainly true, as ER stress has also been shown to promote intracellular lipid accumulation independent of diet through SREBP activation (76). Thus, assessing these effects individually can provide an insight as to which of these conditions plays a bigger factor in attributing to the progression of renal disease.

What is the effect of liver-specific knockout of PCSK9 under HFD conditions? Based on our previous studies, we have shown that PCSK9 deficiency promotes increased lipid uptake in mice fed a HFD. Likewise, Seidah and colleagues have reported that liver-specific knockout of PCSK9 completely reduces circulating PCSK9 while leaving its intracellular expression in the kidney intact (84). As such, liver-specific *Pcsk9*$^{-/-}$ mice and its relative controls will be placed under HFD conditions for 12 weeks and assessed for renal injury. The results of this experiment will provide a greater insight as to whether the observed diet-induced renal ER stress and injury is solely attributed to extracellular circulating PCSK9.

Collectively, the findings that were made over the duration of my masters studies further establishes the initial link made between PCSK9 and its role in modulating liver injury in a diet-

induced model. By initially assessing its extracellular effects, these observations imply that PCSK9 has an extensive effect beyond hepatic lipid homeostasis and may have in turn, a protective stance in renal injury through a manner dependent on surface CD36 on renal epithelia. On the other hand, the intracellular role of PCSK9 localized in the kidney also suggests an additional beneficial effect at directly attenuating ER stress-driven renal injury by stabilizing ER-resident chaperones, which are critical for the mitigation of UPR activation and polypeptide folding. Throughout this thesis, we support the notion that the role of PCSK9 has a crucial effect beyond lipid homeostasis and may potentially represent a novel therapeutic target for CKD progression.

Appendix A: Publication into Journal of Hepatology Reports

Research Article JHEP|Reports

Pcsk9 knockout exacerbates diet-induced non-alcoholic steatohepatitis, fibrosis and liver injury in mice

Paul F. Lebeau,[1,†] Jae Hyun Byun,[1,†] Khrystyna Platko,[1,†] Ali A. Al-Hashimi,[1] Šárka Lhoták,[1] Melissa E. MacDonald,[1] Aurora Mejia-Benitez,[1] Annik Prat,[2] Suleiman A. Igdoura,[3] Bernardo Trigatti,[4,5] Kenneth N. Maclean,[6] Nabil G. Seidah,[2] Richard C. Austin[1,*]

[1]*Department of Medicine, Division of Nephrology, McMaster University, St. Joseph's Healthcare Hamilton, Ontario L8N 4A6, Canada;* [2]*Laboratory of Biochemical Neuroendocrinology, Clinical Research Institute of Montreal, affiliated to the University of Montreal, Montreal, Quebec H2W 1R7, Canada;* [3]*Department of Biology and Pathology, McMaster University, Hamilton, Ontario, L8S 4K1, Canada;* [4]*Thrombosis and Atherosclerosis Research Institute (TaARI), Hamilton Health Sciences and McMaster University, Hamilton, Ontario L8L 2X2, Canada;* [5]*Department of Biochemistry and Biomedical Sciences, McMaster University, Hamilton, Ontario L8S 4L8, Canada;* [6]*the Department of Pediatrics, University of Colorado School of Medicine, Aurora, Colorado, USA, 80045*

JHEP Reports **2019.** https://doi.org/10.1016/j.jhepr.2019.10.009

Background & Aims: The fatty acid translocase, also known as CD36, is a well-established scavenger receptor for fatty acid (FA) uptake and is abundantly expressed in many metabolically active tissues. In the liver, CD36 is known to contribute to the progression of non-alcoholic fatty liver disease and to the more severe non-alcoholic steatohepatitis, by promoting triglyceride accumulation and subsequent lipid-induced endoplasmic reticulum (ER) stress. Given the recent discovery that the hepatocyte-secreted proprotein convertase subtilisin/kexin type 9 (PCSK9) blocks CD36 expression, we sought to investigate the role of PCSK9 in liver fat accumulation and injury in response to saturated FAs and in a mouse model of diet-induced hepatic steatosis.

Methods: In this study, we investigated the role of PCSK9 on the uptake and accumulation of FAs, as well as FA-induced toxicity, in a variety of cultured hepatocytes. Diet-induced hepatic steatosis and liver injury were also assessed in *Pcsk9*$^{-/-}$ mice.

Results: Our results indicate that PCSK9 deficiency in cultured hepatocytes increased the uptake and accumulation of saturated and unsaturated FAs. In the presence of saturated FAs, PCSK9 also protected cultured hepatocytes from ER stress and cytotoxicity. In line with these findings, a metabolic challenge using a high-fat diet caused severe hepatic steatosis, ER stress inflammation and fibrosis in the livers of *Pcsk9*$^{-/-}$ mice compared to controls. Given that inhibition of CD36 ablated the observed accumulation of lipid *in vitro* and *in vivo*, our findings also highlight CD36 as a strong contributor to steatosis and liver injury in the context of PCSK9 deficiency.

Conclusions: Collectively, our findings demonstrate that PCSK9 regulates hepatic triglyceride content in a manner dependent on CD36. In the presence of excess dietary fats, PCSK9 can also protect against hepatic steatosis and liver injury.

Introduction

Given that the liver plays a central role in glucose and lipid metabolism, it is no surprise that non-alcoholic fatty liver disease (NAFLD) has emerged as a contributor to other chronic diseases, such as type 2 diabetes and cardiovascular disease (CVD).[1,2] Severity ranges from simple steatosis to progressive stages of non-alcoholic steatohepatitis (NASH), depending on the presence or absence of inflammation, fibrosis and hepatocyte injury. Excessive consumption of dietary saturated fats and sugars is widely accepted as the primary driver of NAFLD and its prevalence is currently on the rise; affecting 30 to 46% of individuals in Western societies.[3]

Although the exact mechanisms by which NAFLD progresses to NASH are not well understood, an accumulation of events including oxidative stress, mitochondrial dysfunction, adipokine alteration, lipid peroxidation and Kupffer cell activation are all believed to contribute to the currently accepted *multiple hit* hypothesis.[4] Chief among these *hits* is the process by which misfolded polypeptides accumulate in the ER and cause ER stress. Paradoxically, this cellular stress pathway is also known to promote oxidative stress, mitochondrial dysfunction and Kupffer cell-mediated inflammation.[5,6] In a manner similar to other secretory cells, hepatocytes are rich in ER and the signaling cascades associated with its state of stress have been shown to promote apoptotic cell death, lipotoxicity, inflammation and insulin resistance; all of which are commonly observed in patients with obesity, NAFLD and NASH.[4]

In response to ER stress, the unfolded protein response (UPR) is activated via 3 signaling cascades that include (a) the highly conserved inositol-requiring 1α (IRE1α)-X-box-binding protein 1 (XBP1) pathway required for hepatic lipid regulation during conditions of ER stress,[7] (b) the PKR-like ER kinase (PERK)-activating transcription factor (ATF)4 pathway known to modulate *de novo* lipogenesis through fatty acid synthase (FAS) and the sterol regulatory element-binding protein-1C (SREBP1-C),[8] and (c) ATF6, which in its nuclear active form interacts directly with nuclear SREBP-2,

Key words: ER stress; CD36; HFD; NAFLD; Liver disease; Cardiometabolic disease; CVD.
Received 13 April 2019; received in revised form 16 October 2019; accepted 24 October 2019
* Corresponding author. Address: Dr. Richard C. Austin, 50 Charlton Ave East, Room T-3313, Hamilton, Ontario, L8N 4A6. Tel.: 905-522-1155 x35175; Fax: 905-540-6589.
E-mail address: austinr@taari.ca (R.C. Austin).
† Authors contributed equally to this work.

Please cite this article as: Lebeau PF et al. *Pcsk9* knockout exacerbates diet-induced non-alcoholic steatohepatitis, fibrosis and liver injury in mice. JHEP Reports (2019), https://doi.org/10.1016/j.jhepr.2019.10.009

thereby attenuating the expression of lipid regulatory genes.[9] Overall, canonical UPR activation increases the folding capacity of the ER and blocks global protein synthesis in order to reduce ER burden. In a manner similar to NAFLD, ER stress and ER stress-induced apoptosis are also well-established contributors to CVD.[10]

In recent years, CVD has been considered the leading cause of mortality in the USA, accounting for 34% of total deaths in individuals <75 years of age.[11] The discovery of PCSK9[12] and its ability to induce the degradation of the low-density lipoprotein (LDL) receptor (LDLR) once secreted from the liver, firmly positioned PCSK9 as a target for the management of CVD.[13] These seminal discoveries have since led to the development of human anti-PCSK9 monoclonal antibodies capable of reducing circulating LDL levels by 60% in patients at high risk of CVD.[14] In addition to its ability to induce the degradation of cell-surface LDLR, secreted PCSK9 was recently shown to promote the degradation of several other receptors known to be involved in the uptake of lipid from the circulation into the liver, such as the very low-density lipoprotein receptor (VLDLR),[15,16] LDLR-related protein-1,[17] the apolipoprotein E (ApoE) receptor-2[15] and CD36.[18]

Based on these studies, circulating PCSK9 may impact the levels of these receptors on the cell surface of hepatocytes, thereby increasing liver burden via enhanced hepatic lipid uptake and accumulation. The purpose of this study was to determine whether the previously reported increase in hepatic lipid content observed in *Pcsk9*$^{-/-}$ mice[18] correlated with the hallmark features of NASH, such as ER stress, apoptosis, inflammation and fibrosis.

Materials and methods

Cell culture and free FA treatments

HuH7 and HepG2 immortalized human hepatocytes were cultured at 37°C with 5% CO_2 in complete Dulbecco's Modified Eagles Medium (Gibco, Thermorfisher Scientific) containing 10% fetal bovine serum (Sigma-Aldrich) and 50 U/ml of penicillin and streptomycin (Sigma-Aldrich). HepatoSure 100-donor primary human hepatocytes were purchased from Xenotech and cultured in complete William's E medium as per manufacturer's instructions. FAs used for cell treatment such as oleate (OA; Sigma-Aldrich), linoleate (LA; Sigma-Aldrich), stearate (SA; Sigma-Aldrich) and palmitate (PA; Sigma-Aldrich) were conjugated to FA-free bovine serum albumin (BSA; Sigma-Aldrich), as previously described,[19] to a stock concentration of 1 mM. Cells were also treated with LDL (Lee Biosolutions), high-density lipoprotein (HDL; Alpha Aesar) and oxidized (ox)LDL (Alpha Aesar). Additional treatments used in cell culture studies included recombinant human PCSK9 (Cayman Chemical), DiI-LDL (Alpha Aesar) and sulfo-N-succinimidyl oleate (SSO; Cayman Chemical). All cell treatments were carried out for 24 h, unless specified otherwise. Small interfering RNA (siRNA) targeted against *PCSK9* (si*PCSK9*) and *CD36* (si*CD36*) were purchased from siGenome, Dharmacon, and transfections were carried out as per manufacturer's instructions using RNAiMAX (ThermoFisher Scientific). The overexpression of human wild-type *PCSK9*^{WT} and the secretion-deficient *PCSK9*^{Q152H}, as well as human *CD36* (Addgene, # 52025) was achieved using X-tremeGENE transfection reagent as per manufacturer's instructions.

Animal studies

Hepatic lipid accumulation was first examined in 12-week-old male *Pcsk9*$^{-/-}$ mice (n = 10) on a C57BL/6J background and age-matched C57BL/6J controls (*Pcsk9*$^{+/+}$; n = 10) fed normal control diet (NCD). Experiments were then repeated in a second cohort of *Pcsk9*$^{-/-}$ mice (n = 5) on a C57BL/6J background and age-matched *Pcsk9*$^{+/+}$ controls (n = 5), which were fed either NCD or a high-fat diet (HFD) (60% fat/kcal, ENVIGO #TD.06414), starting at 6 weeks of age for an additional 12 weeks prior to sacrifice. A final cohort of 12-week-old male *Pcsk9*$^{-/-}$ mice on a C57BL/6J background (n = 6) were treated with SSO (10 mg/kg; intraperitoneal injection) and 1 h later with OA (1 g/kg, intraperitoneal injection) for an additional 2 h prior to study endpoint. All animals were housed in a vented rack system, had access to food and water *ad libitum* and were exposed to 12 h light:dark cycles. Animal experiments were performed in strict accordance with the McMaster University animal care guidelines.

Statistical analysis

All data are presented as the mean and error bars as SD. Statistical differences between 2 groups were determined using the unpaired *t* test. For analysis of experiments involving multiple groups, the one-way ANOVA was performed. All comparisons were considered statistically significant when $p < 0.05$. For further details regarding the materials used, please refer to the CTAT table and supplementary information.

Results

PCSK9 reduces lipid accumulation in cultured hepatocytes treated with FAs and lipoproteins

The effect of PCSK9 on cellular lipid accumulation was first examined in cultured HepG2 hepatocytes stably transfected with short hairpin RNA (shRNA) targeted against *PCSK9* or control shRNA. Knockdown of PCSK9 in these cells was first confirmed via ELISA for secreted PCSK9 and immunoblotting of PCSK9-regulated receptors, LDLR and CD36 (Fig. 1A and B). Consistent with previous studies, PCSK9 expression was inversely correlated with LDLR and CD36 expression.[13,18] Increased uptake of fluorescently labelled DiI-LDL cholesterol was also observed in *PCSK9* shRNA knockdown cells compared to shRNA controls (Fig. S1A and S1B). Staining with Oil red O (ORO), as well as triglyceride extraction and quantification, revealed a marked increase in triglyceride accumulation in *PCSK9* shRNA cells treated with dietary saturated FAs (PA and SA), unsaturated FAs (OA and LA) and lipoproteins (LDL and HDL) (Fig. 1C and D). The dose-dependent effect of exogenously added extracellular PCSK9 on intracellular lipid accumulation was also examined in OA-treated HepG2 cells using recombinant human PCSK9 (Fig. 1E). Modest but significant reductions in CD36 expression and in OA-induced lipid accumulation were also observed in HepG2 cells and primary mouse hepatocytes transfected with *PCSK9*^{WT} compared to those transfected with a loss-of-function *PCSK9*^{Q152H} variant that fails to be secreted (Fig. S1C to S1F).[20] Transfection efficiency in these cells was confirmed via immunoblotting for PCSK9 and GFP encoded by the bicistronic plasmid utilized in these studies (Fig. S1G). Lipid uptake and accumulation was also assessed in primary human hepatocytes that were exposed to medium harvested from HuH7 cells transfected with either *PCSK9*^{WT} or the secretion-deficient *PCSK9*^{Q152H} variant (Fig. 1F). Consistent with cultured HepG2 cells, secreted *PCSK9*^{WT} significantly reduced OA-induced lipid accumulation in primary human hepatocytes.

The CD36 inhibitor SSO reduces OA-induced lipid droplet accumulation in PCSK9 knockdown hepatocytes

Our next aim was to assess the recently described inhibitory role of PCSK9 on CD36 (using a pharmacologic antagonist of CD36,

Please cite this article as: Lebeau PF et al. *Pcsk9* knockout exacerbates diet-induced non-alcoholic steatohepatitis, fibrosis and liver injury in mice. JHEP Reports (2019), https://doi.org/10.1016/j.jhepr.2019.10.009

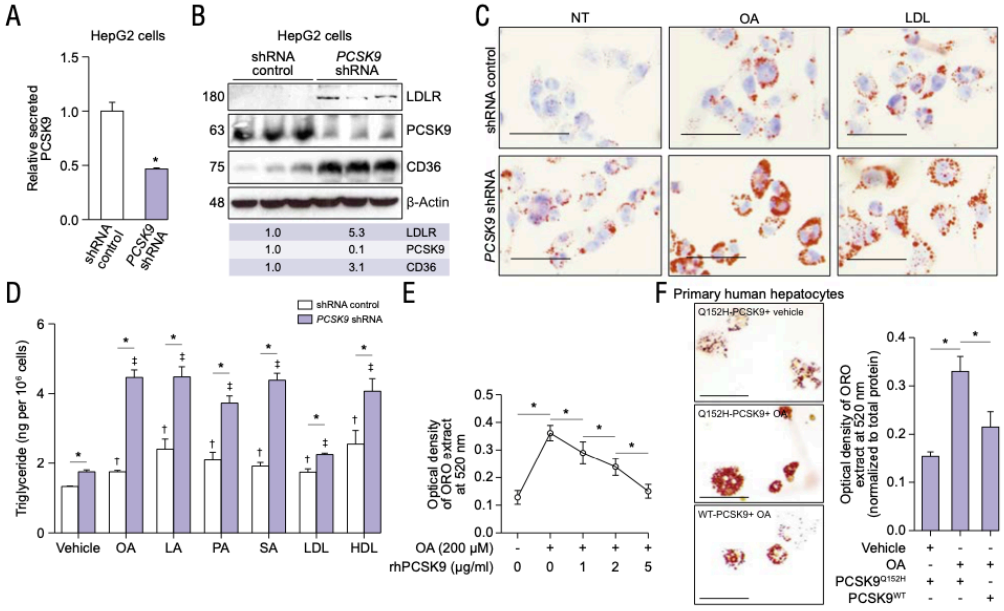

Fig. 1. PCSK9 reduces the triglyceride content of HepG2 cells and primary human hepatocytes. (A,B) PCSK9 knockdown in *PCSK9* shRNA HepG2 cells was confirmed via ELISA for secreted PCSK9 (*p <0.05) and immunoblots for PCSK9-regulated receptors LDLR and CD36. (C) ORO lipid droplet staining of HepG2 control cells (shRNA control) and PCSK9 knockdown cells (*PCSK9* shRNA) in the presence or absence of OA (200 μm) and LDL (50 μg/ml). (D) Intracellular triglyceride content was also quantified in cells treated with either OA (200 μM), LA (200 μM), PA (200 μM), SA (200 μM) and lipoproteins LDL (50 μg/ml) and HDL (50 μg/ml) for 24 h (*p <0.05; †p<0.05 *vs.* vehicle-shRNA control; ‡p<0.05 *vs.* vehicle-*PCSK9* shRNA). (E) The effect of recombinant human PCSK9 on OA uptake was examined in HepG2 cells via quantification of the density of ORO extracts (*p <0.05). (F) ORO staining was carried out in primary human hepatocytes that were exposed to medium harvested from HuH7 cells transfected with either secreted *PCSK9*^{WT} or a *PCSK9* variant that fails to exit the cell,[20] *PCSK9*^{Q152H}, and treated with OA (200 μM) for 24 h. ORO extracts from primary human hepatocytes were also quantified (*p <0.05). Results are shown as the mean and error bars as SD. Differences between groups were determined via Student's *t* test or one-way ANOVA. Scale bars, 50 μm. HDL, high-density lipoprotein; LA, linoleate; LDL, low-density lipoprotein; OA, oleate; ORO, Oil red O; PA, palmitate; SA, stearate; SSO, sulfo-N-succinimidyl oleate.

SSO) as this is the mechanism by which PCSK9 is thought to regulate hepatic lipid levels.[21] Consistent with *PCSK9* shRNA knockdown HepG2 cells, the knockdown of *PCSK9* in HepG2 and HuH7 cells using siRNA increased intracellular lipid content; a result that was further exacerbated by incubating cells in OA (Fig. 2A and B). No such increase in lipid accumulation, however, was observed in cells pre-treated with SSO. Consistently, SSO pre-treatment also attenuated hepatic lipid accumulation in *Pcsk9*$^{-/-}$ mice exposed to a bolus injection of OA (Fig. 2C). The knockdown of CD36 using siRNA (si*CD36*) also reduced lipid accumulation in HepG2 cells challenged with OA (Fig. 2D and E). Lastly, to confirm the role of CD36 as a driver of lipid accumulation in the context of PCSK9 deficiency, experiments were repeated in cells co-transfected with si*PCSK9* and si*CD36*. ORO extract and quantification from these cells demonstrates that ablation of CD36 expression markedly reduced lipid accumulation occurring as a result of PCSK9 knockdown in the presence or absence of OA (Fig. 2F). Similar findings were observed in HuH7 cells (Fig. S2A). The difference in lipid accumulation between control and *PCSK9* shRNA cells was also lost in cells overexpressing CD36 (Fig. 2G). Effective knockdown of PCSK9 and CD36, as well as overexpression of CD36 in HepG2 cells, was confirmed via immunoblotting (Fig. S2B to S2D). Collectively, these data suggest that increased expression of CD36 strongly contributes to the heightened levels of intracellular lipids observed in hepatocyte cell lines with reduced PCSK9 expression.

PCSK9 protects cultured hepatocytes from palmitate-induced ER stress and cytotoxicity

To substantiate our findings, we next investigated whether PCSK9 would protect from the well-established ER stress-associated effects of increased CD36 expression, such as ER Ca^{2+} depletion, reactive oxygen species (ROS) production and cytotoxicity.[22] First, increased expression levels of the ER stress markers IRE1α and glucose-regulated protein of 78-kDa (*GRP78*), and the pro-apoptotic markers CCAAT/enhancer-binding protein homologous protein (*CHOP*), *ATF6* and s*XBP1* were observed in *PCSK9* shRNA compared to control shRNA HepG2 cells treated with PA, via immunoblotting and quantitative real-time PCR (Fig. 3A and B). Similarly, primary human hepatocytes exposed to medium harvested from HuH7 cells transfected with *PCSK9*^{Q152H} also yielded increased PA-induced expression of ER stress markers compared to those exposed to medium containing *PCSK9*^{WT} (Fig. 3C). Consistent with previous studies,[19] treatment with OA and lipoproteins did not cause ER stress in HepG2 cells (Fig. S3A, S3B and S3C).

PCSK9 shRNA HepG2 cells also exhibited increased cytotoxicity in response to PA relative to controls (Fig. 3D and S3D). Interestingly, although SSO-mediated CD36 inhibition failed to reduce

Please cite this article as: Lebeau PF et al. *Pcsk9* knockout exacerbates diet-induced non-alcoholic steatohepatitis, fibrosis and liver injury in mice. JHEP Reports (2019), https://doi.org/10.1016/j.jhepr.2019.10.009

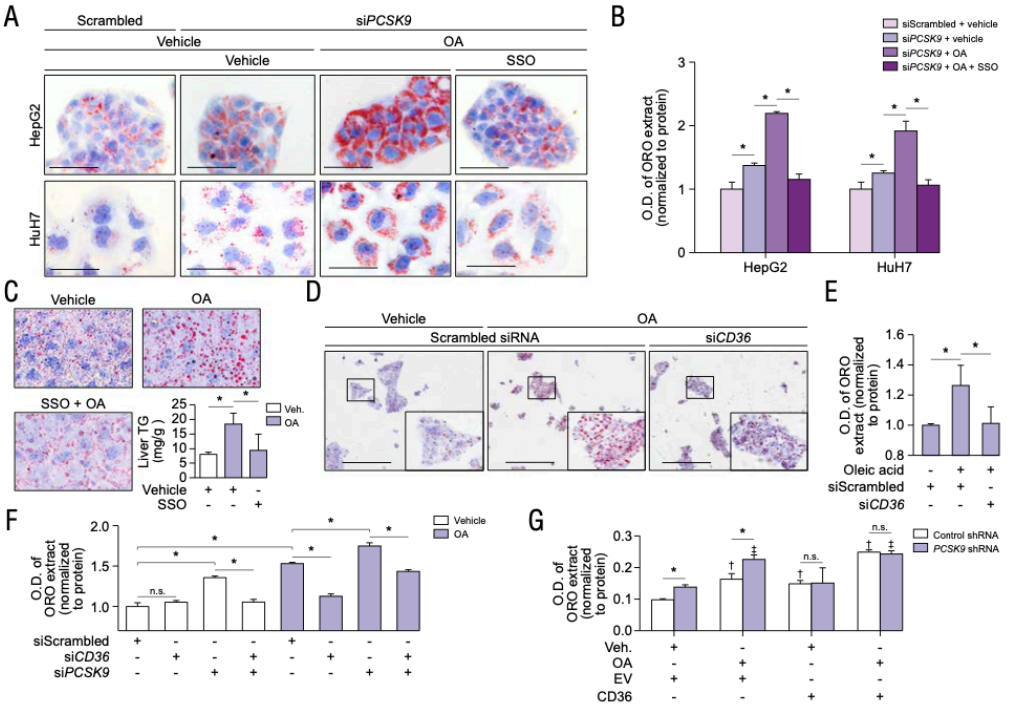

Fig. 2. PCSK9 regulates FA uptake in immortalized hepatocytes through CD36. (A,B) HepG2 and HuH7 cells were transfected with si*PCSK9* or scrambled control siRNA. Cells were subsequently treated with OA and or SSO (10 μM), for an additional 24 h (**p* <0.05). (C) 12-week-old male C57BL/6J mice were pre-treated with SSO (10 mg/kg) for 1 h and subsequently administered with OA for an additional 2 h. Hepatic lipid accumulation was visually examined via ORO staining and quantified using a triglyceride assay. (D,E) The effect of CD36 inhibition on OA uptake was also assessed using si*CD36* (**p* <0.05). Finally, intracellular lipid accumulation was examined in HepG2 cells co-transfected with si*PCSK9* and si*CD36*, via ORO extract and quantification using a spectrophotometer (**p* <0.05). (G) The effect of CD36 overexpression on lipid accumulation was examined in HepG2 cells via quantification of ORO extract (**p* <0.05; †*p*<0.05 *vs.* control shRNA; ‡*p*<0.05 *vs. PCSK9* shRNA). Results are shown as the mean and error bars as SD. Differences between groups were determined via Student's *t* test or one-way ANOVA. Scale bars, (A) 50 μm, (D) 200 μm. FA, fatty acid; OA, oleate; ORO, Oil red O; SSO, sulfo-N-succinimidyl oleate.

PA-induced cytotoxicity in shRNA control cells, the CD36 inhibitor attenuated cytotoxicity in *PCSK9* shRNA knockdown cells (Fig. 3D). Given the role of ER stress in the production of ROS, the ability of PCSK9 to protect from PA-induced ROS was also examined in HepG2 cells (Fig. 3E). We observed that PA treatment led to a significant increase in ROS production in *PCSK9* shRNA HepG2 cells compared to shRNA controls during the course of the experiment.

Next, we assessed ER Ca^{2+} depletion, which represents another established outcome of ER stress in cells treated with PA.[23] The fluorometric cytosolic Ca^{2+} indicator utilized in these studies, Fura-2-AM, increases in fluorescence intensity as Ca^{2+} exits the ER into the cytosol.[24] To measure relative ER Ca^{2+} content, HepG2 cells pre-treated with PA (5 h; 500 μM) were exposed to a potent sarco/endoplasmic reticulum ATPase (SERCA) pump inhibitor, cyclopiazonic acid (CPA; 50 μM; Fig. 3F). In response to CPA, we observed that PA-treated shRNA control cells exhibited ER Ca^{2+} loss to a similar extent as untreated controls. In contrast to this result, *PCSK9* shRNA knockdown cells pre-treated with PA failed to exhibit loss of ER Ca^{2+} in response to CPA, suggesting that PA induced ER Ca^{2+} depletion during pre-treatment in these cells. In support of these results, a time-course study in which ER Ca^{2+} depletion was monitored over a 210 min period yielded similar findings (Fig. S3E). Increased ER expansion, another hallmark feature of ER stress, was also observed in HepG2 cells transfected with a splice-switching oligomer that causes ER retention of PCSK9 in response to PA[25] (Fig. S4A and S4B). Appropriate splice-switching and ER retention of PCSK9 in these cells was confirmed by immunoblotting (Fig. S4C).

Pcsk9$^{-/-}$ mice exhibit compensatory changes in biliary cholesterol excretion and in the expression of hepatic lipid regulatory proteins

Given the observed increase in lipid droplet content in cultured hepatocytes, PCSK9-dependent changes in hepatic lipid content were also examined *in vivo*. The livers of NCD-fed 12-week-old *Pcsk9*$^{-/-}$ mice exhibited increased ORO staining of lipid droplets and protein levels of the lipid droplet marker perilipin (Fig. 4A) compared to controls. Consistent with previous reports, immunohistochemical staining also demonstrated a marked increase in cell-surface levels of LDLR, VLDLR and CD36 expression in the livers of *Pcsk9*$^{-/-}$ mice compared to controls.[13,16,18] We also report the novel finding that *Pcsk9*$^{-/-}$ mice exhibit increased levels of the cholesterol efflux transporter ABCA1 compared to controls (Fig. 4A and S5A). In contrast to the LDLR, CD36 and the VLDLR,

Please cite this article as: Lebeau PF et al. *Pcsk9* knockout exacerbates diet-induced non-alcoholic steatohepatitis, fibrosis and liver injury in mice. JHEP Reports (2019), https://doi.org/10.1016/j.jhepr.2019.10.009

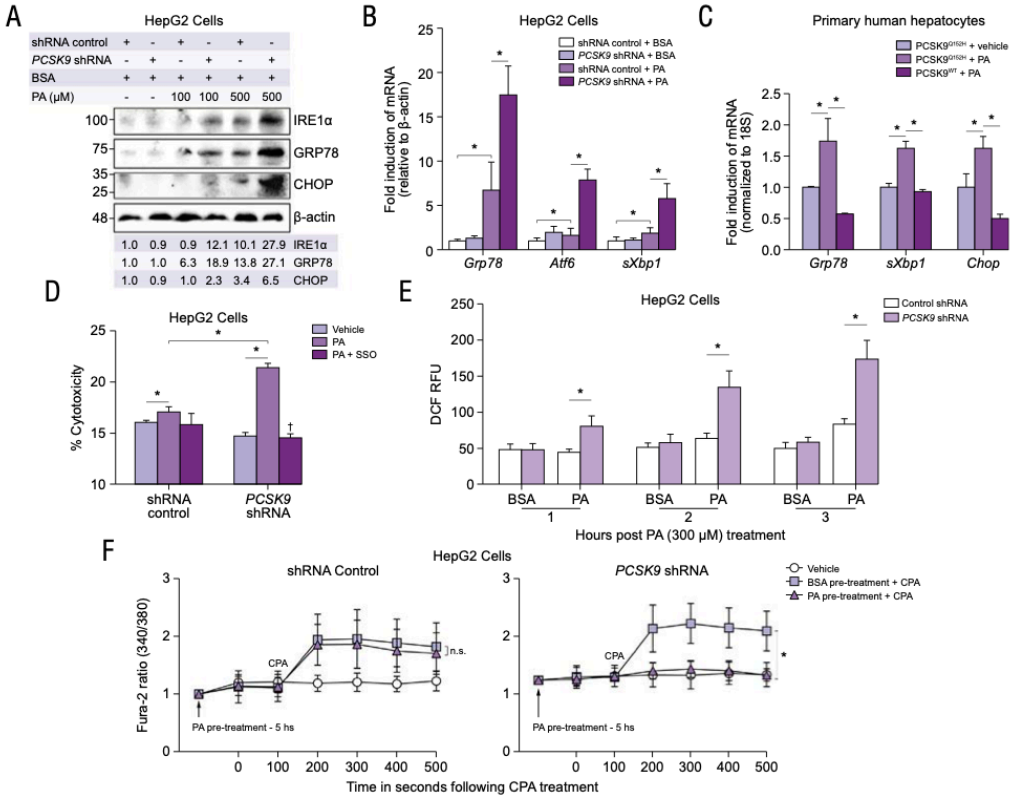

Fig. 3. PCSK9 blocks palmitate-induced ER stress in HepG2 cells. (A,B), Immunoblot and real-time PCR analysis of ER stress marker expression in shRNA control and *PCSK9* shRNA HepG2 cells treated with vehicle (BSA) or PA (100 or 500 μM) for 24 h (**p* <0.05). (C) Primary human hepatocytes were exposed to medium harvested from HuH7 cells transfected with either $PCSK9^{WT}$ or a $PCSK9^{Q152H}$ variant that fails to be secreted. Hepatocytes were then treated with PA (500 μM) for 24 h and assessed for ER stress marker expression via real-time PCR (**p* <0.05). (D) Cytotoxicity of PA-treated HepG2 cells was also examined using a lactate dehydrogenase assay in the presence or absence of CD36 inhibitor, SSO (10 μM; **p* <0.05; †*p* <0.05 *vs.* PA). (E) ROS production was assessed by pre-loading cells with DCF, a ROS-sensitive fluorogenic dye, at 1, 2 and 3 h in HepG2 cells following PA treatment (**p* <0.05). (F) The Fura-2-AM Ca^{2+} indicator was used to examine PA-induced ER Ca^{2+} release. Following the incubation of HepG2 cells with PA for 5 h (500 μM), the SERCA blocker CPA (50 μM) was used to promote the spontaneous release of ER Ca^{2+} to examine total ER Ca^{2+} content (**p* <0.05). Results are shown as the mean and error bars as SD. Differences between groups were determined by Student's *t* test or one-way ANOVA. CPA, cyclopiazonic acid ER, endoplasmic reticulum; PA, palmitate; SSO, sulfo-N-succinimidyl oleate.

changes in hepatic ABCA1 expression in $Pcsk9^{-/-}$ mice likely occurred as a result of increased mRNA transcript expression (Fig. S5B). Elevated expression of hepatic PCSK9-regulated receptors, LDLR, VLDLR and CD36 was also confirmed using immunoblots (Fig. 4B). Given that hepatic biliary secretion or transintestinal cholesterol excretion are established mechanisms of cholesterol clearance,[26,27] fecal cholesterol content was also assessed (Fig. 4C). The feces of $Pcsk9^{-/-}$ mice contained increased levels of cholesterol compared to controls. The positive correlation between PCSK9 and circulating cholesterol and triglycerides was also confirmed via colorimetric assays (Fig. 4D). Consistent with our hypothesis that elevated hepatic lipid content in $Pcsk9^{-/-}$ mice occurs as a result of increased lipid uptake, no difference was observed in the FA oxidation marker, β-hydroxybutyrate (Fig. 4E). Furthermore, we observed that the livers of $Pcsk9^{-/-}$ mice exhibited (a) a significant reduction in peroxisome proliferator-activated receptor gamma (PPARγ) coactivator 1-alpha (PGC1α), a protein commonly associated with *de novo* cholesterol synthesis and PPARγ-mediated NAFLD; (b) a modest but significant increase in mRNA levels of the lipolysis markers ACOX1 and APOC2; and (c) no change in the expression of the FA oxidation marker PPARα (Fig. 4F). Consistent with immunohistochemistry data, a significant increase of perilipin at the mRNA level was also observed in $Pcsk9^{-/-}$ mice relative to controls (Fig. 4F). Although additional studies are required to confirm that *de novo* lipogenesis and lipid oxidation do not contribute to the observed phenotype, our data suggest that lipid accumulation in the livers of $Pcsk9^{-/-}$ mice occurs largely as a result of increased lipid uptake at the cell surface.

Pcsk9 knockout exacerbates diet-induced hepatic steatosis in mice

Although we did not observe profound differences in gross liver morphology or injury in NCD-fed $Pcsk9^{-/-}$ mice compared to $Pcsk9^{+/+}$ counterparts, this diet is not lipid-rich or used for the

Please cite this article as: Lebeau PF et al. *Pcsk9* knockout exacerbates diet-induced non-alcoholic steatohepatitis, fibrosis and liver injury in mice. JHEP Reports (2019), https://doi.org/10.1016/j.jhepr.2019.10.009

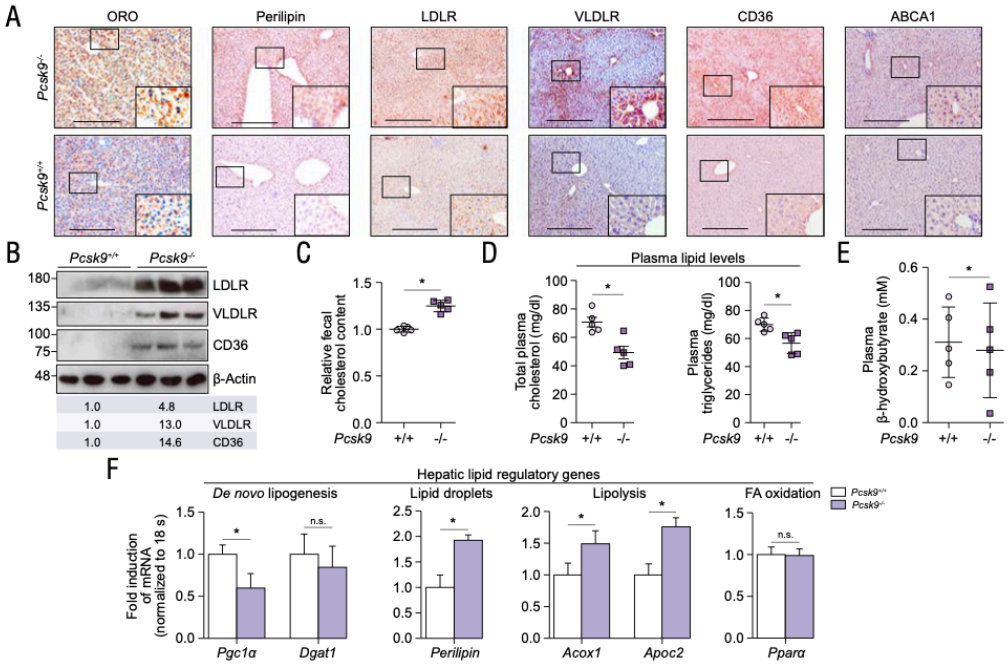

Fig. 4. *Pcsk9*$^{-/-}$ mice exhibit compensatory changes in the expression of lipid regulatory proteins. (A) Representative ORO staining of hepatic lipid droplets in *Pcsk9*$^{+/+}$ and *Pcsk9*$^{-/-}$ mice (n = 10; C57BL/6J). Protein levels of the lipid droplet marker, perilipin, as well as LDLR, VLDLR, CD36 and the cholesterol efflux transporter, ABCA1, were also examined by immunohistochemistry. (B) Hepatic expression of LDLR, VLDLR and CD36 was also examined using immunoblots. (C, D,E) Fecal cholesterol, total plasma cholesterol and triglycerides, as well as a circulating marker of FA oxidation, β-hydroxybutyrate, were measured using colorimetric assays (n = 5). (F) mRNA levels of genes known to play a role in FA metabolism (n = 5). Results are shown as the mean and error bars as SD. **p* <0.05 by Student's *t* test or one-way ANOVA. Scale bars, 200 μm. FA, fatty acid; ORO, Oil red O.

study of hepatic steatosis. Therefore, our next aim was to assess the effect of a HFD on liver function and injury in the context of PCSK9 deficiency and increased hepatic CD36 expression. Accordingly, 6-week-old *Pcsk9*$^{-/-}$ mice and *Pcsk9*$^{+/+}$ controls were fed either NCD or HFD for 12 weeks. Upon removal of the liver from these animals during sacrifice, an apparent increase in size and change in color were observed in the HFD-fed *Pcsk9*$^{-/-}$ mice compared to controls (Fig. 5A). Assessment of hepatic lipid droplets via ORO and H&E staining also demonstrated an increase in lipid droplets in the livers of HFD-fed *Pcsk9*$^{-/-}$ mice compared to HFD-fed controls (Fig. 5B). Although total body weight was not affected by PCSK9 (Fig. 5C) in these experiments, significant increases in liver weight (Fig. 5D) and liver triglyceride and cholesterol content (Fig. 5E) were observed in HFD-fed *Pcsk9*$^{-/-}$ mice compared to controls. A trend was also apparent for elevated gonadal, inguinal and brown adipose tissue weights in the *Pcsk9*$^{-/-}$ mice on HFD, but the differences between genotypes were not statistically significant in this experiment (Fig. 5F).

Pcsk9 knockout mice exhibit increased diet-induced liver injury and insulin resistance

We next examined hepatic ER stress in these mice; a process well known to contribute to hepatic steatosis.[4–6] Increased expression levels of ER stress markers, pro-apoptotic markers, and pro-fibrotic markers were observed in the livers of HFD-fed *Pcsk9*$^{-/-}$ mice compared to HFD-fed *Pcsk9*$^{+/+}$ control mice (Fig. 6A, B). Increased staining of F4/80, a marker of pro-inflammatory Kupffer cells, and increased hepatic mRNA expression of pro-inflammatory markers were also observed in the livers of HFD-fed *Pcsk9*$^{-/-}$ mice compared to controls (Fig. 6A,C). A modest increase in fibrosis was also observed in these mice via Mason's trichrome staining of collagen (blue), as well as immunohistochemical staining of fibronectin. Assessment of plasma alanine aminotransferase (ALT) activity, as well as apoptosis using a TUNEL assay, also revealed that *Pcsk9*$^{-/-}$ mice were more prone to diet-induced hepatic injury compared to controls (Fig. 6D and E). Similarly, an increase in protein aggregate accumulation was observed in HFD-fed *Pcsk9*$^{-/-}$ mice compared to controls using thioflavin-T (Fig. S6)

Hepatic steatosis is also an established driver of insulin resistance and diabetes as it tends to promote chronically elevated circulating glucose levels resulting from constitutively activated gluconeogenic pathways.[28] For this reason, our last aim was to examine the effect of *Pcsk9* knockout on markers of hepatic insulin resistance in HFD-fed mice. First, however, we examined glucose production in vehicle- and PA-treated primary hepatocytes isolated from *Pcsk9*$^{-/-}$ and *Pcsk9*$^{+/+}$ littermate control mice. Glucose production was also examined in PA-treated primary hepatocytes isolated from C57BL/6J mice in the presence or absence of recombinant PCSK9 (1 μg) for 24 h. In both cases, the presence of PCSK9 attenuated PA-induced glucose production. Assessment in HepG2 cells also revealed that PA treatment induced glucose

Please cite this article as: Lebeau PF et al. *Pcsk9* knockout exacerbates diet-induced non-alcoholic steatohepatitis, fibrosis and liver injury in mice. JHEP Reports (2019), https://doi.org/10.1016/j.jhepr.2019.10.009

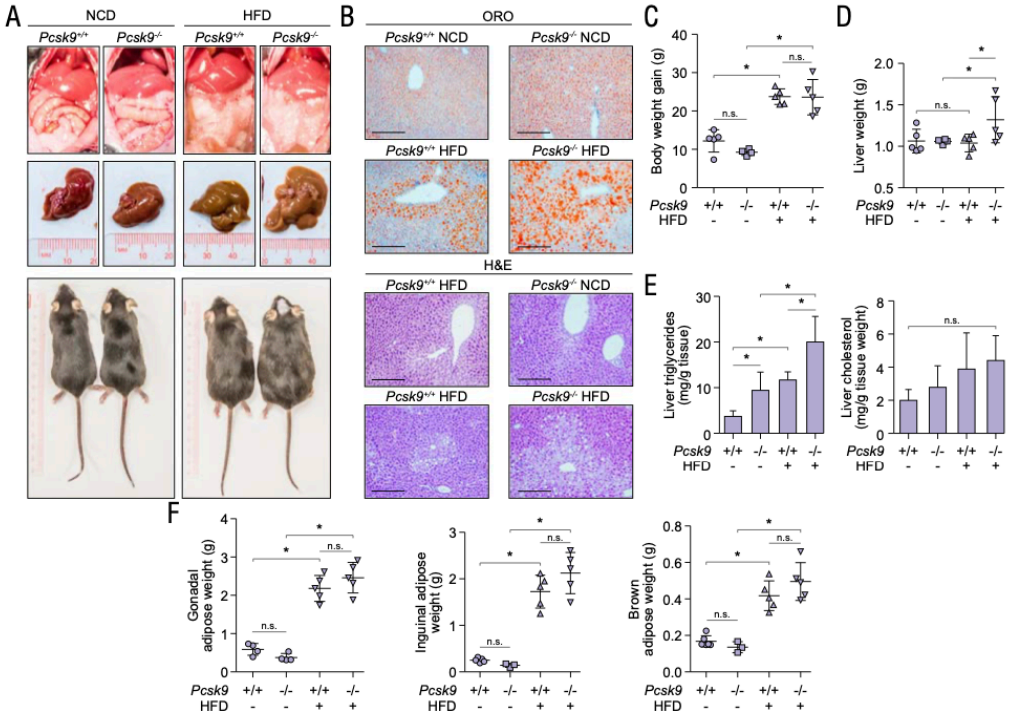

Fig. 5. PCSK9 reduces ER stress-induced hepatic lipid accumulation. (A) Changes in liver size and gross morphology were first visualized and imaged following the sacrifice of NCD- and HFD-fed *Pcsk9*$^{-/-}$ and *Pcsk9*$^{+/+}$ mice (n = 5). (B) Hepatic lipid accumulation was then examined via ORO and H&E. Changes in body and liver weight (C and D), as well as liver triglycerides and cholesterol levels (E) and adipose weights (F) were also examined. Results are shown as the mean and error bars as SD. **p* <0.05 by Student's *t* test or one-way ANOVA. Scale bars, 200 μm. ER, endoplasmic reticulum; HFD, high-fat diet; NCD, normal control diet, ORO, Oil red O.

production to a greater extent in PCSK9 knockdown cells than in control cells (Fig. S7A). Further, exposure of naive HepG2 cells to medium harvested from HuH7 cells transfected with either *PCSK9*^{WT} or the secretion-defective *PCSK9*^{Q152H} also demonstrated that PCSK9 protected against PA-induced gluconeogenesis (Fig. S7B).

In mice, glucose and insulin tolerance tests (GTT and ITT, respectively) revealed that HFD-fed *Pcsk9*$^{-/-}$ mice exhibited a reduction in glucose uptake in response to a bolus injection of glucose or insulin (Fig. 7C), indicative of resistance to insulin.[29,30] A significant increase in resting glucose levels, which represents another characteristic of insulin resistance, was also observed in HFD-fed *Pcsk9*$^{-/-}$ mice compared to HFD-fed controls (Fig. 7D). In contrast to other models of diet-induced insulin resistance,[31] plasma insulin levels were reduced in *Pcsk9*$^{-/-}$ mice compared to controls, but this likely involved pancreatic islet abnormalities, as reported previously (Fig. 7E).[29,30] Mice were also injected with insulin 1 h prior to sacrifice in order to examine the phosphorylation/activation status of protein kinase B (AKT); a central regulator and strong promoter of hepatic glucose uptake and metabolism (Fig. 7F).[31] As expected, insulin treatment led to the phosphorylation of AKT in the livers of NCD-fed mice, but no difference was observed between *Pcsk9*$^{-/-}$ and *Pcsk9*$^{+/+}$ mice. In HFD-fed mice, however, the ability of insulin to activate hepatic AKT was reduced to a greater extent in *Pcsk9*$^{-/-}$ mice than in the *Pcsk9*$^{+/+}$ control mice. Consistent with other studies, hepatic steatosis severity in the mice was positively correlated with the mRNA abundance of hepatic gluconeogenic markers, including signal transducer and activator of transcription 3 (*Stat3*), glucose 6 phosphatase (*G6p*), stearoyl-CoA desaturase-1 (*Scd1*), pyruvate dehydrogenase kinase 4 (*Pdk4*) and the dimethylaniline monooxygenase [N-oxide-forming] 2 (*Fmo2*) (Fig. 7G).[32] In line with the other endpoints examined in these mice, increased gluconeogenic marker expression was observed in the livers of *Pcsk9*$^{-/-}$ compared to *Pcsk9*$^{+/+}$ mice. Collectively, these data suggest that PCSK9 can reduce liver lipid accumulation and protect against ER stress, hepatic insulin resistance and glucose production in response to a HFD.

Discussion

Previous studies have demonstrated that the equilibrium of hepatic lipid levels can favor hepatic steatosis during conditions of (a) increased *de novo* lipogenesis, (b) heightened lipid uptake (c) reduced lipid efflux and (d) reduced lipid oxidation.[32] In the case of *Pcsk9*$^{-/-}$ mice, our studies as well as those of others,[18] suggest that PCSK9 prevents the uptake of lipid into the liver by downregulating the expression of CD36. Consistent with our observations, previous studies have also shown that increased expression of CD36 can promote fatty liver disease and contribute

Please cite this article as: Lebeau PF et al. *Pcsk9* knockout exacerbates diet-induced non-alcoholic steatohepatitis, fibrosis and liver injury in mice. JHEP Reports (2019), https://doi.org/10.1016/j.jhepr.2019.10.009

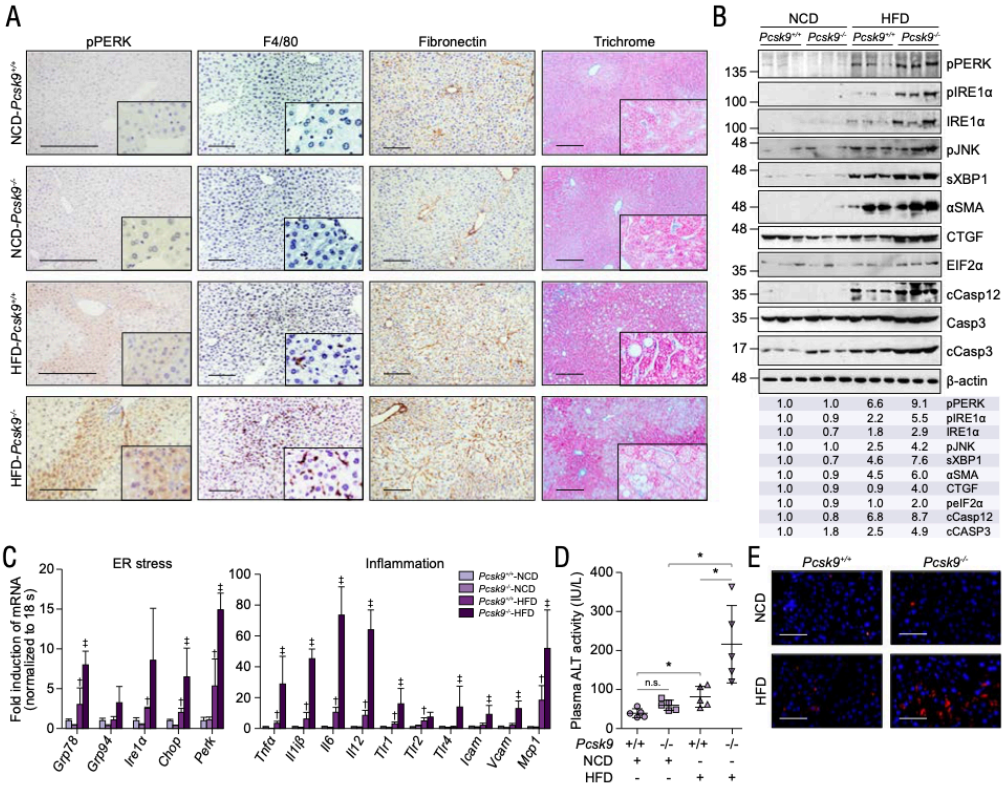

Fig. 6. *Pcsk9* knockout exacerbates diet-induced ER stress and inflammation in the livers of mice. (A, B and C) Markers of ER stress (pPERK, pIRE1α, IRE1α, pJNK, sXBP1, peIF2α and *Chop*), inflammation (F4/80, *Tnfα*, *Il1β*, *Il6*, *Il12*, *Tlr1*, *Tlr2*, *Tlr4*, *Icam*, *Vcam* and *Mcp1*), fibrosis (fibronectin, αSMA, CTGF) and apoptosis (cCasp12 and Casp12) were examined in the livers of NCD- and HFD-fed mice via immunohistochemical staining, immunoblotting and real-time PCR. Hepatic collagen deposition (blue) was also examined via Masson's Trichrome. (D,E) Liver injury was examined via assessment of plasma ALT activity, as well as liver TUNEL staining of apoptotic cells (DAPI staining shown as blue and TUNEL-positive apoptotic cells shown as red). Results are shown as the mean and error bars as SD. **p* <0.05 by Student's *t* test or one-way ANOVA. Scale bars, 100 μm. ALT, alanine aminotransferase; ER, endoplasmic reticulum; HFD, high-fat diet; NCD, normal control diet.

to hepatic insulin resistance.[33] Furthermore, CD36-mediated FA uptake is known to promote ER stress and lipotoxicity in cell types with high capacity for FA metabolism including adipocytes, cardiomyocytes, hepatocytes, endothelial cells, macrophages, pancreatic β cells, podocytes and neurons.[22] Here, we demonstrate that PCSK9 prevents CD36-mediated FA uptake and accumulation in cultured hepatocytes. We also show that under normal dietary conditions, several compensatory mechanisms in the livers of *Pcsk9*$^{-/-}$ mice may act in concert to suppress hepatic steatosis. During a HFD metabolic challenge, however, we observed a significant increase in the expression of markers of ER stress, fibrosis, inflammation and apoptosis, as well as plasma levels of ALT in *Pcsk9*$^{-/-}$ mice compared to *Pcsk9*$^{+/+}$ controls.

The current landscape of studies examining the role of PCSK9 in hepatic steatosis in humans remains controversial. However, pre-clinical data have been largely consistent, demonstrating that circulating PCSK9 can prevent hepatic lipid uptake and accumulation in mice. Demers and coworkers were the first to demonstrate that PCSK9 negatively regulates the expression of CD36 and also reported a 3- to 4-fold increase in hepatic triglyceride levels in NCD-fed *Pcsk9*$^{-/-}$ mice.[18] Recent studies have also identified *E2f1* as a major regulator of hepatic lipid homeostasis in a manner dependent on PCSK9.[34] Lai and colleagues reported increased hepatic lipid content in *E2f1*$^{-/-}$ mice and also discovered that these mice exhibit significantly reduced circulating PCSK9 levels. Upon re-expression of PCSK9 in these mice, the fatty liver phenotype was lost. Consistent with this growing body of literature, a recent network analysis done in primary human hepatocytes identified PCSK9 as a gene linked to liver fat content and NAFLD.[35]

Two independent clinical studies have now demonstrated consistent findings with regards to the association between liver fat content and circulating PCSK9 levels. The Dallas heart study reported a modest but significant positive correlation between liver fat content and circulating PCSK9 levels (n = 2,027; p <0.0001).[36] Ruscica and colleagues have now also reported a positive correlation between circulating PCSK9 and liver steatosis grade (p = 0.0011) as well as necroinflammation, ballooning and

Please cite this article as: Lebeau PF et al. *Pcsk9* knockout exacerbates diet-induced non-alcoholic steatohepatitis, fibrosis and liver injury in mice. JHEP Reports (2019), https://doi.org/10.1016/j.jhepr.2019.10.009

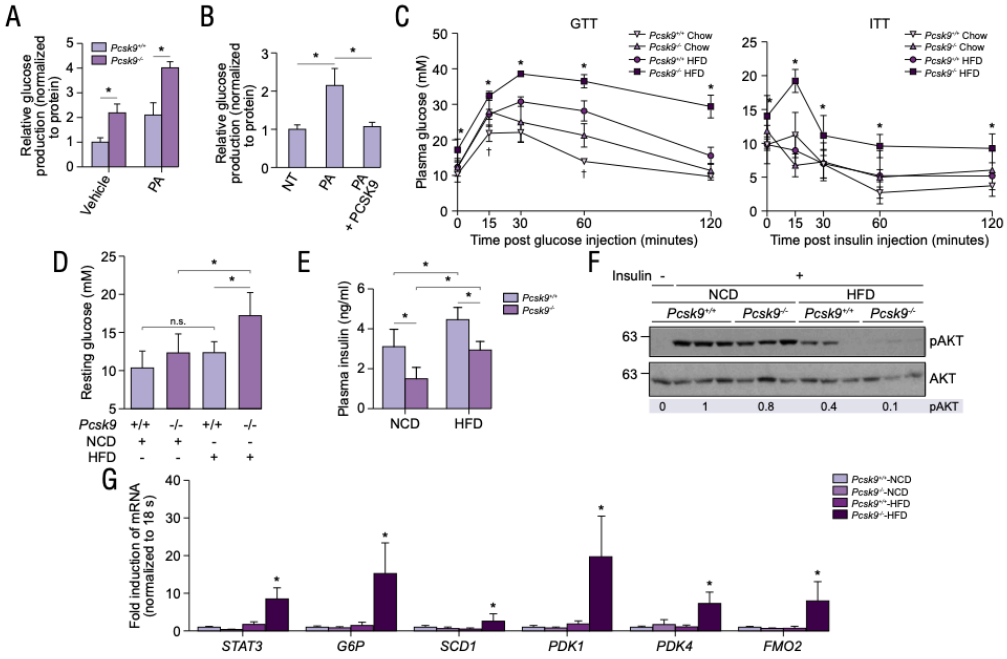

Fig. 7. *Pcsk9* knockout contributes to gluconeogenesis and diet-induced insulin resistance. (A) Gluconeogenesis was first examined in primary hepatocytes isolated from $Pcsk9^{-/-}$ and $Pcsk9^{+/+}$ littermate control mice (n = 5) treated with PA. (B) Gluconeogenesis was also assessed in primary hepatocytes isolated from male C57BL/6J mice (n = 4) treated with PA in the presence or absence of recombinant human PCSK9 (1 μg; p <0.05). (C) One week prior to sacrifice, mice were injected with either insulin (1 IU/kg) or glucose (0.8 g/kg) (ITT and GTT, respectively) to assess insulin resistance in NCD- and HFD-fed $Pcsk9^{+/+}$ and $Pcsk9^{-/-}$ mice (*p <0.05 *vs.* $Pcsk9^{+/+}$). (D) Resting glucose levels were also assessed prior to injections. (E) Resting plasma insulin levels in these mice were examined using an ELISA. (F) Mice were injected with insulin 1 h prior to sacrifice to assess hepatic insulin resistance via phosphorylation of AKT by immunoblotting. (G) The expression of pro-gluconeogenic markers (*Stat3, G6p, Scd1, Pdk1, Pdk4 and Fmo2*) was examined in the livers of HFD-fed mice by real-time PCR (*p <0.05. *vs.* HFD-fed $Pcsk9^{+/+}$). Results are shown as the mean and error bars as SD. *p <0.05. Differences between groups were determined via Student's t test or one-way ANOVA. GTT, glucose tolerance test; HFD, high-fat diet; ITT, insulin tolerance test; NCD, normal control diet; PA, palmitate.

fibrosis stage (n = 201).[37] Consistent with these findings our research group has observed that diet-induced steatosis promotes *de novo* hepatic PCSK9 expression and increases circulating PCSK9 levels in mice.[38] In contrast to these data, Wargny and colleagues failed to observe a significant correlation between circulating PCSK9 levels and plasma aminotransferases, liver fat content, histological liver lesions, steatosis severity, NASH activity score, lobular and/or portal inflammation or ballooning in 3 patient cohorts with advanced stages of NASH (n = 478).[39] Given the severity of steatosis in the patients from this study, however, the authors highlight that variations between studies suggest that in humans, PCSK9 likely plays a role in the early development of NAFLD and not in the late stages of NASH.

Beyond liver fat content, Mbikay and colleagues have reported abnormalities in pancreatic islets of $Pcsk9^{-/-}$ mice, which were shown to contribute to insulin resistance.[29] Consistent with these findings, we also report the novel finding that diet-induced hepatic steatosis attenuates insulin-induced phosphorylation and activation of AKT in the livers of $Pcsk9^{-/-}$ mice to a significantly greater extent than in controls. We have consistently shown that HFD-fed $Pcsk9^{-/-}$ mice exhibit reduced rates of glucose uptake and insulin sensitivity, all of which represent hallmark features of hepatic insulin resistance. In line with these findings, a recent study also identified a positive correlation between loss-of-function *PCSK9* mutations and increased fasting glucose, body weight, waist-to-hip ratio and odds ratio of type 2 diabetes.[40]

Accumulating evidence demonstrates that PCSK9 regulates the uptake and accumulation of lipid in the livers of mice. Given the current inconsistencies in clinical data sets, additional studies are required before strong conclusions can be made in the context of human disease. Interestingly, recent studies have demonstrated that FDA-approved monoclonal antibodies targeted against the LDLR-binding domain of circulating PCSK9 increase its concentrations 7-fold as a result of antagonizing LDLR-mediated clearance.[41] Given that it is likely that the domain utilized by PCSK9 to interact with CD36 differs from its LDLR-binding domain,[18] it remains possible and even likely that such antibodies may also reduce CD36 expression as a byproduct of increasing the circulating pool of PCSK9. Additional studies, however, are required to answer this important question and to determine whether anti-PCSK9 antibodies could be utilized to protect against CD36-driven diseases like NAFLD and NASH.

Overall, the abundance of data characterizing PCSK9 as a modulator of circulating cholesterol strongly suggest that its influence on the latter exceeds that of its effect on circulating and peripheral triglyceride levels. Nonetheless, our findings as well as

Please cite this article as: Lebeau PF et al. *Pcsk9* knockout exacerbates diet-induced non-alcoholic steatohepatitis, fibrosis and liver injury in mice. JHEP Reports (2019), https://doi.org/10.1016/j.jhepr.2019.10.009

those discussed herein, suggest that hepatic PCSK9 expression is upregulated during conditions of steatosis to prevent further lipid uptake and accumulation in the liver, thus acting as a classical feedback modulator of hepatic lipid levels. Moreover, our data demonstrate that in mice, PCSK9 can protect against ER stress, fibrosis and injury of the liver in response to conditions of excessive fat consumption.

Abbreviations

ABCA1, ATP-binding cassette subfamily A member 1; ACOX1, acyl-coA Oxidase 1; AKT, protein kinase B; ALT, alanine aminotransferase; APOC2, apolipoprotein C2; ApoE, apolipoprotein E; ATF, activating transcription factor; cCasp, cleaved-caspase; CHOP, CCAAT/enhancer-binding protein homologous protein; CPA, cyclopiazonic acid; CTGF, connective tissue growth factor, CVD, cardiovascular disease; eIF2, eukaryotic initiation factor 2; ER, endoplasmic reticulum; FA, fatty acid; FAS, fatty acid synthase; FMO2, flavin containing monooxygenase 2; GRP78, 78-kDa glucose regulated protein; GRP94, 94-kDa glucose regulated protein; GTT, glucose tolerance tests; G6P, glucose 6-phosphate; HDL, high-density lipoprotein; HFD, high-fat diet; IL, interleukin; IRE1α, Inositol-requiring enzyme-1 alpha; ITT, insulin tolerance tests; JNK, c-Jun N-terminal kinase; LA, linoleate; LDL, low-density lipoprotein; LDLR, LDL receptor; MCP-1, monocyte chemoattractant protein-1; NAFLD, non-alcoholic fatty liver disease; NASH, non-alcoholic steatohepatitis; NCD, normal control diet; NS, non-significant; OA, oleate; ORO, Oil Red O; oxLDL, oxidized LDL; PA, palmitate; PCSK9, proprotein convertase subtilisin/kexin type 9; PDK1, pyruvate dehydrogenase kinase 1; PDK4, pyruvate dehydrogenase kinase 4; PERK, Protein kinase RNA-like endoplasmic reticulum kinase; PGC1α, PPAR gamma coactivator 1-alpha; PPAR, peroxisome proliferator-activated receptors; PPARγ, peroxisome proliferator-activated receptor gamma; PSR, Picrosirius Red; ROS, reactive oxygen species; SA, stearate; SCD1, stearoyl-coA desaturase-1; SERCA, sarco/endoplasmic reticulum ATPase; shRNA, short hairpin RNA; siRNA, small interfering RNA; αSMA, alpha smooth muscle actin; SREBP, sterol regulatory element-binding protein; SSO, sulfosuccinimidyl oleate; STAT3, signal transducer and activator of transcription 3; TLR, toll-like receptor; TM, tunicamycin; TNFα, tumor necrosis factor alpha; UPR, unfolded protein response; VCAM, vascular cell adhesion protein 1; VLDLR, very low-density lipoprotein receptor; WT, wild-type; XBP1, X-box-binding protein.

Financial support

This work was supported in part by research grants to Richard C. Austin from the Heart and Stroke Foundation of Canada (G-13-0003064 and G-15-0009389), the Canadian Institutes of Health Research (74477), to Nabil G. Seidah and Annik Prat from the Leducq Foundation (13 CVD 03), CIHR Foundation grant (148363) and Canada Research Chair (216684). Kenneth N. Maclean gratefully acknowledges financial support from the William R. Hummel Homocystinuria Research Fund and holds the Ehst-Hummel-Kaufmann Family Endowed Chair in Inherited Metabolic Disease. Financial support from the Research Institute of St. Joseph's Healthcare Hamilton is acknowledged. Richard C. Austin is a Career Investigator of the Heart and Stroke Foundation of Ontario and holds the Amgen Canada Research Chair in the Division of Nephrology at St. Joseph's Healthcare Hamilton and McMaster University.

Conflict of interest

The authors declare no conflicts of interest that pertain to this work.

Please refer to the accompanying ICMJE disclosure forms for further details.

Authors' contributions

PL, NGS and RCA conceived the studies. PL, JHB, KP, AAA, SL, and MEM performed all of the *in vitro* and *in vivo* studies. The manuscript was written by PL and RCA and revised by AMB, AP, SAI, KNM, BT and NGS.

Acknowledgements

The mammalian expression plasmid encoding His-CD36 was a gift from Gavin Wright (Addgene plasmid # 52025).

Supplementary data

Supplementary data associated with this article can be found, in the online version, at https://doi.org/10.1016/j.jhepr.2019.10.009.

References

[1] Francque SM, van der Graaff D, Kwanten WJ. Non-alcoholic fatty liver disease and cardiovascular risk: Pathophysiological mechanisms and implications. J Hepatol 2016;65:425–443.
[2] Patil R, Sood GK. Non-alcoholic fatty liver disease and cardiovascular risk. World J Gastrointest Pathophysiol 2017;8:51–58.
[3] Vernon G, Baranova A, Younossi ZM. Systematic review: the epidemiology and natural history of non-alcoholic fatty liver disease and non-alcoholic steatohepatitis in adults. Aliment Pharmacol Ther 2011;34:274–285.
[4] Zhang XQ, Xu CF, Yu CH, Chen WX, Li YM. Role of endoplasmic reticulum stress in the pathogenesis of nonalcoholic fatty liver disease. World J Gastroenterol 2014;20:1768–1776.
[5] Puri P, Mirshahi F, Cheung O, Natarajan R, Maher JW, Kellum JM, et al. Activation and dysregulation of the unfolded protein response in nonalcoholic fatty liver disease. Gastroenterology 2008;134:568–576.
[6] Rinella ME, Elias MS, Smolak RR, Fu T, Borensztajn J, Green RM. Mechanisms of hepatic steatosis in mice fed a lipogenic methionine choline-deficient diet. J Lipid Res 2008;49:1068–1076.
[7] Zhang K, Wang S, Malhotra J, Hassler JR, Back SH, Wang G, et al. The unfolded protein response transducer IRE1alpha prevents ER stress-induced hepatic steatosis. EMBO J 2011;30:1357–1375.
[8] Bobrovnikova-Marjon E, Hatzivassiliou G, Grigoriadou C, Romero M, Cavener DR, Thompson CB, et al. PERK-dependent regulation of lipogenesis during mouse mammary gland development and adipocyte differentiation. Proc Natl Acad Sci U S A 2008;105:16314–16319.
[9] Zeng L, Lu M, Mori K, Luo S, Lee AS, Zhu Y, et al. ATF6 modulates SREBP2-mediated lipogenesis. EMBO J 2004;23:950–958.
[10] Minamino T, Kitakaze M. ER stress in cardiovascular disease. J Mol Cell Cardiol 2010;48:1105–1110.
[11] Mozaffarian D, Benjamin EJ, Go AS, Arnett DK, Blaha MJ, Cushman M, et al. Heart disease and stroke statistics–2015 update: a report from the American Heart Association. Circulation 2015;131:e29–322.
[12] Seidah NG, Benjannet S, Wickham L, Marcinkiewicz J, Jasmin SB, Stifani S, et al. The secretory proprotein convertase neural apoptosis-regulated convertase 1 (NARC-1): liver regeneration and neuronal differentiation. Proc Natl Acad Sci U S A 2003;100:928–933.
[13] Maxwell KN, Breslow JL. Adenoviral-mediated expression of Pcsk9 in mice results in a low-density lipoprotein receptor knockout phenotype. Proc Natl Acad Sci U S A 2004;101:7100–7105.
[14] Sabatine MS, Giugliano RP, Keech AC, Honarpour N, Wiviott SD, Murphy SA, et al. Evolocumab and Clinical Outcomes in Patients with Cardiovascular Disease. N Engl J Med 2017;376:1713–1722.
[15] Poirier S, Mayer G, Benjannet S, Bergeron E, Marcinkiewicz J, Nassoury N, et al. The proprotein convertase PCSK9 induces the degradation of low density lipoprotein receptor (LDLR) and its closest family members VLDLR and ApoER2. J Biol Chem 2008;283:2363–2372.
[16] Roubtsova A, Munkonda MN, Awan Z, Marcinkiewicz J, Chamberland A, Lazure C, et al. Circulating proprotein convertase subtilisin/kexin 9 (PCSK9) regulates VLDLR protein and triglyceride accumulation in visceral adipose tissue. Arterioscler Thromb Vasc Biol 2011;31:785–791.
[17] Canuel M, Sun X, Asselin MC, Paramithiotis E, Prat A, Seidah NG. Proprotein convertase subtilisin/kexin type 9 (PCSK9) can mediate degradation of the low density lipoprotein receptor-related protein 1 (LRP-1). PLoS One 2013;8:e64145.

Please cite this article as: Lebeau PF et al. *Pcsk9* knockout exacerbates diet-induced non-alcoholic steatohepatitis, fibrosis and liver injury in mice. JHEP Reports (2019), https://doi.org/10.1016/j.jhepr.2019.10.009

[18] Demers A, Samami S, Lauzier B, Des Rosiers C, Ngo Sock ET, Ong H, et al. PCSK9 Induces CD36 Degradation and Affects Long-Chain Fatty Acid Uptake and Triglyceride Metabolism in Adipocytes and in Mouse Liver. Arterioscler Thromb Vasc Biol 2015;35:2517–2525.
[19] Wei Y, Wang D, Topczewski F, Pagliassotti MJ. Saturated fatty acids induce endoplasmic reticulum stress and apoptosis independently of ceramide in liver cells. Am J Physiol Endocrinol Metab 2006;291:E275–E281.
[20] Lebeau P, Platko K, Al-Hashimi AA, Byun JH, Lhotak S, Holzapfel N, et al. Loss-of-function PCSK9 mutants evade the unfolded protein response sensor GRP78 and fail to induce endoplasmic reticulum stress when retained. J Biol Chem 2018;293:7329–7343.
[21] Kuda O, Pietka TA, Demianova Z, Kudova E, Cvacka J, Kopecky J, et al. Sulfo-N-succinimidyl oleate (SSO) inhibits fatty acid uptake and signaling for intracellular calcium via binding CD36 lysine 164: SSO also inhibits oxidized low density lipoprotein uptake by macrophages. J Biol Chem 2013;288:15547–15555.
[22] Park YM. CD36, a scavenger receptor implicated in atherosclerosis. Exp Mol Med 2014;46:e99.
[23] **Xu S, Nam SM,** Kim JH, Das R, Choi SK, Nguyen TT, et al. Palmitate induces ER calcium depletion and apoptosis in mouse podocytes subsequent to mitochondrial oxidative stress. Cell Death Dis 2015;6:e1976.
[24] Samtleben S, Jaepel J, Fecher C, Andreska T, Rehberg M, Blum R. Direct imaging of ER calcium with targeted-esterase induced dye loading (TED). J Vis Exp 2013;(75):e50317, https://doi.org/10.3791/50317.
[25] Rocha CS, Wiklander OP, Larsson L, Moreno PM, Parini P, Lundin KE, Smith CI. RNA therapeutics inactivate PCSK9 by inducing a unique intracellular retention form. J Mol Cell Cardiol 2015;82:186–193, https://doi.org/10.1016/j.yjmcc.2015.03.009.
[26] **Le May C, Berger JM,** Lespine A, Pillot B, Prieur X, Letessier E, et al. Transintestinal cholesterol excretion is an active metabolic process modulated by PCSK9 and statin involving ABCB1. Arterioscler Thromb Vasc Biol 2013;33:1484–1493.
[27] **Su K, Sabeva NS,** Wang Y, Liu X, Lester JD, Liu J, et al. Acceleration of biliary cholesterol secretion restores glycemic control and alleviates hypertriglyceridemia in obese db/db mice. Arterioscler Thromb Vasc Biol 2014;34:26–33.
[28] Capeau J. Insulin resistance and steatosis in humans. Diabetes Metab 2008;34:649–657.
[29] Mbikay M, Sirois F, Mayne J, Wang GS, Chen A, Dewpura T, et al. PCSK9-deficient mice exhibit impaired glucose tolerance and pancreatic islet abnormalities. FEBS Lett 2010;584:701–706.
[30] Da Dalt L, Ruscica M, Bonacina F, Balzarotti G, Dhyani A, Di Cairano E, et al. PCSK9 deficiency reduces insulin secretion and promotes glucose intolerance: the role of the low-density lipoprotein receptor. Eur Heart J 2019;40:357–368.
[31] Guo S. Insulin signaling, resistance, and the metabolic syndrome: insights from mouse models into disease mechanisms. J Endocrinol 2014;220:T1–T23.
[32] Song S, Andrikopoulos S, Filippis C, Thorburn AW, Khan D, Proietto J. Mechanism of fat-induced hepatic gluconeogenesis: effect of metformin. Am J Physiol Endocrinol Metab 2001;281:275–282.
[33] Wilson CG, Tran JL, Erion DM, Vera NB, Febbraio M, Weiss EJ. Hepatocyte-Specific Disruption of CD36 Attenuates Fatty Liver and Improves Insulin Sensitivity in HFD-Fed Mice. Endocrinology 2016;157:570–585.
[34] Lai Q, Giralt A, Le May C, Zhang L, Cariou B, Denechaud PD, et al. E2F1 inhibits circulating cholesterol clearance by regulating Pcsk9 expression in the liver. JCI Insight 2017;2.
[35] **Lee S, Zhang C,** Liu Z, Klevstig M, Mukhopadhyay B, Bergentall M, et al. Network analyses identify liver-specific targets for treating liver diseases. Mol Syst Biol 2017;13:938.
[36] Lakoski SG, Lagace TA, Cohen JC, Horton JD, Hobbs HH. Genetic and metabolic determinants of plasma PCSK9 levels. J Clin Endocrinol Metab 2009;94:2537–2543.
[37] Ruscica M, Ferri N, Macchi C, Meroni M, Lanti C, Ricci C, et al. Liver fat accumulation is associated with circulating PCSK9. Ann Med 2016;48:384–391.
[38] Lebeau P.F., Byun J.H., Platko K., MacDonald M.E., Poon S.V., Faiyaz M., et al. Diet-induced hepatic steatosis abrogates cell-surface LDLR by inducing de novo PCSK9 expression in mice. J Biol Chem 2019;294:9037–9047.
[39] Wargny M, Ducluzeau PH, Petit JM, Le May C, Smati S, Arnaud L, et al. Circulating PCSK9 levels are not associated with the severity of hepatic steatosis and NASH in a high-risk population. Atherosclerosis 2018;278:82–90.
[40] **Schmidt AF, Swerdlow DI, Holmes MV,** Patel RS, Fairhurst-Hunter Z, Lyall DM, et al. PCSK9 genetic variants and risk of type 2 diabetes: a mendelian randomisation study. Lancet Diabetes Endocrinol 2017;5:97–105.
[41] Shapiro MD, Miles J, Tavori H, Fazio S. Diagnosing resistance to a proprotein convertase subtilisin/kexin type-9 inhibitor. Ann Intern Med 2018;168:376–379.

Please cite this article as: Lebeau PF et al. *Pcsk9* knockout exacerbates diet-induced non-alcoholic steatohepatitis, fibrosis and liver injury in mice. JHEP Reports (2019), https://doi.org/10.1016/j.jhepr.2019.10.009

Appendix B: Publication into the Journal of Toxicology and Applied Pharmacology

Toxicology and Applied Pharmacology 349 (2018) 1–7

Contents lists available at ScienceDirect

Toxicology and Applied Pharmacology

journal homepage: www.elsevier.com/locate/taap

High impact short article

Pharmacologic inhibition of S1P attenuates ATF6 expression, causes ER stress and contributes to apoptotic cell death

Paul Lebeau[1], Jae Hyun Byun[1], Tamana Yousof, Richard C. Austin*

Department of Medicine, Division of Nephrology, McMaster University, St. Joseph's Healthcare Hamilton, Hamilton Centre for Kidney Research, Hamilton, Ontario L8N 4A6, Canada

ARTICLE INFO

Keywords:
S1P inhibition
SREBP
ATF6
PF-429242
ER stress
UPR inhibition

ABSTRACT

Mammalian cells express unique transcription factors embedded in the endoplasmic reticulum (ER) membrane, such as the sterol regulatory element-binding proteins (SREBPs), that promote *de novo* lipogenesis. Upon their release from the ER, the SREBPs require proteolytic activation in the Golgi by site-1-protease (S1P). As such, inhibition of S1P, using compounds such as PF-429242 (PF), reduces cholesterol synthesis and may represent a new strategy for the management of dyslipidemia. In addition to the SREBPs, the unfolded protein response (UPR) transducer, known as the activating transcription factor 6 (ATF6), is another ER membrane-bound transcription factor that requires S1P-mediated activation. ATF6 regulates ER protein folding capacity by promoting the expression of ER chaperones such as the 78-kDa glucose-regulated protein (GRP78). ER-resident chaperones like GRP78 prevent and/or resolve ER polypeptide accumulation and subsequent ER stress-induced UPR activation by folding nascent polypeptides. Here we report that pharmacological inhibition of S1P reduced the expression of ATF6 and GRP78 and induced the activation of UPR transducers inositol-requiring enzyme-1α (IRE1α) and protein kinase RNA-like ER kinase (PERK). As a consequence, S1P inhibition also increased the susceptibility of cells to ER stress-induced cell death. Our findings suggest that S1P plays a crucial role in the regulation of ER folding capacity and also identifies a compensatory cross-talk between UPR transducers in order to maintain adequate ER chaperone expression and activity.

1. Introduction

The ER is the intracellular compartment that plays a central role in the synthesis and folding of nascent polypeptides (Austin, 2009). One third of the proteome originates in the ER, consisting primarily of cell-surface and secretory proteins, which undergo post-translational modifications, including disulfide bond formation, *N*-linked glycosylation and proline *cis-trans* isomerization (Schwarz and Blower, 2016; Vincenz-Donnelly and Hipp, 2017).

Due to the constant influx of newly synthesized polypeptides entering the ER, the expression of ER-resident chaperones burdened with the task of protein folding is tightly regulated. GRP78 is a ubiquitously expressed ER chaperone known to promote polypeptide folding, enhance nascent polypeptide chain translocation and resolve the accumulation of misfolded proteins. Perhaps its most well-studied role is its ability to prevent constitutive activation of the UPR by blocking the release of ATF6, IRE1α and PERK at the ER luminal surface (Shen et al., 2002; Lee, 2005; Gardner et al., 2013). Conditions that cause the protein folding requirements of the cell to exceed the protein folding capacity of the ER lead to an accumulation of misfolded polypeptides in the ER lumen. This state of ER stress is associated with numerous human diseases including heritable ER storage diseases, cardiovascular disease, neurodegenerative disease and metabolic disorders (Rutishauser and Spiess, 2002; McAlpine et al., 2010; Xiang et al., 2017).

In order to prevent further misfolding of *de novo* polypeptide chains, GRP78 dissociates from the ER luminal domain of ATF6, IRE1α and PERK, thereby leading to the release of these transducers from the ER and causing UPR activation. Among these "arms of the UPR" is the ATF6 transcription factor; IRE1α which utilizes intrinsic endoribonuclease activity to cleave the X-box-binding protein-1 (XBP1) mRNA to form the active spliced-XBP1 (sXBP1) transcription factor; as well as PERK, which promotes the expression of the pro-apoptotic CCAAT-enhancer-binding protein homologous protein (CHOP). Collectively, this UPR signaling cascade increases the protein folding capacity of the ER, while reducing its burden by blocking global *de novo* protein synthesis (Basseri and Austin, 2008).

Chief among the transcription factors capable of binding to the

* Corresponding author at:50 Charlton Ave East, Room T-3313, Hamilton, Ontario L8N 4A6, Canada.
E-mail address: austinr@taari.ca (R.C. Austin).
[1] Co-first authors.

https://doi.org/10.1016/j.taap.2018.04.020
Received 19 December 2017; Received in revised form 12 April 2018; Accepted 16 April 2018
Available online 22 April 2018
0041-008X/

CCAAT consensus sequence of the ER stress element, is the basic leucine zipper protein ATF6 (Okada et al., 2003). Upon its release from the ER by GRP78, ATF6 translocates to the Golgi complex where it undergoes proteolytic activation by S1P. Other ER stress-inducible transcription factors known to reside in the ER and to be cleaved and activated by S1P are the SREBPs (Brown and Goldstein, 1999); isoforms of the SREBPs consist of SREBP1 and SREBP2, which regulate triglyceride and cholesterol synthesis, respectively. Because SREBPs play a central role in *de novo* lipogenesis, S1P has recently been identified as a putative therapeutic target for the management of dyslipidemia (Hay et al., 2007; Hawkins et al., 2008; Basu et al., 2015).

In the present study we used a pharmacological approach to examine whether blocking S1P would reduce ATF6 expression and lead to UPR activation. Due to the well-established role of the liver in cholesterol synthesis, these studies were carried-out in HuH7 cultured human hepatocytes. S1P was blocked using the aminopyrrolidineamide small-molecule reversible inhibitor, PF, which was first characterized for its hypolipidemic properties from a high throughput screen done in a Pfizer compound library (Hay et al., 2007; Hawkins et al., 2008; Uchida et al., 2016). We show here for the first time that reducing the activation of ATF6, *via* PF-mediated S1P inhibition, is associated with an induction of IRE1α and increased phosphorylation of PERK. We also observed that S1P inhibition increased the susceptibility of cells to cytotoxicity in the presence of ER stress-inducing agent thapsigargin (TG). Because ATF6 is a major regulator of GRP78 expression, which modulates the activation of the UPR, the observed downregulation of GRP78 is a likely cause of IRE1α and PERK induction. Indeed, a compensatory UPR activation to account for reduced ATF6 activity may represent another explanation for these observations. Upon inhibition of IRE1α activity *via* STF-083010 (STF), which did not reduce GRP78 expression, we also observed that cells were more susceptible to TG-induced UPR activation and apoptosis. Taken together, our findings demonstrate that S1P plays a critical role in maintaining the protein folding capacity of the ER and that there exists a compensatory cross-talk between UPR transducers.

2. Materials and methods

2.1. Cell culture and reagents

HuH7, HepG2, HEK293 and DU145 cells were routinely grown in Dulbecco's Modified Eagle's Medium (Gibco, Thermofisher Scientific) supplemented with 10% (v/v) fetal bovine serum (Sigma-Aldrich) and 50 U/ml of penicillin and streptomycin (Sigma-Aldrich). TG, AEBSF, PF, STF and 4-phenylbutyrate (4PBA) were purchased from Sigma-Aldrich (St. Louis, MO, USA). Cells were treated with TG (100 nM), AEBSF (300 μM), PF (10 μM), STF (60 μM) and/or 4PBA (1 mM) for 24 h prior to lysis.

2.2. Transfection and plasmids

Transfection of HuH7 cells was carried-out using XtremeGene HP (Roche Applied Sciences) at a 3:1 ratio with plasmid DNA (3 μl transfection reagent, 1 μg DNA per ml media). The ER stress-activated indicator (ERAI) plasmid used in our studies encodes XBP1 that displays a FLAG antigen upon splicing and removal of the ER stress-specific intron by IRE1α (Iwawaki et al., 2004). This form of FLAG-sXBP1 is lacking its DNA-binding domain and serves strictly as a marker of IRE1α activity with no transcriptional capacity. Inhibition of SREBP2 was achieved using siRNA (200 nM, #4390824, Thermofisher Scientific), which was transfected into HuH7 cells using Lipofectamine RNAiMAX (X13778-030, Invitrogen).

2.3. Immunoblotting and antibodies

Cells were lysed in 4× SDS-PAGE lysis buffer and protein lysates were resolved on 10% polyacrylamide gels in denaturing conditions, as described previously (Lebeau et al., 2017). Following gel electrophoresis, resolved proteins were transferred to nitrocellulose membranes. Membranes were then blocked in 5% skim milk dissolved in 1× Tris-buffered saline with 1% Tween-20 (TBS-T). Incubation of membranes with primary antibodies was carried-out for 18 h at 4 °C. Primary antibodies were diluted in TBS-T containing 1% skim milk, which included the following: anti-ATF6, (70B1413.1, Novus Biologicals), anti-CHOP (#SC-793, Santa Cruz Biotechnology), anti-GRP78 (#610979, BD Bioscience), anti-GRP94 (#ADI-SPA-850, Enzo Life Sciences), anti-IRE1α (#14C10 Cell Signaling Technology), anti-pPERK (#3179S, Cell Signaling Technology) and anti-SREBP2 (#557037, BD Bioscience). Membranes were visualized using the EZ-ECL chemiluminescent reagent (#20-500-500, FroggaBio) and quantified using ImageLab software (BioRad). Quantification of band intensities represent the mean of three replicates, normalized against membranes re-probed for β-actin.

2.4. Reverse transcription and quantitative real-time PCR

Total RNA was extracted using RNeasy Mini kits (#74104, Qiagen) and reverse transcribed to cDNA using Superscript Vilo cDNA Synthesis kit (#11754050, Life Technologies). Real-time PCR was completed using Fast SYBR Green (#4385610, Life Technologies), as described previously (Al-Hashimi et al., 2010).

2.5. Immunofluorescent staining

HuH7 cells were seeded in 4-well chamber slides, transfected with the ERAI plasmid for 48 h and treated with PF or TG 24 h prior to fixation in 4% paraformaldehyde. Following fixation, cells were permeabilized with phosphate-buffered saline (PBS) containing 0.025% Triton-X, blocked in PBS containing 1% bovine serum albumin and incubated in primary antibodies targeted against FLAG (1:100; F3165, Sigma Aldrich) for 1 h. Cells were then washed in PBS containing 1% tween and incubated with Alexa 488 fluorescently-labelled secondary antibody (1:200; #A32723, ThermoFisher Scientific) for 45 min. Actin and nuclei were stained using rhodamine phalloidin (#R415, ThermoFisher Scientific) and DAPI (Sigma-Aldrich), respectively. Immunofluorescent staining of ATF6 was carried-out with the same protocol as mentioned above using an anti-ATF6 antibody (1:100; Enzo Life Sciences, 70B1413.1). TUNEL assays, which stain DNA damage, were used to assess cell apoptosis. After fixation of cells in 4% paraformaldehyde, TUNEL assays were carried-out as per manufacturer's instructions (#4810–30-CK, Trevigen). Briefly, HuH7 cells were incubated with terminal deoxynucleotidyl transferase, which biotinylates damaged DNA, for 1 h at 37 °C. Biotinylated DNA was then labelled *via* incubation with streptavidin-594 (1:200 in PBS) for an additional hour at room temperature. 5 representative images of TUNEL-stained cells from each treatment group were quantified using ImageJ software (U. S. National Institute of Health).

2.6. Lactate dehydrogenase cytotoxicity assay

Lactate dehydrogenase cytotoxicity assays were performed as per manufacturer's instructions (#04744926001, Roche Applied Sciences).

2.7. Measurement of cellular reactive oxygen species

HuH7 cells were seeded in a black clear-bottom 96-well plate and permitted to adhere for 24 h. Live cells were then washed with Hank's Balanced Salt Solution (HBSS) containing 20 mM HEPES and loaded with DCFDA (25 μM, #D6883, Sigma-Aldrich) *via* incubation for 1 h at 37 °C. DCFDA-containing HBSS was then washed off and an additional 100 μl of HBSS and treatments were added to each well. DCFDA relative fluorescence units (RFU) were measured using the Gemini EM Microplate Reader at 37 °C for 18 h with the excitation and emission

wavelengths of 480 and 515 nm, respectively.

2.8. Isolation of primary hepatocytes

A two-step hepatic perfusion of collagenase (0.05% in HEPES buffer, Sigma) and EGTA (500 M in HEPES buffer, Sigma) was used in 12-week-old male C57bl/6 mice to isolate fresh primary hepatocytes. Following harvest, cells were washed, separated *via* centrifugation and cell strainers and plated at a confluence of 1×10^6 cells/well in William's E medium (Gibco, Thermo Fisher Scientific) supplemented with 10% fetal bovine serum, 100 IU/ml penicillin, and 100 g/ml streptomycin.

2.9. Statistical analysis

Error bars are represented as standard deviation of the mean. Statistical significance was calculated using unpaired Student's *t*-tests. Comparisons between means of immunoblot quantifications was done using one-way ANOVA.

3. Results

3.1. PF blocks ATF6 activation and GRP78 expression

The role of S1P in the activation of ATF6 and expression of GRP78 was explored in HuH7 cells *via* treatment with PF for 24 h. Our data demonstrate that PF significantly reduced the abundance of nuclear ATF6 (nATF6; Fig. 1A) and expression of GRP78, whether in the presence or absence of the ER stress-inducing agent TG (Fig. 1B). Consistent with our previous findings (Lebeau et al., 2017), we observed that PF blocked SREBP2 activation and reduced the abundance of a downstream target of SREBP2 transcriptional activity, the proprotein convertase subtilisin/kexin type-9 (PCSK9). Immunoblot findings were confirmed *via* real-time PCR of cells treated with PF as well as the serine protease inhibitor AEBSF (Fig. 1C). The effect of PF on GRP78 and ATF6 expression was also examined in HepG2 immortalized human hepatocytes *via* real-time PCR (Fig. 1D). Given that PF blocks the S1P-mediated proteolytic cleavage of ATF6 in the Golgi complex, we also examined the effect of PF on TG-induced nuclear localization of ATF6 *via* immunofluorescence staining (Fig. 1E). Our findings demonstrate that upon treatment of HuH7 cells with TG, ATF6 localizes to the nucleus, as well as the perinuclear region of the cell. In the presence of PF, however, TG-induced nuclear localization of ATF6 was not observed; rather a distinct accumulation of ATF6 was observed in the perinuclear compartments of the cell (white arrows), likely the ER or Golgi.

3.2. Pharmacologic inhibition of S1P induces UPR activation

Given the well-established role of GRP78 as a sensor/repressor of UPR transducers, and that inhibition of S1P downregulates GRP78 (Okada et al., 2003), we investigated whether treatment of PF would lead to UPR activation. After a 24 h treatment with PF, a significant upregulation of the remaining two arms of the UPR, PERK and IRE1α, was observed in HuH7 cells (Fig. 2A). We also observed a marked increase in the expression of GRP94; another member of the heat-shock protein (HSP) family of proteins, which in contrast to GRP78 was not downregulated by S1P inhibition. Given the significant induction of IRE1α by PF, the splicing of XPB1 was also examined in HuH7 cells transfected with the ERAI plasmid *via* immunofluorescence staining. Consistent with the observed PF-mediated increase in IRE1α expression was a concomitant increase in cells that stained positive for sXBP1 (Fig. 2B and C). The effect of PF on UPR activation was also confirmed in freshly isolated primary mouse hepatocytes (Fig. 2D), human embryonic kidney (HEK293) and HepG2 cells *via* real-time PCR (Fig. 2E and F) and immunoblots (Fig. 2G and H). Consistent with our observations in immortalized cultured human hepatocytes (HuH7), we

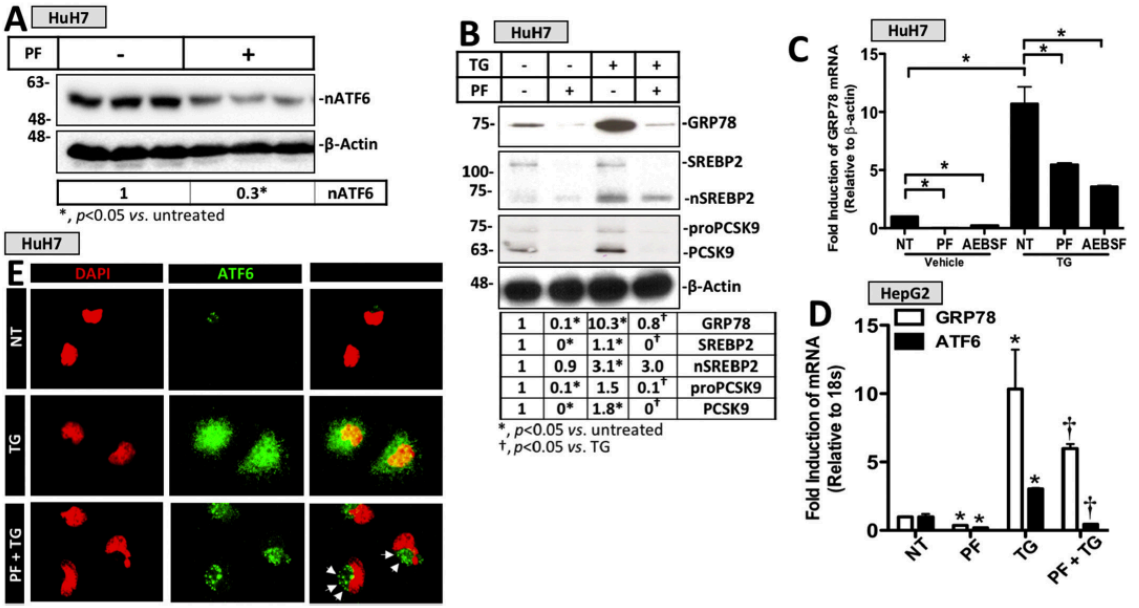

Fig. 1. PF-429242 (PF) blocks ATF6 activation and GRP78 expression. (a and b) Immunoblots of HuH7 cells incubated with PF (10 μM) in the presence or absence of thapsigargin (TG; 100 nM) for 24 h show that PF blocks nuclear ATF6 (nATF6), GRP78, nuclear SREBP2 (nSREBP2) and PCSK9 expression. (c) Transcriptional repression of GRP78 mRNA by S1P inhibitors AEBSF and PF was also examined using real-time PCR 8 h post-treatment (*, $p < 0.05$). (d) PF-mediated inhibition of GRP78 and ATF6 was also examined in HepG2 cells *via* real-time PCR (*, $p < 0.05$ *vs.* NT; †, $p < 0.05$ *vs.* TG). (e) PF-mediated inhibition of ATF6 nuclear localization was also observed in HuH7 cells treated with TG *via* immunofluorescence staining.

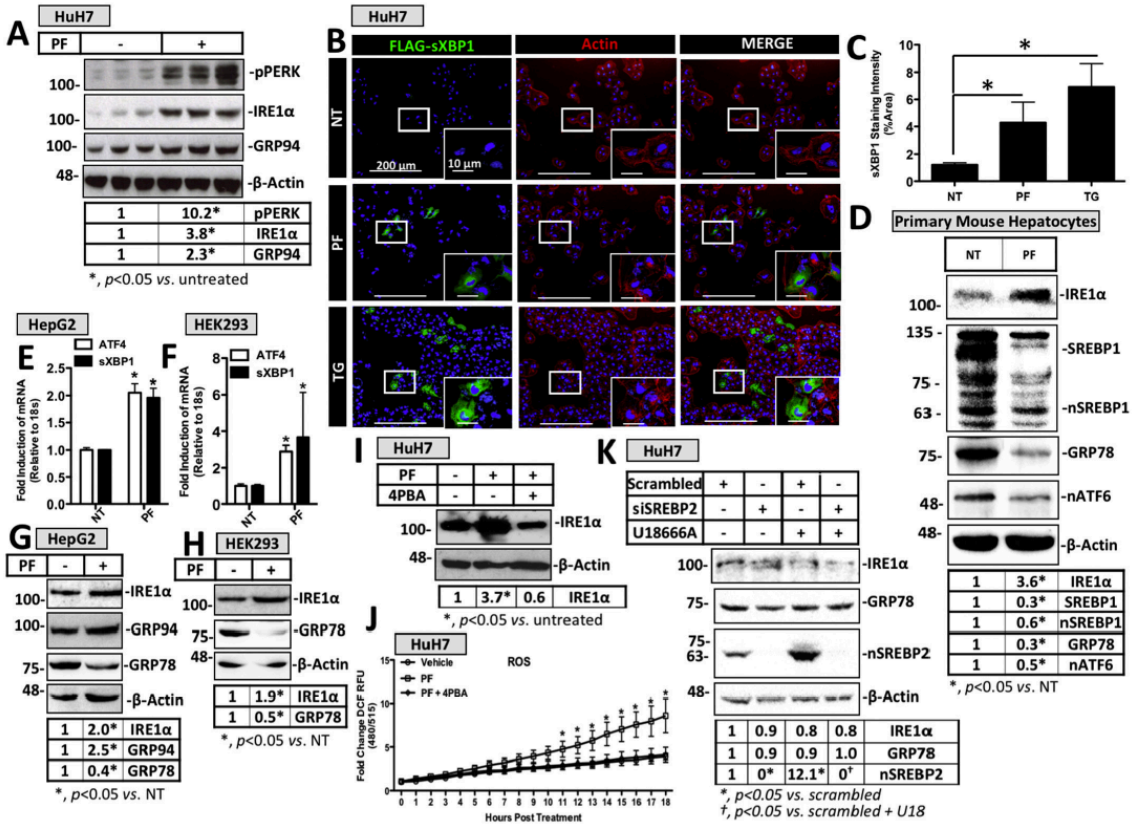

Fig. 2. Pharmacologic inhibition of S1P induces UPR activation. (a) UPR markers phospho-PERK (pPERK), IRE1α and GRP94 were examined in HuH7 cells incubated with PF-429242 (PF; 10 μM), *via* immunoblots. (b) The PF-mediated splicing of XBP1 (sXBP1) was examined in HuH7 cells transfected with the ER-activated indicator (ERAI) plasmid using immunofluorescence staining. ERAI-transfected cells were also treated with ER stress-inducing agent thapsigargin (TG; 100 nM) to serve as a positive control. (c) Quantification of ERAI positive staining using ImageJ (*, $p < 0.05$ *vs.* NT). (d, e, f, g and h) The effect of PF on UPR marker expression was confirmed *via* real-time PCR and immunoblots in mouse primary hepatocytes, HepG2 and HEK293 cells. (i) The reversibility of PF-induced ER stress was also examined *via* pre-treatment of cells with the small chemical chaperone 4-phenylbutyrate (4PBA, 1 mM) using immunoblots. (j) PF-mediated cellular reactive oxygen species (ROS) production was also examined in HuH7 cells in the presence and absence of 4PBA using a DCF assay during an 18 h treatment time-course (*, $p < 0.05$ *vs.* Vehicle). (k) The effect of SREBP2 inhibition on UPR marker expression was examined in HuH7 cells transfected with siRNA targeted against SREBP2 (siSREBP2) in the presence and absence of an agent that induces SREBP2 activation, U18666A (Basu et al., 2015).

observed that a 24 h treatment of PF (10 μM) blocked the expression of GRP78 but increased the expression of UPR markers ATF4, sXBP1, IRE1α and GRP94. SREBP1 expression was also examined in PF-treated primary hepatocytes and found to be significantly reduced, which is consistent with that of the other S1P-regulated transcription factors, ATF6 and SREBP2.

To confirm that the PF-mediated induction of IRE1α occurred in a manner dependent on ER stress, HuH7 cells were treated with 4PBA; a small chemical chaperone well-known to alleviate ER stress (Basseri et al., 2009; Liu et al., 2016). Consistent with our findings in Fig. 2A, we observed that PF increased the cellular abundance of IRE1α and that this increase was blocked in the presence of 4PBA (Fig. 2I). The production of reactive oxygen species (ROS), a process closely related to ER stress (Zeeshan et al., 2016), was also examined in PF-treated HuH7 cells (Fig. 2J). Our data show that PF caused a significant increase in cellular ROS starting at the 11 h time point, which persisted until the 18 h endpoint. Consistent with findings in Fig. 2I, we also observed that 4PBA abolished PF-mediated ROS production, likely due to its ability to attenuate ER stress. Because of the dual role of S1P in activation of the SREBPs and ATF6, we next examined whether the inhibition of SREBP2 would lead to UPR activation. Despite the significant siRNA-mediated reduction in the nuclear form of SREBP2 (nSREBP2), immunoblots reveal that GRP78 and IRE1α were not affected (Fig. 2K). Furthermore, the expression of UPR markers was not altered upon induction of SREBP2 *via* U18666A, an agent that causes intracellular sterol deprivation (Basu et al., 2015).

3.3. Inhibition of S1P leads to ER stress-induced cell death

It is well-established that prolonged ER stress promotes programmed cell death in a manner dependent on the UPR mediator CHOP (Szegezdi et al., 2006). Despite the observed UPR activation in response to PF, our findings demonstrate that an additional stimulus by the ER stress-inducing agent TG was required for PF to elicit an effect on CHOP expression (Fig. 3A) and cytotoxicity (Fig. 3B) in HuH7 cells. Given that a number of inhibitors of the UPR have been shown to reduce the onset and progression of a variety of cancer types, the pro-apoptotic effect of PF-mediated ATF6 inhibition was also examined in a well-established prostate cancer cell line DU145 (Fig. 3C). Consistent with our previous observation that 4PBA attenuated PF-induced UPR activation, we also

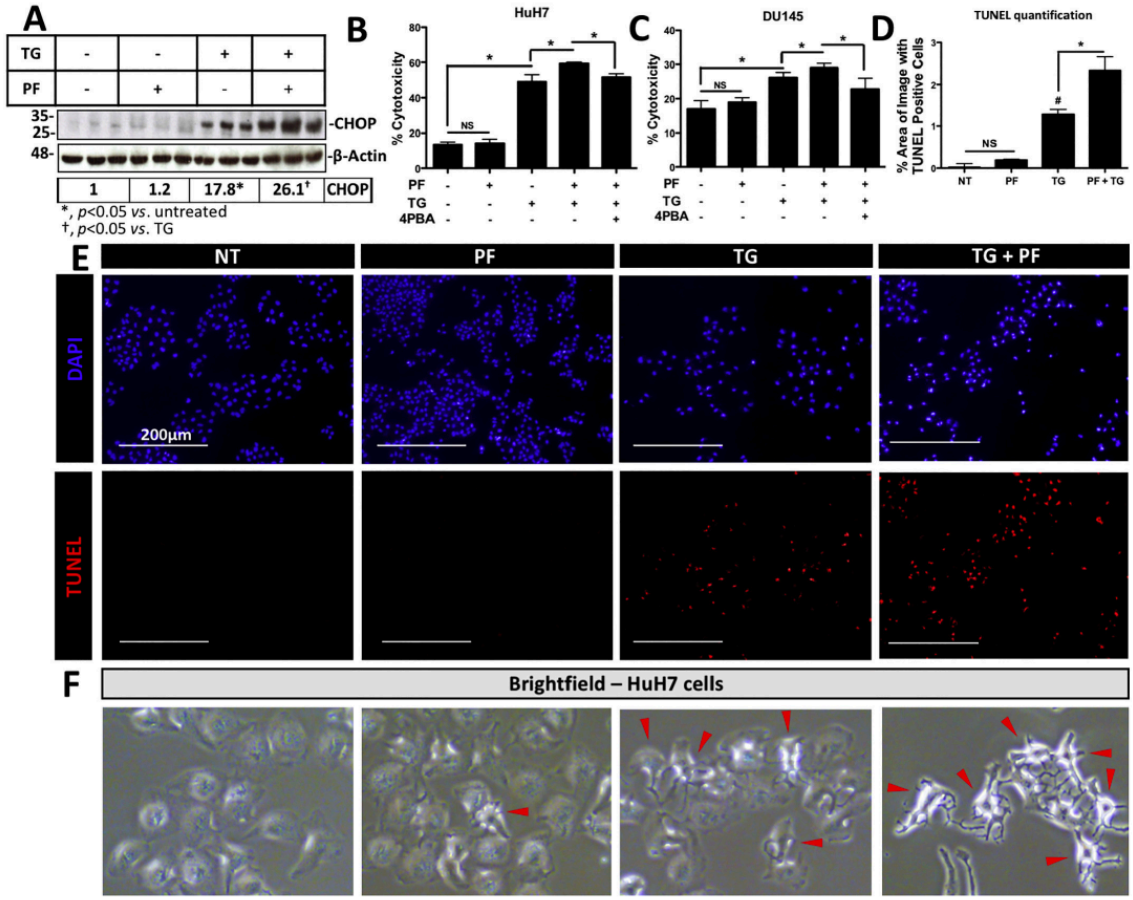

Fig. 3. Inhibition of S1P leads to ER stress-induced cell death. (a) Expression of the pro-apoptotic UPR marker, CHOP, was examined in HuH7 cells treated with PF-429242 (PF, 10 µM) in the presence and absence of ER stress-inducing agent thapsigargin (TG; 100 nM) using immunoblots. (b and c) Cell death was assessed in these cells, as well as DU145 prostate cancer cells, *via* lactate dehydrogenase cytotoxicity assays (*, $p < 0.05$). The role of ER stress in the observed cell death was confirmed *via* pre-treatment of cells with the small chemical chaperone 4-phenylbutyrate (4PBA; 1 mM), which significantly reduced cytotoxicity. (d and e) Apoptosis was also examined in PF-treated HuH7 cells in the presence and absence of TG using a TUNEL assay (red) (#, $p < 0.05$ *vs.* NT; *, $p < 0.05$). (f) PF-mediated changes in cell morphology were examined in the presence and absence of TG using light microscopy. (For interpretation of the references to colour in this figure legend, the reader is referred to the web version of this article.)

observed that 4PBA reduced PF-induced cytotoxicity in HuH7 and DU145 cells. To examine apoptosis specifically, a TUNEL assay was carried-out and also revealed that TG is required to attain a PF-mediated increase in cell death (Fig. 3D and E). Furthermore, we observed an increase in the TG-mediated shrinking and budding of cells (red arrows) in the presence of PF; a well-established morphological hallmark of apoptosis (Fig. 3F).

3.4. Inhibition of IRE1α, via STF, exacerbates TG-mediated UPR activation but does not block GRP78 expression

To investigate whether PF-mediated UPR activation occurred solely as a result of reduced GRP78 expression, or also as a result of a compensatory response of the UPR, cells were treated with an inhibitor of IRE1α that fails to reduce GRP78 expression. To confirm effective STF-mediated inhibition of IRE1α activity, sXBP1 was examined *via* real-time PCR. These data demonstrate that STF significantly reduced the cellular abundance of sXBP1, the downstream marker of IRE1α activity, whether in the presence or absence of TG (Fig. 4A). The STF-mediated effect on UPR marker expression was then examined *via* real-time PCR and immunoblot analysis (Fig. 4B and C). In a consistent manner, these data demonstrate that STF treatment failed to induce GRP78 and CHOP expression; however, in the presence of TG, STF significantly increased the cellular abundance of both UPR markers. In support of the PF findings, TUNEL assay data also demonstrate that STF treatment required an additional ER stress-inducing stimulus to elicit a significant increase in cell death (Fig. 4D and E).

4. Discussion

Accumulating evidence implicates S1P as a major regulator of cholesterol due to its role in the activation of SREBP1/2 (Brown and Goldstein, 1999; Hawkins et al., 2008; Hyrina et al., 2017). In support of this, we have recently demonstrated that inhibition of S1P, *via* AEBSF and PF, blocks the activation of SREBP2 and PCSK9 expression (Lebeau et al., 2017). In addition to the SREBPs, S1P is also known to mediate

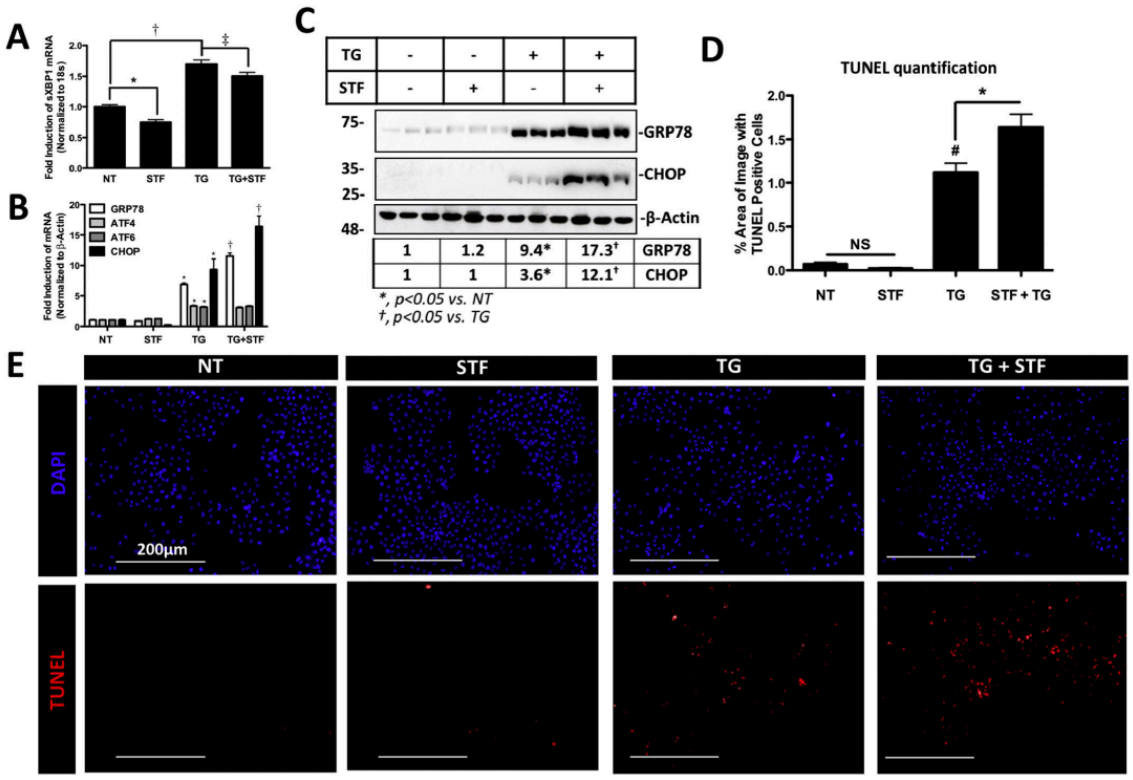

Fig. 4. Inhibition of IRE1α, *via* STF-083010 (STF), exacerbates thapsigargin (TG)-mediated UPR activation but does not block GRP78 expression. (a) STF-mediated IRE1α inhibition was assessed *via* analysis of mRNA levels of spliced-XBP1 (sXBP1); a downstream target of IRE1α endoribonuclease activity. (b and c) Real-time PCR and immunoblots of UPR markers GRP78, ATF4, ATF6 and CHOP in HuH7 cells incubated with STF in the presence or absence of ER stress-inducing agent TG (100 nM; *, $p < 0.05$ *vs.* NT; †, $p < 0.05$ *vs.* TG). (d and e) Apoptosis in STF/TG-treated cells was also examined *via* TUNEL assay (red). (For interpretation of the references to colour in this figure legend, the reader is referred to the web version of this article.)

the activation of the ATF6 transcription factor that plays a central role in the transcriptional regulation of ER chaperones, such as GRP78 (Li et al., 2000). Given that GRP78 promotes the folding and maturation of nascent polypeptides and acts as a repressor of ATF6, IRE1α and PERK function, we investigated whether S1P inhibition would lead to UPR activation.

Despite the potential benefits associated with S1P inhibitor-mediated cholesterol lowering (Hawkins et al., 2008; Basu et al., 2015), the major finding of this study suggests that S1P plays a crucial role in maintaining ER chaperone expression and ER folding capacity. Our findings demonstrate that inhibition of S1P leads to UPR activation in the absence of additional ER stress-inducing stimuli (Fig. 2). While S1P inhibition did not induce a significant level of cytotoxicity, a significant increase in cytotoxicity was observed in the presence of TG (Fig. 3).

Given that S1P regulates the activation of SREBP1/2 and ATF6 (Velho et al., 2017), which are both ER stress-inducible proteins (Colgan et al., 2007), we also examined whether inhibition of SREBP2 corresponded with UPR activation using small-interfering RNA (Fig. 2K). We observed that inhibition of SREBP2 expression did not yield UPR activation, suggesting that S1P inhibition promotes UPR activation in a manner dependent on ATF6 and/or GRP78. Because GRP78 has intrinsic chaperone activity and plays a major role in the repression of UPR activation, it remains unclear whether PF-mediated downregulation of GRP78 contributes to UPR activation *via* liberation of the UPR transducers from the ER or as a compensatory response to reduced ATF6 and GRP78 chaperone activity.

In support of the notion by which S1P inhibition promotes UPR activation as a compensatory response, we also observed that IRE1α inhibition increased the susceptibility of cells to TG-induced ER stress despite not having an effect on GRP78 expression (Fig. 4C). Accumulating evidence suggests that the three arms of the UPR work in concert to maintain ER folding capacity and cellular homeostasis. ATF6$^{-/-}$ mice exhibit increased hepatic lipid accumulation and UPR activation in response to ER stress-inducing agent tunicamycin (Yamamoto et al., 2010). Similarly, liver-specific PERK$^{-/-}$ mice exhibit increased tunicamycin-mediated hepatic apoptosis (Teske et al., 2011). Inhibition of the UPR was also shown to cause severe atrophy in cultured myotubules, a process known to contribute to skeletal muscle wasting in cancer patients (Bohnert et al., 2016).

The UPR is emerging as a therapeutic target due to its well-established role in the onset and progression of a variety of human diseases (Maly and Papa, 2014; Nagelkerke et al., 2014). Inhibitors of IRE1α activity and PERK have been shown to reduce the progression of atherosclerosis and various cancers including multiple myeloma and pancreatic cancer (Atkins et al., 2013; Chien et al., 2014; Feng et al., 2017; Tufanli et al., 2017). The present study supports the notion that networks of the UPR are fully integrated and act in concert to maintain ER chaperone activity. Inhibitors of S1P and the UPR may confer significant protection against dyslipidemia or disease in tissues laden by chronic UPR activation. However, given that blocking ATF6 and IRE1α can promote cell death in conditions that increase ER burden, the long-term systemic effect of such inhibitors remains to be elucidated.

Funding

This work was supported in part by research grants to Richard C. Austin from the Heart and Stroke Foundation of Ontario (T-6146), the Heart and Stroke Foundation of Canada (G-13-0003064 and G-15-0009389) and the Canadian Institutes of Health Research (74477).

Conflicts of interest

The McMaster University Animal Research Ethics Board approved all procedures used for primary hepatocyte isolation.

Acknowledgements

We would like to thank Dr. Masayuki Miura, University of Tokyo, for the ERAI plasmid. "Dr. Richard C. Austin is a career investigator of the Heart and Stroke Foundation of Ontario" and that "this research was made possible by the generous support of St. Joseph's Healthcare Hamilton."

References

Al-Hashimi, A.A., Caldwell, J., Gonzalez-Gronow, M., Pizzo, S.V., Aboumrad, D., Pozza, L., Al-Bayati, H., Weitz, J.I., Stafford, A., Chan, H., Kapoor, A., Jacobsen, D.W., Dickhout, J.G., Austin, R.C., 2010. Binding of anti-GRP78 autoantibodies to cell surface GRP78 increases tissue factor procoagulant activity via the release of calcium from endoplasmic reticulum stores. J. Biol. Chem. 285, 28912–28923.

Atkins, C., Liu, Q., Minthorn, E., Zhang, S.Y., Figueroa, D.J., Moss, K., Stanley, T.B., Sanders, B., Goetz, A., Gaul, N., Choudhry, A.E., Alsaid, H., Jucker, B.M., Axten, J.M., Kumar, R., 2013. Characterization of a novel PERK kinase inhibitor with antitumor and antiangiogenic activity. Cancer Res. 73, 1993–2002.

Austin, R.C., 2009. The unfolded protein response in health and disease. Antioxid. Redox Signal. 11, 2279–2287.

Basseri, S., Austin, R.C., 2008. ER stress and lipogenesis: a slippery slope toward hepatic steatosis. Dev. Cell 15, 795–796.

Basseri, S., Lhotak, S., Sharma, A.M., Austin, R.C., 2009. The chemical chaperone 4-phenylbutyrate inhibits adipogenesis by modulating the unfolded protein response. J. Lipid Res. 50, 2486–2501.

Basu, D., Huq, A., Iqbal, J., Hussain, M.M., Jiang, X.C., Jin, W., 2015. Hepatic S1P deficiency lowers plasma cholesterol levels in apoB-containing lipoproteins when LDLR function is compromised. Nutr. Metab. (Lond.) 12, 35.

Bohnert, K.R., Gallot, Y.S., Sato, S., Xiong, G., Hindi, S.M., Kumar, A., 2016. Inhibition of ER stress and unfolding protein response pathways causes skeletal muscle wasting during cancer cachexia. FASEB J. 30, 3053–3068.

Brown, M.S., Goldstein, J.L., 1999. A proteolytic pathway that controls the cholesterol content of membranes, cells, and blood. Proc. Natl. Acad. Sci. U. S. A. 96, 11041–11048.

Chien, W., Ding, L.W., Sun, Q.Y., Torres-Fernandez, L.A., Tan, S.Z., Xiao, J., Lim, S.L., Garg, M., Lee, K.L., Kitajima, S., Takao, S., Leong, W.Z., Sun, H., Tokatly, I., Poellinger, L., Gery, S., Koeffler, P.H., 2014. Selective inhibition of unfolded protein response induces apoptosis in pancreatic cancer cells. Oncotarget 5, 4881–4894.

Colgan, S.M., Tang, D., Werstuck, G.H., Austin, R.C., 2007. Endoplasmic reticulum stress causes the activation of sterol regulatory element binding protein-2. Int. J. Biochem. Cell Biol. 39, 1843–1851.

Feng, Y.X., Jin, D.X., Sokol, E.S., Reinhardt, F., Miller, D.H., Gupta, P.B., 2017. Cancer-specific PERK signaling drives invasion and metastasis through CREB3L1. Nat. Commun. 8, 1079.

Gardner, B.M., Pincus, D., Gotthardt, K., Gallagher, C.M., Walter, P., 2013. Endoplasmic reticulum stress sensing in the unfolded protein response. Cold Spring Harb. Perspect. Biol. 5, a013169.

Hawkins, J.L., Robbins, M.D., Warren, L.C., Xia, D., Petras, S.F., Valentine, J.J., Varghese, A.H., Wang, I.K., Subashi, T.A., Shelly, L.D., Hay, B.A., Landschulz, K.T., Geoghegan, K.F., Harwood Jr., H.J., 2008. Pharmacologic inhibition of site 1 protease activity inhibits sterol regulatory element-binding protein processing and reduces lipogenic enzyme gene expression and lipid synthesis in cultured cells and experimental animals. J. Pharmacol. Exp. Ther. 326, 801–808.

Hay, B.A., Abrams, B., Zumbrunn, A.Y., Valentine, J.J., Warren, L.C., Petras, S.F., Shelly, L.D., Xia, A., Varghese, A.H., Hawkins, J.L., Van Camp, J.A., Robbins, M.D., Landschulz, K., Harwood Jr., H.J., 2007. Aminopyrrolidineamide inhibitors of site-1 protease. Bioorg. Med. Chem. Lett. 17, 4411–4414.

Hyrina, A., Meng, F., McArthur, S.J., Eivemark, S., Nabi, I.R., Jean, F., 2017. Human Subtilisin Kexin Isozyme-1 (SKI-1)/Site-1 protease (S1P) regulates cytoplasmic lipid droplet abundance: a potential target for indirect-acting anti-dengue virus agents. PLoS One 12, e0174483.

Iwawaki, T., Akai, R., Kohno, K., Miura, M., 2004. A transgenic mouse model for monitoring endoplasmic reticulum stress. Nat. Med. 10, 98–102.

Lebeau, P., Al-Hashimi, A., Sood, S., Lhotak, S., Yu, P., Gyulay, G., Pare, G., Chen, S.R., Trigatti, B., Prat, A., Seidah, N.G., Austin, R.C., 2017. Endoplasmic reticulum stress and Ca2+ depletion differentially modulate the sterol regulatory protein PCSK9 to control lipid metabolism. J. Biol. Chem. 292, 1510–1523.

Lee, A.S., 2005. The ER chaperone and signaling regulator GRP78/BiP as a monitor of endoplasmic reticulum stress. Methods 35, 373–381.

Li, M., Baumeister, P., Roy, B., Phan, T., Foti, D., Luo, S., Lee, A.S., 2000. ATF6 as a transcription activator of the endoplasmic reticulum stress element: thapsigargin stress-induced changes and synergistic interactions with NF-Y and YY1. Mol. Cell. Biol. 20, 5096–5106.

Liu, S.H., Yang, C.C., Chan, D.C., Wu, C.T., Chen, L.P., Huang, J.W., Hung, K.Y., Chiang, C.K., 2016. Chemical chaperon 4-phenylbutyrate protects against the endoplasmic reticulum stress-mediated renal fibrosis in vivo and in vitro. Oncotarget 7, 22116–22127.

Maly, D.J., Papa, F.R., 2014. Druggable sensors of the unfolded protein response. Nat. Chem. Biol. 10, 892–901.

McAlpine, C.S., Bowes, A.J., Werstuck, G.H., 2010. Diabetes, hyperglycemia and accelerated atherosclerosis: evidence supporting a role for endoplasmic reticulum (ER) stress signaling. Cardiovasc Hematol Disord Drug Targets 10, 151–157.

Nagelkerke, A., Bussink, J., Sweep, F.C., Span, P.N., 2014. The unfolded protein response as a target for cancer therapy. Biochim. Biophys. Acta 1846, 277–284.

Okada, T., Haze, K., Nadanaka, S., Yoshida, H., Seidah, N.G., Hirano, Y., Sato, R., Negishi, M., Mori, K., 2003. A serine protease inhibitor prevents endoplasmic reticulum stress-induced cleavage but not transport of the membrane-bound transcription factor ATF6. J. Biol. Chem. 278, 31024–31032.

Rutishauser, J., Spiess, M., 2002. Endoplasmic reticulum storage diseases. Swiss Med. Wkly. 132, 211–222.

Schwarz, D.S., Blower, M.D., 2016. The endoplasmic reticulum: structure, function and response to cellular signaling. Cell. Mol. Life Sci. 73, 79–94.

Shen, J., Chen, X., Hendershot, L., Prywes, R., 2002. ER stress regulation of ATF6 localization by dissociation of BiP/GRP78 binding and unmasking of Golgi localization signals. Dev. Cell 3, 99–111.

Szegezdi, E., Logue, S.E., Gorman, A.M., Samali, A., 2006. Mediators of endoplasmic reticulum stress-induced apoptosis. EMBO Rep. 7, 880–885.

Teske, B.F., Wek, S.A., Bunpo, P., Cundiff, J.K., McClintick, J.N., Anthony, T.G., Wek, R.C., 2011. The eIF2 kinase PERK and the integrated stress response facilitate activation of ATF6 during endoplasmic reticulum stress. Mol. Biol. Cell 22, 4390–4405.

Tufanli, O., Telkoparan Akillilar, P., Acosta-Alvear, D., Kocaturk, B., Onat, U.I., Hamid, S.M., Cimen, I., Walter, P., Weber, C., Erbay, E., 2017. Targeting IRE1 with small molecules counteracts progression of atherosclerosis. Proc. Natl. Acad. Sci. U. S. A. 114, E1395–E1404.

Uchida, L., Urata, S., Ulanday, G.E., Takamatsu, Y., Yasuda, J., Morita, K., Hayasaka, D., 2016. Suppressive effects of the site 1 protease (S1P) inhibitor, PF-429242, on dengue virus propagation. Viruses 8.

Velho, R.V., De Pace, R., Klunder, S., Di Lorenzo, G., Schweizer, M., Braulke, T., Pohl, S., 2017. Site-1 protease and lysosomal homeostasis. Biochim. Biophys. Acta 1864 (, 2162–2168.

Vincenz-Donnelly, L., Hipp, M.S., 2017. The endoplasmic reticulum: a hub of protein quality control in health and disease. Free Radic. Biol. Med. 108, 383–393.

Xiang, C., Wang, Y., Zhang, H., Han, F., 2017. The role of endoplasmic reticulum stress in neurodegenerative disease. Apoptosis 22, 1–26.

Yamamoto, K., Takahara, K., Oyadomari, S., Okada, T., Sato, T., Harada, A., Mori, K., 2010. Induction of liver steatosis and lipid droplet formation in ATF6alpha-knockout mice burdened with pharmacological endoplasmic reticulum stress. Mol. Biol. Cell 21, 2975–2986.

Zeeshan, H.M., Lee, G.H., Kim, H.R., Chae, H.J., 2016. Endoplasmic reticulum stress and associated ROS. Int. J. Mol. Sci. 17, 327.

9. References

1. Hill, N. R., Fatoba, S. T., Oke, J. L., Hirst, J. A., O'Callaghan, C. A., Lasserson, D. S., & Hobbs, F. D. R. (2016). Global Prevalence of Chronic Kidney Disease – A Systematic Review and Meta-Analysis. *Plos One*, *11*(7). doi: 10.1371/journal.pone.0158765

2. United States Renal Data System. 2016 Annual data report, chapter 1: CKD in the general population. https://www.usrds.org/2016/view/v1_01.aspx.

3. Levey, A. S., & Coresh, J. (2012). Chronic kidney disease. Lancet, 379(9811), 165-180.

4. Metcalfe, W. (2007). How does early chronic kidney disease progress? A background paper prepared for the UK Consensus Conference on early chronic kidney disease. Nephrol Dial Transplant, 22 Suppl 9, ix26-30.

5. Bigot A, Gusto G, Copin N, Sautenet B, Lantieri O, Halimi J-M: Body mass index, fatty liver index and other metabolic disturbances differentially affect albuminuria and glomerular filtration rate in the general population. *J. Diabetes Metab.* 05: 1000387, 2014

6. Singh GM, Danaei G, Farzadfar F, Stevens GA, Woodward M, Wormser D, Kaptoge S, Whitlock G, Qiao Q, Lewington S, Di Angelantonio E, vander Hoorn S, Lawes CMM, Ali MK, Ezzati M: The age-specific quantitative effects of metabolic risk factors on cardiovascular diseases and diabetes: A pooled analysis. PLoS One 8: e65174, 2013

7. GBD 2015 Obesity Collaborators: Health effects of overweight and obesity in 195 Countries over 25 years. N. Engl. J. Med. 377: 13–27, 2017

8. Lee SM, Park M, Yoon H-J: Association of body mass index with estimated glomerular filtration rate and incident proteinuria In: Proceedings of the 11th International Joint Conference on Biomedical Engineering Systems and Technologies, pp 587–590, 2018

9. Lakka, H. M., Laaksonen, D. E., Lakka, T. A., Niskanen, L. K., Kumpusalo, E., Tuomilehto, J., and Salonen, J. T. (2002) The metabolic syndrome and total and cardiovascular disease mortality in middle-aged men. JAMA 288, 2709–2716

10. Isomaa, B., Almgre, P., Tuomi, T., Forsen, B., Lahti, K., Nissen, M., Taskinen M. R., and Groop, L. (2001) Cardiovascular morbidity and mortality associated with the metabolic syndrome. Diabetes Care 24, 683–689

11. Chen, J., Muntner, P., Hamm, L. L., Jones, D. W., Batuman, V., Fonseca, V., Whelton, P. K., and He, J. (2004) The metabolic syndrome and chronic kidney disease in U.S. adults. Ann. Intern. Med. 140, 167–174

12. Bagby, S. P. (2004) Obesity-initiated metabolic syndrome and the kidney: a recipe for chronic kidney disease? J. Am. Soc. Nephrol. 15, 2775–2791

13. Henegar, J. R., Bigler, S. A., Henegar, L. K., Tyagi, S. C., and Hall, J. E. (2001) Functional and structural changes in the kidney in the early stages of obesity. J. Am. Soc. Nephrol. 12, 1211–1217

14. Praga, M. (2002) Obesity- a neglected culprit in renal disease. Nephrol. Dial. Transplant. 17, 1157–1159

15. Guan, Y. (2004) Peroxisome proliferator-activated receptor family and its relationship to renal complications of the metabolic syndrome. J. Am. Soc. Nephrol. 15, 2801–2815

16. El-Atat, F. A., Stas, S. N., McFarlane, S. I., and Sowers, J. R. (2004) The relationship between hyperinsulinemia, hypertension and progressive renal disease. J. Am. Soc. Nephrol. 15, 2816–2827

17. Kimmelstiel, P., and Wilson, C. (1936) Intercapillary Lesions in the Glomeruli of the Kidney. Am. J. Pathol. 12, 83–98

18. Yamagata K., Ishida K., Sairenchi T., Takahashi H., Ohba S., Shiigai T., Narita M., Koyama A. Risk factors for chronic kidney disease in a community-based population: A 10-year follow-up study. Kidney Int. 2007;71:159–166. doi: 10.1038/sj.ki.5002017.

19. Weiner D.E., Sarnak M.J. Managing dyslipidemia in chronic kidney disease. J. Gen. Intern. Med. 2004;19:1045–1052. doi: 10.1111/j.1525-1497.2004.40049.x.

20. C. Hetz, The unfolded protein response: controlling cell fate decisions under ER stress and beyond, Nat Rev Mol Cell Biol 13 (2012) 89-102.

21. R.C. Austin, The unfolded protein response in health and disease, Antioxid Redox Signal 11 (2009) 2279-2287.

22. A. Al-Hashimi, E. Crane, R. Austin, oxidative stress and the endoplasmic reticulum, in: K. Pantopoulos, H.M. Schipper (Eds.), Principles of free radical biomedicine, Nova Science Publishers, New York, NY, 2011, pp. 1-20.

23. B.M. Gardner, D. Pincus, K. Gotthardt, C.M. Gallagher, P. Walter, Endoplasmic reticulum stress sensing in the unfolded protein response, Cold Spring Harb Perspect Biol 5 (2013) a013169.

24. Cinaroglu A, Gao C, Imrie D, Sadler KC. KC. Activating transcription factor 6 plays protective and pathological roles in steatosis due to endoplasmic reticulum stress in zebrafish. Hepatology 2011;54:495-508.

25. Brown MS, Goldstein JL. A proteolytic pathway that controls the cholesterol content of membranes, cells, and blood. Proc Natl Acad Sci USA 1999;96:11041-11048

26. Calfon M, Zeng H, Urano F, Till JH, Hubbard SR, Harding HP, et al. IRE1 couples endoplasmic reticulum load to secretory capacity by processing the XBP-1 mRNA. Nature 2002;415:92-96.

27. Hetz C, Martinon F, Rodriguez D, Glimcher LH. The unfolded protein response: integrating stress signals through the stress sensor IRE1alpha. Physiol Rev 2011;91:1219-1243.

28. Back SH, Schroder M, Lee K, Zhang K, Kaufman RJ. ER stress signaling by regulated splicing: IRE1/HAC1/XBP1. Methods 2005;35:395-416.

29. Rozpedek W, Pytel D, Mucha B, Leszczynska H, Diehl JA, Majsterek I. The Role of the PERK/eIF2alpha/ATF4/CHOP Signaling Pathway in Tumor Progression During Endoplasmic Reticulum Stress. Curr Mol Med 2016;16:533-544.

30. B'Chir W, Maurin AC, Carraro V, Averous J, Jousse C, Muranishi Y, et al. The eIF2alpha/ATF4 pathway is essential for stress-induced autophagy gene expression. Nucleic acids research 2013;41:7683-7699.

31. Iagi R, Ishimoto Y, Nangaku M: Proteostasis in endoplasmic reticulum—new mechanisms in kidney disease. Nat. Rev. Nephrol. 10: 369–378, 2014

32. Dickhout JG, Carlisle RE, Austin RC: Interrelationship between cardiac hypertrophy, heart failure, and chronic kidney disease. *Circ. Res.* 108: 629–642, 2011

33. Cybulsky, A. V. (2017). Endoplasmic reticulum stress, the unfolded protein response and autophagy in kidney diseases. Nature Reviews Nephrology, 13(11), 681–696. doi: 10.1038/nrneph.2017.129

34. Wright, G., Noiret, L., Damink, S. W. M. O., & Jalan, R. (2011). Interorgan ammonia metabolism in liver failure: the basis of current and future therapies. Liver Int, 31(2), 163-175.

35. Miller, A. C., Cohen, S., Stewart, M., Rivas, R., & Lison, P. (2011). Radioprotection by the histone deacetylase inhibitor phenylbutyrate. Radiat Environ Biophys, 50(4), 585-596.

36. Xiao, C., Giacca, A., & Lewis, G. F. (2011). Sodium phenylbutyrate, a drug with known capacity to reduce endoplasmic reticulum stress, partially alleviates lipid-induced insulin resistance and beta-cell dysfunction in humans. Diabetes, 60(3), 918-924.

37. Yam, G. H., Gaplovska-Kysela, K., Zuber, C., & Roth, J. (2007). Sodium 4-phenylbutyrate acts as a chemical chaperone on misfolded myocilin to rescue cells from endoplasmic reticulum stress and apoptosis. Invest Ophthalmol Vis Sci, 48(4), 1683-1690.

38. Mimori, S., Ohtaka, H., Koshikawa, Y., Kawada, K., Kaneko, M., Okuma, Y., . . . Hamana, H. (2013). 4-Phenylbutyric acid protects against neuronal cell death by

primarily acting as a chemical chaperone rather than histone deacetylase inhibitor. Bioorg Med Chem Lett, 23(21), 6015-6018.

39. Mohammed-Ali, Z., Lu, C., Marway, M. K., Carlisle, R. E., Ask, K., Lukic, D., Krepinsky, J. C., … Dickhout, J. G. (2017). Endoplasmic reticulum stress inhibition attenuates hypertensive chronic kidney disease through reduction in proteinuria. Scientific reports, 7, 41572. doi:10.1038/srep41572

40. Wilson, C. G., Tran, J. L., Erion, D. M., Vera, N. B., Febbraio, M., & Weiss, E. J. (2016). Hepatocyte-Specific Disruption of CD36 Attenuates Fatty Liver and Improves Insulin Sensitivity in HFD-Fed Mice. Endocrinology, 157(2), 570–585. doi: 10.1210/en.2015-1866

41. Alkhatatbeh, M. J., Enjeti, A. K., Acharya, S., Thorne, R. F., & Lincz, L. F. (2013). The origin of circulating CD36 in type 2 diabetes. Nutrition & Diabetes, 3(2). doi: 10.1038/nutd.2013.1

42. Wang, J., & Li, Y. (2019). CD36 tango in cancer: signaling pathways and functions. Theranostics, 9(17), 4893–4908. doi: 10.7150/thno.36037

43. Susztak K., Ciccone E., McCue P., Sharma K., Bottinger E.P. Multiple metabolic hits converge on CD36 as novel mediator of tubular epithelial apoptosis in diabetic nephropathy. PLoS Med. 2005;2:e45. doi: 10.1371/journal.pmed.0020045.

44. Kennedy D.J., Chen Y., Huang W., Viterna J., Liu J., Westfall K., Tian J., Bartlett D.J., Tang W.H., Xie Z., et al. CD36 and Na/K-ATPase-alpha1 form a proinflammatory signaling loop in kidney. Hypertension. 2013;61:216–224. doi: 10.1161/HYPERTENSIONAHA.112.198770.

45. Yang P., Xiao Y., Luo X., Zhao Y., Zhao L., Wang Y., Wu T., Wei L., Chen Y. Inflammatory stress promotes the development of obesity-related chronic kidney disease via CD36 in mice. J. Lipid Res. 2017;58:1417–1427. doi: 10.1194/jlr.M076216.

46. Okamura D.M., Lopez-Guisa J.M., Koelsch K., Collins S., Eddy A.A. Atherogenic scavenger receptor modulation in the tubulointerstitium in response to chronic renal injury. Am. J. Physiol. Ren. Physiol. 2007;293:F575–F585. doi: 10.1152/ajprenal.00063.2007.

47. Hua W., Huang H.Z., Tan L.T., Wan J.M., Gui H.B., Zhao L., Ruan X.Z., Chen X.M., Du X.G. CD36 Mediated Fatty Acid-Induced Podocyte Apoptosis via Oxidative Stress. PLoS ONE. 2015;10:e0127507. doi: 10.1371/journal.pone.0127507.

48. Ruan X.Z., Varghese Z., Powis S.H., Moorhead J.F. Human mesangial cells express inducible macrophage scavenger receptor. Kidney Int. 1999;56:440–451. doi: 10.1046/j.1523-1755.1999.00587.x.

49. Seidah NG, Benjannet S, Wickham L, Marcinkiewicz J, Jasmin SB, Stifani S, et al. The secretory proprotein convertase neural apoptosis-regulated convertase 1 (NARC-1): liver regeneration and neuronal differentiation. Proc Natl Acad Sci USA 2003;100-928-933

50. Maxwell KN, Breslow JL, Adenoviral mediated expression of Pcsk9 in mice results in a low-density lipoprotein receptor knockout phenotype. Proc Natl Acad Sci USA 2004;101;7100-7105

51. Grefohort, A, McNutt MC, Lagace TA, Horton JD. Plasma PCSK9 preferentially reduces liver LDL receptors in mice. J Lipid Res 2008;49:1303-1311

52. Dubuc G, Chamberland A, Wassef H, Davignon J, Seidah NG, Bernier L, et al. Statins upregulate PCSK9, the gene encoding the proprotein convertase neural apoptosis-regulated convertase-1 implicated in familial hypercholesterolemia. Arterioscler Thromb Vasc Biol 2004;24:1454-1459

53. Brown MS, Goldstein JL. The SREBP pathway: regulation of cholesterol metabolism by proteolysis of a membrane-bound transcription factor. Cell 1997;89:331-340

54. Humphries SE, Neely RD, Whittall RA, Troutt JS, Konrad RJ, Scartezini M, et al. Healthy individuals carrying the PCSK9 p.R46L variant and familial hypercholesterolemia patients carrying PCSK9 p.D374Y exhibit lower plasma concentrations of PCSK9. Clin Chem 2009;55:2153-2161

55. Sabatine M.S., Giugliano R.P., Wiviott S.D., et al., for the Open-Label Study of Long-Term Evaluation against LDL Cholesterol (OSLER) Investigators (2015) Efficacy and safety of evolocumab in reducing lipids and cardiovascular events. N Engl J Med 372:1500–1509.

56. Giugliano R.P., Sabatine M.S. (2015) Are PCSK9 inhibitors the next breakthrough in the cardiovascular field? J Am Coll Cardiol 65:2638–2651.

57. Ray K.K., Landmesser U., Leiter L.A., et al. (2017) Inclisiran in patients at high cardiovascular risk with elevated LDL cholesterol. N Engl J Med 376:1430–1440.

58. Nordestgaard B.G., Nicholls S.J., Langsted A., Ray K.K., Tybjærg-Hansen A. (2018) Advances in lipid-lowering therapy through gene-silencing technologies. Nat Rev Cardiol 15:261–272.

59. Surdo PL, Bottomley MJ, Calzetta A, Settembre EC, Cirillo A, Pandit S, Ni YG, Hubbard B, Sitlani A, Carfi A. Mechanistic implications for LDL receptor degradation from the PCSK9/LDLR structure at neutral pH. EMBO Rep. 2011;12:1300–1305.

60. Jinek M, Chylinski K, Fonfara I, Hauer M, Doudna JA, Charpentier E. A programmable dual-RNA-guided DNA endonuclease in adaptive bacterial immunity. Science. 2012;337:816–821.

61. Cong L, Ran FA, Cox D, Lin S, Barretto R, Habib N, Hsu PD, Wu X, Jiang W, Marraffini LA, Zhang F. Multiplex genome engineering using CRISPR/Cas systems. Science. 2013;339:819–823.

62. Poirier S, Mayer G, Benjannet S, Bergeron E, Marcinkiewicz J, Nassoury N, Mayer H, Nimpf J, Prat A, Seidah NG: The proprotein convertase PCSK9 induces the degradation of low density lipoprotein receptor (LDLR) and its closest family members VLDLR and ApoER2. *J. Biol. Chem.* 283: 2363–2372, 2008

63. Roubtsova A, Munkonda MN, Awan Z, Marcinkiewicz J, Chamberland A, Lazure C, Cianflone K, Seidah NG, Prat A. Circulating proprotein convertase subtilisin/kexin 9 (PCSK9) regulates VLDLR protein and triglyceride accumulation in visceral adipose tissue. Arterioscler Thromb Vasc Biol. 2011;31:785–791.

64. Labonte P, Begley S, Guevin C, Asselin MC, Nassoury N, Mayer G, Prat A, Seidah NG. PCSK9 impedes hepatitis C virus infection in vitro and modulates liver CD81 expression. Hepatology. 2009;50:17–24.

65. Sharotri, V., Collier, D. M., Olson, D. R., Zhou, R., & Snyder, P. M. (2012). Regulation of Epithelial Sodium Channel Trafficking by Proprotein Convertase Subtilisin/Kexin Type 9 (PCSK9). Journal of Biological Chemistry, 287(23), 19266–19274. doi: 10.1074/jbc.m112.363382

66. Picard, C., Poirier, A., Bélanger, S., Labonté, A., Auld, D., & Poirier, J. (2019). Proprotein convertase subtilisin/kexin type 9 (PCSK9) in Alzheimer's disease: A genetic and proteomic multi-cohort study. Plos One, 14(8). doi: 10.1371/journal.pone.0220254

67. Lebeau P, Byun JH, Platko K, et al. Pcsk9 knockout exacerbates diet-induced non-alcoholic steatohepatitis, fibrosis, and liver injury in mice. (2019) j.hepr.2019.10.009

68. Mayne J, Ooi TC, Raymond A, Cousins M, Bernier L, Dewpura T, et al. Differential effects of PCSK9 loss of function variants on serum lipid and PCSK9 levels in Caucasian and African Canadian populations. Lipids in health and disease 2013;12:70.

69. Lebeau, P.*, et al.* Loss-of-function PCSK9 mutants evade the unfolded protein response sensor GRP78 and fail to induce endoplasmic reticulum stress when retained. *J Biol Chem* **293**, 7329-7343 (2018).

70. Konarzewski M, Szolkiewicz M, Sucajtys-Szulc E, Blaszak J, Lizakowski S, Swierczynski J, Rutkowski B: Elevated circulating PCSK-9 concentration in renal failure patients is corrected by renal replacement therapy. Am. J. Nephrol. 40: 157–163, 2014

71. Sucajtys-Szulc E, Szolkiewicz M, Swierczynski J, Rutkowski B: Up-regulation of liver Pcsk9 gene expression as a possible cause of hypercholesterolemia in experimental chronic renal failure. Mol. Cell. Biochem. 411: 281–287, 2016

72. Haas ME, Levenson AE, Sun X, Liao W-H, Rutkowski JM, de Ferranti SD, Schumacher VA, Scherer PE, Salant DJ, Biddinger SB: The role of proprotein convertase subtilisin/kexin type 9 in nephrotic syndrome-associated hypercholesterolemia. *Circulation* 134: 61–72, 2016

73. Kuwahara S, Hosojima M, Kaneko R, Aoki H, Nakano D, Sasagawa T, Kabasawa H, Kaseda R, Yasukawa R, Ishikawa T, Suzuki A, Sato H, Kageyama S, Tanaka T, Kitamura N, Narita I, Komatsu M, Nishiyama A, Saito A: Megalin-mediated tubuloglomerular alterations in high-fat diet–induced kidney disease. *J. Am. Soc. Nephrol.* 27: 1996–2008, 2016

74. Lebeau, P., et al. Loss-of-function PCSK9 mutants evade the unfolded protein response sensor GRP78 and fail to induce endoplasmic reticulum stress when retained. J Biol Chem 293, 7329-7343 (2018).

75. Lebeau PF, Byun JH, Platko K, MacDonald ME, Poon SV, Faiyaz M, et al.
Diet-induced hepatic steatosis abrogates cellsurface LDLR by inducing de novo PCSK9 expression in mice. J Biol Chem 2019;294:9037-9047.

76. Lhoták, Š., Sood, S., Brimble, E., Carlisle, R. E., Colgan, S. M., Mazzetti, A., … Austin, R. C. (2012). ER stress contributes to renal proximal tubule injury by increasing SREBP-2-mediated lipid accumulation and apoptotic cell death. American Journal of Physiology-Renal Physiology, 303(2). doi: 10.1152/ajprenal.00482.2011

77. Poirier, S., Mamarbachi, M., Lee, A., & Mayer, G. (2015). GRP94 regulates circulating cholesterol levels through blockade of PCSK9-induced LDLR degradation. Atherosclerosis, 241(1). doi: 10.1016/j.atherosclerosis.2015.04.072

78. Dongiovanni, P., Ruscica, M., Ferri, N., Macchi, C., Lanti, C., Rametta, R., … Valenti, L. (2015). Liver fat accumulation is associated with circulating PCSK9 levels. *Digestive and Liver Disease*, *47*. doi: 10.1016/j.dld.2015.07.033

79. Iwawaki, T., Akai, R., Kohno, K., and Miura, M. (2004). A transgenic mouse model for monitoring endoplasmic reticulum stress. Nat. Med. 10, 98–102

80. Han J, Kaufman RJ. The role of ER stress in lipid metabolism and lipotoxicity. J Lipid Res 2016;57:1329-1338.

81. Dubuc G, Chamberland A, Wassef H, Davignon J, Seidah NG, Bernier L, et al. Statins upregulate PCSK9, the gene encoding the proprotein convertase neural apoptosis-regulated convertase-1 implicated in familial hypercholesterolemia. Arterioscler. Thromb Vasc Biol 2004;24:1454-1459.

82. Maimaitiyiming, H., Zhou, Q. & Wang, S. Thrombospondin 1 deficiency ameliorates the development of adriamycin-induced proteinuric kidney disease. PLoS ONE 11, e0156144 (2016).

83. Lopez-Carmona, M.D., Plaza-Seron, M.C., Vargas-Candela, A. et al. CD36 overexpression: a possible etiopathogenic mechanism of atherosclerosis in patients with prediabetes and diabetes. Diabetol Metab Syndr 9, 55 (2017) doi:10.1186/s13098-017-0253-x

84. Zaid, A., Roubtsova, A., Essalmani, R., Marcinkiewicz, J., Chamberland, A., Hamelin, J., … Prat, A. (2008). Proprotein convertase subtilisin/kexin type 9 (PCSK9): Hepatocyte-specific low-density lipoprotein receptor degradation and critical role in mouse liver regeneration. Hepatology, 48(2), 646–654. doi: 10.1002/hep.22354

85. Yang, X., Okamura, D. M., Lu, X., Chen, Y., Moorhead, J., Varghese, Z., & Ruan, X. Z. (2017). CD36 in chronic kidney disease: novel insights and therapeutic opportunities. Nature Reviews Nephrology, 13(12), 769–781. doi: 10.1038/nrneph.2017.126

86. Fraser, S. D., Roderick, P. J., & Taal, M. W. (2016). Where now for proteinuria testing in chronic kidney disease?: Good evidence can clarify a potentially confusing message. Br J Gen Pract, 66(645), 215-217.

87. Seidah, N. G. (2017). The PCSK9 revolution and the potential of PCSK9-based therapies to reduce LDL-cholesterol. Global Cardiology Science and Practice, 2017(1). doi: 10.21542/gcsp.2017.2

88. Carlisle, R. E., Brimble, E., Werner, K. E., Cruz, G. L., Ask, K., Ingram, A. J., & Dickhout, J. G. (2014). 4-Phenylbutyrate Inhibits Tunicamycin-Induced Acute Kidney Injury via CHOP/GADD153 Repression. PLoS ONE, 9(1). doi: 10.1371/journal.pone.0084663

89. Okamura, D. M., Pennathur, S., Pasichnyk, K., López-Guisa, J. M., Collins, S., Febbraio, M., … Eddy, A. A. (2009). CD36 Regulates Oxidative Stress and Inflammation in

Hypercholesterolemic CKD. Journal of the American Society of Nephrology, 20(3), 495–505. doi: 10.1681/asn.2008010009